Master's thesis

NTNU
Norwegian University of Science and Technology
Faculty of Engineering
Department of Geoscience and Petroleum

Juan Manuel Montoza

Design and Implementation of an Autonomous Miniature Drilling Rig for Directional Drilling

Contribution to the Drillbotics Competition 2019

Master's thesis in Petroleum Engineering
Supervisor: Alexey Pavlov, Tor Berge Gjersvik and Sigve Hovda
June 2019

NTNU
Norwegian University of
Science and Technology

Juan Manuel Montoza

Design and Implementation of an Autonomous Miniature Drilling Rig for Directional Drilling

Contribution to the Drillbotics Competition 2019

Master's thesis in Petroleum Engineering
Supervisor: Alexey Pavlov, Tor Berge Gjersvik and Sigve Hovda
June 2019

Norwegian University of Science and Technology
Faculty of Engineering
Department of Geoscience and Petroleum

Abstract

The current report will showcase the work done by the NTNU team during Phase II of Drillbotics. Drillbotics is an international drilling competition organized by DSATS for the fifth consecutive year that challenges university students to build and automate a miniature drilling rig. Each year a different challenge is introduced and autonomous directional drilling and downhole measurements are the main focus of this year's competition.

During Phase I of the competition, a design proposal was presented to tackle the main challenges [35]. Such a design serves as a starting point for the current work and will focus on implementing two different mechanical alternatives to deviate the well while taking downhole measurements.

Several changes had to be made to the rig to be able to deviate the well. The top drive had to be changed to be able to steer the BHA precisely and the wiring inside the drill string had to be optimized and shrunk to be able to have a stable connection with the downhole sensor card. Besides, a new pump had to be installed in order to fulfill the high-pressure requirements in the hydraulic system.

A 9-axis sensor card which includes an accelerometer, magnetometer, and a gyroscope has been used to track the trajectory of the well and as feedback for the control system. An active magnetic ranging method has been implemented to overcome the magnetic disturbances in the vicinity of the magnetometer. This solution helps keeping better track of the magnetic North and thus, the direction of the well.

This year's control system is implemented using NI LabVIEW and includes numerous new features. A better GUI helps the driller visualize and interpret what is going on in the well through a live log panel. The script also increases HSE by including a safety sequence that automatically takes control over the rig and prevent a complete rig halt should any dysfunction appear.

Many challenges and limitations were encountered along the way. Manufacturing miniature downhole tools from scratch comes with a lot of practicalities that need to be understood and overcome. These aspects are included and thoroughly explained in the report, as well as the lessons learned.

The competition day for Drillbotics 2019 will be held on June 13th in Celle, Germany. All the finalists from Europe will compete and start drilling at the same time. Due to deadline limitations, this report could not include the NTNU rig performance in the competition.

Sammendrag

Denne rapporten viser arbeidet gjort av NTNU-laget under andre fase av Drillbotics. Drillbotics er ein internasjonal borekonkurranse som blir arrangert av DSATS for femte år på rad i 2019, der universitetsstudentar vert utfordra til å bygga og automatisera ein miniatyrborerigg. Kvart år blir ei ny utfordring introdusert, og fokuset dette året er på nedihullsmålingar og automatisering av retningsboring.

I fyrste fase av konkurransen vart eit designforlag presentert for korleis hovudutfordringane skulle taklast [35]. Dette designet presenterte to ulike mekaniske alternativ for å oppnå retningsboring ut frå nedihullsmålingar.

Fleire endringar måtte gjerast på riggen for å gjera retningsboring mulig. Top-drive-motoren måtte byttast ut for å mogeleggjera presis styring av nedihullsutstyret, og leidningane inne i borestrengen måtte forbetrast og gjerast mindre for å ha stabil kopling med nedihulls sensorkort. Ei ny pumpe måtte monterast for å tilfredsstilla dei høge trykk-krava frå det hydrauliske systemet.

Eit 9-akse sensorkort med akselerometer, magnetometer og gyroskop har blitt brukt for å måla brønnbanen. Ein elektromagnet har blitt brukt for å gjera opp for magnetisk forstyrring i nærleiken av magnetometeret. Denne løysinga gjer det enklare for sensoren å måla magnetisk nord, og det blir difor enklare å bora brønnen i ønska retning.

Kontrollsystemet er implementert i NI LabVIEW, og inneheld fleire nye funksjonalitetar. Eit forbetra grafisk brukargrensesnitt hjelper operatør med å visualisera og tolka det som foregår i brønnen ved bruk av eit live loggpanel. HMS har blitt styrka, og nedetid redusert, ved innføring av ein tryggleikssekvens som blir aktivert av mindre advarslar frå systemet, og jobbar for å redusera problemet før det blir så stort at riggen må stoppast.

Fleire utfordringar og begrensningar vart møtt under prosjektet. Å laga nedihullsutstyr i miniatyr frå grunnen av fører med seg mange praktiske utfordringar som må forståast og løysast. Dette aspektet av prosjektet, samt det laget lærte av utfordringane, er skildra og forklart i rapporten.

Konkurransen for Drillbotics 2019 blir haldt 13. juni i Celle i Tyskland. Alle finalistane frå Europa skal delta her, og starta boringa samtidig. Sidan leveringsfristen til oppgåva er før konkurransedagen, vil denne rapporten ikkje innehalda NTNU sine resultat i denne konkurransen.

Acknowledgements

We would like to express our thanks to our professors and supervisors Alexey Pavlov, Sigve Hovda, Tor Berge S. Gjersvik, Sigbjørn Sangesland and John-Morten Godhavn for continuously sharing their knowledge and experience in finding the solution of the problems that came along the way. The meetings, knowledge-sharing sessions and the feedback on the progress helped us improve the project. Thank you for supporting us and always being available for guidance and help.

We would like to give a special recognition to all the support crew in the workshop. They have always prioritized our work for which we are extremely grateful. It has been a great learning experience working in close collaboration with such a talented technical crew. They have always been welcoming and nice to us whenever a problem occurred or any help was needed. Without their help and time, this project would have been much more difficult to complete.

Thanks to Noralf Vedvik for helping us out in all the mechanical work related to the rig and its components. The time and effort you have spent towards the project is highly appreciated.

Thanks to Steffen W. Moen for assisting us with all the electrical and electronics associated with the rig. The time spent on setting up the top drive communication and electrical swivel is highly valued.

Thanks to Terje Bjerkan and Håkon Myhren for fabricating different components in the BHA. The precision combined with the elegant solutions have always been workable and priceless. The efforts they made in fixing the mechanical problems is highly admired.

We would also like to express our gratitude to Lyng Drilling for helping us in designing the drill bits and also for sponsoring us with four new drill bits for the competition. Thank you Are Funderud for inviting us to the company and showing us the whole bit manufacturing process. Thank you for supporting the team and always being available.

Last but not least, we would like to thank the Department of Geoscience and Petroleum at NTNU for providing us the opportunity to work in such a comprehensive multidisciplinary project. Thank you to the Department for providing us the economic support to the project. The Drillbotics project requires significant resources to achieve the different tasks and that would have never been possible without their support.

Table of Contents

List of Tables

List of Figures

Nomenclature

BHA	=	Bottom hole assembly
PDM	=	Positive displacement motor
NPT	=	Non-productive time
DSATS	=	Drilling Systems Automation Technical Section
EMM	=	Electric Miniature Motor
PPE	=	Personal Protective Equipment
SP	=	Set point
GUI	=	Graphical User Interface
RSS	=	Rotary Steerable System
PLA	=	Polylactic acid

Chapter 1

Introduction

Many industries have gone through the process of mechanizing and automating their operations and manufacturing processes. The benefits are numerous and range from reducing costs to improving the safety of the personnel. The drilling industry has seen these advantages in the past decades and has been developing new ways of drilling more efficiently ever since.

Even though levels of automation vary from rig to rig, the industry is working towards fully automated drilling rigs that will allow remote operations in the future. Nowadays, many drilling operations such as tripping operations are already automated and the use of downhole sensors that implement feedback control to detect drilling dysfunctions are becoming more and more popular.

There exist many drives for drilling automation. Among the most evident and important is safety. Removing people from the rig floor reduces the risks involved with pipe handling, heavy lifting, and unforeseen accidents. Besides, having a lower headcount on the rig also signifies fewer costs for the operator, service company and drilling contractor.

Another major drive is efficiency. By implementing downhole sensors and a control system on the rig, one can create internal algorithms that use real-time drilling parameters to detect drilling dysfunctions. This feature allows the driller to react on time and thus reduce the non-productive time (NPT) and the costs associated with it.

With the idea to ”help accelerate the uptake of automation in the drilling industry” a group of SPE (Society of Petroleum Engineers) members created the Drilling Systems Automation Technical Section (DSATS) in 2008. To further develop these ideas, in 2014 the Drillbotics competition was created, which engages university students at all levels in an international competition.

The Norwegian University of Science and Technology (NTNU) had the opportunity to participate in this competition for the first time in 2017, landing a decent second place

worldwide. After obtaining excellent results in the competition, the NTNU Drillbotics Team took the first place in 2018, finishing way ahead of the competition. This year marks the third time NTNU will participate in the competition, with the hopes to maintain previous excellence.

The challenge for this year is autonomous directional drilling. Teams have to drill a vertical pilot hole and then kick off to reach a predefined target along the north axis of the rock sample. Closed loop control of the rig is mandatory and those teams who are able to maintain direction and have a longer vertical section will receive more points by the judges.

The current thesis describes the work done by the NTNU Drillbotics Team during the testing phase of the project. Several changes had to be made to the proposed designed presented in Phase I [35], due to a series of challenges encountered along the way. Because of the magnitude of the project and time constraints, project management techniques were necessary to ensure that critical tasks were completed on time and all risks involved in the system were minimized.

Chapter 2

Project Overview

2.1 About the competition, NTNU history and objective

The Drillbotics competition is an international competition between teams from universities from around the world. The goal is to design and build the best fully automated miniature drilling rig. NTNU participated for the first time in 2017, placing second in the competition. The NTNU's team then went on to win the first place in 2018. The challenge for the first two years was to drill a vertical well through rock with unknown and changing formations. For the 2019 competition, the challenge is to drill a deviated well in a sandstone of known strength. The competition spans two semesters, which are considered separate phases of the competition. The first phase is the design phase or Phase I. In this part of the competition, the teams design the equipment which has to be built and tested in the second phase.

2.2 About work done in Phase I

In the first phase of the competition, the NTNU team worked to find a design that could be implemented in Phase II. This was done by considering the mechanical and budget limitations and time constraints of the competition. It was decided to steer using a bent housing and downhole power section, meaning that the bit is at an angle to the drill pipe. This allows for deviated drilling by rotating the bit using the downhole power section and only requires drill pipe rotation when drilling straight ahead or orienting the tool face for steering. The angle is fixed, meaning that the angle build rate is constant and that the maximum deviation is limited by this angle [1].

[1] In the case of an overgauged hole, WOB plays also a part in how much the BHA can deviate.

The available downhole power section is also a limitation of the design. Two alternative solutions for downhole power sections were decided on: an electric miniature motor and a positive displacement motor. The main one of these was the positive displacement motor, often referred to as a mud motor or a PDM. The power section consists of a stator, which is fixed to the external parts of the BHA and drill pipe, and a rotor, which is connected to the bit via a drive shaft and a universal joint. Water is pumped through the power section, driving the motor. This ensures that the water flow, which is required for hole cleaning, is better utilized than when using an electric motor. However, mud motors at this scale are not commercially available and needed to be designed and manufactured for the project. The team designed a PDM and used a plastic 3D printer during the design process to check the fit and configuration of the design. The plan was then to finally 3D-print the motor in metal and apply an elastomer coating to either the rotor or the stator in order to adjust the fit and avoid metal on metal friction. However, this plan was considered risky, due to the amount of work and testing required to ensure the motor could be used for drilling. An electric miniature motor, hereafter referred to as **EMM**, was therefore used as a backup downhole motor.

Using the rig, bit and BHA from the previous year's competition, the team drilled in sandstone to find an approximate minimum output needed from the downhole power section to be able to finish the well within the competition time limits. An EMM that fulfilled these requirements was chosen and a BHA for this solution was designed. The motor housing required channels in the wall to allow water to flow past the motor without exposing the motor to water, which restricted the diameter of the motor. The length of the motor was kept as short as possible to limit the BHA length. These limitations in size also limited the amount of power it was possible to get from the EMM. The output from the motor is therefore not much higher than the minimum that is expected to be needed. Differences in rock softness and bit aggressiveness, friction in the BHA and inaccuracies of the torque measurements in the drilling tests in Phase I may therefore, lead to the competition well not being completed within the competition time limits. This was considered an acceptable risk due to the EMM being the backup solution.

Only the power section and the bent housing differ between the two alternatives. The PDM power section is 8 cm long, while the EMM housing is 10 cm long. A single U-joint transmits the rotation from the EMM to the bit, while a double U-joint is required to take up the planetary motion from the PDM rotor. Therefore, the PDM requires a longer bent housing than the EMM. As the angle of the bent housing depends on the distance between the contact points on the BHA, two different bent housing angles are required for the alternatives.

The general BHA consists of the following parts: bit sub, thrust bearing, bearing assembly, bent housing, power section, sensor housing and drill pipe connector. The drill pipe connector is the same as was used in 2018 and the bearings are purchased off-the-shelf. All other parts were designed by the students and manufactured in the mechanical workshop at the institute.

A 9-axis sensor is used to log the position while drilling. The sensor consists of a 3D accelerometer, 3D gyroscope and 3D magnetometer. It was planned to use the magne-

tometer to measure the BHA's orientation in the earth's magnetic field. A testing version of the sensor card was designed and made at the electronics workshop. The sensor data would be used in a closed-loop system to orient the drill pipe when drilling the deviated section of the well. The drill pipe should be oriented by a servo motor functioning as a top drive. Since the previous top drive did not have position control and was inaccurate at low speeds, a new motor had to be purchased for this purpose.

The circulation system was planned to be similar to the 2018 system, with some modification. Due to low water flow rate from the outlet at the wall and uncertainties about the flow rate at the competition location, it was decided to use two 200 liter tanks to store water. These could then be filled before the drilling started. If the tanks were to run out of water, a pressure sensor at the bottom would allow the control system to stop pumping until the tank could be refilled. The pump, which was controlled manually the previous year, needed to be implemented in the control system for the PDM-solution to work. This was intended to be done using the same pump motor and drive as was already in place.

The electrical system was mostly unchanged from the previous year. An electric cabinet sits at the rear end of the rig and all communication and power to drives, sensors and actuators go through it. The rig is powered by 3-phase 400V, with some equipment running on 240V. Of the sensors in the system, the load cell and pump pressure sensor were the same as in the previous year, while a pressure sensor was added to the tanks to measure the water level in the tanks. The hoisting motor and pump motor were planned to be unchanged, while the top drive motor should be replaced by a servo motor with position control.

The control system was planned to be written in NI LabVIEW. The system should be capable of first drilling vertically for 3 inches and then deviating in the north direction until exiting the rock sample. When drilling the vertical section, the control sequence should be similar to last year's code. A WOB controller and a top drive torque controller were then used to control the weight on bit and top drive RPM. In addition to these, a position control script needed to be made from scratch.

A Kalman filter should be implemented to filter the downhole sensor data before the data is used in a PID controller for position control. If the load cell data filtering from 2018 turned out to be inadequate, a Kalman filter would be used for this data as well.

More details about the plans and designs after Phase I of the project can be found in the project report [35]. As these plans were implemented and acted on in Phase II, changes were made. These changes will be further described in this thesis.

Chapter 3

Organization

In order to complete a group task successfully, roles within a team should be decided early on in the project. In the Drillbotics competition, students from petroleum and cybernetics background join hands to work in a multi-disciplinary team and resolve different engineering problems that come in a way of completing the task. To have an effective teamwork, a structured organization, splitting of tasks and proper distribution of duties are required. Moreover, an accurate methodology is required to engage all the participants towards a common vision and goal. Since the Drillbotics project covers all aspects of engineering, the learning outcomes for all the group members have been enormous in terms of solving the engineering problems, project management issues and time planning. In this section, a brief introduction to all the members of NTNU Drillbotics team, followed by roles and overall management is described.

3.1 Team Drillbotics

According to the Drillbotics competition guidelines, a maximum of five students can form a team. Thus, the NTNU team consists of four students: three from the petroleum engineering department and one from the industrial cybernetics department. The team is also supported by four supervisors from the respective departments. Moreover, two lab engineers from mechanical and electronics background also help the team throughout the project. Figure 3.1 and Figure 3.2 and represents a brief background for all the team members.

Figure 3.1: Project team background chart

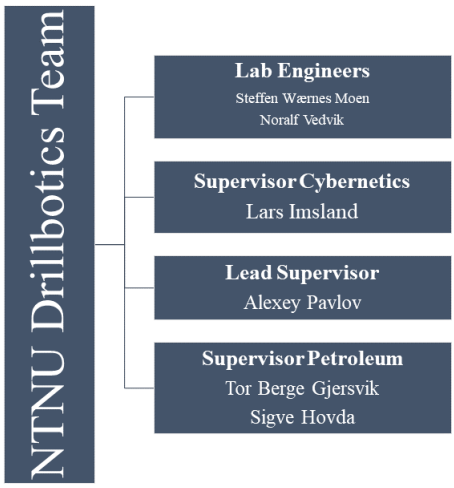

Figure 3.2: Support Team Chart

3.2 Distribution of Roles

The splitting of a big project into smaller tasks and the distribution of these tasks among the individuals is very important to ensure the efficient workflow in a team. Before assigning different roles within the team members, the team arranged a meeting and enlisted all the areas required for the successful completion of the project. The duties and tasks are then chosen by each of the team members based on their interest, technical knowledge and experience. The roles of all the team members is mentioned in Figure 3.3. Since all the tasks are interrelated, the team decided to update the progress of the tasks to ensure a good communication flow. Apart from the assigned roles, each team member helped each other throughout the project.

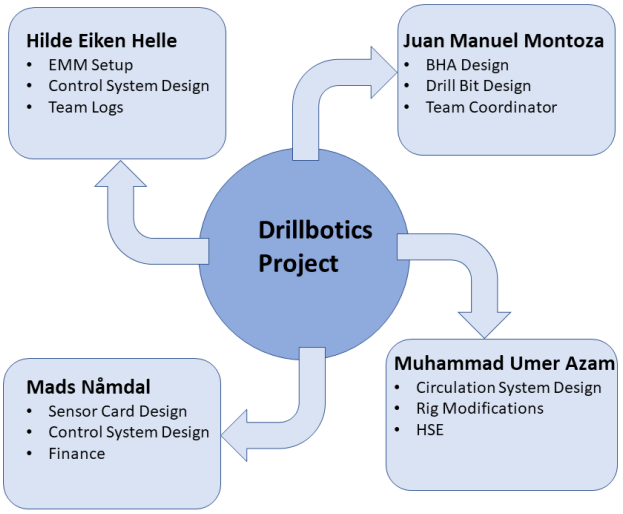

Figure 3.3: Team organization chart

The regular meetings with the supervisors were also arranged throughout the project to keep them updated and get guidance and inspiration. The meetings became more frequent towards the end of the project to solve different challenges. The support team from the mechanical and electrical lab collaborated on a daily basis while discussing the issues encountered in the project.

3.3 Project Management

The Drillbotics project is divided into two phases: Phase I includes the detailed plan of the setup, safety, programming and cost analysis. Whereas Phase II requires ordering of the components needed, the construction of the rig and overall implementation of the design. As soon as the components arrived to the rig site, they were programmed in NI Labview based on their operating limits.

A continuous flow of information among team members and smart planning of tasks, are the key for a successful project. After the formation of the team, a separate office was established near the support team and the workshop to have short communication channels. The purpose of a separate office for the Drillbotics team was to discuss the challenges, their solutions and keep the team updated on the overall progress of the tasks. During Phase I, three meetings a week were planned to analyze the progress with the supervisors. The meetings used to last from 30 minutes to an hour, to discuss any problem that may have occurred since the last meeting and followed by individual work or teamwork sessions. However, in Phase II these meetings were intensified and prolonged due to the continuous challenges that needed to be solved.

The progress was tracked by taking some important actions that included the formulation of notes and logs from each meeting. The online documentation of these notes helped each member get updated quickly. Some of the important routines are described below:

Meetings with Supervisors The meetings with supervisors were held every two weeks during Phase I. The meetings helped getting feedback on the progress and possible solutions to the different problems. During Phase II and towards the end, the team decided to meet the supervisors twice a week to get them updated about the project progress and solve the problems quickly. The notes from the meeting were formulated for later use.

Activity Logs All the activities that were done related to the project were listed and put online. This helped each team member knowing about what was done in the project at a given time.

Inventory List The inventory list was made in Phase I of the project to keep track of the equipment available. This list helped preventing delays if any component was unavailable or needed to be ordered.

Budgeting Whenever anything was ordered, all related information about the component and its cost was listed to keep track of the budget, since the budget was restricted to USD 10,000.

Order follow-up During Phase II, several electrical and mechanical components were ordered. The proper tracking order of these components and enlisting in the inventory list, helped avoiding any unusual delays.

Google Drive A Google drive was set up for the project. All the tasks, problems, solutions, theoretical background, notes from the meeting and other documentation was regularly uploaded to get the team updated.

3.4 Time Management

Having a good time management and good control over all the associated tasks in a project, is of utmost importance. Since the Drillbotics project is highly practical, time management becomes one of the most critical aspects to consider. Also, the project consists of several smaller tasks which are dependent on each other. Therefore, the completion of each of these tasks well on time is essential. A time planner was made available to all the team members to have a clear picture of the critical tasks and their deadlines. A part of such a time planner is shown in Figure 3.4.

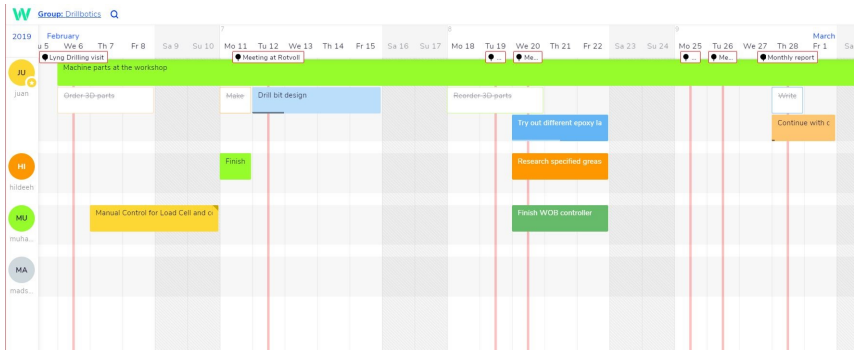

Figure 3.4: Part of Drillbotics team time planner. Milestones are indicated by red lines.

In Phase II, the ordering of the equipment became an important part. The team set up several meetings to discuss different aspects of the competition, components/equipment required for the rig and their ordering. All the necessary components were ordered by keeping the delays in mind. However, the team experienced unusual delays in the delivery of smaller components associated with the main equipment. Whenever an order was placed, it was written down with expected date of arrival to keep better track of it. The

support team in the mechanical workshop had several other projects from different students and was not always available. However, the Drillbotics project was their priority and delays were not very long on this side.

The visits to companies ended up being very time consuming, though helpful. All the planned visits were regularly added in the Time Planner to keep the team informed about the date and time of visit.

The programming of any electrical components depends on their functionality. The delivery time of servo motor and pump motor communication caused unexpected delays in the construction of the script and debugging. A great amount of time was spent setting up the software for the EMM and its wiring. Besides, fixing all magnetic distortions in the sensor card's magnetometer due to the presence of steel, took a fair amount time. However, these delays were accounted for in the Time Planner as the semester passed.

Chapter 4

Safety

For any engineering project, the safety of all the personnel, environment and machinery should always be a priority. There occur thousands of accidents and incidents every year in the industry. Most of them reported to HSE are due to the lifting, moving of equipment and falling objects [26]. A complete system analysis should be performed to identify any dangerous aspect present in the system and possible corrections to them. System safety is a comprehensive examination of the engineering design and control of any potential hazards that could injure people or cause any damage to the equipment [20].

The oil and gas industry is considered one of the most hazardous energy sectors and therefore has comprehensive safety programs. The excessive usage of powerful equipment, high-pressure processes and flammable chemicals can lead to precarious incidents if not handled with proper care. Despite having safety procedures, the fatality rate in the oil and gas industry is seven times higher compared to all other industries in the U.S from 2003-2010 [3]. The events that caused most of the fatalities includes transportation, contact injuries and fires or explosions. The biggest threats to the worker's safety are human error, working culture, negligence, lack of PPE, miscommunication and misuse of equipment. With the dawn of digitization and automation in the oil and gas industry, contact injuries and failure to the human error can be fewer than before.

Students' projects like Drillbotics, in which a lot of manual work is involved, require extra attention. The construction of a rig and the services of its parts were done in the presence of qualified personnel in the workshop. A complete safety course for lab work had to be completed by each of the team members to work in the workshop. This helped to understand any possible hazardous situation that can occur during working hours. The precautionary measures to eliminate those situations were also briefed in the course. The team members were also trained about the usage of PPEs, fire extinguishers and about the emergency exits. Hence, each team member was trained properly about the health, safety and environment before starting working in the lab.

In this chapter, the possible hazards during the construction, repair, service and operation are explained. As this project is a continuation from the previous years and most of the construction work on the rig has been done already, safety measures from the previous year's team have been diminished for this year. The safety measures during the construction of the rig are explained in [32]. However, the hazards involved during the operation and testing are explained here. Whereas the risk assessment is performed in chapter 5.

4.1 Hazards During the Construction of the Rig

During the construction of the rig, the safety hazards can be mechanical or electrical. Since most of the construction work has been done already, the small changes in the rig have been implemented carefully. The disassembling and assembling of different components was done with proper guidance from the workshop personnel. It was made sure that while doing any mechanical job, all related PPE were being used.

NTNU has made proper rules and regulations for working in labs, according to that, all the processes which involve high voltage must be performed by authorized and qualified personnel. The most common and potential hazards while working with the electrical systems are shocks and short circuits, that can lead to the damage of the equipment. Such risks have been removed by keeping all the electrical wires and sources away from water and making sure that rig power is shut down while making any connection. Above all, all the wires must be insulated to prevent short circuits and potential hazards for the personnel.

4.2 Hazards During Operations

It is important for all the team members to get themselves familiarized with the possible hazards during testing and while working on the rig. The Phase II of the competition involves a lot of testing and experimentation before going to the competition. Therefore, all the team members spent time identifying any potential hazards and safety measures to mitigate them. This section describes all probable risks involved during the operation and measures to avoid or eliminate them.

Circulation System In this year's competition, high pressure is involved due to the use of a downhole mud motor which requires high pressure for its operation. The possible danger while working with high pressure can be bursting the drill pipe or their connections. The debris with high pressure can seriously harm the personnel nearby. Before applying high pressures, it was made sure that all the connections were tight enough to withstand the pressure. Also, the pressure applied by the water pump should be less than the burst limit of the drill pipe. For safety purposes, drill pipe burst pressure calculations were done with a proper safety margin. The control system of the pump and the pressure sensor is enabled to monitor the pressure in the system and stop the pump if the internal pressure gets too high. Moreover, a pop-off valve has also been installed at the pump for

safety precautions. This valve will be activated if the pressure in the system reaches 100 bar, which is also the maximum limit of the pump [1]. While testing, it is ensured that the acrylic glass is covering the drilling area. This way, everybody is at safe distance from the rig.

The circulation system also involves a water tank as a water supply for the pump. The possible risks with a water tank can be the overflow of water from the tank and potential short circuits. A solenoid valve was installed on the water tank which automatically stops the water supply into the tank if a particular level has been reached. A level sensor was also installed on the tank that controls the level of water in the tank, hence eliminating the risk of water overflow. Besides, the tank was put on a metallic frame to keep it in balance and at the same level as the pump.

Due to the high flow rates in the circulation system, the bell nipple in the riser was not able to direct all the cuttings and water towards the drain. A possible leakage from the top of the riser was expected. To minimize it, a comparatively larger bell nipple was installed on the new riser system to be able to handle these flow rates.

Hoisting System Among the important drilling parameters, weight on bit control deserves particular attention. WOB is applied on the rock sample through the hoisting motor. This weight travels from drill pipe down to BHA. An excessive WOB can cause buckling of drill pipe with risks of injury from debris. The reduction of this kind of risk involves buckling limit testing with a proper design factor. The maximum value of WOB is set in the control script of the motor, such that all motors will return to the safety sequence if WOB reaches a certain limit. This feature is further explained in Section 10.2.7.

The maximum limit of the drill string position is set up in the script to avoid the drill string drilling beyond the limits. For safety reasons, two stop switches are installed on the roller guide. The top switch prevents the guide frame from moving over the top of the guide frame, whereas the bottom switch stops the rotary motor before hitting the rig floor. Whenever the guide frame touches any of the switches, the motor stops working immediately.

Electrical System The electrical components such as motors and drives can cause serious fire hazards due to improper winding and overheating. In the case of a fire emergency, everybody is familiarized with the emergency exits and muster points. It is always recommended that the working site should be clean and tidy to avoid any incidents.

[1] This is the theoretical pressure limit, the true limit after the pump wore down is actually 35 bar

Safety Measures Since the rig contains several heavy moving parts during its operation, serious injuries might happen if somebody is not standing in the safe zone [2]. To prevent this, it is strictly prohibited to use any loose clothing while working on the workshop and women should tie their hair before getting close to the rig. All PPEs including coverall and safety shoes are always recommended while testing. For safety reasons, all the power must be shut down while making or breaking any connection.

Emergency Stop Button An emergency stop button has been installed on the rig, as well as on the graphical user interface (GUI) to the stop the drilling operation immediately in the case of an emergency. The stop button on the GUI however, has a lag time as the WOB and the rotation ramp up to zero. In order to get a quick response, the emergency stop button outside the electrical cabinet should be used. Whenever the button is pressed, all the operation will be stopped immediately without any delays. The button must be pulled back again before starting any operation again.

[2] Defined as outside the Plexiglass

Chapter 5

Risk Analysis and System Evaluation

5.1 Risk Analysis and Risk Mitigation for the Different Design Options

5.1.1 Risk Mitigating Backup Solution

Due to the design choices of the team and the challenge of directional drilling, the bottom hole assembly ended up being much more complicated than it was in the previous years. Failure of the bottom hole assembly was therefore identified as one of the main risks to the project. As a risk mitigating measure, an investigation was carried out on an alternative design that would simplify the BHA and move the power section to the surface. This design would also need to be steered using a bent sub, as a rotary steerable system (RSS) would be more complicated than the original design.

In this alternative design, two topside motors are required: one to drive the drill string and one to drive a flexible shaft that passes through the drill string and provides torque and rotation to the bit. The drill pipe must be rotated without interfering with the internal shaft. A similar set up to the current one can then be used, with the rotation being transmitted from the top drive to a shaft through the hydraulic swivel.

The flexible inner shaft diameter must be less than the pipe ID, which is 7 mm. An initial search for flexible shafts shows that shafts below this size can commonly take up to 2.4 Nm of torque. The rate of rotation will be limited by drilling efficiency or vibrations to a value well above the limits of a downhole power section. A higher drilling rate can therefore be expected when rotation is provided by a stronger topside motor. Figure 5.1 shows a sketch that illustrates how this solution works. A hollow bore servo motor would be used to steer

the BHA, together with the sensor wires. To be able to achieve this, a special type of flange needs to be designed and its connection to the drill pipe as well. A shorter piece of drill pipe could be used to connect this flange to the hydraulic swivel. Besides, a protective sleeve needs to be added between the flange and the electric swivel to protect the sensor wires from the servo motor.

It is worth mentioning that this design is not well suited to minimize vibrations while drilling. This is because no stabilizer can be used on the drill pipe. Doing this would cause immediate damage to the sensor wires.

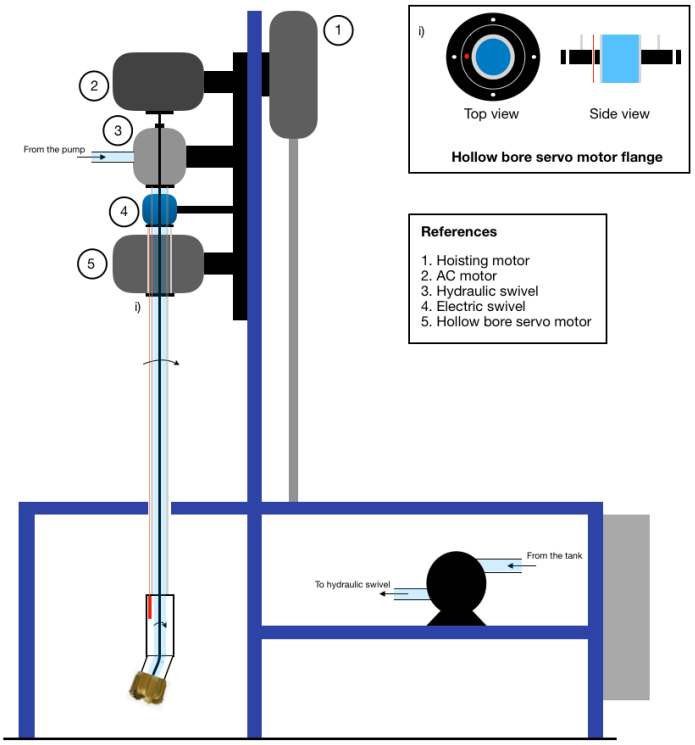

Figure 5.1: Alternative solution using an internal steel wire to provide torque and RPM to the drill bit

There are a more challenges with this design. The top connection in the hydraulic swivel would have to be redesigned to prevent any leakage while packing against the steel wire. Another issue is the location of the sensor wires. These wires need to go on the outside of the drill pipe, as the inside is taken up by the flexible shaft. This poses a problem when drilling the vertical section, where the drill pipe will need to be rotated. The wires will therefore have to be rotated which also represents a risk.

A wireless sensor communication would make this alternative a lot more viable, since no electric swivel would need to be used. However, this method will also require a lot of

design work and rebuilding of the rig. It was therefore concluded that while this method may be an alternative for future teams needing a greater drilling speed, it is too complex to have as a back-up solution for this year's competition.

5.2 Risk Analysis of Rig Components

In order to more closely understand which components carried the greatest risk of delaying or hindering the project, an analysis was carried out of all important parts in the system. The probability of failure and the consequences in the case of failure for each part is described, and summed up in Figure 5.2 (see also Appendix chapter B.

Probability	Rig parts risk analysis Severity 1 (low)	2	3	4	5 (Severe)
1 (low)		Tank			
2	Water tube Riser seal	Water supply Drill floor stabilizer	Bit sub Bit	Bearing sub Electric swivel Pump Sensor sub Bent housing DP connections	Hoisting motor
3	Bell nipple	Tank valve	Downhole motor shafts Hydraulic swivel	PC Sensor	Top drive
4	Drill pipe	Tank pressure sensor Pump pressure sensor Riser	EMM housing	EMM PDM	Wire connections
5 (certain)					

Figure 5.2: Figure showing a risk matrix where the individual components of the system have been analyzed to determine the risk they pose to the project as a whole

5.2.1 PDM

The primary option for a downhole motor was a PDM. Without a downhole motor, the rig is unable to drill a deviated well. Designing and manufacturing a miniature PDM was however considered a risky option, due to the team's lack of experience with design, time limitations and budget constraints. Several risk mitigating measures were therefore put in place. First among these was the design of a backup solution, an EMM as a downhole motor. Additionally, as it became clear that extensive testing would be required to develop the design, a modular design was created to allow for cheaper, more efficient testing.

5.2.2 EMM and EMM Housing

The use of an EMM was prepared as a backup solution to the risky PDM alternative, but still carried several risks of its own. Due to the size limitations of the motor, the RPM and torque output were not much higher than the expected minimum required to drill the rock. Uncertainties in the drilling tests used to determine these parameters and friction in the BHA could therefore lead to buying a weaker EMM, than the one actually required. The risk of motor failure due to inadequate protection from the drilling fluid was also an issue. Mitigation of these issues was done by drilling with a sealed BHA as soon as the components were ready, to verify the motor could provide sufficient torque and RPM and be run with water. Once the performance was verified, two backup motors were ordered.

5.2.3 Sensor Card

The sensor card is required to function in order to use position control while drilling and the worst-case consequence of the sensor card not working could be having to drill without downhole sensors, which is an automatic failure in the competition. The sensor card is sensitive to water damage and the connection between the sensor card and sensor wires can easily be damaged by careless handling. Several sensor cards were made and different methods of water sealing and protecting the wires were tested. Thus, the risk of each sensor card failing was reduced, as well as the risk of being left without a functioning card altogether.

5.2.4 Wire Connections and Electric Swivel

Poor wire connections can lead to the EMM and the sensor card losing power and communication with topside. The drilling must then be stopped and the connections remade. Both the connection between the hydraulic and electric swivel and the connections inside the drill pipe are vulnerable points. Poor wire connections were an issue in 2018 and were considered likely to continue to be an issue in 2019. Limiting the top drive rotation and water flow, as well as testing different kinds of connections, helped reduce the risk of poor connections, but this remains one of the major risks to uninterrupted drilling. Remaking wire connections also turned out to be a major limitation on testing, due to the time required to fix broken connections. As the upper part of the hydraulic swivel is necessary for containing water flow inside the swivel, no testing of the PDM could take place when this part was being repaired. Therefore, the consequences of poor wires and connections went beyond hindering the use of the EMM and sensor, to hindering nearly all possible testing.

5.2.5 Downhole Motor Shafts

The metal shafts connecting the shaft of the downhole motor to the U-joint and the U-joint to the bit sub, are some of the weak points in the BHA. They are difficult to manufacture, due to being thin and hollow. They can be deformed or detached by incorrectly assembling the BHA and small errors in manufacturing can lead to the parts breaking under normal use. Extra u-joints have therefore been purchased, so a spare can always be at hand. The connection with the EMM shaft has also been strengthened.

5.2.6 Bent Housing

The bent housing is less likely to fail than the internal shafts, but it takes a longer time to produce in the workshop. Due to this manufacturing time, no extra bent housings have been made. Directional drilling is impossible without a bent housing and the part is therefore critical to the system. The manufacture of the bend is also an issue.

Due to project delays and early shipping time, only two wells have been drilled in deviated mode. The deviation of these wells does not conform with the expected deviation from the design calculations. Ideally, more tests should have been performed to find the expected deviation with the current bend angle in the competition well. Without these tests, there is a possibility that the angle is not great enough to achieve the desired deviation. This will reduce the score in the competition but still, allow for a well to be drilled.

5.2.7 Hydraulic Swivel

The hydraulic swivel was made in the university workshop for the first year's competition and can be repaired at the workshop if needed. The consequences of small dysfunctions in the swivel are limited to leakage of water and extra friction when rotating the shaft. The swivel is therefore not as critical as some of the other components and has not been prioritized to the same degree as the BHA. However, at least a week must be expected for making a new internal shaft and the packers inside the swivel can have a long delivery time. In NTNU's first year in the Drillbotics competition, the first drilling tests were performed the night before the competition, due to waiting for delivery of these packers. Extra parts were therefore ordered at the beginning of the semester and care was taken while disassembling the swivel. Some damages have still occurred, as evidenced by a small leakage from the swivel.

5.2.8 Drill Pipe Connections

The drill pipe connections are comprised of the threaded lower end of the hydraulic swivel shaft, the threaded upper end of the BHA, two mini chucks threaded connectors to the BHA and two slotted spring-type straight pins. These pins sit inside the mini chucks and the connectors on the BHA and swivel so that they are tightened against the drill pipe when the mini chuck connections are torqued up. Of these, only straight pins are spare. The risk of the connections being broken is considered low, due to the lower torque and RPM expected in the 2019 competition compared to 2018, where the connections worked well. Since there are no spares for most of the parts, care should be taken to not misplace these during transportation. It is also important to use the correct make up torque, to avoid disconnecting accidentally during drilling.

5.2.9 Pump

The pump was not initially identified as one of the major risks. According to the specifications, it should be able to provide pressure higher than the expected pressure losses in the system and it had worked well the two previous years. However, the pump suffered a reduction in performance during the last weeks of testing and eventually had to be changed out for a newer one, two days before shipping. Therefore, the newer pump will be nearly untested at the time of the competition, making it one of the major uncertainties at the competition.

5.2.10 Water Supply

Insufficient water supply can lead to poor hole cleaning and reduced PDM performance. A tank is therefore implemented as part of the circulation system, allowing water to be filled up before and while drilling. The tank is equipped with a solenoid valve and a pressure sensor which allows the tank to be monitored and filled by the control system. With the EMM solution, water supply is not predicted to be an issue, as the low expected drilling rates will not require high flow rates for cutting transportation.

5.2.11 Tank

The tank is used as a reservoir for drilling fluid in the case of a too low water supply. The possibility of the tank leaking, or otherwise becoming unusable is considered small and the consequence of this would be to have to use the water supply from the tap directly into the pump instead, which is only expected to have a noticeable effect on drilling if the PDM is used. The risk associated with the tank is therefore considered low.

5.2.12 Pump Pressure Sensor

The pump pressure sensor is used in the control system to prevent overly high pressures and is one of several safety measures in the system. It is also used for measuring the pressure drop during PDM testing. Therefore, it is an important component of the system, though limited tests can be carried out without it.

The part is easily replaceable, though expensive, and will therefore not lead to major delays if lost.

5.2.13 Tank Pressure Sensor

The tank pressure sensor is used to determine the water level in the tank and must be input to the control system in order to use the tank solution. If the tank pressure sensor is not working, one could risk either overfilling the tank or running the pump without sufficient water available and damaging the pump. If the tank pressure sensor should break, the pump should either be supplied with water directly from the outlet at the wall or the tank level should be monitored manually.

5.2.14 Tank Valve

A solenoid valve that is operated through NI DAQ allows for remote control of the tank filling. It is a simple component in terms of both design and control. It is therefore not considered likely to fail. The consequence of the valve failing is that the tank filling must either be done manually, or the water to the pump must be supplied directly to the pump from the outlet at the wall.

5.2.15 PC

A computer with NI LabVIEW 2018 and Lenze engineer is required to run the control script. The conditions in the workshop where the rig is situated are dusty and often wet, which is not ideal for a computer. Therefore, there is a risk of the computer being damaged. To minimize the impact of this occurrence, all important files should be saved often and backed up. The morning of the shipping of the rig, the control computer failed and could therefore not be shipped. The hard drive from the original computer was put into several alternative computers before one that was functioning well was found. This computer must be shipped to the competition site in Germany in the luggage of the team, which carries the risk of the luggage being lost or damaged. It was therefore decided to bring a laptop with all the required files and programs as a backup solution for the competition.

5.2.16 Sensor Sub and Bearing Sub

The sensor sub and bearing sub function as an upper and lower stabilizer in the drill string. They have thick walls and are considered unlikely to be damaged during normal operations. The sensor sub is more at risk than the bearing sub, due to the thinner wall thickness between the sensor hole and the center hole in the part. If damaged, both parts can be fixed or replaced in the NTNU workshop. The bearings inside the bearing sub may need to be replaced during the life of the bearing sub. It is possible to drill with damaged bearings, though it runs the risk of causing damage to other BHA parts, such as shaft between the bit sub and U-joint. These parts are required for drilling and losing or destroying them will delay testing. Spare parts will be made for the competition.

5.2.17 Drill Floor Stabilizer

The drill floor stabilizer is a roller bearing which is fixed relative to the drill floor by a metal housing, and through which the drill pipe passes. Without this stabilizer, the stability of the drill string is drastically reduced, particularly when drilling the pilot hole. Its function as a stabilizer is however still good even with minor wear and damages on the bearing. Both the probability and consequence of the failure of this part is therefore considered low. Should the bearing be damaged beyond usefulness, the bearing used as riser stabilizer in 2018 can be used as a spare.

5.2.18 Bit Sub

The bit sub is among the quickest parts to manufacture in the workshop. Some scratches can occur on the surface between the bit sub and the thrust bearing, which will influence the friction between the bit sub and the bearing housing. Apart from this, the bit sub is not likely to suffer any damages. No replacements are therefore made for the competition, though a separate bit sub has been made for the three types of bit. It will, therefore, be an option to change both bit and bit sub if the bit sub should fail during drilling.

5.2.19 Bit

Due to the softness of the rock and the planned low drilling rate, the bits are not expected to be much damaged. Some wear can be expected over time but should not be enough to drastically affect the competition results. Several bits are in store, though most of different designs. It is, therefore, possible to change between bit designs if one bit should be damaged while drilling.

5.2.20 Drill pipe

Though the drill pipe is a weak point when drilling, it is less so this year than in 2018, due to the weakness of the downhole motor. Several drill pipes have been ordered and they are easy to change. The drill pipes are therefore considered a low-risk item.

5.2.21 Riser

The function of the riser is mainly to contain the water flow from the bit and direct it into the bell nipple (diverter), where a hose is connected. If the riser is removed, the water spreads more out when exiting the borehole and loses velocity. This leads to cuttings being deposited on the rock surface. Some drill pipe stability is gained from the seal at the top of the riser, as it touches the drill pipe if the pipe moves more than 2 mm from the center, but no roller bearing is in place this year. The consequence of drilling riserless is therefore mostly poorer hole cleaning and slightly less support for the drill pipe in the case of vibrations in the drill string.

5.2.22 Riser Seal

The riser seal is a 3D printed elastomer cap with a hole for the drill pipe in the center. The purpose of this seal is to prevent water flowing out at the top of the riser. The flow rates are not very high and leakage is not considered a serious problem, so there is a clearance of 2 mm between the drill pipe and the seal. If the drill pipe should deviate or buckle into the seal, some stability will be provided, but this is not counted on in the safety limits. The seal improves HSE by limiting water leakage and therefore the risk of someone slipping in the water, or electrical equipment being exposed to water. Though this is not crucial for drilling. The material of the seal is strong and the seal is not expected to fail completely, but it may be deformed by the drill pipe in the case of buckling or vibrations.

5.2.23 Diverter

The diverter allows the drilling fluid to exit the riser through a tube through which the water can flow to the drain. Drilling without the diverter will lead to the water being impossible to direct into a tube, which can lead to water ending up on the floor surrounding the rig. The rig is normally situated next to a drain, so some leakage is considered acceptable. While testing, a thick cable has been taped to the floor around the rig, with an opening towards the drain, to further prevent water from reaching unwanted areas.

5.2.24 Top Drive

The top drive is required both for drilling the vertical section of the well and for steering in the deviated section. As the previous top drive did not have position control, a new Schneider servo motor was purchased in Phase II to function as a top drive. As this was a new kind of motor to set up, the likelihood of problems arising with this motor was considered larger than the likelihood of problems occurring with the tried and tested motors. This motor turned out to be one of the major limiting factors. This was due to some setup files initially missing from the motor and the only university employee available with the ability to help set up the motor having a tight schedule.

Chapter 6

Limits and Constraints

The Drillbotics project is restricted by various limits and constraints that affect the mechanical design as well as the control design of the rig. Some of the limitations are marked by DSATS in the competition guidelines (see Appendix A), whereas some are from different components used in the rig. This chapter outlines all the mechanical limits and logistical constraints in the Drillbotics project.

6.1 Mechanical Limitations

Disclaimer: The contents of the mechanical calculations are, with minor modifications, taken from the project report[35].

6.1.1 Buckling

Weight on bit is an important drilling parameter for optimum and effective drilling. In a full-scale drilling rig, weight on bit is applied through the heavyweight drill pipes and drill collars used in the BHA. In the miniature scale, the BHA is not heavy enough to meet the WOB requirements for drilling. WOB is applied by the hoisting motor turning a ball screw, which is attached to the hoisting frame. This WOB is transferred from the drill pipe down to the BHA. Excessive WOB can increase the risk of the drill pipe buckling due to compression. By considering the drill pipe as a slender column, the well known Euler's equation (Equation 6.1) is used to estimate the buckling limits of a drill pipe under static conditions [8]. A slender column has a high slenderness ratio, which can be found by using Equation 6.2.

$$F_{cr} = \frac{\pi^2 EI}{(KL)^2} \tag{6.1}$$

$$R_s = \frac{L}{r_g} \tag{6.2}$$

where F_{cr} (N) is the critical force before buckling, E (Pa) is the elastic modulus of the material, I (m^4) is the second moment of area, K is the effective length factor, L (m) is the unsupported pipe length, R_s is the slenderness ratio and r_g is the radius of gyration. The radius of gyration can be found by using Equation 6.3.

$$r_g = \sqrt{\frac{I}{A}} \tag{6.3}$$

Euler's formula assumes a perfectly straight pipe and that all the load is applied through the pipe centroid. The second moment of area (I) in Equation 6.1 is also known as area moment of inertia, which is given by Equation 6.4 [1].

$$I = \frac{\pi}{64}(OD^4 - ID^4) \tag{6.4}$$

where OD and ID are outer and inner diameters of pipes in m. K in the Euler's equation accounts for different end conditions of the column. The Figure 6.1 shows different end conditions for pipe whereas Table 6.1 shows the theoretical and recommended values for the effective length K [8]. It should be noted that recommended values are more conservative than the theoretical values.

End Condition:	Pinned-Pinned	Fixed-Fixed	Fixed-Pinned	Fixed-Free
Illustration:	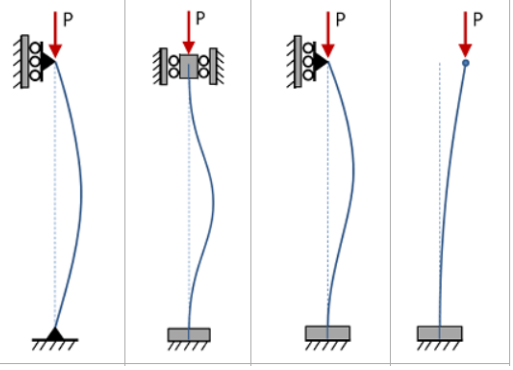			

Figure 6.1: Pipe end conditions [8]

The slenderness ratio defined in Equation 6.2 shows the susceptibility of the pipe towards buckling. The pipes having large slenderness ratio are more sensitive to buckling and are

Table 6.1: Theoretical and recommended effective length factor, K, for different end conditions of the column

End condition	Pinned-pinned	Fixed-fixed	Fixed-pinned	fixed-free
Theoretical K	1	0.5	$\frac{1}{\sqrt{2}}$	2
Recommended K	1	0.9	0.9	2.1

classified as long columns. Euler's formula is used to analyze such columns. Lower slenderness ratio columns will fail at lower loads than calculated by Euler's formula. These columns are classified as intermediate columns and are analyzed with Johnson formula[8], which is given in Equation 6.6, and is based on empirical data for intermediate columns.

The intermediate columns are identified by transition slenderness ratio defined in Equation 6.5. This slenderness ratio is the ratio at which Euler's formula and Johnson's formula predict the same buckling stress.

$$R_{trans} = \sqrt{\frac{2\pi^2 E}{K^2 S_y}} \tag{6.5}$$

where S_y is the material's yield strength. Columns exceeding this slenderness ratio are considered long columns, while columns under this ratio are considered intermediate columns.

$$F_{cric} = S_y - \left(\frac{S_y}{2\pi}\frac{KL}{r}\right)^2 \left(\frac{1}{E}\right) \tag{6.6}$$

The buckling limit of the drill pipe was calculated by last year's team using both the yield strength and the fatigue strength as material compressive strength. As the fatigue strength is not the strength of a weakened pipe that has been exposed to fatigue stress, but rather a measure of the material's resistance to fatigue from cyclic stress, the buckling limits based on the fatigue strength are lower than the actual buckling limits. This only affected the buckling limits for shorter columns, as Euler's formula is not dependent on the material's yield strength.

Based on the theory above, the maximum allowable WOB against the unsupported length of 0.375" OD and 0.049" thick drill pipe is calculated at different values of effective length factors, K. The results are shown in Figure 6.2, the dimensions and the material for the drill pipe are the same as mentioned in the competition guidelines.

Since the effective length factor depends upon the end condition of the pipe, the drill pipe can be divided into three sections, if a roller bearing is used as stabilizer in the riser. One section is above the kelly bushing, the second is below the kelly bushing and above the riser and the third is inside the riser above the BHA. The longest section among three will determine the buckling limit of the drill pipe. Thus, maximum allowable WOB depends upon rock height, riser height, BHA and bit length, total drill pipe length and total drill depth.

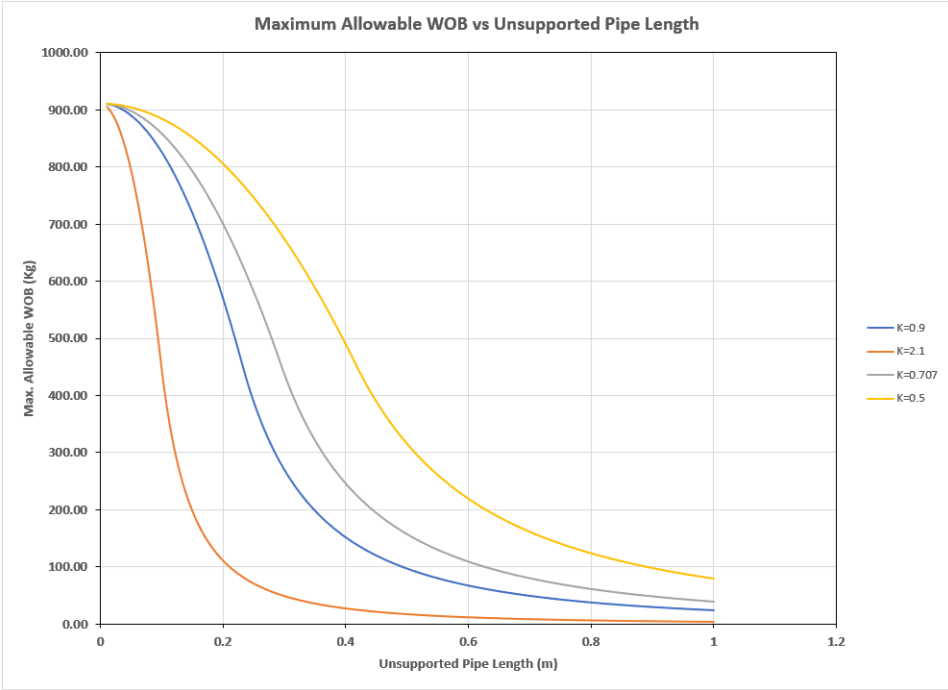

Figure 6.2: Maximum Allowable WOB against unsupported length of drill pipe for different effective length factors

The upper two sections of the drill pipe can be considered as fixed-fixed end conditions, whereas the lower end bears most resemblance with the fixed-pinned end condition. Table 6.2 shows maximum allowable weight on bit for different unsupported pipe lengths. It can be seen that the weight on bit requirements for the fixed free case are quite low i.e. 5.3 kg and 11.6 kg for the total length of drill pipe and the total well length respectively. The lower WOB values show the need for stabilizing the drill pipe above the rock surface. The presence of stabilizers increases the allowed WOB for the aforementioned sensitive cases. Also, while passing through the well, the drill pipe will be supported by the rock walls after some buckling and the buckling limit is expected to be over-estimated by these equations.

The maximum allowable weight on bit values mentioned in Table 6.2 are without the BHA. The BHA will take a part of length in the hole, and reduce the unsupported pipe length and increase the WOB limits. The Table 6.3 shows the allowed WOB with the BHA. It can be seen that the allowable WOB has increased for fixed free end condition as well. In reality, due to the presence of stabilizers and the curved section after 4” vertical section, there will be support from the borehole and the buckling limits for the drill pipe are expected to be more than mentioned here.

The maximum allowable WOB changes with the drilled depth of the hole. The WOB as a

Table 6.2: Maximum allowable WOB for different unsupported pipe length and effective length factors

	K	0.5	0.71	0.9	2.1
	L (m)	**max. allowed WOB (kg)**			
Total pipe length	0.91	93.0	46.5	28.7	5.3
Pipe length in well	0.61	204.7	102.3	63.2	11.6
Pipe length in the Curved section	0.51	291.0	145.5	89.8	16,5
Pipe length above finished well	0.3	657.5	409.4	252.7	46.4

Table 6.3: Max. allowable WOB for unsupported pipe length including BHA and different effective length factors

	K	0.5	0.71	0.9	2.1
	L(m)	**max. allowed WOB (kg)**			
Total pipe length in the well with BHA	0.406	476.31	238.66	147.32	27.06
Pipe length in curved section with BHA	0.306	664.03	420.13	259.34	47.63

function of drilled depth has been calculated and the results are shown in Figure 6.3. All the data used for the calculations are shown in Table 6.4.

Table 6.4: Data used for WOB limit Vs drilled depth plot, Aluminum 6061 T6 pipe is used

Rock height	0.65 m	BHA length	0.21 m
Riser height	0.25 m	DP length + BHA	1.12 m
Rig floor height	0.95 m	Tensile yield strength of pipe	276 MPa
Vertical sec. length	0.10 m	Fatigue strength	96.5 MPa
Curve horizontal displacement	0.08 m	Drill pipe OD	0.375 in
Curve vertical displacement	0.51 m	Drill pipe ID	0.277 in
Radius of curvature	1.65 m	Drill pipe thickness	0.049 in
Angle	0.31 rad	Length	36 in
Curve length	0.52 m	Area	0.0502 in
Total well length	0.62 m	Radius of gyration	0.1165 in

In the Figure 6.3, the drill pipe is divided into two sections, the upper and lower sections are above and below the rotary table, respectively. It can be seen that, as the drilled depth increases the pipe length below the riser increases which in return causes lower value of allowable WOB. The actual maximum allowable WOB is the minimum value for the two cases.

Since the space between the riser and the rig floor is very low, only 5 cm, the need of the second stabilizer inside the riser is diminished. If a stabilizer is used both in the top of the riser and at the rig floor while drilling the vertical section, the chances of the pipe suffering fatigue is increased, as aligning the riser perfectly with the rig floor can be challenging. It was therefore decided to remove the riser stabilizer. However, the flow towards the top of

riser will be restricted through a plastic cap placed inside the riser.

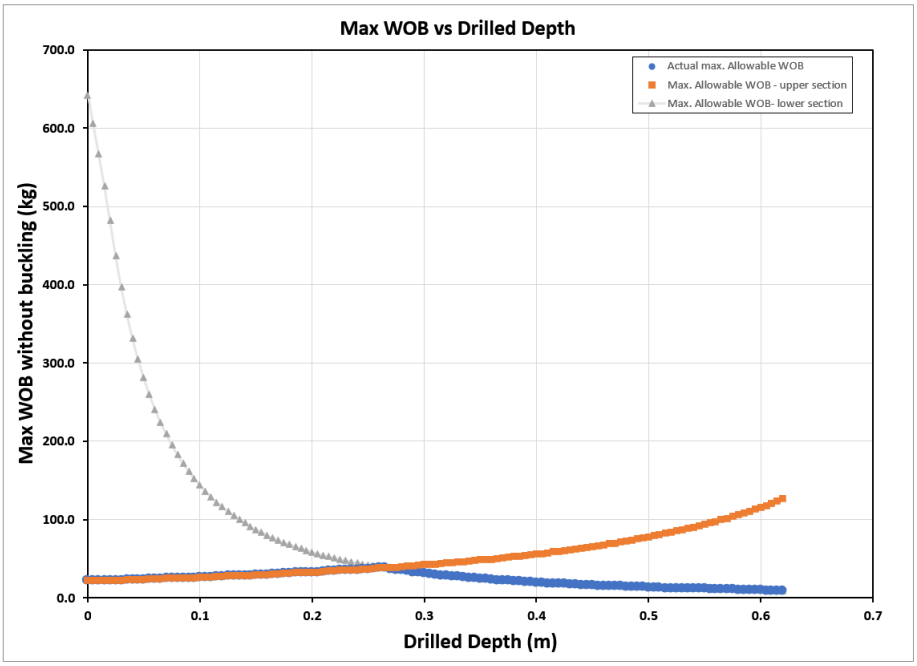

Figure 6.3: Maximum allowable WOB before buckling as a function of drilled depth

Setting up a changing WOB limit in the control system based on buckling limits was considered, but testing has shown that the EMM is likely to stall long before the WOB reaches the buckling limit. The buckling limits are therefore only used when drilling without the EMM in the vertical section. No further testing on buckling limits in the deviated well has been carried out, due to both the lack of deviated wells in which to do testing and the observation that the buckling limits are unlikely to be a limitation with the current downhole motor.

6.1.2 Burst

When the internal pressure of the pipe exceeds its internal yield strength, the pipe is no longer able to withstand the pressure and burst under that loading. The most common equation used to find the burst pressure for the tubular in the industry is **Barlow's equation**. It calculates the internal pressure at which the tangential stress at the inner wall of the pipe reaches the yield strength of the material [25]. To account for the uncertainties in the pipe thickness, a reduction factor of 0.875 is used in the Barlow equation for API burst ratings [21]. The Barlow equation is given by:

$$P_{burst} = 0.875 \left[\frac{2Y_p t}{OD} \right] \tag{6.7}$$

where P_{burst} is the internal pressure, Y_p is the yield strength of the material, t is the wall thickness and OD is the outer diameter of the pipe.

The maximum limit for flow rate in the drilling system depends upon the pressure loss across the bit nozzles. The burst pressure of the pipe is reached when the pressure inside gets too high, due to some sort of restriction in the drill string. By using specifications for the used drill pipe i.e. 0.049" thickness of the pipe, 276 MPa yield strength for aluminum 6061 T6, 0.375" OD and safety factor of 3, the burst limit is calculated to be **210.4 bar** by using Equation 6.7.

During the testing of different design for the PDM as presented in section 7.3.1, the team experienced a lot of pressure loss in the power section of the PDM, especially for the tight rotor-stator configurations. The maximum pressure experienced during the PDM testing was 35 bars which is far lower than the burst limit for the drill pipe. For safety purposes, the pump pressure limit in the control system is set up and this turns off the pump motor if the pressure reaches the set limit. Moreover, a pop-off valve at the pump is activated when the pressure reaches to 100 bar.

6.1.3 Twist off

Twist off is the limiting factor to the torque applied on the drill string. When the shear stress acting on the drill string gets higher than the material shear strength, a twist off occurs. The maximum theoretical torque that can be applied to the drill string is given by Equation 6.8 [28].

$$T_{DP,max} = \tau_{max} \frac{\pi}{16} \left(OD^2 - ID^2 \right) (OD + ID) \tag{6.8}$$

where τ_{max} is the maximum shear strength of the material.

Static Twist off Static twist off in the drill pipe can occur while the drill pipe is not moving. The maximum static torque for 6061-T6 Aluminum drill pipe before it fails is **27.8 Nm**. The shear strength of the drill pipe used is 207 MPa, OD is 3/8" and the wall thickness is 0.049". Nevertheless, during the drilling process drill pipe is continuously under the induced stresses that can affect the maximum torque limit for the drill pipe.

Dynamic Twist off During drilling, the drill string can experience excessive torque. These high torques can be due to a hard formation or could be a stuck pipe case. The maximum torque that a pipe can handle before it fails can be governed by the von-Mises criterion for failure, given in Equation 6.9

$$\sigma_{ys}^2 = \frac{1}{2}[(\sigma_{11} - \sigma_{22})^2 + (\sigma_{22} - \sigma_{33})^2 + (\sigma_{33} - \sigma_{11})^2 + 6(\sigma_{12}^2 + \sigma_{23}^2 + \sigma_{31}^2)] \quad (6.9)$$

where σ_{11}, σ_{22}, σ_{33} are the three normal stress components whereas σ_{12}, σ_{23}, σ_{31} are the shear stresses acting on a drill pipe and σ_{23}, σ_{31} are assumed to be zero. These stress components acting on the drill pipe are due to WOB, internal pressure due to the circulation system and torque applied on drill string by the top drive. The stress components acting on the drill pipe are shown in Figure 6.4. The stresses due to the internal pressure of the pipe are provided by Equation 6.10 through Equation 6.12. [28][29].

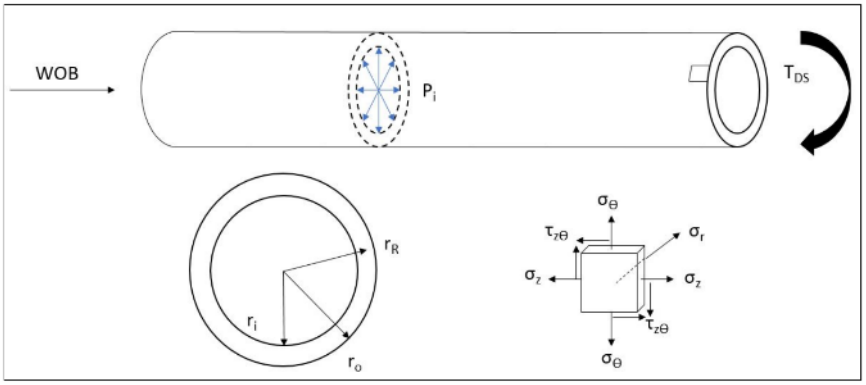

Figure 6.4: Stresses on drill pipe due to internal pressure, WOB and torque [29]

$$\sigma_r = \frac{\left(\frac{r_i}{r_o}\right)^2 - \left(\frac{r_i}{R}\right)}{1 - \left(\frac{r_i}{r_o}\right)^2} p \quad (6.10)$$

$$\sigma_\theta = \frac{\left(\frac{r_i}{r_o}\right)^2 + \left(\frac{r_i}{R}\right)^2}{1 - \left(\frac{r_i}{r_o}\right)^2} p \quad (6.11)$$

$$\sigma_z^p = \frac{\left(\frac{r_i}{r_o}\right)^2}{1 - \left(\frac{r_i}{r_o}\right)^2} p \quad (6.12)$$

In the equation above, σ_z^p is the axial stress in the drill pipe that is due to the drilling fluid flowing continuously during the drilling. The maximum shear stress of the pipe that includes both the effect of induced stresses and von-Mises failure criterion is given by Equation 6.13.

$$\tau_{max} = \sqrt{\frac{2\sigma_{ys}^2 - [(\sigma_z - \sigma_\theta)^2 + (\sigma_\theta - \sigma_r)^2 + (\sigma_r - \sigma_z)^2]}{6}} \tag{6.13}$$

The Equation 6.10 through Equation 6.12 are used to find the stresses inside the drill pipe due to the internal pressure. The maximum shear stress of the pipe before the twist off is determined by Equation 6.13. The total axial stress acting on the pipe is the sum of internal pressure stress and the stress due to the WOB and it is assumed that the hoop and radial stresses are due to the internal pressure in the pipe. Figure 6.5 shows the twist-off torque as a function of WOB for different bending stress cases. The bending stress is an axial stress and has an effect on the maximum shear stress for the pipe, so it is added with the other axial stresses in the calculations. It can be seen in Figure 6.5 that the effect of internal pressure on the twist-off torque is negligible, whereas the WOB and the trajectories have a remarkable effect on the torque handling limits for the drill pipe. The maximum and minimum calculated torque limits for the drill pipe are at different WOB and internal pressure are shown in Table 6.5.

Table 6.5: Twist-off torque for bending stresses with no horizontal displacement, 2 3/8" displacement and 4" displacement over 20" vertical depth. All stresses calculated for center of pipe wall.

	No Bending Stress	**2 3/8" Hor. Displacement**	**4" Hor. Displacement**
Torque limit at 1 bar and 1 kg (Nm)	21.4	18.8	13.3
Torque limit at 1 bar and 1 kg (Nm)	21.2	17.9	11.2
Mean torque limit	21.3	18.4	12.3

As for the directional drilling in this year's competition, most of the hole length will be drilled in the sliding mode with EMM or PDM as a power section in the BHA. During testing, the initial 4" vertical hole was drilled with a top drive servo motor, and the maximum torque that was experienced was **3.34 Nm** which is well inside the safe limits of maximum allowable torques before twist-off. This was with a mechanically fixed bit. When drilling with a rotating EMM or PDM, the TD torque limits would likely be even lower. Twist off is therefore not anticipated to be a problem in this year's competition.

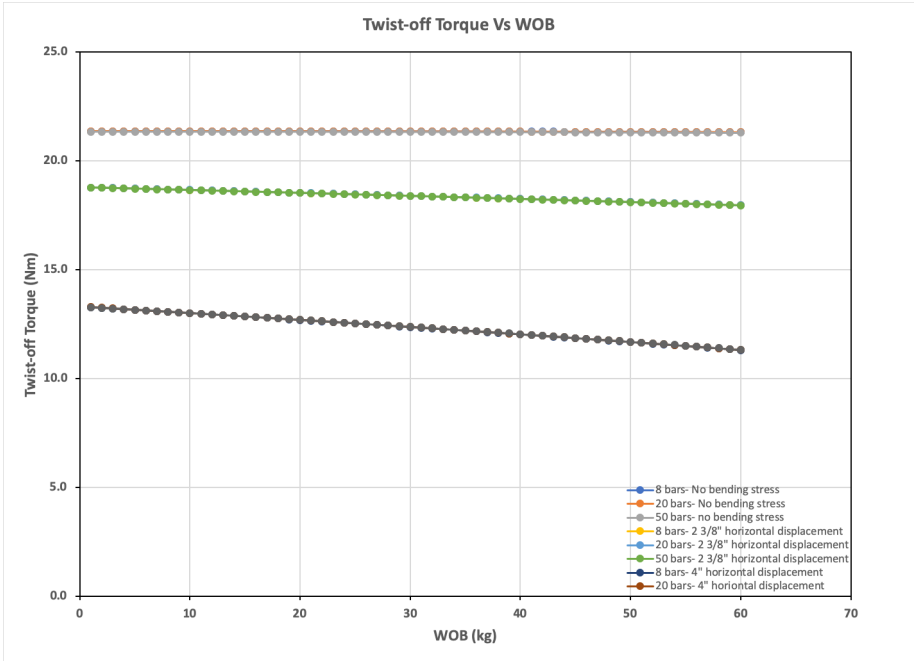

Figure 6.5: Twist off torque as a function of WOB for different internal pressures and trajectories

6.1.4 Bending

The bending stress is the form of normal stress that is caused by the bending moment. When a pipe is bent by the action of force, the stress that is induced in the pipe is bending stress. The bending stress is calculated by the flexure formula mentioned in Equation 6.14 [16].

$$\sigma_b = \frac{My}{I} \tag{6.14}$$

where M is the bending moment along the length of the pipe where the stress is calculated, ”y” is the distance from the point of interest to the neutral axis and I is the moment of inertia (or second moment of area) along the horizontal axis. The assumption in the equation is that the cross section of the pipe remains unchanged, whereas in reality, while bending the pipe the wall gets thinner at the outer end of the curve where it is stretched and gets thicker where it is compressed. The internal bending moment of the pipe is given in Equation 6.15.

$$M = \frac{EI}{RC} \tag{6.15}$$

where E is modulus of elasticity and RC is the radius of curvature. The moment of inertia for the pipe is given by Equation 6.16.

$$I = \frac{\pi}{4}\left(\frac{OD}{2}^4 - \frac{ID}{2}^4\right) \tag{6.16}$$

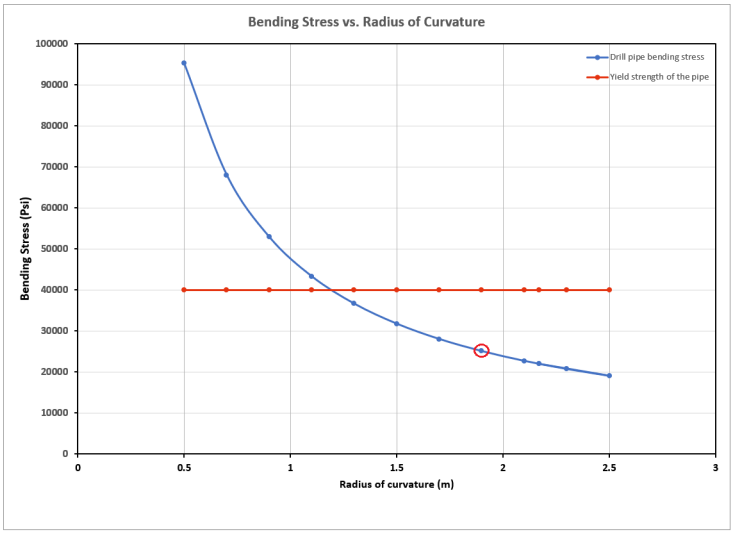

Figure 6.6: Bending stress as a function of radius of curvature

The bending stress of the drill pipe is highly dependent on the radius of curvature. Bending stress as a function of the radius of curvature is shown in Figure 6.6. If the drilled hole follows the minimum required radius of curvature (1.65 m) for exiting the rock bottom 2 3/8" from the center line towards the horizontal plane, the bending stress the pipe experiences will be **25000 psi** as marked with a red circle in Figure 6.6. This bending stress is below the yield strength (40000 psi) of the pipe, so the pipe will remain in the elastic zone. For the radius of curvature less than 1.189 m, the bending stress on the drill pipe gets larger than the yield strength of the pipe and pipe will enter into the plastic zone.

6.1.5 WOB Limitations for EMM

The EMM is used as a downhole motor in the BHA. It can provide a maximum torque of 0.84 Nm and speed of 87 rpm with the gearbox installed. A detailed description of its performance is included in Section 9.1.8.

During testing, the EMM was used frequently in the sliding mode to push its specified working limits. Different rock samples and bits were used to check the performance of the EMM. It was observed that the stalling torque of the motor is highly dependent on

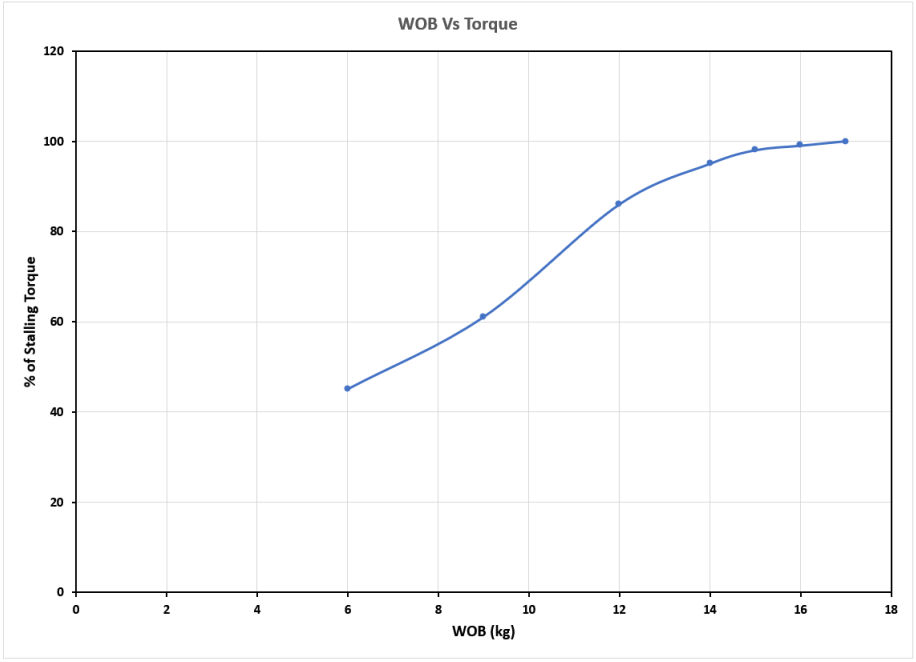

Figure 6.7: EMM torque as a function of WOB

applied WOB, rock type and the drill bit performance. During testing, the EMM was run at different WOBs and the result of one of the tests is shown in Figure 6.7.

These results are from the rock sample provided in the last year's competition and the bit provided by DSATS. It can be seen that the bit stalls at **17 kg** WOB when running the motor at maximum rpm. Since the EMM is not very strong in terms of nominal torque, the WOB during sliding mode of drilling could be a major limitation during the competition.

6.1.6 Pump Pressure Limits for PDM

The PDM is planned to be used in the bottom hole assembly for directional drilling as an option, besides EMM. A detail description of the different PDM designs that were tested is given in section 7.3.1. As the PDM works with the hydraulic energy provided by the pump, it is necessary that the pump has enough energy to overcome the resistance in the system.

During testing, different PDM designs were used to check their performance. It was observed that some versions of the PDM started rotating with some outside help and then stopped rotating because the pump was unable to overcome the pressure loss in the power section. As a result, the pump motor started struggling to reach the set rpm. As testing went on, the pump became weaker, probably due to wear of the internals. The maximum

pressure the pump could provide at maximum motor RPM was around **35 bars**, which was less than the required RPM for the higher torque versions of the PDM. The pump (pressure) was labeled as a major limitation for testing and implementing the PDM. The pump pressure profile for one of the PDM tests is shown in Figure 6.8.

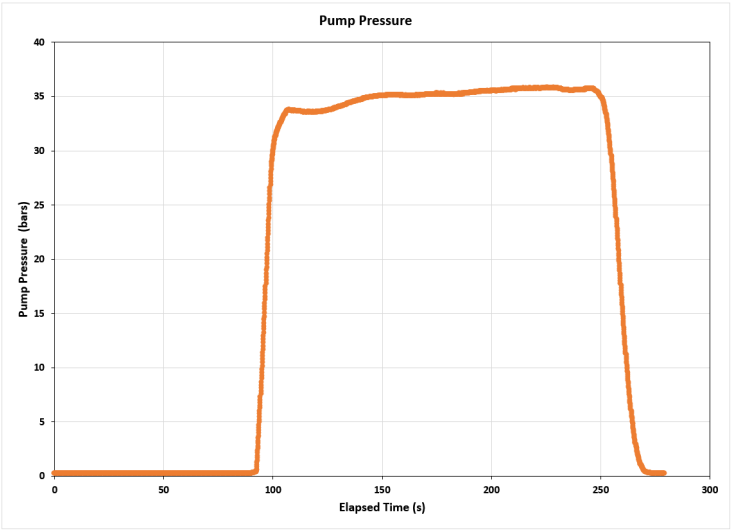

Figure 6.8: Pump pressure profile for PDM testing

During the last week before the shipment of rig, the pump decreased its output to just 40% of the set RPM that it had previously been able to provide at the same pressures. The team then decided to change the pump and replace it with a relatively newer available pump in the workshop. Two days before the rig was shipped for the competition, the pump was then replaced. That pump was not tested due to issues with its drive and time constraints, but it has reportedly performed well in other projects and should be an improvement from the old pump. This way, the pump limitation has been overcome, but it was done too late to perform any new PDM tests. The Figure 6.9 shows the new and old pump installed on the rig.

6.2 Power Consumption

One of the limitations set by the competition committee is that each team can only use a maximum of 25 HP (18.64 KW) to operate the rig autonomously. The rig gets the power (3 phase and 400 V) from the main electrical supply in the workshop. The power is then consumed by the top drive servo motor to rotate the string, hoisting motor to move the drill string up and down, ball screws, pump motor for circulation system and all the top side sensors. In addition to that, computers consume some of the power from the system. This section briefly describes the power consumed by each of the components during drilling and if it is within the set limitations by the guidelines.

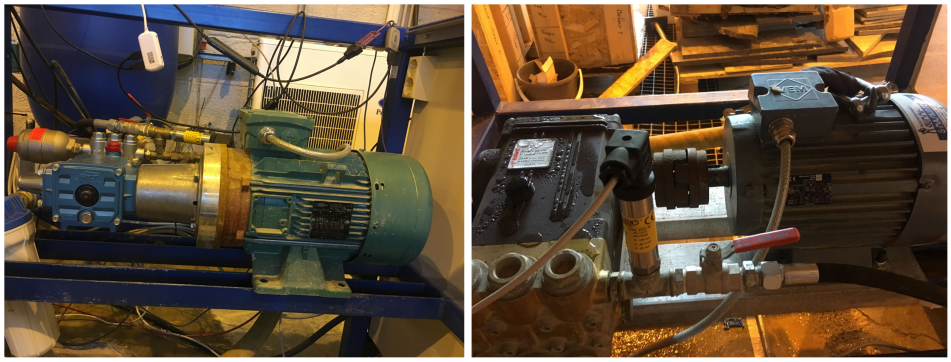

Figure 6.9: Upgraded pump (left) and old pump (right)

6.2.1 Top Drive Servo Motor

The top drive servo motor is used to give torque and rotation to the whole drill string. For the directional drilling purposes, the initial 3" (1" pre-drilled) pilot hole is to be drilled with the top drive servo motor and after 4", the hole has to be kicked off to some specified angle and the servo is used to orient the toolface for slide drilling. The torque and rotation provided by the servo consume power, which can be calculated by using Equation 6.17.

$$P = \frac{T\omega}{\eta} \tag{6.17}$$

$$\omega = \frac{2\pi N}{60}$$

where T is the torque provided by the servo motor to overcome the rock resistance and ω is the angular velocity. The servo motor of selected type can provide a maximum output torque of 28.4 Nm but the nominal torque is 8.34 Nm and maximum speed is 2000 rpm.

The performance of the servo motor was tested towards the end of the semester and the results for torque and rotational speed for one of the tests is shown in Figure 6.10 and Figure 6.11.

The servo motor was run at 100 rpm to avoid stick and slip in the drill string at set WOB. The 100 rpm speed gave satisfactory results of ROP. The torque that the TD motor experienced was changing between 2 and 4 Nm, with some peaks towards the end of the test. At 100 rpm speed and 4 Nm of torque the power consumed by the top drive servo is **52 W** with an efficiency of 80%. The power consumed at a different speed and torque will be different and is shown in Table 6.6.

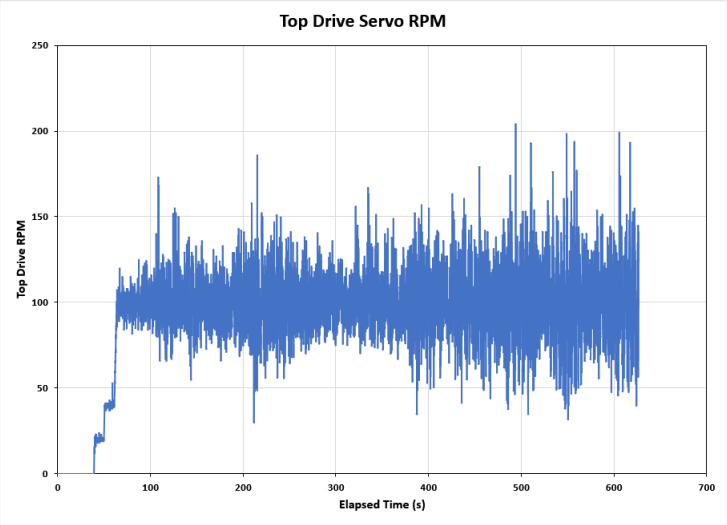

Figure 6.10: Top drive servo RPM for one of the test runs

Table 6.6: Top drive servo power consumption at different speeds and torques at 80% efficiency

	Top Drive Motor Torque (Nm)					
	2	3	4	6	8	8.34
Rotary Speed (RPM)	**Power Consumption (W)**					
50	13	20	26	39	52	55
100	26	39	52	79	105	109
200	52	79	105	157	209	218
400	105	157	209	314	419	437
600	157	236	314	471	628	655
1000	262	393	524	785	1047	1092
2000	524	785	1047	1571	2094	2183

6.2.2 Hoisting Motor

The upward and downward motion of the drill string is provided by the hoisting motor. The hoisting motor acts through the ball screw which converts the rotational motion into vertical motion. The ball screw lead is related to the torque applied by the hoisting motor. Since no changes to the hoisting system have been made from previous years, the already installed ball screw has the same 5 mm lead [29]. The power calculations are done using the same equation as for servo motor i.e. Equation 6.17, whereas the torque is calculated using the following Equation 6.18[5].

$$T = \frac{F.l}{2\pi\varepsilon_{BS}} \tag{6.18}$$

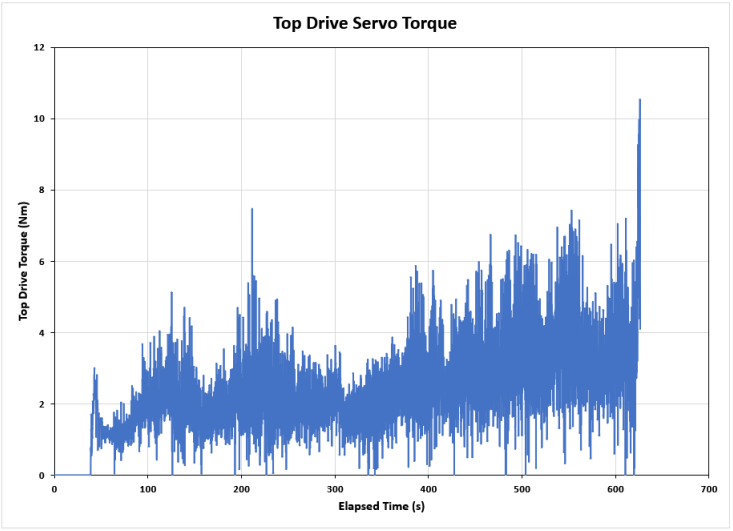

Figure 6.11: Top drive servo torque for one of the test runs

where F (N) is the axial force acted on the ball screw, l (m) is the ball screw lead that is set to 5 mm and ε_{BS} is the hoisting motor and ball screw efficiency factor which is set to 0.90 by the manufacturer [5].

The total axial force acting on the ball screw is due to the weight of motors installed topside (approx. 490 N) and the applied WOB. The RPM and torque of the hoisting motor for one of the test runs are shown in Figure 6.12 and Figure 6.13 respectively.

The low speed and torque is due to the small drilling rates. Since the WOB controller works with the hoisting motor and it always tries to keep the WOB at the set point, the hoisting motor continuously rotates clock and counterclockwise to keep the WOB constant.

The power consumption by the hoisting motor is calculated by first calculating the torque at a specified WOB using Equation 6.18 and then Equation 6.17. If a maximum and constant WOB of 20 kg (196 N) is used, then the axial force acting on the ball screw will be 686 N and the estimated torque provided by the hoisting motor will be 0.606 Nm. From Figure 6.12, it can be seen that the RPM of the hoisting motor is continuously moving between positive and negative values which is due to the WOB controller effect to keep the WOB at the set point. However, the maximum speed of the hoisting motor that the motor provides during the test is 80 rpm. So the power consumed will be **6.35 Watt** at 80% efficiency. As the power is dependent on the torque and speed, the Table 6.7 shows the power consumption at various speeds. It should be noted that the speed of the hoisting motor depends on the rate of penetration.

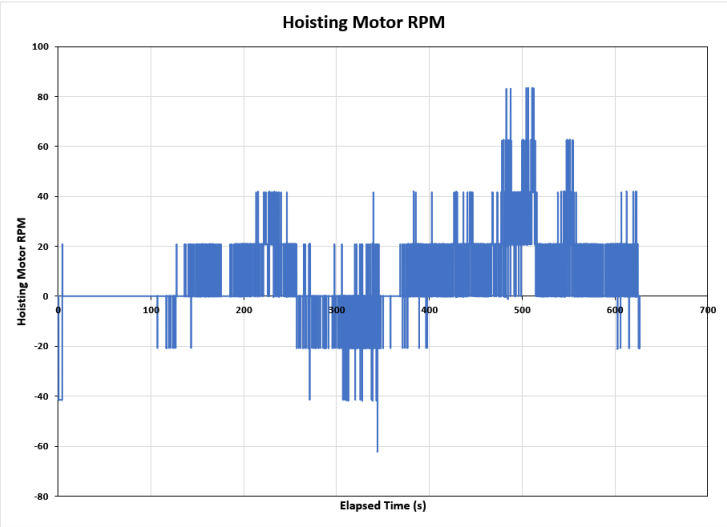

Figure 6.12: Hoisting motor rpm for one of the test runs

6.2.3 Pump Motor

The pump provides the circulation of fluid in the whole system for hole cleaning, cooling of the bit and lubrication. It also cools the EMM and provides enough hydraulic energy for the PDM to rotate. The PDM has not been tested for the optimum pressure and flow rate due to pressure limitations of the old pump and time constraints in installing the new pump. However, the power required for the pump depends upon the pressure and flow rate as given in Equation 6.19.

$$P_p = \frac{P * q}{\eta} \tag{6.19}$$

where P is the pressure at the downstream end of the pump and q is the flow rate. The pump pressure is directly measured by the pressure gauge installed at the downstream end of the pump. The Table 6.8 shows the power consumed by the pump at different flow rates and pressures with 80% frequency.

The maximum power that the pump can consume at maximum flow rate and pressure is used in the total pressure calculations.

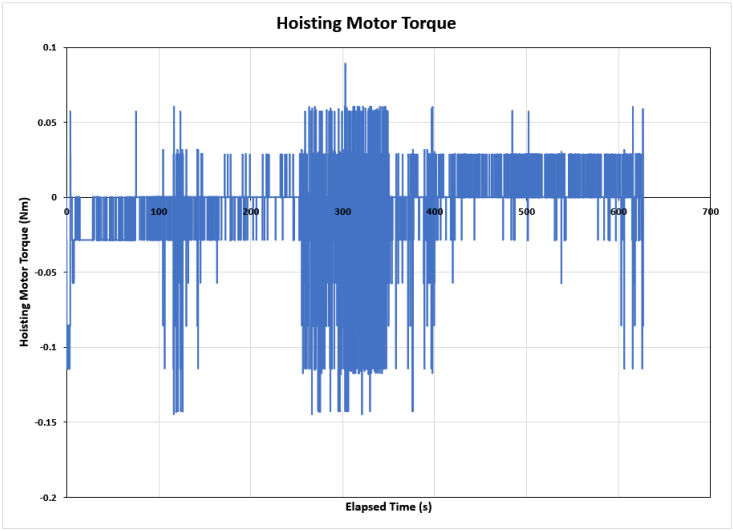

Figure 6.13: Hoisting Motor torque for one of the test runs

6.2.4 Downhole EMM

The downhole EMM with a bent housing in the BHA is used to drill a directional hole at a specific angle. During slide drilling, only the bit will be rotating and that rotation will be provided by the motor shaft. The motor itself is powered from topside through the wires that pass through the drill pipe and are connected to the drive topside.

The maximum speed of the motor with the gear installed is 87 rpm whereas the nominal torque is 0.80 Nm. The motor is planned to operate slightly below its maximum limit during the competition. By using an efficiency of 82.3% provided by the supplier, the maximum power consumed by the EMM will be **8.85 W**.

6.2.5 Electromagnet

A sensor card that is placed in the sensor sub above the downhole power section is used for downhole measurements . One of the components in the sensor card is a magnetometer that measures the azimuth of the drilled hole. Since there is a lot of steel around the sensor card and that steel causes magnetic distortion, a more reliable source of direction should be used. Therefore, the plan is to use an external electromagnet near the rock sample as shown in Figure 8.3 that would help the sensor card to correct any magnetic disturbances.

The power to the electromagnet will be provided from the rig's power supply. The maximum voltage that the electromagnet uses is 12 V and it has an internal resistance of 7 ohm. Hence, the maximum current the electromagnet would take will be 1.71 A. The consumed power by the electromagnet will then be **20 W**.

Table 6.7: Power consumption of hoisting motor at various speeds and constant torque of 0.606 Nm calculated at set WOB of 20 kg with 80% efficiency.

Rotary Speed (RPM)	Power Consumption (W)
50	3.97
80	6.35
100	7.94
200	15.88
500	39.70
1000	79.40
2000	158.80
3000	238.19

Table 6.8: Power consumption by pump at different flow rates and pressure

	Pump Pressure (bars)						
	10	20	40	60	80	100	110
Pump Flow rate (lpm)	**Power Consumption (W)**						
4	83	167	333	500	667	833	917
8	167	333	667	1000	1333	1667	1833
12	250	500	1000	1500	2000	2500	2750
14	292	583	1167	1750	2333	2917	3208
16	333	667	1333	2000	2667	3333	3667
18	375	750	1500	2250	3000	3750	4125
23	479	958	1917	2875	3833	4792	5271

6.2.6 Computer

All the communication in the rig is controlled through the computer, which is part of the rig. The computer used in the rig is **Dell OptiPlex 7440 AIO** and the maximum power it can use is 700 W. Since it is used for some specific tasks just related to the control system, the maximum expected power consumption by the computer will be 100 W.

6.2.7 Total Consumption

The total power consumption by all the components in the rig should be less than 18.64 kW to remain within the set limitations. Table 6.9 shows the expected and maximum power consumption by each of the rig components. It can be seen that the expected power consumption by the rig is just 29 % of the total power and if all the components use their maximum power, they still represent only 45 % of the total available power.

Table 6.9: Expected and maximum power consumption by each component of the rig

Rig Component	Expected Power Consumption (W)	Maximum Power Consumption (W)
Top drive servo	52	2183
Hoisting motor	6.35	238
Pump motor	5271	5271
Downhole el. motor	8.85	8.85
Electromagnet	20	20
Computer	100	700
Total	5458	8421
Limit	29 %	45 %

6.3 Budget Limitations

According to the Drillbotics competition guidelines, the budget for the Drillbotics project is only limited to USD 10,000. If any team exceeds this limit, then a penalty will be given in the overall results. The budget discussed here covers all the equipment and components that will be used during the competition. The allocated budget should cover all the hardware used to build the rig, software for the control system and the labor to construct the rig.

In-kind contributions from the university laboratory are not part of the budget. Two different rock samples were made for testing purposes and the wooden block and the cement used for the rock also comes under the in-kind contributions. Hence, they are not added in the budget. Different consumable items such as pressure gauge and can-open gates are not included in the budget and can be used in any other university project(s). The team just used 1/3 of the total drill pipes ordered so the price of only used drill pipe is included in the budget. The rest of the pipes are university property and can be used by the next year's team. Also, the drill bits were fully sponsored by Lyng Drilling and the expenses of their fabrication is unknown and therefore not listed in the budget.

The cost that is mentioned here just covers the hardware for the rig or drill string. In a real project, a huge sum of the budget goes towards a company's payroll. Since Drillbotics is a student project and the labor done by the students for designing and construction is free, it is not included in the budget. The students involved in the project spent 37.5 hours a week that includes team meetings, designing, testing and report writing. The supervisor's role in the project was to advise and guide throughout the project. The meetings were held every two weeks in the start and twice a week in the last month. Table 6.10 shows the overall time spent by students, professors and support crew, and expected wages as per Norwegian rules and regulations. All the equipment used for the competition is listed in Table 6.11.

At the beginning of the project, the team contacted some of the potential sponsors for sponsoring the Drillbotics. Unfortunately none of the companies were able to provide sponsorship and all the expenditures for the project were taken care by the Department of Petroleum and Geoscience of NTNU.

Table 6.10: Overview of the labour expenses in the Drillbotics Competition

	Hours per week	**No. of weeks**	**Hourly Wage [NOK]**	**Total Cost [NOK]**
Students	37.5	18	165	445500
Supervisors	1.5	14	520	32760
Support Crew	5	18	370	66600
Total				**544860 NOK** **$ 62896**

Table 6.11: Budget for the equipment ordered for the Drillbotics 2018-19 project, the exchange rate used for the things bought in Norwegian Kroners is 8.67 NOK/USD

Objects	**Cost per item [USD]**	**# of items**	**Total Cost [USD]**
Drill pipes	8.56	17	143
Alibaba bits	25	3	75
Maxon motor, gear, sensor, controller	1006	1	1006
Servo motor	761	1	761
Servo drive	807	1	807
Can-open gate valve	415	1	415
Schneider Can-open converter	58	1	58
Water Tanks	92.5	2	185
O-rings and packers	890	-	890
U-joints	27	5	135
3D printed PDM parts	2631	-	2631
Parts for servo drive	231	-	231
Extra maxon motor	490.5	2	981
Tank pressure sensor	238	1	238
Electric swivel	304	1	304
Universal coupling	103	1	103
Extra u-joints	42	5	210
Sensor card	6.9	10	690
Nano connectors	115	-	115
Total Sum [USD]			**8634**

Chapter 7

Mechanical Design

The drilling efficiency of the autonomous drilling rig is highly affected by its mechanical design. The overall system's efficiency, stability, hole quality and integrity can be improved by constructing a strong mechanical structure. A robust and reliable mechanical and control system design enhances the operational window of drilling parameters by pushing the physical limits of the components involved; that improves the overall drilling performance of the system. Based on the design proposal from Phase I of the competition, this chapter explains the mechanical design of the overall miniature drilling rig and all the components being used for drilling.

7.1 Miniature Drilling Rig

The miniature drilling rig used for the Drillbotics competition 2018-2019 was designed and built by the teams from the previous years. The team evaluated the design and structure of the already available rig throughout the semester. Based on the evaluations and discussions, multiple improvements and upgrades in the design were proposed, as discussed in the design proposal (Phase I of the competition)[35].

This section of the chapter describes the overview of the original rig and all its components followed by the improvements in the old design. Moreover, the final design for the competition is explained in this section.

7.1.1 Original Rig

The autonomous drilling rig was designed according to the guidelines given by DSATS. The main focus in the design is on drilling functionality, safety, mobility and performance. Several design features such as framework, hoisting motor, fluid pump, ball screws, load cell, hydraulic and electrical swivel remained the same in the final design. However, the service and maintenance measures were carried out throughout the semester for all the components to improve their efficiency. Figure 7.1 shows the unchanged components of the rig from the original design.

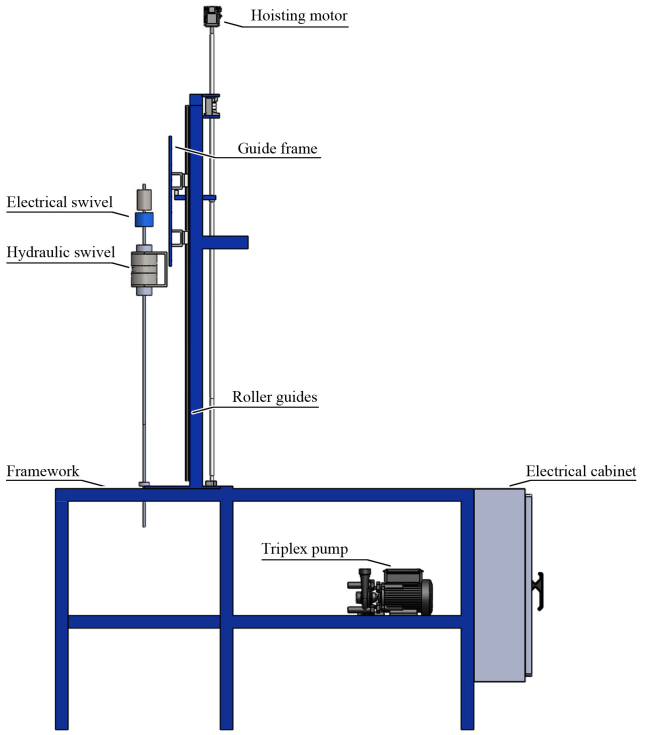

Figure 7.1: The miniature rig and its components from last year

Framework of the Rig

The framework of the autonomous miniature drilling rig is made of 5×5 hollow steel beams. The vertical height of the rig is 285 cm from the ground and width is 70 cm, that counts the total weight of approximately 100 kg. The framework of the rig is designed and constructed to integrate all the mechanical and electrical equipment required to drill the rock sample. The rig floor is 90 cm above the ground, so the rig has the capacity to adjust a rock sample of less than 90 cm tall. To make the transportation feasible, the derrick can be folded down with the hinges that make the rig 253 cm long. The caster wheels are installed on each leg of the rig for its movement. The folded rig structure is shown in the Figure 7.2.

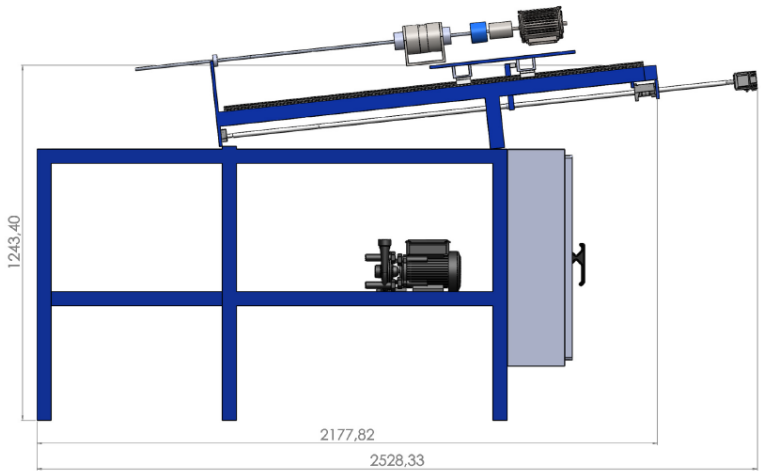

Figure 7.2: Folded rig for the transportation purposes, all measurements in mm

The structure of the rig can be divided into four compartments as shown in Figure 7.3. The rig mast separates two compartments above the rig floor; one used for the rotary motor and the traveling block whereas the other one for the computer to control the drilling operation. The other compartments below the rig floor accommodate the rock sample to be drilled and the pump and hoses for the hydraulic system.

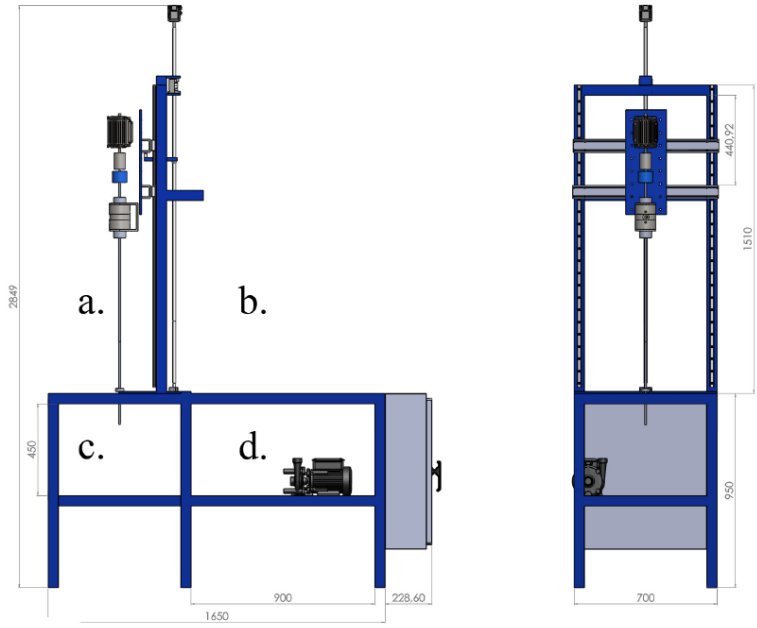

Figure 7.3: The rig compartments a) Drilling area for hoisting motor and drill string b) Space for placing the computer to control the drilling operation c) Rock sample placement area d) Area for hoses and circulation pump, all dimensions are mentioned in mm

7.1.2 Drilling Rig Systems

In a real drilling operation, different systems on the rig function for efficient drilling and so does the miniature drilling rig. Different systems include hoisting system, rotary system, circulation system and the power system. These systems are used simultaneously during the drilling process. This section discusses the function of each system along with the components involved them.

Hoisting System

The upward and downward movement of the drill string and the related components is controlled by the hoisting system. The hoisting system consists of a hoisting motor mounted at the top of the mast, a ball screw and a roller guide. The hoisting motor "Lenze GST AC gear motor" acts through the ball screw that translates the rotational motion into vertical motion. The ball screw installed on the rig is "KGT KGT16x5 FGR RH 1 S 1500 G9 AEG" and is selected due its high precision, efficiency and better step resolution[19]. The installed package of the ball screw is shown in Figure 7.4.

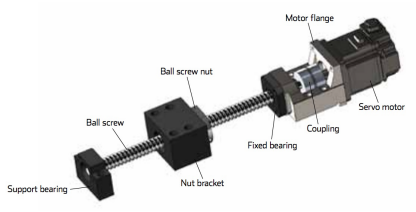

Figure 7.4: Ball screw package used in the hoisting system

The roller guide is attached to the mast that enables the vertical movement. The guide frame that carries the drill string, electrical and hydraulic swivel and the rotary motor, is fixed with the roller guide to move it up and down while keeping it horizontally fixed. The roller guide installed on the rig is shown in Figure 7.5. The connection between the guide frame and the horizontal beam is made through the horizontal beam, ball screw nut and nut bracket. When the hoisting motor works, the rotation in the ball screw allows the guide frame to move vertically.

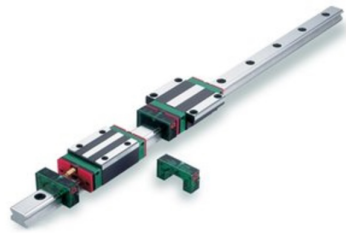

Figure 7.5: Roller guide used in hoisting system [6]

WOB is applied by adding heavy weight drill pipes and drill collars in a full scale drilling rig. In the miniature replica of a full-scale rig the weight of the drill string is not enough to drill the rock, hence the hoisting motor is used to do so. It pushes the drill string downwards to put the required weight on the bit.

Rotary System

In the conventional full-scale drilling, a swivel-kelly system has been used to provide rotation and torque to the drill string. However, in modern drilling, top drive systems replace the swivel-kelly due to its safety and efficiency in the overall drilling process[7]. The miniature drilling rig is designed on the modern principles of drilling and uses the top drive motor for the rotation of drill string. The motor is installed above the swivels (as shown in Figure 7.3) and is capable of moving up and down along the mast. For this year's competition, the previously installed electrical rotary motor has been replaced with servo motor due to the requirements of directional drilling (see section 7.2.2).

Circulation System

The circulation system provides hydraulic fluid at desired pressures and flow rates to the drilling rig in order to meet the drilling requirements. The drilling fluid used in the miniature drilling rig is water that is supplied from the local water supply. The main functions of the drilling fluid are to cool and lubricate the drill string components, clean the hole by transporting the cuttings out of the hole and provide stability to the drilled hole[4].

The circulation system consists of a hydraulic pump (triplex) along with the motor, water hoses, a water tank and swivels. The pump receives water from the tank, pressurizes it and sends it towards the hydraulic swivel through the water hose. The pressure at the outlet of the pump is measured through the pressure transducer mounted on the hydraulic hose. The hydraulic swivel receives the water and forwards it towards the drill string where water travels all the way down and comes out of the drill bit through the nozzles. It then carries the drilled out cuttings and comes out from the outlet in the riser. Another water hose is then used to guide the water into the drainage system. Some modifications has been made in the circulation system of the rig to improve the efficiency of the operation. These modifications are explained in Section 7.2.

In the full-scale drilling, the circulation system involves cleaning the drilling fluid from the cuttings and use it again. The separated cuttings are then examined to know about the geology of the formation. In the competition, a homogeneous sandstone will be provided for drilling, therefore the examination of cuttings is considered irrelevant for the design.

Power System

The electrical power to all the electrical components of the drilling rig is supplied by the power system. In the full-scale drilling rig, the power is generated through the diesel generators on site and that power counts for the actual power of the rig. Most of that generated power is used by the hydraulic pumps used in the circulation system and the draw works used in hoisting system[21].

In a small scale, the rig is limited to use the power of 25 HP (18.64 KW) by the competition guidelines. The required power is supplied through the main electrical supply available in the workshop. The main electrical supply is 3-phase 400 volts, which is input to the electrical cabinet. From the electrical cabinet, different phases and voltages are fed to the drives and sensors based on their requirements. The power distribution to the different components in the rig is shown in Figure 7.6. All the electrical wires are secured properly from the hydraulic system and are placed in the electrical cabinet to avoid any hazard(s). Most of the electrical power is utilized by the hydraulic pump, hoisting motor and the top drive rotary motor. The power consumed by all the components is described in the section 6.2.

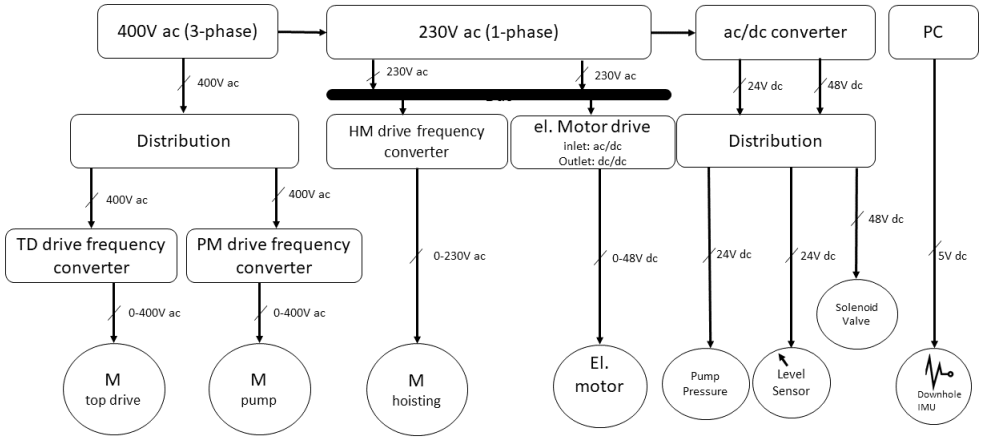

Figure 7.6: Power distribution flow chart

Control System

The control system is the most important system for an autonomous drilling rig. It consists of different algorithms and programs to control the whole drilling process automatically. The drives associated with all the electrical components and the sensors are programmed in the computer to control the drilling operation. All the control system design, algorithms used, sensors and drives are explained in chapter 10.

Other Components

Load Cell As discussed earlier, WOB is an important drilling parameter for efficient drilling. The hoisting motor is used to put the WOB. The applied WOB is measured and recorded through the hollow cylindrical load cell (acts as a top side weight measuring sensor) that is installed around the ball screw on the nut bracket. The location of the load cell in the drilling rig is shown in Figure 7.7.

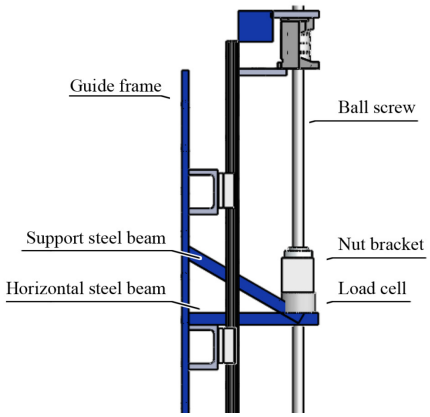

Figure 7.7: Location of load cell

The load cell acts as an integral part in the control system. WOB controller is programmed to achieve the desired weight on the rock sample. Load cell as a WOB controller is explained in chapter 10.

Swivels Below the rotary motor, electrical and hydraulic swivels are installed. The electrical swivel acts as a bridge between the top side and bottom hole electrical connections and transfers the rotary motion from the top drive motor to the drill string. All the connections for the downhole components and sensors are made in the electrical swivel.

The hydraulic swivel receives the high-pressure drilling fluid from the pump and directs it towards the drill string. The hydraulic swivel provides the back pressure of 7.4 bar through oil. A piston enables the hydraulic connection between the water supply network and oil. The swivels installed on the rig are shown in Figure 7.8.

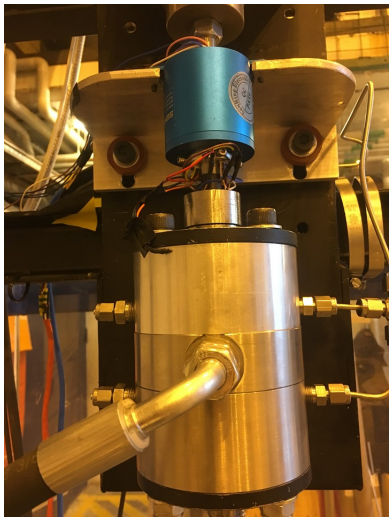

Figure 7.8: Electrical swivel (top) and hydraulic swivel (bottom) installed on the rig

Universal Coupling The universal coupling is placed in between the electrical swivel and the top drive motor. The main purpose of the universal coupling is to mitigate the lateral vibration caused by the high rotational speed of the top drive motor. Also, the misalignment caused by the top drive motor to the components below is also removed by the universal coupling. Figure 7.9 shows the location of the universal coupling on the rig.

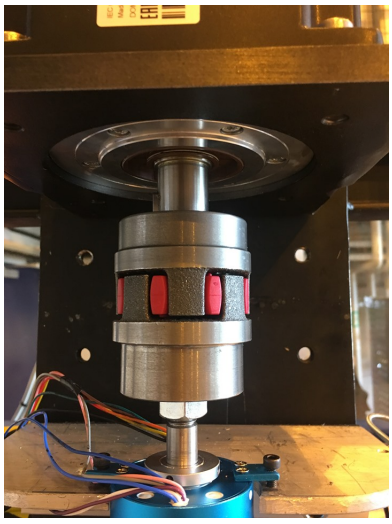

Figure 7.9: Picture of universal coupling installed on the rig

Stabilizers The topside stabilizer is installed on the rig floor through which the whole drill string passes. The stabilizer minimizes the lateral vibrations on the drill string during drilling. The effective length of the free pipe reduces due to the stabilizer which leads to less risk of pipe buckling, hence enhances the drilling performance.

The stabilizer is a roller bearing with a diameter of 9.52 mm equal to the outer diameter of the pipe and is fixed on the rig floor as can be seen Figure 7.10.

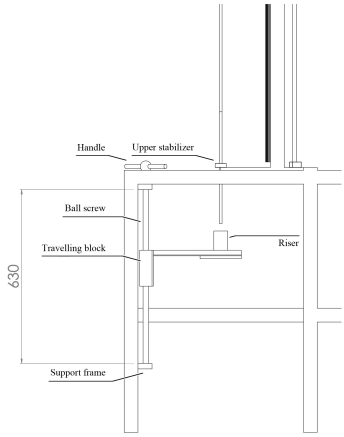

Figure 7.10: Stabilizer Location

7.2 Modifications on the Rig

During Phase I of the competition, the rig was analyzed and tested. Based on the analysis and nature of this year's competition, a few modifications on the rig were applied and are described in this section.

7.2.1 Circulation System

In this year, the competition intends to drill a directional hole to reach the target given by DSATS committee. The team decided to drill the directional hole with a PDM as used in the industry. The mud motor works on the principle of hydraulic energy conversion into mechanical (rotational) energy. The hydraulic energy (flow rate) is provided by the pump.

In the previous setup, the pump gets water supply directly from the water tap available in the workshop. Since the supply from the water tap is constant, the pump was unable to increase the flow rate against the constant supply at the inlet. The mud motor required high flow rate for the desired torque and speed to get the optimum rate of penetration. So the team planned to include the tank system in the previous setup to achieve the drilling targets. The schematics of the rig with the tank system is shown in the Figure 7.11.

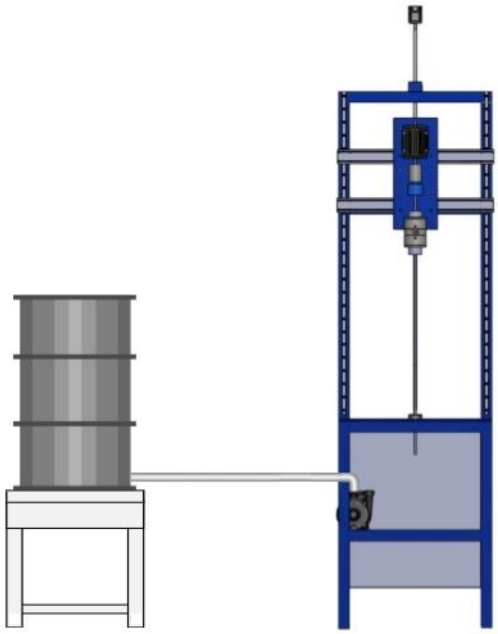

Figure 7.11: Rig with Tank System

The tank system consists of 200-liter tank. The tank has been modified with a level sensor and a solenoid valve. The level sensor allows the solenoid valve to be opened and closed depending on the volume of water inside the tank. All the instrumentation used in the tank system is explained in chapter 9.

7.2.2 Rotary System

In the previous years, the main objective of the competition was to drill a vertical hole so a simple top drive electrical motor has been used to rotate the whole drill string.

As for this year's competition, a directional hole is to be drilled in sliding mode (no rotation from the surface). For this, the orientation of the directional tool (toolface) becomes important. The already installed electrical motors can not orient the tool at the desired position but can only rotate at required RPM (or torque). Therefore, the team decided to change the electrical motor with a servo motor that would use a close-loop feedback to adjust its voltage and current according to given parameters of RPM, torque and position. The toolface of the BHA is then adjusted at any point during drilling. A detailed description of the servo motor and its control system is included in chapter 9.

7.2.3 Riser and stabilizer Alignment

Due to the bent housing in the BHA and a larger bit size, the riser needed to be re-designed. Now the new riser has an inner diameter of 4.5 cm and a total height of 25 cm. The riser and the guideframe material is also changed from steel to stainless steel to avoid any magnetic distortion with the sensor card. The engineering drawings and calculations of its diameter are shown in Appendix H.

The space between the top of riser and the rig floor is small, so the need of an extra bearing in the riser is diminished. However the return flow will be blocked by a 3D printed plastic cap that has an OD equal to the riser ID (4.5 cm) and an ID (1.1 cm) slightly larger than the drill pipe size to avoid any friction.

7.3 BHA design

7.3.1 Positive Displacement Motor

Even though Rotary Steerable Systems (RSS) are the go to solution for many operators when it comes to directional drilling, Positive Displacement Motors (PDM) remain an important share of the directional drilling market due to their low operational costs [42].

When looking for solutions to deviate the miniature well, designing a PDM from scratch seemed more reasonable than a RSS. It took several iterations to make this solution work, due to many challenges regarding the power section of the mud motor. This section will explain in detail what were the difficulties encountered along the way and how the team tried to overcome them.

Initial Design

The initial PDM design from Phase I included a top sub which functions as a sensor card holder and a stabilizer. A 1:2 configuration was chosen for the power section, using steel on both the stator and rotor. Even though the torque generated with this configuration is usually low, the team knew beforehand that the rock to be drilled in the on-site test was a sandstone. Based on last year experience, this rock does not require a lot of torque to drill.

The transmission and bent housing had two universal joints, one single and one double, working inside. As Figure 7.12 shows, this made the overall design longer, adding up to 20.4 cm for the entire BHA. The bearing housing includes a near-bit stabilizer on the outside, increasing bit stability and further improving directional control and hole quality [1].

[1] For more design details, refer to the Phase I report [35]

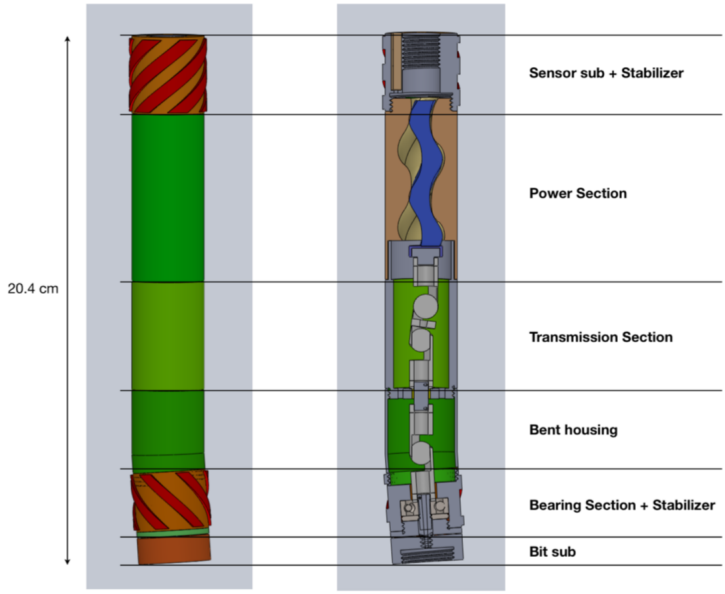

Figure 7.12: Initial design from Phase I [35]

After careful consideration, it was decided to get rid of the transmission housing and the single universal joint. Instead, the lower end of the power section will be connected to the bent housing and the double universal joint will connect the rotor on one end and the drive shaft on the other end. This initial modification reduced the length of the BHA down to 16.76 cm. Figure 7.13 shows the modified initial design.

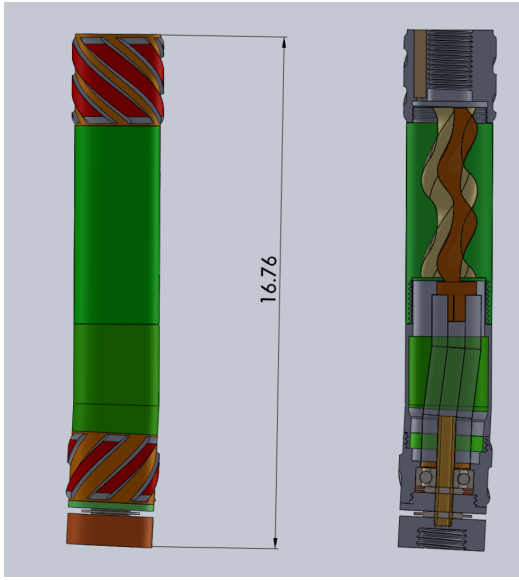

Figure 7.13: Modified version of the initial design. Dimensions in centimeters.

Figure 7.14: Real version of the modified initial design.

Iteration I: Steel on Steel

Due to the difficulty in the design, the team opted for 3D printing the rotor and stator in maraging steel. Since high metal-to-metal wear was expected between the parts, they were hardened to extend their life. Figure 7.15 shows both and how they fit together.

Figure 7.15: Steel rotor and stator.

Since the interference fit between the rotor and stator was negative for this case and water is a low viscosity fluid, there was a lot of slippage between the parts and the rotor was not able to move the rest of the transmission. In an attempt to fix this issue, high viscosity grease was applied on the rotor to try to reduce the gaps in between the parts. As a result, the PDM delivered more than 200 rpm with 28 lpm.

After a few successful runs, the rotor and stator wore down to a point where the slippage was too big to make the rotor run again. An epoxy layer was applied on the rotor later to reduce the fit, but the irregularities along the surface and the poor bonding between the two materials made the epoxy layer peel off easily when rotated inside the stator. Figure 7.15 shows the rotor with an epoxy layer on the left and Figure 7.16 shows the same rotor after a run inside the stator.

Additional setbacks occurred when testing this setup. The heat treatment given to both rotor and stator hardened the parts making them more resistant to wear but also makes the material brittle. While assembling the BHA for future runs, the lower end of the stator broke due to the high makeup torque and low thickness in the threaded zone. Figure 7.17 shows the repaired stator after the failure.

Figure 7.16: Peeled off rotor after a run inside the stator.

Figure 7.17: Repaired stator after a brittle failure in the threaded zone.

The lessons learned on this iteration are listed below:

- Making a PDM power section entirely out of steel is very challenging. Only zero and negative interference fits can be tried out.
- Even hardened parts can wear down and reduce the interference fit even further.
- Even though epoxy is temperature and wear resistant, a slight imperfection on the surface of the rotor or stator will peel it off.
- Avoid high loads on thin and hardened materials. These are very susceptible to break.

Iteration II: Modular Design in Plastic

In order to fix the previous design, it was decided to implement a solution that moves towards a real PDM power section. With that purpose in mind, a modular plastic design was created. It consists of a 3D-printed hard plastic housing, which holds a 3D-printed flexible stator inside. The outer housing can be seen in Figure 7.18 and Figure 7.19 shows how the flexible stator fits inside the housing. These parts were 3D printed with a Prusa i3 MK2S, using a 0.4 mm brass nozzle.

The benefits of implementing this solution are the flexibility it offers, in terms of different rotor/stator configurations that can be tried out. If one wants to try different lobe ratios, only the flexible stator and rotor need to be printed again. The outer housing will remain the same.

Figure 7.18: Modular design showing the outer plastic housing that holds the stator inside. Notice the splines inside the housing that take up the torque induced in the stator.

(a) (b)

Figure 7.19: (a) Flexible stator. (b) Flexible stator and housing assembled together.

Different filaments were chosen when 3D-printing these two parts. The reason behind was because of the functionality each of the parts has. The material chosen for the flexible stator was TPU (Thermoplastic Polyurethane), also known as NinjaFlex commercially. This elastomer offers high elongation percentages which allow for repeated movement of the rotor without wear or cracking and it is chemically resistant to many materials. On the other hand, the outer housing needs to be strong and stiff enough to take up the makeup torque on the threads and any external loads applied to the BHA. This is why PETG (Glycol-modified Polyethylene Terephthalate) was chosen for this component, this material has good impact resistance and high tensile strength.

When it comes to the rotor, it was decided to try both the old steel rotor and an entirely new 3D-printed part with a different design. For the 3D-printed version, PLA (Polylactic acid) was used which provides good tensile strength and surface quality. Table 7.1 summarizes the mechanical specifications for both materials. Figure 7.20 shows the new rotor used in this iteration.

		NinjaFlex	**PLA**	**PETG**
General Properties	**Units**			
Specific Gravity	g/cc	1.19	1.24	1.29
Mechanical Properties				
Tensile strength, Yield	MPa	4	49.5	53
Tensile strength, Ultimate	MPa	26	45.6	45.8
Tensile modulus	MPa (GPa)	12	(2.3)	(2.1)
Elongation at Yield	%	65	3.3	14
Hardness	Shore	85A	83D	85D
Thermal Properties				
Melting point	^{o}C	216	45 - 160	73

Table 7.1: Mechanical specifications of the materials used in this iteration

Figure 7.20: New rotor 3D-printed in PLA. Notice the four lobes following a spiral along the rotor. This feature provides more torque and less rpm to the power section.

When testing this newly designed power section, two problems were encountered. First, the threads that connect the outer housing with the sensor sub broke at their base. This could be due to a high metal-to-plastic makeup torque that weakened the threads or due to a high-pressure buildup at the beginning of the power section or a combination of both, as illustrated in Figure 7.21. The actual result can be seen in Figure 7.22. Second, the coupling that connects the rotor and the universal joint broke when trying to rotate the bit manually. This is an indication that the plastic coupling is too weak to take the required torque. Figure 7.23 shows where the failure in the rotor took place.

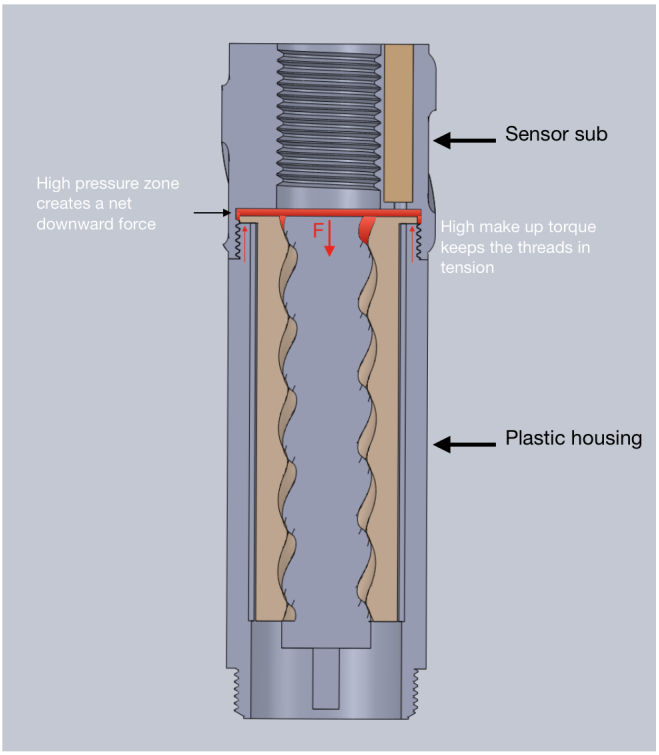

Figure 7.21: Root cause of the housing failure.

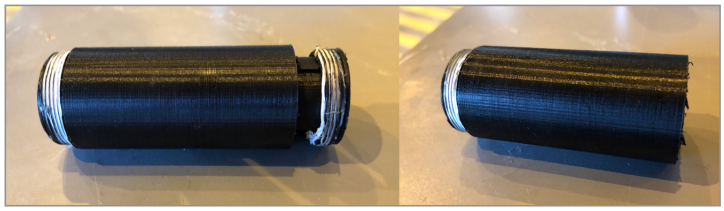

Figure 7.22: Plastic housing thread failure.

Figure 7.23: Rotor coupling failure.

The lessons learned on this iteration are listed below:

- Metal-to-plastic threads are not ideal. Plastic threads tend to break or deform when they are tightened.
- High pressure builds up at the beginning of the power section, therefore it is important to seal all possible leakage points and use materials that can withstand the stress.
- The rotor coupling needs to be stronger to take up the required torque.

Iteration III: Modular Design in Steel

To solve the issues encountered in Iteration II, a modular design in steel was proposed. The idea behind this new design is essentially the same, with the difference that now the torque between the housing and the stator is taken up by two set screws instead of the four previous splines.

In this new design, the stator is 3D-printed using the same material as before but it is permanently glued into a stainless steel sleeve. This sleeve containing the stator is then placed inside a steel housing where it is fixed in place using two set screws.

With respect to the rotor, now only the outside is 3D-printed in plastic using the same material. However, the core and the coupling are now made out of steel and permanently glued with the rest of the rotor, as it can be seen in Figure 7.24b. The entire power section is shown in Figure 7.25.

(a) (b)

Figure 7.24: (a) Steel sleeve with stator inside. (b) Rotor and stator working together. Notice the steel core inside the rotor.

(a) (b)

Figure 7.25: New power section assembly. (a) The inner sleeve can be retrieved and replaced without affecting the outer housing. (b) Power section ready to be used.

After testing this new design, both solutions on the rotor and outer housing worked as planned. Minor leaks were experienced on the set screws with low flow rates. However, these leaks were stopped after increasing the pressure on the rubber lip atop of the stator, which occurs when the flow rate is increased over a certain value.

Different rotors with different interference fits were tested. Starting with negative fits, the motor started rotating with almost the maximum flow rate available from the pump and with some help from the outside, signaling high slippage in the power section. In order to solve this issue, new rotors were 3D-printed with tighter fits. The tests that followed

showed that the higher the fit between rotor and stator, the lower the flow rate needed to start the PDM. [2].

Based on these results, the lessons learned can be listed below:

- What might seem a lot of friction to the human hand when trying to rotate the rotor, actually indicates a good sign for the PDM performance. If the rotor can be easily rotated with one's hand, it usually means the motor will be weak and there will be a lot of slippage in the power section.

- By increasing the interference fit, the PDM can be started with lower flow rates.

It took three iterations to have a working design and a steep learning curve was experienced along the way. The next step in the process is to check whether the PDM performance is good enough to drill a deviated well or not. The performance tests are detailed in Section 11.1.

7.3.2 Electric BHA

As mentioned in the Phase I report [35], a back-up solution was planned and designed in case the main alternative does not work. This section will go through the design details of this alternative solution and the main modifications introduced to the initial design.

Initial design

The initial design for the electric BHA includes an electric motor as the down hole power section. The rest of the assembly consists of a top stabilizer, a bent-housing, a bearing housing and the bit sub. The overall design can be seen in Figure 7.26.

[2] No rpm or torque tests were performed at this stage. For more information on this matter, please refer to Section 11.1

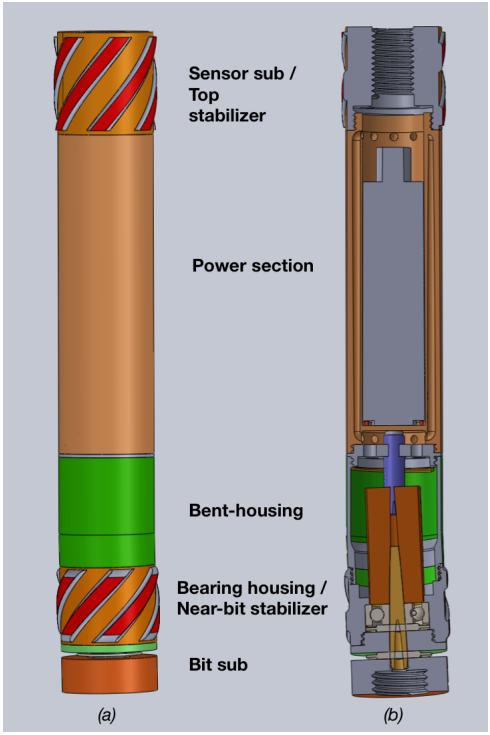

Figure 7.26: Initial electric BHA design (a) Overall design (b) Cross-section

Modifications

When testing this BHA for the first time, a few issues were encountered. These issues were found in the transmission section of the assembly, as Figure 7.27 shows. First, the metal 3D-printed coupling that connects the electric motor shaft with the rest of the transmission, became deformed after an attempt to drill a hard sandstone. The high counter-torque experienced on the bit's face, traveled along the transmission up to the failure zone. At first the motor simply stalled out when this happened, but as the stalling tests continued, the cylindrical coupling became oval up to a point where the motor shaft simply slipped inside without transmitting any torque further down the transmission.

The main reason behind this issue was the small wall thickness, which was 0.45 mm and the fact that all the torque was being applied only on one side of the coupling. Therefore, to overcome the problem it was decided to first try increasing the wall thickness by permanently fixing an outer steel cylinder on the coupling. This solution proved to be successful for the following runs, but the same issue appeared after some time as Figure 7.28 shows.

To increase the strength of the coupling, the wall thickness was further increased and instead of using an inner edge that latches onto the motor shaft, two set screws keep it in place. Figure 7.29 shows how the new coupling design will work together with the motor

shaft. The other end of the coupling fits inside the universal joint, which is part of the transmission.

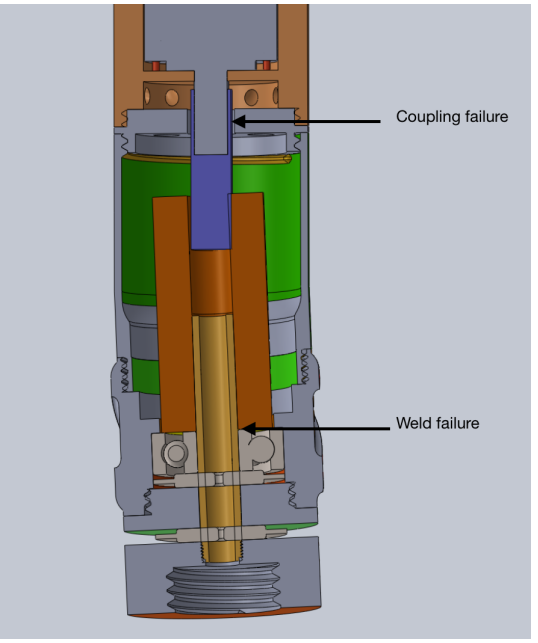

Figure 7.27: Summary of failure zones inside the electric BHA.

Figure 7.28: Different views of the reinforced coupling. On the right, the coupling has taken a slight oval shape enough to cause issues with the rest of the transmission.

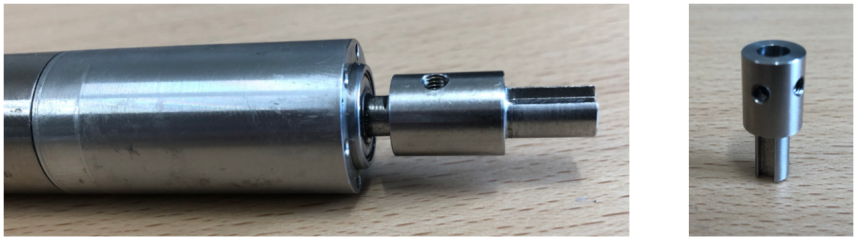

(a) (b)

Figure 7.29: (a) Electric motor and new coupling design. (b) New coupling design after two previous iterations that did not work.

Another issue found when testing the electric BHA was the weld at the bottom of the universal joint, as illustrated in Figure 7.27. After a few runs, the weld broke leaving the drill bit without any torque and rpm. No modifications were introduced here, the weld most probably broke because of a poor welding procedure.

Electric Motor Performance

The electric motor that was decided to use consists of the motor itself, a planetary gearhead to increase the torque output and a sensor that provides the readings needed to control the motor. Figure 7.30 shows the performance of the parts combined. Due to torque and rpm limitations, it was decided to maximize both of them without entering into any dangerous zones for the motor. Even though the motor would be slightly inside the "out of voltage range", it was decided to use 87 rpm and 0.8 Nm as the operational parameters when drilling the on-site well. This will allow for higher ROP, especially in harder sandstones.

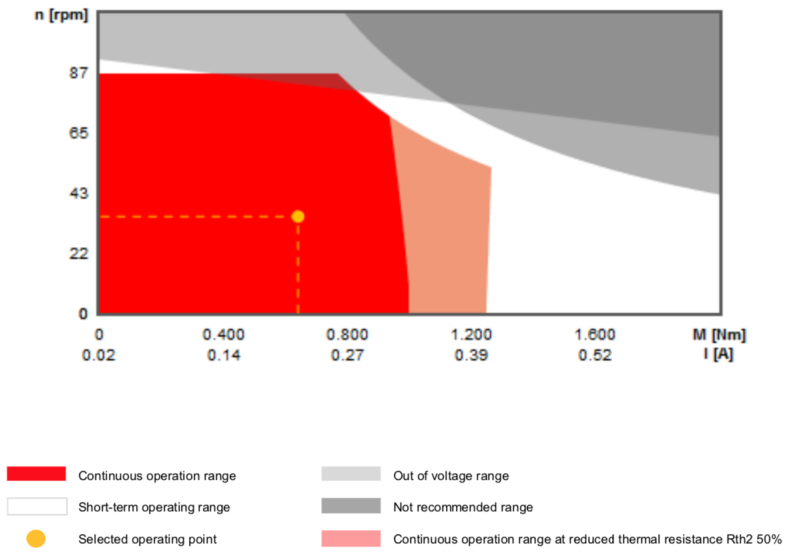

Figure 7.30: Electric motor performance chart.

Motor Seal

The main challenge when using the electric motor as a power source for the BHA, is its proximity with water. As Figure 7.31 shows, water flows around the motor housing through a series of small channels and continues its way at the bottom of the motor. There are basically three areas where water can enter the motor: top, bottom or connection between the gearbox and the motor, as signaled in Figure 7.32. The highest risk zone lies in the gap between the motor and the housing, here water can easily enter the gearbox and travel all the way up to the motor and create a short circuit.

Three motors were initially bought to test out this design and several iterations were needed along the way, which are going to be explained below.

Iteration I: No water, no seals (Motor 1) On a first run, the motor was tested without water flushing through the channels and without any seals. The results were good at first and the motor was able to drill, but water droplets falling from the hydraulic swivel made their way to the top of the motor and burned it in a few hours. However, the motor seemed to work fine after it was left to dry for a day.

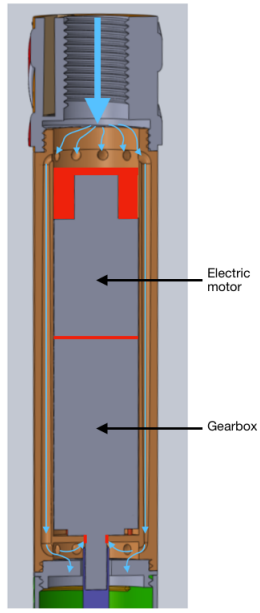

Figure 7.31: Light blue arrows indicate how water gets past the electric motor. Red areas signal dangerous zones where water can enter the motor.

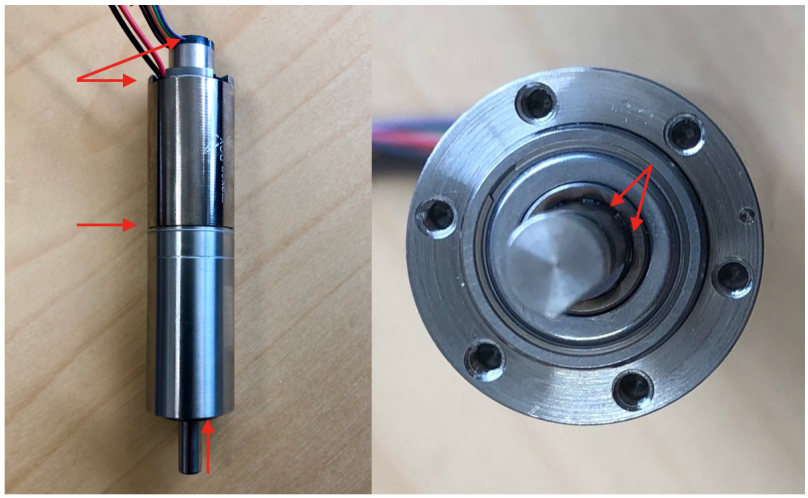

Figure 7.32: (Left) Three main areas for water invasion. (Right) Toughest area to seal properly.

Iteration II: Water and Seals Included (Motor 1) On a new try, the same motor was tested but with seals and water flow included this time. To isolate the top of the motor as Figure 7.31 illustrates, a layer of magic rubber and silicone was applied. Thick grease was applied in the annulus between the motor and its housing, to seal the connection between the electric motor and the gearbox. No seal was applied on the shaft at the bottom. The idea here was to see if grease could stop water from entering the aforementioned areas when pressure from below is applied.

After a few runs, the motor stopped working again. Once the BHA was rigged down, it was noticed that the magic rubber and silicone layer applied on top could not stick well to the steel walls of the housing. This means that water was able to flow in these gaps and flush out all the grease that was placed further down the motor, exposing all the areas that needed to be sealed. This time the motor stopped working completely.

Iteration III: Water and Seals Included (Motor 2) On a following run with a new motor, the top was sealed with a silicone cap this time. The rest of the areas were sealed using the same grease as before. After three hours of testing this solution with water flow, the motor stopped working completely. No drying helped this time.

When trying to find a solution, it was decided to disassemble the faulty motor and measure the resistance inside to check for a short circuit. The resistance of the motor after failure was sufficiently high to suspect that water was not the issue but grease instead.

Iteration IV: Water and Permanent Seals (Motor 3) On a last iteration, it was decided to permanently seal the top of the motor with epoxy and the shaft at the bottom with a V-seal, which can be seen in Figure 7.33. Along the walls of the motor, a dielectric grease was used. [3]

Since this was the last electric motor available, it was decided to leave this setup for the competition day and test it on-site.

[3] A few modifications were necessary on the motor housing to be able to use the V-seal.

Figure 7.33: V-seal on the electric motor shaft. When pressurized this seal makes contact with the plate where the motor sits and prevents any water from going further inside the housing.

7.4 Drill Bit

A directional polycrystalline diamond compact (PDC) bit will be provided by DSATS for this year's competition [4]. According to the Drillbotics guidelines shown in Appendix A, "the students may use the directional drill bit provided by DSATS, or use their own bit design (...)". Encouraged by the latter statement and inspired to create an even better drill bit, it was decided to work in a completely new design in collaboration with Lyng Drilling.

Designing an entirely new drill bit from scratch is a demanding and time-consuming task but it offers many advantages. It offers the possibility to specifically design the bit for the type of well is going to be used in and to be compatible with the proposed bottom hole assembly. Besides, if the rock formations to be drilled are known beforehand, the drill bit can be further optimized to increase its performance and life. In other terms, a proper bit design will provide a good ROP, good borehole quality and reduce the number of bit runs for each well section reducing the non-productive time (NPT).

In this section, a basic drill bit theory is going to be introduced to highlight the most important features a drill bit must have, especially when used in directional drilling applications. Then, the general modeling steps are included to show how to use this theory to go from a basic sketch to a fully designed drill bit. Besides, a new concept [38] has been introduced in the design to create a more stable and efficient directional PDC bit. Finally, different

[4] DSATS drill bit specifications can be found in Appendix A.1

gauge pad lengths are going to be tested to assess their impact on steerability and stability.

7.4.1 Theory

Drill bits play an important role in every drilling operation, they influence borehole quality as well as drilling performance. When designing a drill bit, there are many key aspects that must be understood that will be discussed in this section.

There are mainly two types of drill bits used in the industry today, fixed-cutter bits and roller-cone bits. Both types can be used to drill a variety of formations, ranging from very hard to very soft. This section will focus on Polycrystalline Diamond Compact or PDC bits, which are part of the fixed-cutter group of bits.

PDC Bits

Polycrystalline diamond compact (PDC) bits are the most common type within fixed-cutter bits. They consist of a single rotating body, with a set number of blades where the synthetically made diamond cutters are brazed in place. Figure 7.34 shows the standard nomenclature for a PDC bit.

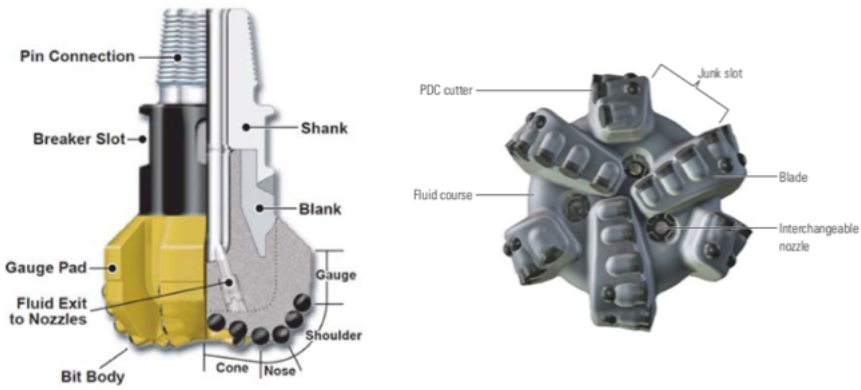

Figure 7.34: Main PDC bit nomenclature [23] [22]

A PDC bit drills by shearing the formation, instead of gouging and crushing the rock like a roller-cone bit does. The energy required to reach plastic limit for rupture is significantly less in shear than by compressive stress. Therefore, PDC bits require less WOB than roller-cone bits [10]. This characteristic is beneficial to the thin-walled aluminum pipes for buckling related issues and also to the PDM to avoid stalling it out.

Bit Profile

The bit profile refers to the shape of the cutting structure and influences many aspects of the bit's performance such as stability, steerability, and ROP.

The type of bit profile influences the hydraulic flow across the bit's face. A good hydraulic flow will help clean out cuttings as fast as they are generated, which in other terms means having higher ROP. A poor hydraulic flow, on the other hand, will let cuttings accumulate on the bit's face and will hinder the removal of new rock, decreasing the ROP. Having a good hydraulic flow it is also important to cool down the cutters and helps prevent cutters damage due to heat degradation [11]. The PDC profile nomenclature is shown in Figure 7.34 to the left and can be divided into four zones, from the center axis to the gauge: cone, nose, shoulder, and gauge.

There are two types of profiles, flat and parabolic, as illustrated in Figure 7.35. A flat bit profile has a single radius on the shoulder and will mainly be used in hard formations since it uniformly places a high load on individual cutters and increases penetration. However, a parabolic profile is more aggressive and produces higher ROP but it also wears faster than a flat profile [11].

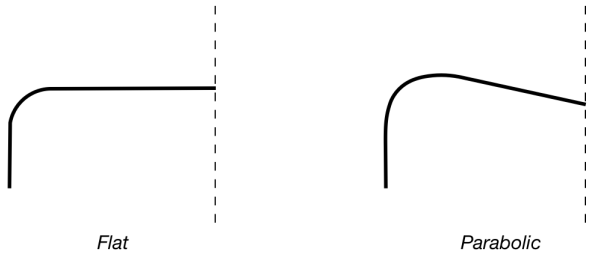

Figure 7.35: Flat profile vs. Parabolic profile

Cutter Density

PDC cutters are placed along the bit profile to ensure complete bottomhole coverage, i.e. no uncut formation. The cutter number and specific placement along the profile can be referred to as cutter density and it is a function of profile shape and length and of cutter size, type and quantity. As the distance from the center axis increases, the cutter is exposed to higher speeds and has to remove more rock than those closer to the centerline [10]. Therefore, to slow down the abrasive wear rate of those cutters near the gauge, it is common to find bit designs where cutter density increases towards the gauge. Figure 7.36 shows the cutter density after each cutter has been projected into a radial plane passing through the bit axis.

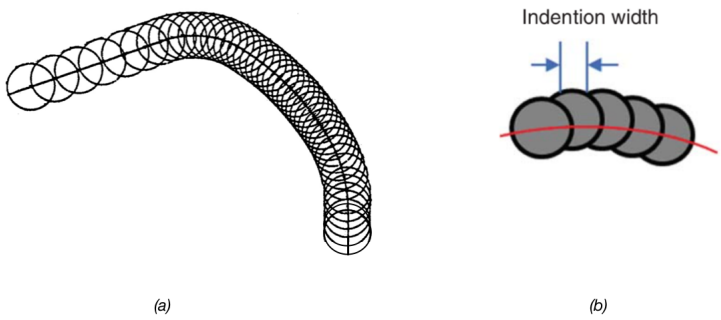

Figure 7.36: (a) Cutter density along bit profile. Note how the density increases towards the gauge where the cutters see more wear [10]. (b) Single-set cutter layout [38]

The cutter density can be manipulated by changing the overlapping between cutters. A single-set cutter layout is defined as having no cutters at the same radial or axial position. Based on field experience, a PDC bit with single-set cutters is able to drill much more efficiently than a PDC with cutters at the same radial positions (also known as ”track-set cutters”) [38].

Cutter-rock Interaction

Cutter orientation influences the way the bit interacts with the rock. PDC cutters are placed on the active edge of the blade at an angle. The attack angle or back rake angle is the angle between the plane perpendicular to the rock's face and the plane coincident with the cutter's face.

Small back rake angles increase the depth of cut and therefore are used in soft formations to increase ROP. On the other hand, bigger back rake angles decrease the depth of cut, ROP and bit vibrations but also increase bit life, making it appropriate for harder formations. As Figure 7.37 shows, typical back rake angles vary between 10 and 30 degrees and individual cutters normally have different angles as they go from the bit's center towards the gauge.

If one looks at the drill bit from its front face, a cutter's side rake angle can be defined. This angle is defined as the angle between a line passing through the center of the bit and the cutter's face, as shown in Figure 7.38. Positive side rake angles help direct the cuttings towards the gauge, improving hole cleaning. However, negative side rake angles would direct the cuttings towards the center of the bit [22].

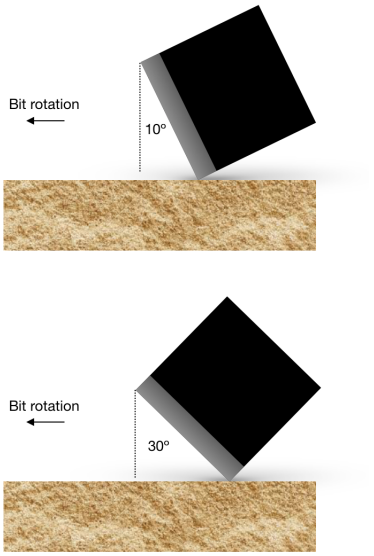

Figure 7.37: Back rake angle for a single PDC cutter. Depending on the rock hardness, this value influences how much the cutter digs into the formation.

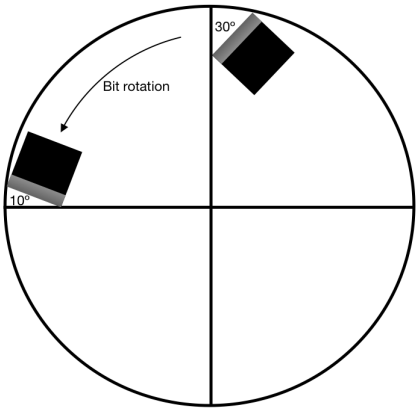

Figure 7.38: Side rake angle for a single PDC cutter. This angle helps removing the cuttings from the bit's face.

7.4.2 Design Considerations

When designing the bit for this year's competition, several aspects had to be considered. Drilling a directional well requires the bit to be steerable and stable at the same time. This means the bit has to be able to follow a predefined well path and minimize all kinds of vibrations, especially those leading to whirl.

The steering methodology also needs to be taken into account. Since the current BHA uses a three-point curvature method to deviate the well ensuring those three points of contact are in place is a mandatory task if one wants to have a decent steerable system.

In this section, a discussion about the main features a directional bit must have is introduced, along with a new concept to improve bit efficiency.

Steerability

When drilling a well, the bit is exposed to a set of lateral and axial forces that tend to initiate a lateral deviation in the hole. The ability of a bit to begin this lateral deviation is defined as bit steerability (B_s) [34].

$$B_s = \frac{D_{lat}}{D_{ax}} \tag{7.1}$$

where D_{lat} is the lateral displacement per bit revolution and D_{ax} is the axial penetration per bit revolution.

The lateral displacement per bit revolution (D_{lat}) depends on the gauge aggressiveness. This aspect has a strong effect on side-cutting ability and hole quality. Therefore, for those cutters placed on the gauge, one has to choose a back rake angle that provides some side-cutting action to change direction. However, if the gauge pad is too aggressive, i.e. low back rake angles, this may lead to ledges, spiraling and hourglass features along the borehole [15].

The face aggressiveness of the bit is also important to consider when it comes to the axial penetration of the bit and tool face control. Small variations in WOB can cause a significant increase in torque, especially on PDC bits. This could lead to tool face control issues and the PDM stalling out. Therefore, even though increasing the back rake angle on the bit's face may decrease the instantaneous ROP, the overall ROP might be higher since motor stalling and tool face resets are avoided [15].

Bit profile and gauge length have proved to influence bit steerability as well. Deep cone angles and a relatively flat nose area, together with a reduction in gauge length, seems to improve bit steerability [34]. Having a short gauge length reduces the overall bit height which is one of the key characteristics of a steerable bit.

Stability

Bit stability is a major concern during the design phase. Several vibration mechanisms may occur in the drill string, but bit stick-slip and whirl are the ones that involve the drill bit the most. Stick-slip can be overcome by reducing WOB and increasing RPM and also by limiting the depth of cut. However, bit whirl can be avoided by choosing the correct bit profile and blade design.

When it comes to bit stability, the profile length plays a part. Generally speaking, shorter profiles are more dynamically stable than longer profiles (Figure 7.39). This is due to a larger contact area with the wellbore wall towards the gauge [24].

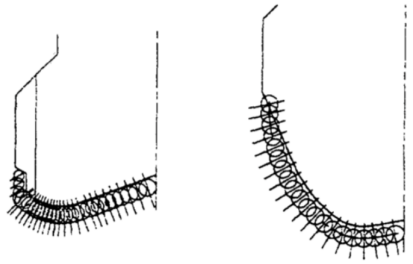

Figure 7.39: Short vs. Long bit profile [24]

Another important aspect of a bit profile that directly influences a bit's stability is its cone depth. Deep cones tend to create a cone of rock at the center of the bit that generates a centralizing effect and reduces the bit's tendency to rotate off-center. The deeper the cone angle, the bigger the restoration force [24].

Finally, to aid in the development of an anti-whirl bit, gauge pad and rock interaction must be understood. When a bit starts whirling it is usually because the radial bit imbalance makes the instantaneous center of rotation to move around the bit face as the bit rotates. By including low-friction spiraled gauge pads, smooth contact with the borehole wall is created and the movement of the center of rotation is interrupted, thus minimizing bit whirl [40].

Force-balanced Design

A relatively new concept, also known as the force-balanced design has shown to improve bit stability and drilling efficiency [38]. In this design, the cutter layout is such that the imbalance forces that tend to offset the bit are minimized.

To minimize these imbalance forces, cutters no longer follow the traditional spiral towards the bit gauge as illustrated in Figure 7.40a, but rather the path shown in Figure 7.40b.

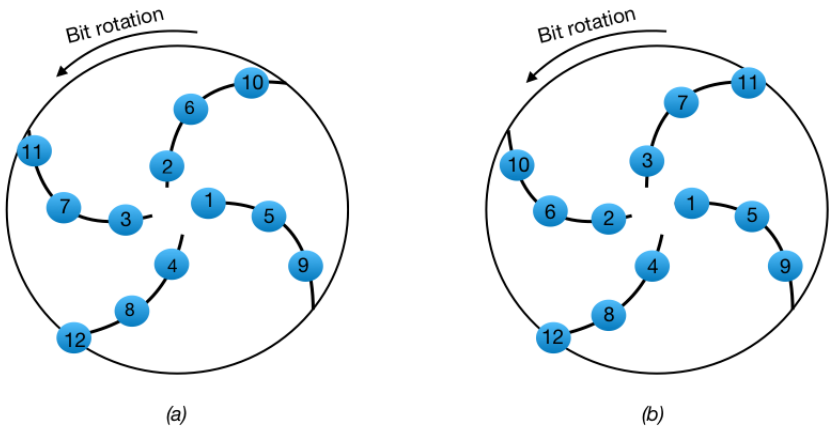

Figure 7.40: (a) Traditional cutter layout. (b) New cutter layout.

The reason why this new cutter layout works can be explained by looking at Figure 7.41. Considering one cutter on each blade, the traditional spiraled cutter layout drills inefficiently due to a poor cutter placement. As depicted in Figure 7.41a, cutters 1 and 2 are placed on the same side of the inner ring of rock and therefore cutter 2 will remove much more rock than cutter 1, leading to inefficient drilling. However, by rearranging the cutters angularly without changing their radial and axial positions, one can drill more efficiently and minimize the imbalance forces. As Figure 7.41b shows, now cutters 1 and 2 are facing each other, such that each cutter can approximately remove the same amount of rock in a complete revolution. Placing the cutters this way minimizes the imbalance forces and leads to more efficient drilling. The same principles apply for the outer ring of rock [38].

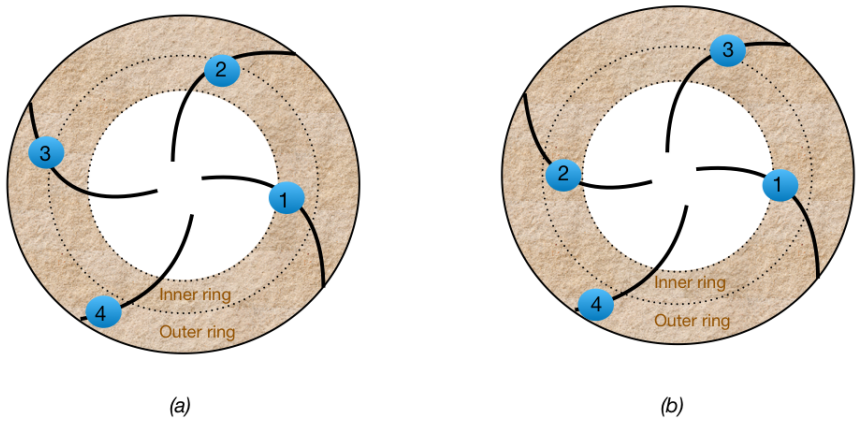

Figure 7.41: (a) Traditional cutter layout. (b) New cutter layout.

7.4.3 3D Bit Modeling

Two drill bits were designed for this year's competition, in collaboration with Lyng Drilling (a Schlumberger company). The main reason for creating two designs was to test the effect of gauge length on steerability and later choose the one that performs best.

This section demonstrates how the NTNU team was able to design the bit using the commercial modeling software SolidWorks. All the previous design considerations were taken into account to reach the final designs

As a first step in the process, a 2D sketch needs to be created which includes all the features the 3D model will have. Once the 2D sketch is done, a 3D model is made. Since small details count in a miniature bit, one will almost always go back and forth between the 2D and 3D model until the final design is reached.

For clarity purposes, this section only walks-through the design steps of one of the bits. The alternative design is presented at the end of the section.

2D Model

The bit design starts with a 2D sketch that contains all the important features the bit will have, such as the bit profile and cutter layout. The bit diameter and length are introduced by defining the distance between the center axis and the gauge pad and the distance from the threads to the nose of the bit, respectively. Figure 7.42 shows the main features of the 2D sketch.

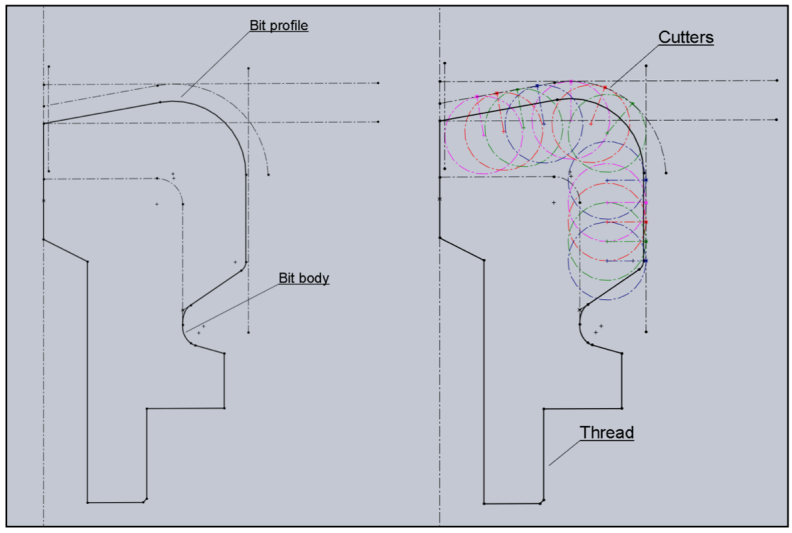

Figure 7.42: 2D sketch.

A short parabolic profile with a moderate deep cone angle was chosen to achieve more stability, together with a short gauge pad to increase steerability. To extend bit life over the testing phase, a total of 12 cutters were placed using a single-set cutter layout, which reduces cutter wear. Besides, cutter support was increased to avoid having chipped cutters, leaving a maximum depth of cut of 1.33 mm as shown in Figure 7.43.

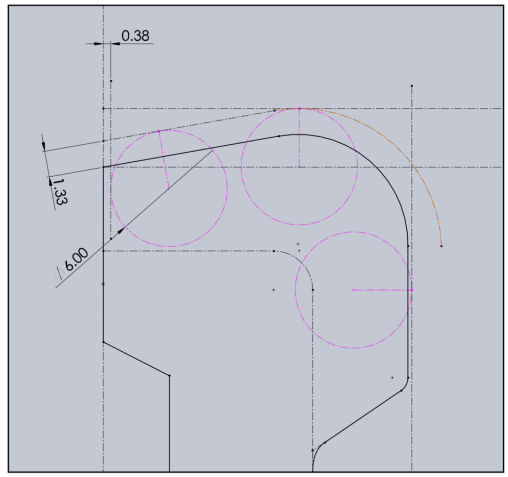

Figure 7.43: Cutter placement. Dimensions in mm.

As illustrated in Figure 7.44, a constant side rake angle of 10 degrees was chosen for all the cutters. Since the rock sample to be used at the on-site test is already known to be sandstone, it was decided to use different back rake angles. For those cutters at the bit's face, a constant back rake angle of 15 degrees was chosen to increase ROP as shown in Figure 7.45. However, for those cutters on the gauge pad, both depth of cut and side aggressiveness was reduced by choosing a back rake angle of 25 degrees. This way, the bit remains steerable and stable at the same time.

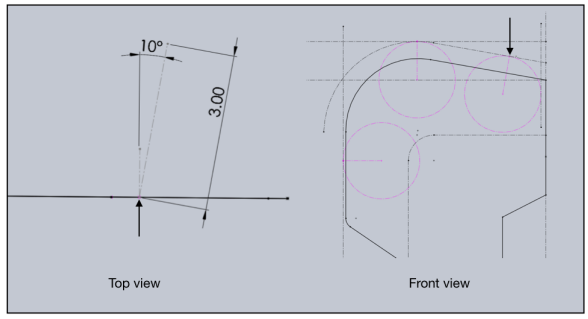

Figure 7.44: Cutter side rake angle. Dimensions in mm.

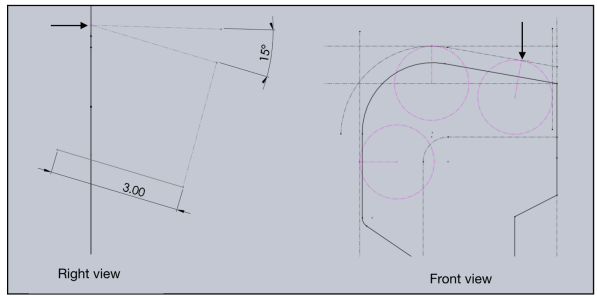

Figure 7.45: Cutter back rake angle. Dimensions in mm.

3D Model

Once the 2D model is finished, the 3D model can be started. By importing the 2D sketch into a new file, one can easily use the features incorporated in the software to start creating the bit.

The first step is to create the bit body by using the revolve feature around the center axis, as depicted in Figure 7.46. The bid body will serve as a foundation for the blade design, which is the next step in the process. To cut the formation smoothly and improve the cleaning efficiency around the blades and cutters, it was decided to design each blade following a 3D spiral that starts on the bit face and ends at the gauge pad. Once the blade is created, it is cut to follow the bit profile designed in the 2D model. Figure 7.47 shows these two steps in the blade design process.

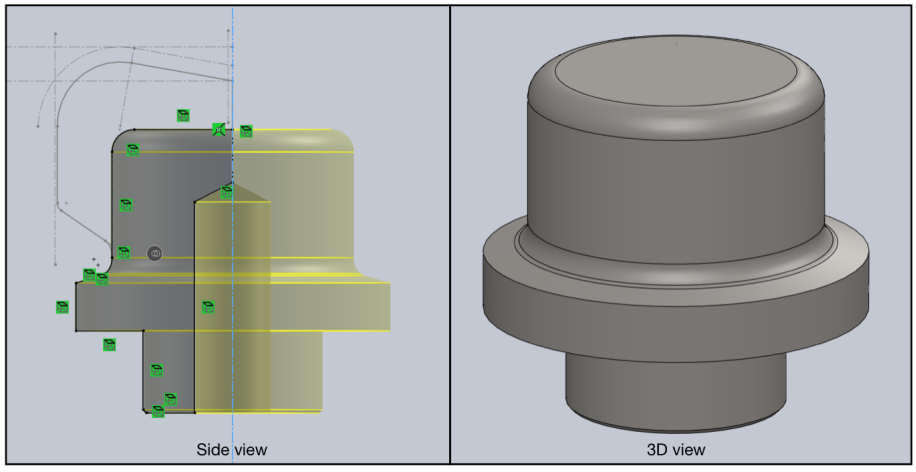

Figure 7.46: Bit body.

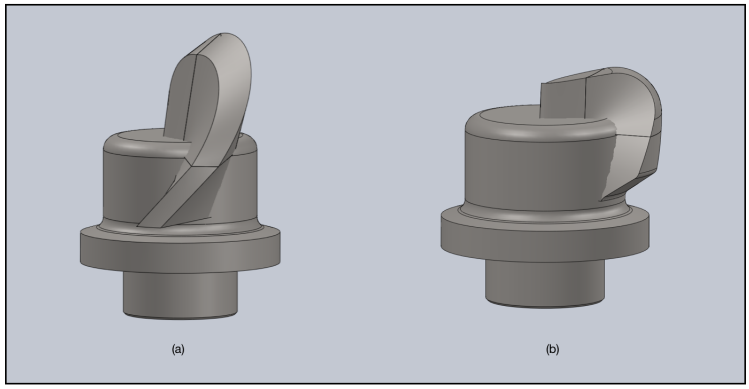

Figure 7.47: (a) Blade design principle. Notice how the blade front profile follows a three-dimensional spiral from the bit center to the gauge pad. (b) Finished blade after applying the bit profile from the 2D sketch.

After all, blades have been placed on the bit body, cutter sockets must be inserted on them. For this purpose, a 3D vector was created in the 2D model that results from the combination of the side rake and back rake angles. By using this vector, one can create a cylinder that resembles the dimensions of a PDC cutter. Keeping in mind the new concept introduced in Section 7.4.2, each cylinder is placed on the corresponding blade as shown in Figure 7.48. By removing these cylinders, each PDC socket is created.

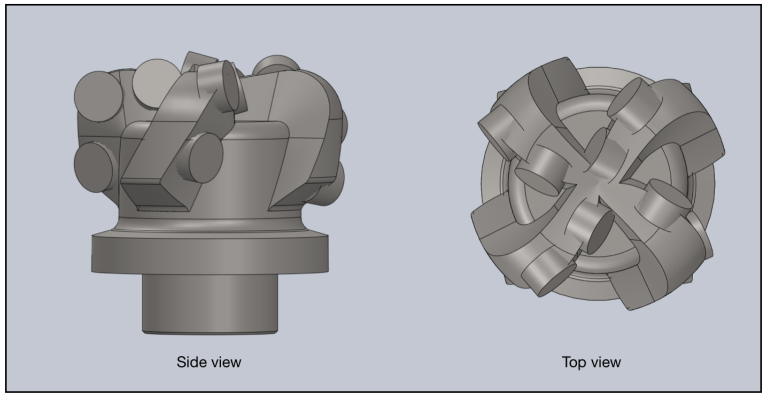

Figure 7.48: Side (left) and top (right) view of the bit showing how sockets that will hold the PDC cutters are created.

It is worth noticing that to increase the integrity of the blades, an angled cross-section was implemented and sharp edges were smoothed out to minimize stress concentrations.

The last step in the process is to create the bit nozzles. Since the miniature bit is 3D printed, curved nozzles were designed to improve the cleaning efficiency at the bit's face.

Once the nozzles are in place, the drill bit design is ready for 3D printing as Figure 7.49 shows. To visualize how to miniature bit will look like when all the PDC cutters are brazed in place, one can create an assembly such as the one shown in Figure 7.50.

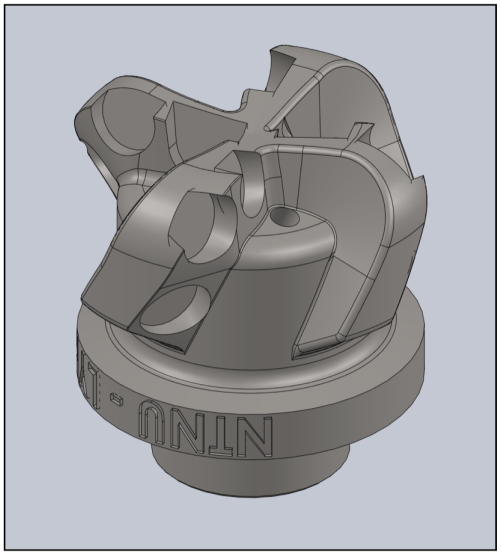

Figure 7.49: Miniature bit design ready for 3D printing.

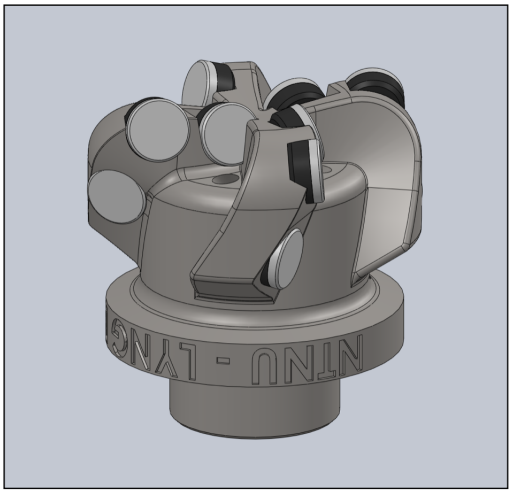

Figure 7.50: Bit design and PDC cutters in place.

Design Alternative

It was previously mentioned that an alternative solution was designed to test the effect of gauge length on steerability. The same modeling steps can be applied to this new design, only slight changes in the 2D sketch are needed. All the features on this new bit are exactly the same as the one previously discussed, except for the longer gauge pad. However, the additional length on the gauge pads provided an opportunity to include three TSP inserts, which generate a low friction surface and lateral control. Figure 7.51 shows the alternative bit design.

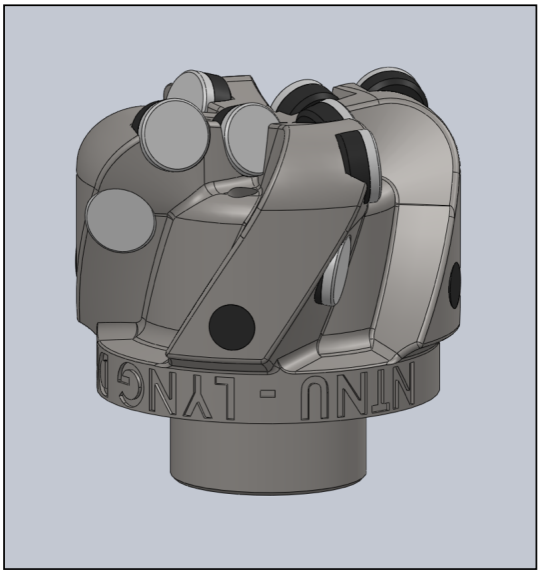

Figure 7.51: Alternative bit design.

Miniature Bit Summary

After having designed two custom bits, the NTNU team plans to test them together with the miniature bit provided by DSATS and an Alibaba bit. Table 7.2 summarizes the specifications for all the bits to be tested, which can be seen in Figure 7.52.

Bit specifications				
	NTNU bit (main)	**NTNU bit (alternative)**	**DSATS bit**	**Alibaba bit**
Bit diameter	1.25”	1.25”	1.25”	1.25”
Length	1.29”	1.3”	1.25”	1.9”
Weight	88 g	100 g	64 g	94 g
Blades	4	4	4	2
PDC cutters	12	12	4	2
Cutter diameter	0.236”	0.236”	0.323”	0.522”
TSP inserts	-	3	-	-
TC inserts	-	-	5	-
Nozzles	4	4	4	1

Table 7.2: Miniature drill bits specifications summary.

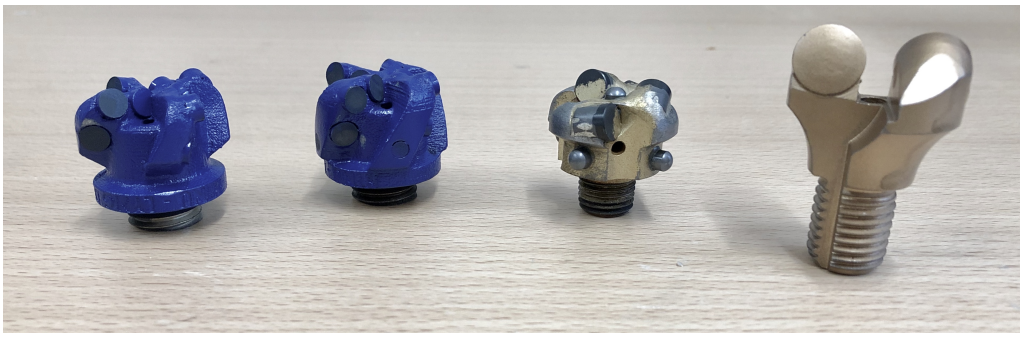

Figure 7.52: From left to right: main NTNU bit, alternative NTNU bit, DSATS bits and Alibaba bit.

7.5 Drill Pipe

When it comes to the drill pipe, the one used in the Drillbotics competition is far from mirroring that used on full scale rigs. Steel pipes are used in real life with higher cross sectional areas on the pipe joints, whereas slick aluminum pipes are used with the down-scaled drilling rig.

The aluminum drill pipe comes with its advantages and disadvantages. Since the hole to be drilled this year is deviated, having a flexible aluminum drill pipe helps building the angle needed to reach the target depth. It was previously tested [35] that having a steel

pipe of about the same dimensions would have resulted in plastic deformation for the pipe with the same inclination.

Two of the main drilling dysfunctions associated with the aluminum drill pipe are pipe buckling and twist off. Buckling issues are likely to arise when the pipe is subject to axial loads that exceed its bending stiffness, which is a function of the Young's Modulus and Moment of Inertia. Since the WOB to be used in the competition is well below the bending stiffness of the pipe, it is safe to say that buckling is not going to be an issue this year.

In this year's competition, the drill pipe will not be rotated all the time, only when drilling the 4-inch vertical section of the well and with a maximum of 150 rpm coming from the servo motor. Twist offs are unlikely to happen at these speeds.

7.5.1 Drill pipe connections

The drill pipe connections to be used this year are the same as the ones used by the NTNU Drillbotics Team last year. These connections are shown in Figure 7.53 and so far they have worked well for the Drillbotics rig. Figure 7.54 shows where these connections are needed in the rig, one at the top that connects to the hydraulic swivel and one at the bottom that connects to the BHA.

Figure 7.53: Drill pipe connector from Vertex.

Figure 7.54: (Left) Top drill pipe connection. (Right) Bottom drill pipe connection.

Chapter 8

Downhole Measurements

In this year's Drillbotics competition, downhole measurements are mandatory, as stated in the guidelines (Appendix A). To achieve this purpose, a downhole sensor card containing a triaxial accelerometer, gyroscope and magnetometer has been used. The inclination of the well is measured by the accelerometer and the azimuth with the magnetometer and accelerometer combined. The sensor card will be placed in the BHA inside the top stabilizer, as shown in Figure 8.1. The wires will exit the sensor slot from the bottom and turn 180 degrees to go inside the drill pipe and connect at the top to the electric swivel.

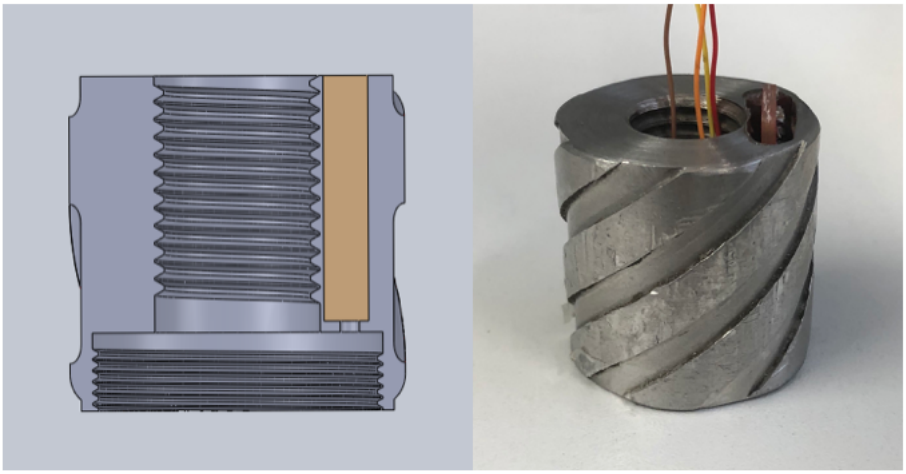

Figure 8.1: (Left) Cross section of the sensor sub where the sensor card will be placed. (Right) Current sensor sub with the sensor card in place.

8.1 Survey Calculation

To accurately predict the wellbore position relative to the rig's site, several survey calculation methods exist nowadays in the drilling industry. A standard within the industry which provides accurate results is the *minimum curvature method*. However, in the current master thesis, a different approach will be used to get azimuth, inclination, and tool face.

This method employs different frames which are needed to get these three values. Each frame is located in a different place on the rig (except for the "world frame") and can be seen in Figure 8.2. The "world frame" (black) is a position-less frame that has the X-axis aligned with the magnetic North. An "inertial frame" is then aligned with the "world frame" and placed on top of the rock sample. A "body frame" (red) is fixed and aligned with the sensor card tool face. The "rig frame" (green) is used to align the rig with the magnetic North. Finally, the "servo motor frame" (purple) is a moving frame that was meant to be used when steering the BHA, but since the drill pipe is twisted while drilling it was decided not to use it.

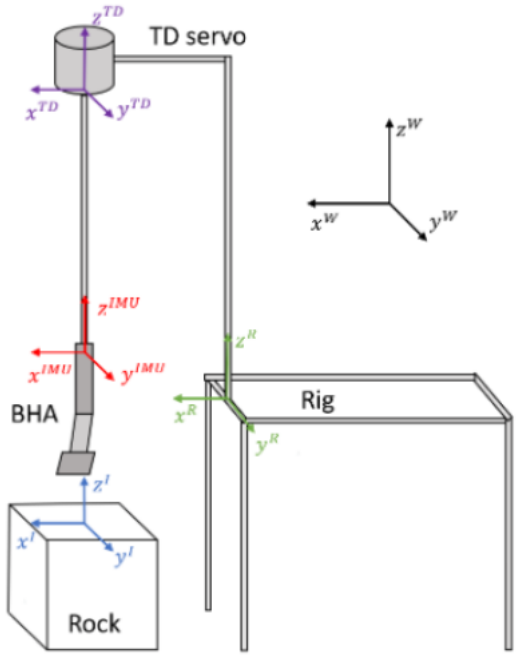

Figure 8.2: Different frames used to calculate the azimuth, inclination and tool face. [37]

To continuously measure the inclination, a rotation matrix is used to describe the orientation of the body frame relative to the inertial frame. Then the angle between the Z-axis of

the body frame and the inertial frame can be retrieved from this matrix and therefore, get the inclination.

In the case of azimuth, both the accelerometer and magnetometer are needed. By projecting the Z-axis of the body frame into the horizontal plane, one can get the azimuth by measuring the angle between the projected vector and the magnetic North. Since the sensor card is placed inside a steel sub and it is surrounded by other static and moving steel parts, there is a lot of magnetic disturbance on the magnetometer side of the card. This is why an electromagnet will be placed outside of the rock to serve as an active magnetic ranging method to help guide the drill string inside the well, Figure 8.3 illustrates the current setup on the rig. Since the magnetic strength varies approximately with the inverse of the squared distance to the source, the closer the tool gets to the electromagnet, the more the control system corrects the toolface of the BHA.

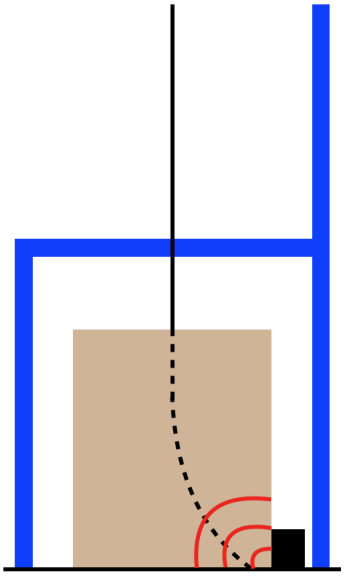

Figure 8.3: Active magnetic ranging setup. The electromagnet (black) is placed on the floor next to the rock sample and helps the sensor card correct any magnetic disturbance.

When it comes to steering the BHA to maintain the direction of the well, the calculated toolface plays an important role. Before the drilling operation starts, the body frame is calibrated relative to the inertial frame. However, there is also an offset angle between the toolface of the sensor card and that of the bent housing, as illustrated in Figure 8.4. Therefore, by drawing two scribe lines one can measure this angle and rotate the body frame accordingly. Once the body frame is aligned with the inertial frame, any deviations from this initial calibration can be measured by the control system and corrected using the position controller and servo motor.

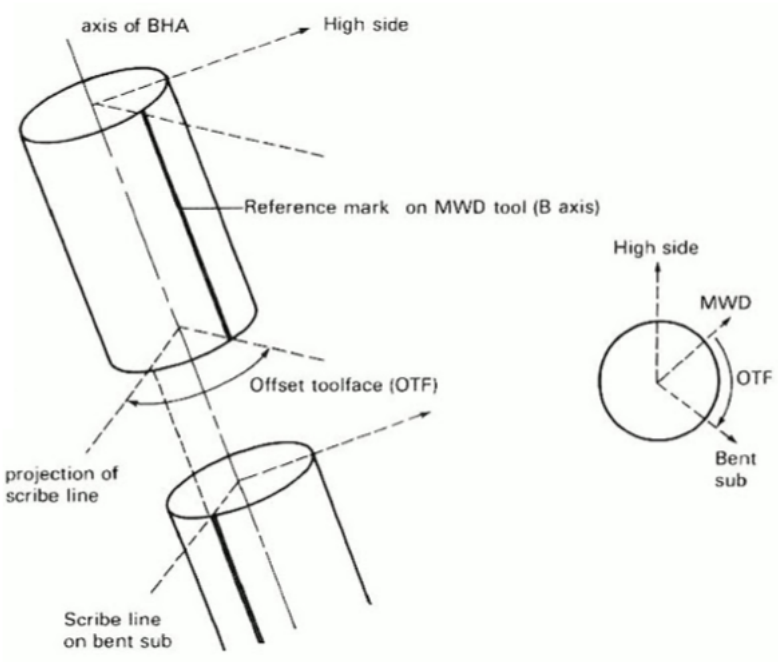

Figure 8.4: Toolface offset between the sensor card and the bent housing. [27]

Chapter 9

Instrumentation

An autonomous drilling rig is an assembly of various electrical and mechanical equipment. All these equipment are incorporated with each other in order to make the rig fully functional. In this chapter all the electrical equipment (and components), its application in the rig and communication protocols are discussed.

9.1 Components of the System

The overall system consists of several motors, drives and sensors. The motors installed are hoisting motor, top drive servo motor and the pump motor. The communication of these motors (through their drives) with the computer is setup using a Modbus adapter and LabVIEW. The sensors used in the rig are load cell, pump pressure sensor, tank level sensor and the solenoid valve. All these sensors are communicated with the computer through NI USB 6212. In this section, all the electrical components, their drives and communication are explained. The overall communication of all the motor drives and sensors with LabVIEW is illustrated in the flow chart in Figure 9.1.

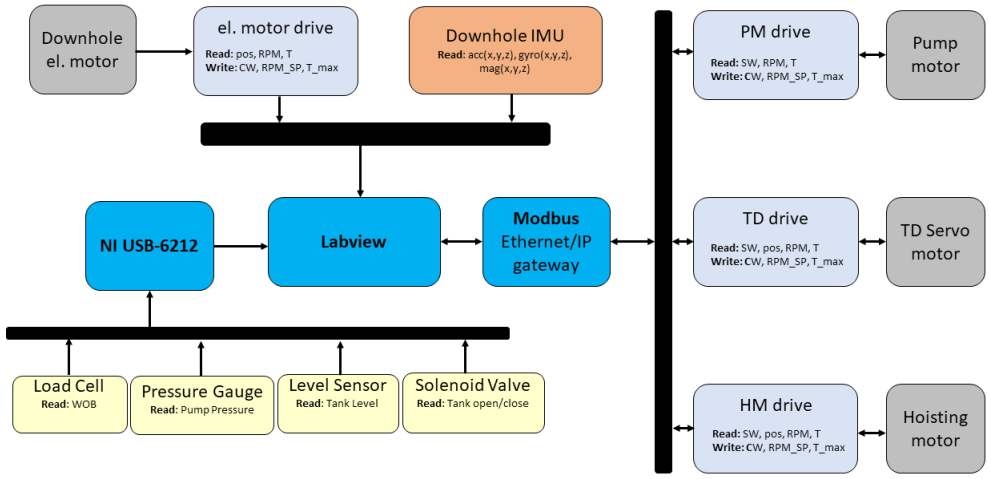

Figure 9.1: Communication flow chart

9.1.1 Hoisting Motor

The hoisting motor is responsible for hoisting the drill string up and down, putting WOB on the rock sample and providing ROP measurements. The hoisting motor on the rig is **Lenze GST 03-2M VBR 063C42** which is connected via a frequency converter **Lenze 8400 Topline C**. The motor is capable of delivering a maximum output power of 0.75 kW. The working frequency for the motor is 120 Hz with a maximum rotary speed of 3400 rpm and a maximum nominal torque of 4.68 Nm. It is connected to a ball screw to convert the rotational motion into linear motion. The gear ratio between the RPM of the hoisting motor and the ball screw RPM is 8.935.

Hoisting Motor Drive The drive used for the hoisting motor control is Lenze 8400 Topline C. The torque and RPM of the hoisting motor are measured by the integrated sensors present in the motor. The drive controls the current and the frequencies for the motor to operate at specific speed and torque. The output signal through the hoisting motor is in voltage which is then changed to torque and RPM. The torque and speed values are first converted to 0-10 V range and then converted to 0-0.468 Nm of torque signal and 0-3400 RPM signal.

The position of the drill string (through the motor rotation) is estimated by the combination of load cell lead and the incremental encoder output of the motor. The hoisting motor and its drive are shown Figure 9.2.

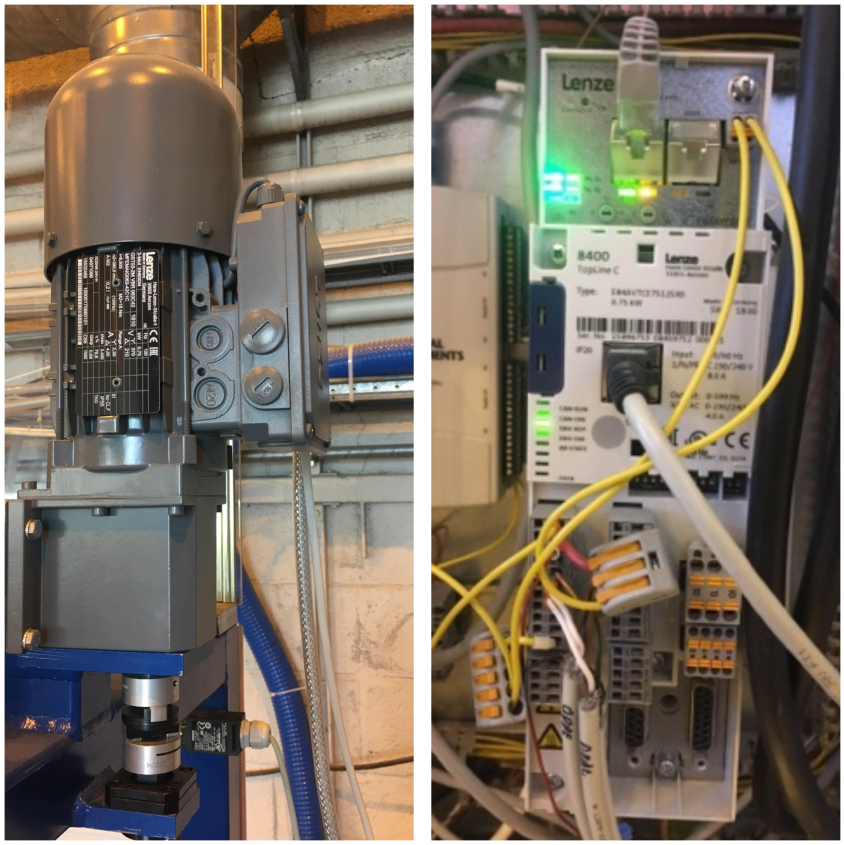

Figure 9.2: Hoisting motor and its drive

Communication The communication of the hoisting motor with the computer is set up with its drive through a Modbus communication protocol. To set up the communication, the motor drive is connected via Ethernet/IP module which establishes the communication using Modbus TCP/IP protocol. A client-server hierarchy is set up between the LabVIEW interface and the drive. This hierarchy allows the server (drive) to perform task(s) only if it gets a request from the client (LabVIEW interface). A wide variety of information can be extracted from the holding registers of the drive. However, the torque and RPM of the motor are desired parameters. The communication protocol also allows to write to the coils of the motor and a binary control word is necessary to be written first to the coil to enable the control. The first bit of the control word is set to zero, which avoids internal PID controllers in the drive from working constantly when not necessary and disables the motor. The LabVIEW code for the communication of hoisting motor is shown in Figure 9.3.

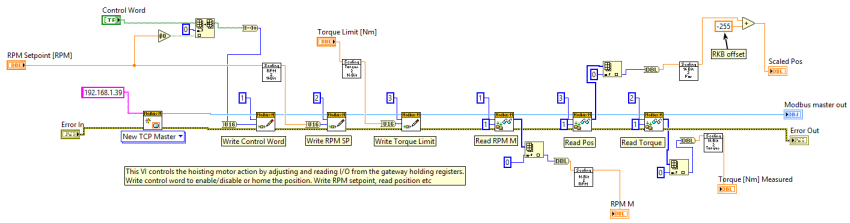

Figure 9.3: Hoisting motor communication SubVI block diagram

In the figure above, the block on the left initiates the code by establishing a master instance which controls the hoisting motor present at the given IP address. The control word, RPM set point and torque limit for the motor can be written in the next three blocks, respectively. The last three blocks read the RPM, position and torque of the motor. The ROP is estimated separately from the current position of the motor calculated through Figure 9.3. The code in Figure 9.4 shows the estimation of ROP.

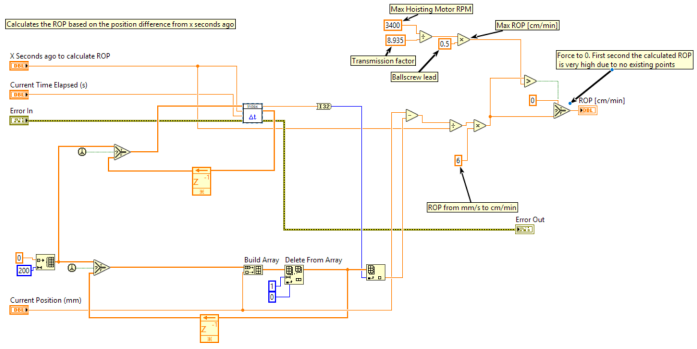

Figure 9.4: ROP estimation from hoisting motor position

Since the hoisting motor is also used to apply WOB, the weight applied is measured by a load cell. A WOB controller is formulated which incorporates both the load cell and the hoisting motor in the same code. WOB controller is a PID controller which tries to keep the WOB close to the set value and stops it from over-shooting. A detailed description of the control is presented in chapter 10. The code for WOB controller incorporating hoisting motor and the load cell is shown Figure 9.5.

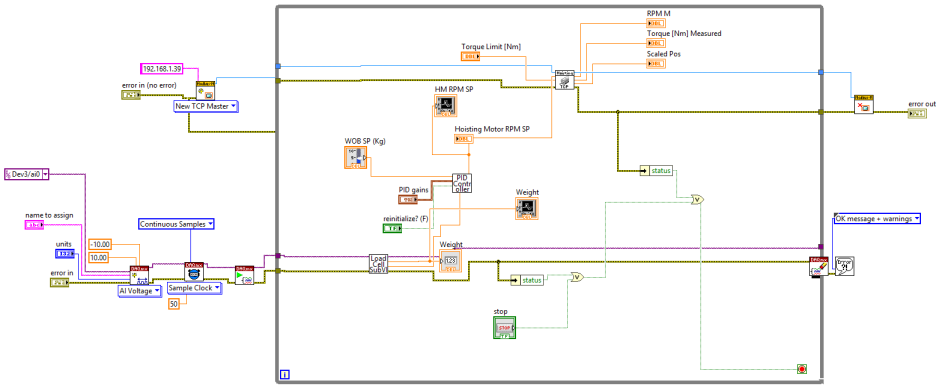

Figure 9.5: WOB controller through PID

The top left block in Figure 9.5 initializes the hoisting motor and bottom left block calls for the load cell, the weight measured by the load cell gets into the PID controller subVI in the loop and compares that value with the set point and then PID operates the hoisting motor accordingly.

9.1.2 Servo Motor

The servo motor acts as the main component in the rotary system of the rig. The top drive electrical motor has been replaced with the top drive servo motor due to the need of precise orientation of the toolface. The servo that is installed on the rig is **Schneider Electric BSH1003P31A2A**. The motor rated for 2 KW power with the nominal speed of 2000 Nm. The maximum torque that it can provide is 28.3 Nm whereas it stalls at 8.34 Nm of continuous torque. The speed and torque provided by the motor are suited for rotary drilling.

Top Drive for Servo Motor The drive used to control the servo motor is **LXM28AU15M3X**. The rated voltage supply is 3-phase 220 V with a supply frequency of 50/60 Hz. The torque and RPM provided by the servo motor is measured by integrated sensors. The internal PID controller in the drive controls the current and frequencies to operate the motor at set limits. The servo motor and its drive are shown in the Figure 9.6.

Figure 9.6: Servo motor and its drive installed on the rig

Communication The communication of the top drive servo motor is set up using CANopen communication protocol. The CANopen communication of the drive was done by lab engineer Steffen W. Moen.

9.1.3 Pump Motor

The pump and its motor are the main components in the circulation system of the miniature rig. The pump **Hawk HC980A** with the motor **VEM motors Thurm GmbH K21R 112 M-6** is connected through **ABBACS880-01-05A6-3**. It gets water from the water tank placed nearby. The importance of flow rate and pressure has increased in this year's competition due to the use of downhole positive displacement motor which works with high flow rate and pressure.

The pump is capable of delivering 140 bars of pressure. The motor that runs the pump is capable of providing 2955 RPM with a maximum power factor of 74%. The output power from the motor is 2.2 KW and 2.6 KW at 50 Hz and 60 Hz, respectively. The overall efficiency of the pump motor is however, 86%.

Pump Motor Drive Since, for this year's competition, the pump motor is implemented in the control loop. The drive that has been used previously for the pump motor was not good enough for this. The team decided to use the previous top drive for the pump motor to control it automatically. The pump motor drive is now "ABBACS880-01-05A6-3" which is capable of controlling the RPM and torque of the motor. The integrated sensor package of the motor provides the measurement for RPM and torque. The internal PID controller in the drive takes the values of RPM (and torque) from the motor sensor, compares with the set point and controls the speed through frequency and current to keep it running at setpoint values.

The pump motor and its drive are shown in Figure 9.7.

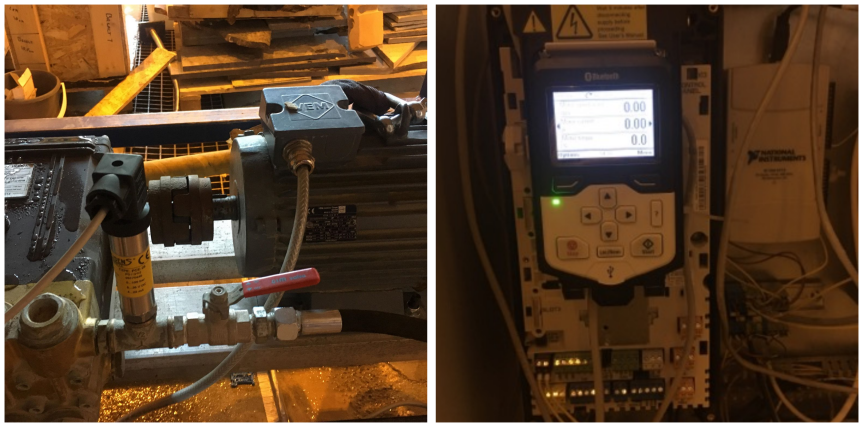

Figure 9.7: Pump motor and its drive installed on the rig

Communication The pump motor communication with the computer is set up with its drive via Modbus communication protocol. The pump motor is connected through Ethernet/IP cable the same way as the hoisting motor. The communication protocol is Modbus TCP/IP which creates a client-server hierarchy to control the drive. The holding registers of the drive allows for the reading of various measurements. However, only RPM and torque readings of the pump motor are desired measurements. The internal PID controller of the drive allows to write the set point for the RPM, so the holding register was set up to give required values of RPM to the drive. Figure 9.8 shows the code for the pump motor communication with its drive through LabVIEW.

The block diagram for the pump motor control is similar to the hoisting motor where the leftmost block starts the code by establishing the master instance to control the pump motor located at the specific IP address. The next blocks first write the control word and RPM set point on the holding register and then read RPM, torque and the status word in the next blocks.

If the set point of the pump motor has been set to zero, the shutdown control word is written to the coils of the drive to turn it off. The reason for doing this is to prevent the

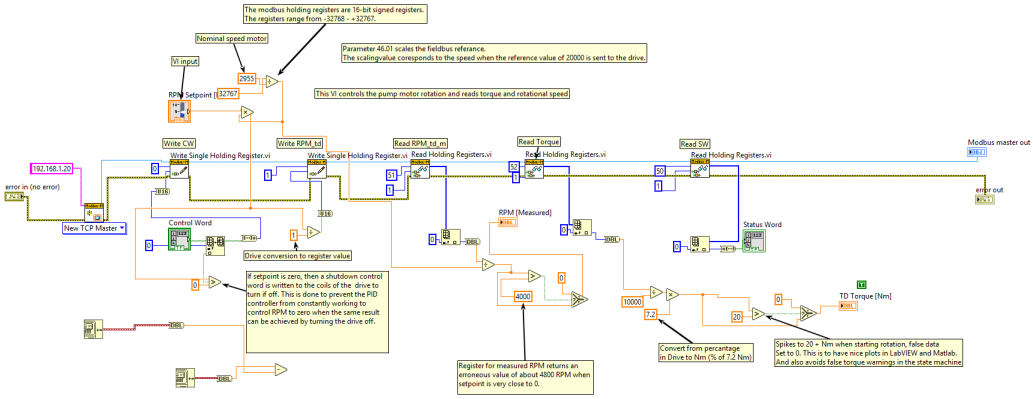

Figure 9.8: Pump motor communication SubVI block diagram

PID controller from working constantly to keep RPM at zero, while the same results can be obtained by simply turning the motor off.

The pump pressure is monitored continuously by a pressure transducer installed at the downstream of the pump. Figure 9.9 shows the combination of the pressure sensor with the pump motor. This SubVI can also be converted into a pressure controller by implementing a PID controller, the same way it was done with the WOB controller.

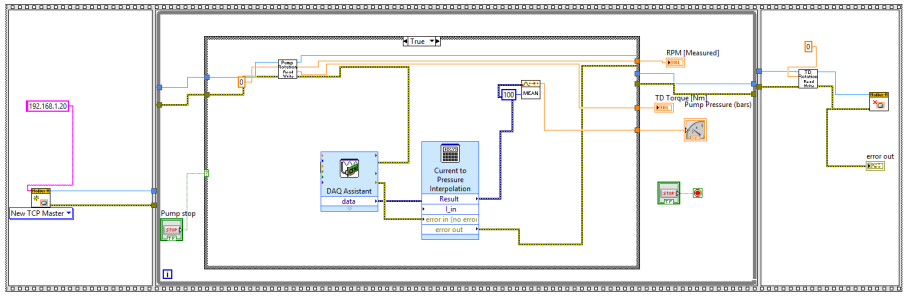

Figure 9.9: Pump motor combined with pressure sensor block diagram

9.1.4 Load cell

The load cell is the WOB measuring sensor that is mounted on the ball screw nut bracket around the ball screw. The hoisting motor is used to put WOB that is measured by load cell. The load cell used on the rig is AEP Transducer **TC4-AMP** and shown in Figure 9.10. It is a force transducer that converts the force from the hoisting motor into a voltage signal, that voltage signal is then interpolated into WOB readings.

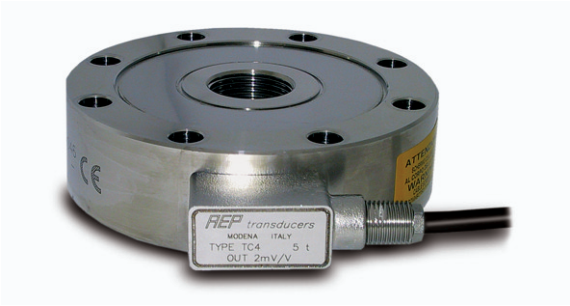

Figure 9.10: AEP TC-AMP cylindrical load cell

Last year's team decided to change the position of the load cell, the setup was analyzed this year as well. The currently installed hollow load cell around the ball screw works fine, therefore it was decided to use the previous setup of load cell and its mounted position for this year as well. Figure 9.11 shows the position of cylindrical load cell on the rig.

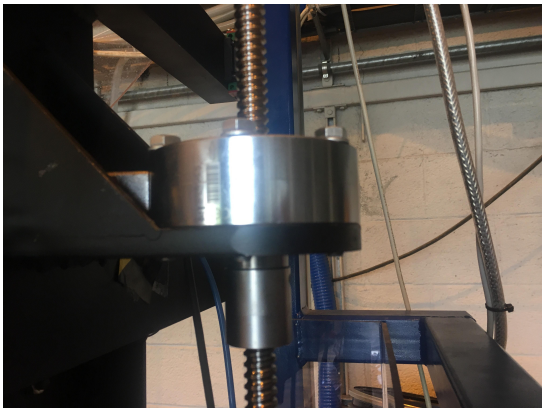

Figure 9.11: Load cell mounted on the rig

Communication The load cell is connected to the computer via NI USB-6212 Multi-function I/O (see section 9.2.1 for details). It is a force transducer that gives the output of the force in the form of an electrical signal. When the WOB is applied on the load cell through the ball screw, the force deforms the strain gauge inside the load cell. The deformation in the strain gauge is measured as change in electrical signal. The continuous change in electrical (voltage) signal is measured by the NI USB and then interpolated to the weight measurements. The range of the load cell is +/- 5 kN, that is converted from the differential input voltage of +/- 10V. The linear interpolation equation of voltage to weight on bit in kg will be:

$$WOB = -509.7\ kg + \frac{V_{in} + 10\ V}{20\ V} 1019.4\ kg \tag{9.1}$$

Figure 9.12 shows the code for the weight measurements from the load cell.

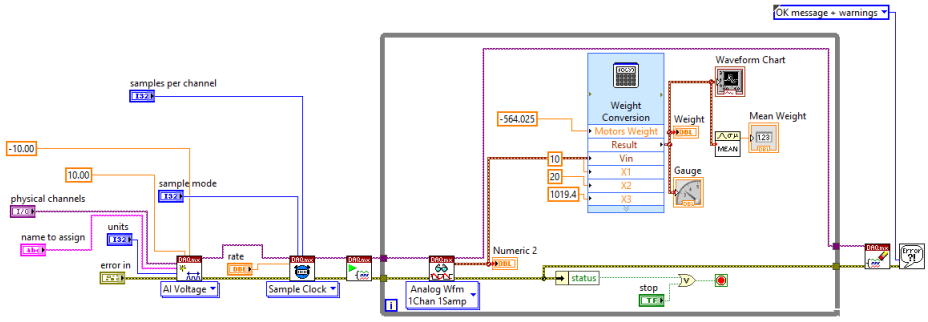

Figure 9.12: Load cell communication block diagram

The blocks outside the loop initiate and read the specific port of the USB where the load cell is wired. The voltage signal is then read in the form of an analog waveform and then converted to the weight on bit measurements through linear interpolation as shown in Equation 9.1.

9.1.5 Pump Pressure Sensor

A pressure sensor **Aplisens PCE-28** is installed downstream of the pump. Due to the introduction of the pump in the control loop and the use of PDM in the BHA (that needs specific pressure drop to get desired torque), the internal measurements of pressure has become important. The pressure sensor has a maximum limit of 100 bars, which is within a designed system pressure limit as maximum pressure in the system during the testing has not increased to 40 bars. The position of pressure sensor on the rig is shown in Figure 9.13.

Figure 9.13: Pressure sensor installed on the rig

Communication The pressure gauge is a pressure transducer that is connected via USB-6212 Multifunction I/O. It converts the pressure into an analog electrical signal. The conversion of pressure into the electrical signal takes place by the physical deformation of strain gauge present in the sensor's diaphragm. The analog current signal is of the range of 4- 20 mA which is converted into the 0-100 bars of pressure by interpolating linearly within the pressure range of the sensor using the equation below:

$$p = \frac{i_{in} - 4\ mA}{20\ mA - 4\ mA} 100\ bar \tag{9.2}$$

Figure 9.14 shows the code for the communication of the pressure sensor in the LabVIEW.

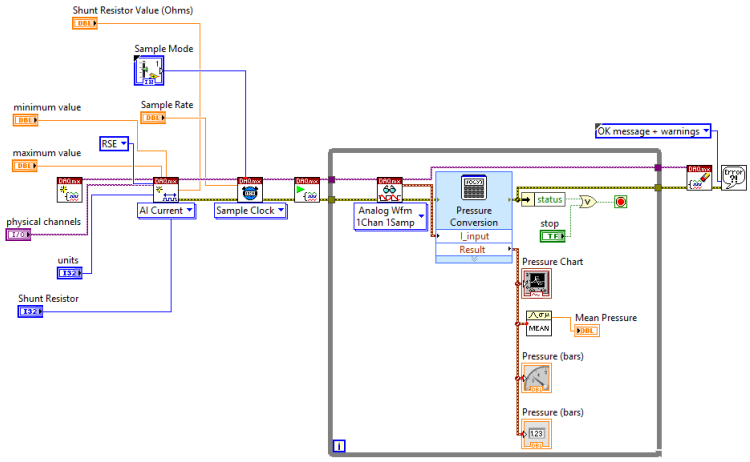

Figure 9.14: Pressure sensor communication block diagram

9.1.6 Tank Level Sensor

As described in 7.2.1, a water tank will be used in the circulation system to provide the water to the pump for its flow in the system. The monitoring of water level in tank is done by pressure sensor **IPSL-G0100-5**, mounted at the bottom of the tank, hence used as a level sensor. The sensor can measure a maximum hydrostatic pressure of 100 mbar which is in the range of static water column pressure in the tank. Figure 9.15 shows the pressure (level) sensor installed on the rig.

Figure 9.15: Pressure (level) sensor installed on the tank

Communication The level sensor is actually a pressure transducer that converts the pressure into the analog current signal. The working principle is explained in the pump pressure sensor section above. The electrical signal is converted to the pressure by linear interpolation described in Equation 9.2 and then pressure is converted to the height of water column by $h = \frac{P}{\rho\, g}$. Figure 9.16 shows the block diagram of the level sensor in the LabVIEW.

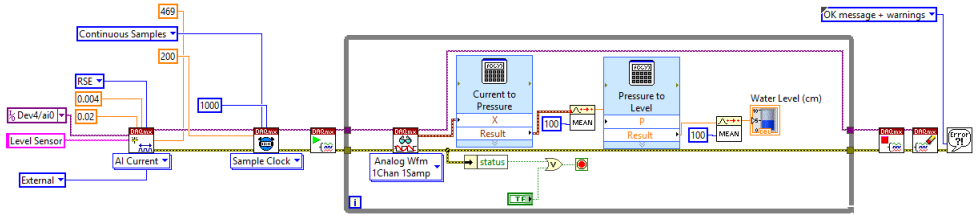

Figure 9.16: Pressure (level) sensor communication block diagram

9.1.7 Solenoid Valve

The water tank is filled continuously from an external water supply to keep the desired water level in the tank. A solenoid valve is installed on the tank that opens and closes automatically when the required water level in the tank is reached. Figure 9.17 shows the solenoid valve installed on the tank.

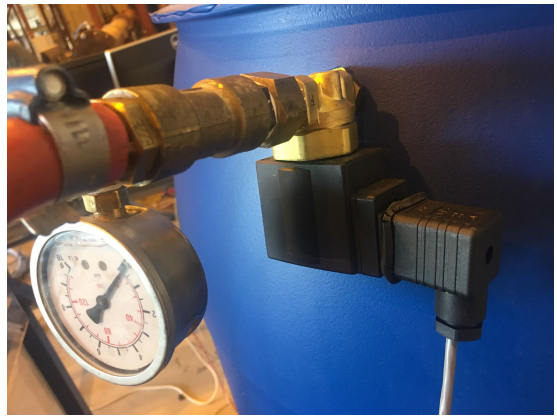

Figure 9.17: Solenoid Valve installed on the tank

Communication The solenoid valve is connected via USB-6212 Multifunction I/O same as other topside sensors. Instead of acquiring the signal as in other sensors, a digital signal is generated that operates the solenoid valve.

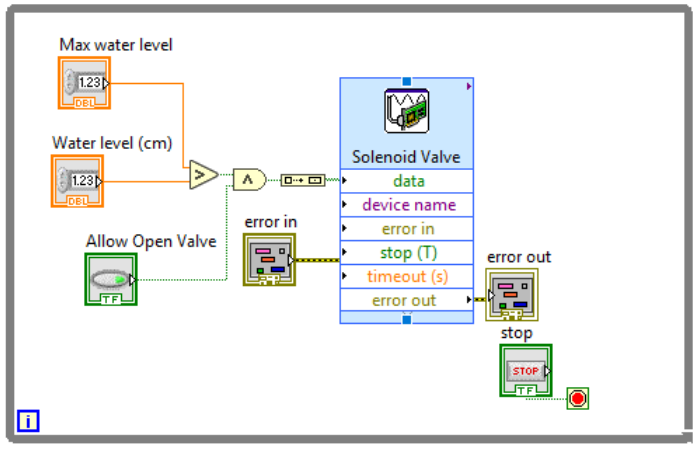

Figure 9.18: Solenoid valve communication block diagram

The minimum and maximum water level for the valve opening has been set up with a Boolean logic. If the current water level is less than the set point then a current signal will activate the valve and it will open. Similarly if the water level gets above the set limit the valve will close automatically.

9.1.8 Downhole EMM

As discussed earlier, the EMM with the bent housing is one of the options as a directional tool. The EMM is from "Maxon Motors" of model **DCX19S GB KL 48V** with the gearhead of **GPX19HP**. The motor comes with different sensors such as position, velocity and torque sensors. The motor is customized by installing a gearhead to increase the nominal torque. With the gearhead installed, the motor can operate at maximum 87 rpm with 0.80 Nm of nominal torque. An illustration of the EMM is shown in Figure 9.19, whereas the detail description of its design and technical specification can be seen in Appendix D.

Figure 9.19: Illustration of EMM

EMM Drive The drive used to operate the EMM is **EPOS4 Module 50/5** which is dynamic OEM positioning controller module. The drive has the capability to operate the motors with up to 250 W. Since the operating voltage for the drive is between 10 and 50 V, a step-down transformer is attached with the drive as shown in Figure 9.20. The torque and the speed of the motor is measured by the integrated sensors installed inside the motors. The drive controls the current for the motor to operate the set RPM and torque. A detailed description of all the specifications of the EMM drive can be found in Appendix E.

Figure 9.20: El. motor drive with the transformer kit

Communication The communication of the EMM with the computer is set up via USB. The power wires from the EMM are fed into the drive which controls the current for the motor to operate it at set torque. The subVI to control the motor's torque is shown Figure 9.21.

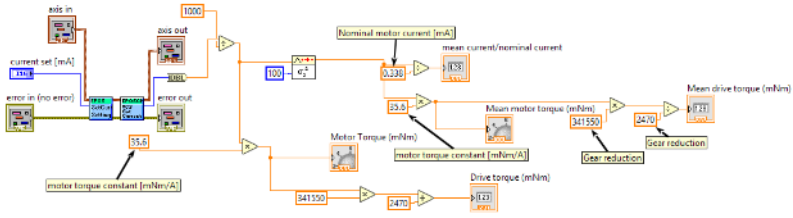

Figure 9.21: El. motor communication SubVI block diagram

The current control subVIs are pre-built by the supplier. The torque is kept at the set point value through the internal PID controller in the drive.

9.1.9 Downhole Sensor

Downhole measurements are mandatory for this year's competition. According to competition guidelines, any team with no downhole measurements will be considered fail. Therefore, the team spent plenty of time and care for the downhole measurements and its communication topside.

The sensor card used for the downhole measurements is shown in Figure 9.23 and Figure 9.24. The details of the components mentioned are described in Table 9.1.

Figure 9.22: TDK InvenSense ICM-20948 9-axis IMU [18]

Table 9.1: PCB components and specifications

Name	Product name	Details	Supplier
U1	REF3318AIDBZT	3,3V-1,8V DC/DC converter	Texas Instruments
U2	ICM-20948	9-axis MotionTracking device	TDK Invensense
U3	EFM32G210F128	Microcontroller	Silicon Labs
U4	CP2104	USB-to-UART-bridge	Silicon Labs
R1-2	1kω	Resistor	RS components
R3-4	10kω	Resistor (later changed to 1kω)	RS components
D1	X	LED diode	RS components
C1+C4-7+C9-12	C0603C105K9RACAUTO	1,0μF Capacitor	RS components
C2-3	C0603C105K9RACAUTO	0,1μF Capacitor	RS components
C8	C0603C105K9RACAUTO	100pF Capacitor	RS components

The downhole measurements are taken by ICM-2094 9-axis motion tracking device from TDK InvenSense as shown in Figure 9.22. This inertial measurements unit (IMU) contains 3-axis accelerometer, 3-axis gyroscope and 3-axis magnetometer. With this IMU in the sensor card, the downhole measurements such as azimuth, inclination and angular velocity and angular acceleration (vibrations) can be measured.

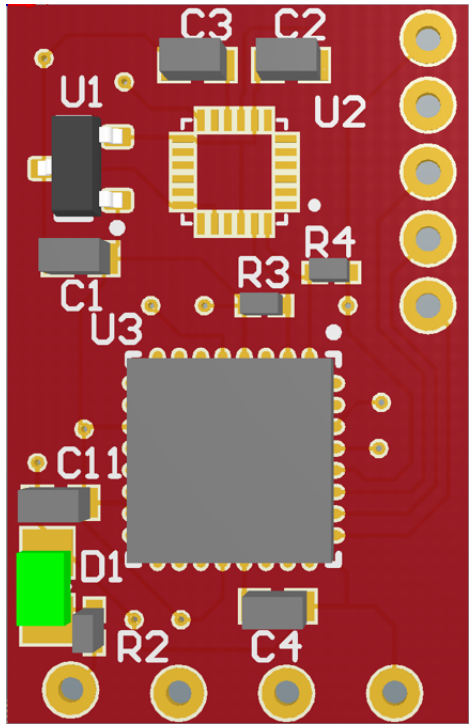

Figure 9.23: Sensor card with all the components (front view)

PCB Design The printed circuit board (PCB) has been designed in Altium Designer which includes the EFM32 Gecko microcontroller (EFM32G210F128-QFN32), ICM-20948 9-axis IMU and CP2104 USB-to-UART bridge as main components. Initially a sensor card of dimensions 15x25x4mm was designed for the initial testing phase. The size was compressed to fit in the BHA and order a pre-soldered board from a third party specialist like JLBPCB.

Top-side-Downhole Communication The downhole sensor is programmed in C to pump out time-series with sensor data at the given frequency. The top-side-down-hole communication is set up through a USB cable connected to the topside computer and soldered on the PCB. The communication with the LabVIEW is configured by the built-in VISA drive in the LabVIEW. The Proper wire-handling is conducted to prevent winding of the wire while drilling and a connection point is located in the electrical swivel.

The 11 pins circular plastic shell connector provided by “Omnetics” (as shown in Figure 9.25) is used to connect the power wires from EMM and the sensor card. The 2 power wires from EMM and 4 from sensor card (2 for power and 2 for data communication). All these wires pass through the BHA and the drill pipe and connect the wires from electrical swivel through the connector at the drill pipe connection point. The connector is then

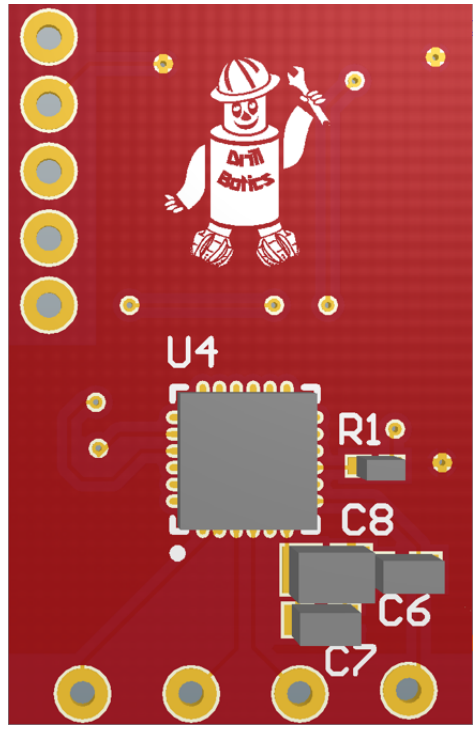

Figure 9.24: Sensor card with all the components (back view)

planned to sealed with the glued shrinking tube to avoid any circuit shorting due to water leakage inside the connectors. During testing, the team faced a lot of challenges regarding the downhole-top-side wiring and explained in Section 12.8.

NB For the detail description of downhole measurements and all the control system, a separate thesis is written by a Drillbotics team member [37].

9.2 National Instruments

In the Drillbotics projects, the control of motor drives and sensors are done by LabVIEW software provided by National Instruments. This section will provide a brief description about the NI USB-6212 that has been used to communicate with the sensors. The software package LabVIEW will be described in chapter 10.

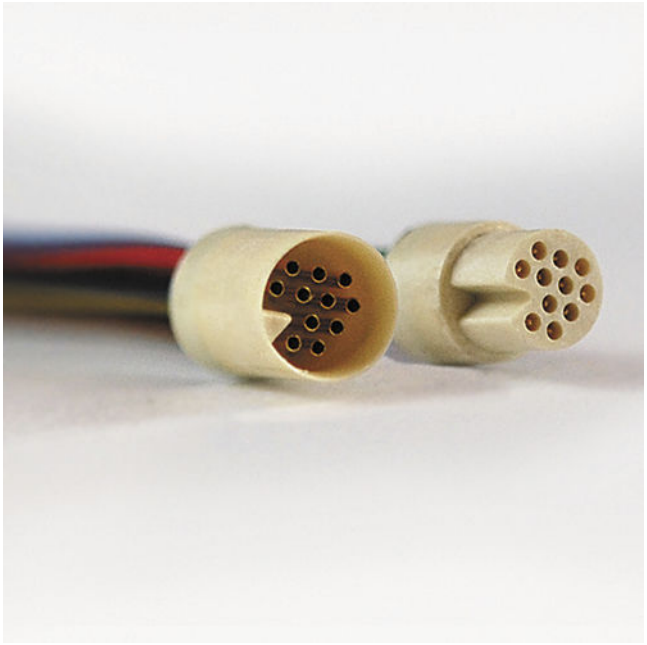

Figure 9.25: 11 pin circular connectors by Omnetics

9.2.1 NI USB-6212

As explained earlier, all the topside sensors are communicated via USB-6212. It is a multi-function DAQ device that can provide digital I/O, analog input and two 32 bit counters. The USB is shown in Figure 9.26.

The presence of onboard amplifier provides fast settling times at high scanning rates[9]. It features thin mechanical enclosure with a bus powered for easy portability.

Figure 9.26: NI USB-6212 for topside sensors

Chapter 10

Control system

10.1 Theory

The cybernetics student Mads Bertheussen Nåmdal has had the primary responsibility for downhole sensoring, PID controllers and filtering. A short description of the work done in these areas is included below. A more comprehensive overview of theory and testing relating to these subjects can be found in his master thesis [37].

10.1.1 Kalman Filter

The theory behind the use of a Kalman-filter to filter measurement data is described in the Phase I project report [35]. The relevant section can be found in Appendix F.

10.1.2 IMU Theory

The inertial measurement unit, or sensor card, outputs measured acceleration, magnetic field strength and turn rate, each in 3 axis. The accelerometer data has the unit $\frac{m}{s^2}$, the magnetometer microTesla and the gyroscope degrees per second. The accelerometer and magnetometer data are used to create a 3x3 rotation matrix which describes the orientation of the sensor card frame in relation to the world frame. This rotation matrix gives information on which direction the sensor card, and by extension, the BHA and drill string, need to be oriented in order to align with a world frame. The world frame can be defined as north-west-up, which correspond to the x-, y- and z-axis respectively.

In order to relate sensor card direction to drilled direction, an inertial frame is designed. This frame is fixed in relation to the rock, starting with the center of the frame at the center of the top of the rock, north is towards one of the 12” sides of the rock, with east being

perpendicular to the north. The rock should be oriented so that the inertial frame and world frame align.

The general Euler equation, equation Equation 10.2 [2], is used to calculate the position of the sensor while drilling.

$$R_{world}^{body} = \begin{bmatrix} r_{1,1} & r_{1,2} & r_{1,3} \\ r_{2,1} & r_{2,2} & r_{2,3} \\ r_{3,1} & r_{3,2} & r_{3,3} \end{bmatrix} \tag{10.1}$$

$$\vec{x_{k+1}} = \vec{x_k} + R \cdot ROP \cdot \delta t \tag{10.2}$$

Where ROP is the velocity of the sensor card along its z-axis, and the rotation matrix is required to relate the velocity in this direction to velocity along axis of the world frame. δt is the time elapsed between step k and k+1.

Tool-face is used to determine in which direction the BHA is facing. It can be found using equation Equation 10.3

$$Toolface = atan2(r_{2,1}, r_{1,1}) \tag{10.3}$$

10.1.3 PID Theory

A PID controller uses proportional, integral and derivative error to adjust a control variable, as shown in equation Equation 10.4.

$$u(t) = K_p \cdot e(t) + K_i \cdot \int_0^t \cdot e(\tau) d\tau + K_d \cdot \frac{de(t)}{dt} \tag{10.4}$$

Often, the integral and derivative coefficients are replaced by the integral and derivative time and the equation becomes Equation 10.5[43].

$$u(t) = K \left(e(t) + \frac{1}{T_i} \cdot \int_0^t \cdot e(\tau) d\tau + T_d \cdot \frac{de(t)}{dt} \right) \tag{10.5}$$

The proportional error is defined as the difference between the process variable and the set point, the integral error is the integral of this error over time, and the derivative error is the derivative of this error. These errors are illustrated in figures Figure 10.1,Figure 10.2 and Figure 10.3.

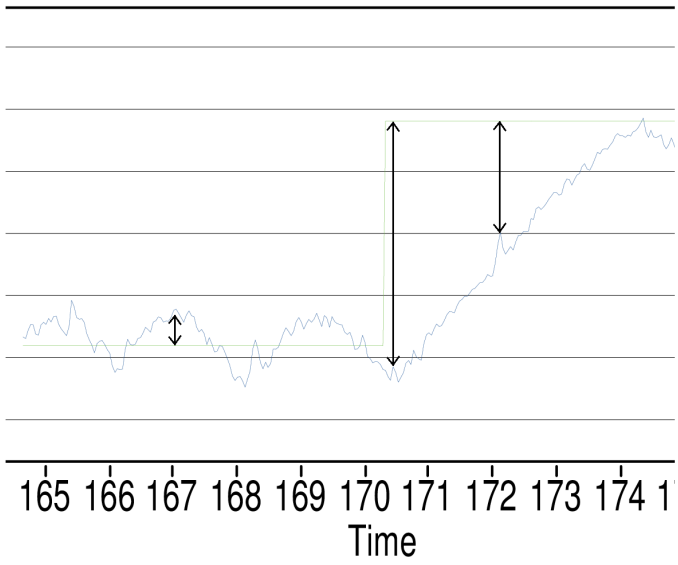

Figure 10.1: Figure illustrating proportional error

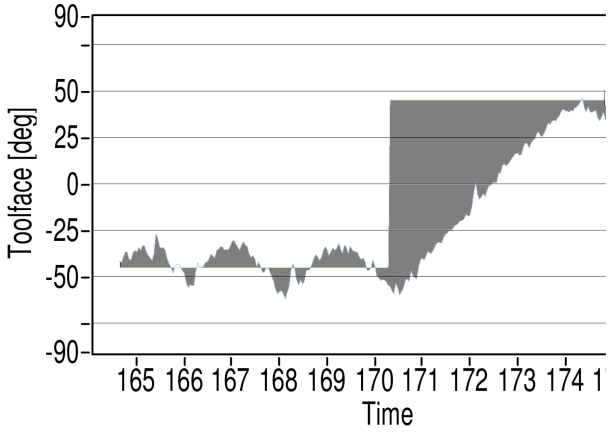

Figure 10.2: Figure illustrating integral error

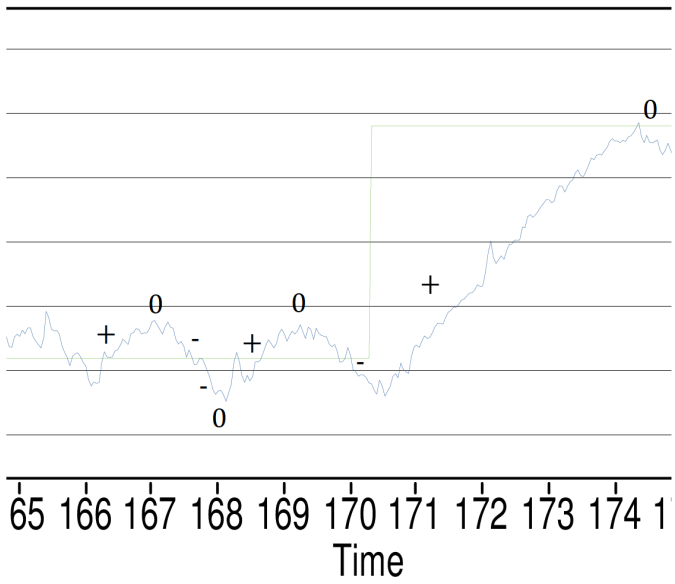

Figure 10.3: Figure illustrating derivative error

In a closed loop system, the system state is changed by the control action of the PID controller, though rarely in a constant manner. In the example of the WOB controller, the PID determines the hoisting motor RPM set point. The WOB that is measured by the load cell changes depending on the hoisting motor RPM, but also depending on drilling rate and friction in the system. The PID controller must therefore continuously adjust the hoisting motor speed to maintain a WOB set point while drilling. PID is also used for toolface control in the control system. In that case, the position of the top drive motor is the control variable, the toolface from magnetometer sensor readings is the process variable and the set point for the tool face will continuously be zero.

10.1.4 PID Tuning

A PID controller must be tuned before it can be used to control a system. This is done by adjusting the constants K_P, K_i and K_d in Equation 10.4. These constants are referred to as proportional gain, integral gain, and derivative gain respectively. A higher value for each of these constants ensures that the corresponding error affects the output from the PID controller more. The process of adjusting these constants to get an appropriately responsive controller is called PID tuning.

How responsive the controller should be, varies from system to system. However, there are some common traits of a well-tuned PID controller. A small overshoot is desirable when going from one set point to the next, as the controller otherwise tends to be very slow in reaching the set point. The settling time should be low, which means that the controller

should stabilize quickly at the set point and oscillations should not be long-lasting. The controller should not be too active, as frequent corrections will cause more wear to the actuators. There exists several methods and algorithms that can be used for tuning a PID controller, but once the effects of each of the gain constants are understood, good results can be achieved by manually adjusting the constants depending on the response from the system.

As a rule, higher gain constants will lead to larger corrections. Changing the proportional gain is often the first step in tuning. The proportional should be increased until there is little to no steady state error, but not so much that the system experiences excessive oscillations around the set point [30]. The derivative and integral gains are then adjusted depending on how the system reaches the set point. Oscillations around the set point will be dampened by a higher derivative gain, but a high derivative gain may lead to an overactive controller. Noisy or quickly changing data will limit the size of the derivative gain. A high derivative gain in a system with noisy data will lead to the PID controller trying to correct for the measurement noise.

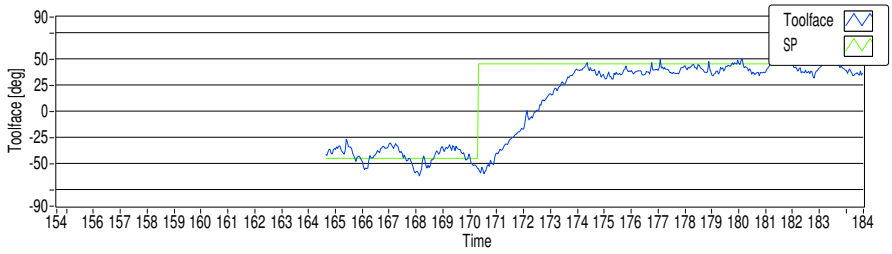

Figure 10.4: Figure showing a step response with a poorly tuned toolface PID controller

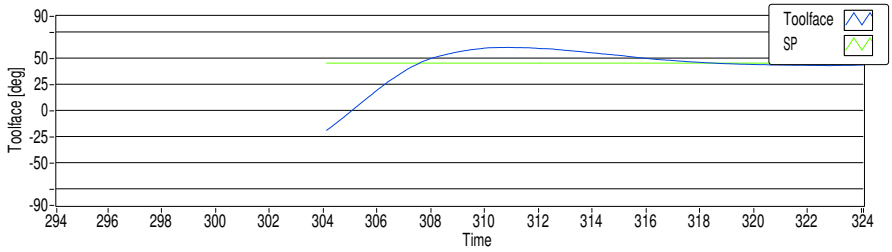

Figure 10.5: Figure showing a step response for a PID toolface controller which overshoots the set point

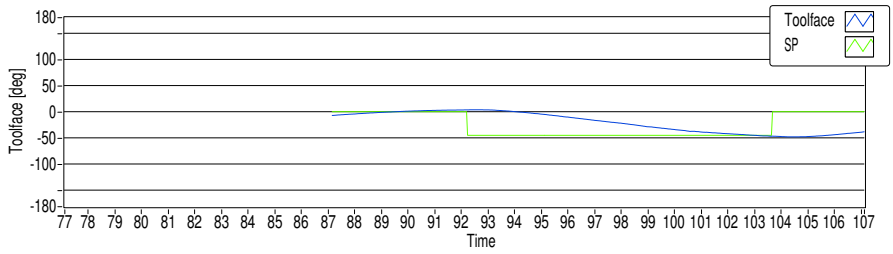

Figure 10.6: Figure showing a slow PID toolface controller step response, ideal for a slow system where overshooting is unwanted.

If the controller stabilizes parallel to the set point in a steady state control offset, the integral gain should be increased. [13]. The integral error grows over time as the accumulated area between the set point and the process variable increases. A larger K_i will, therefore, lead to the system closing the last gap between the set point and toolface quicker. Using an integral gain that is too high, will on the other hand lead to large overshoots if a long time passes from the controller is started until it can reach the set point, as the integral error from before the set point was approached is much larger than the proportional and derivative error when the process variable passes the set point. This build-up of integral error is called integral wind-up and can be limited by several methods. The integral gain can be set to a low value, the system can be brought close to the set point before starting the PID control, the output from the PID can be limited to a maximum value, or the PID can be reset when an unwanted wind-up is detected. All these alternatives have been used at some point in the control system.

Using knowledge about how the different gains affect the PID tuning, the PID controls have been tuned manually. By changing the set point and observing the behaviour of the controller, it is possible to see which constants need to be changed. The aim is to have slow controllers for both the WOB and the toolface. Neither of these controllers are expected to need to respond to any fast changes and frequent and large corrections will lead to more wear on the actuators. Additionally, overshooting the target with the WOB controller can possibly lead to the EMM stalling, which will require the control system to exit drilling mode and go into the safety sequence. If the PID controller then overshoots when returning to directional drilling mode, the controller will return to safety mode, thus getting stuck in a cycle of safety mode and hoisting up. It is therefore of the utmost importance that the WOB PID controller does not overshoot by much. If the toolface controller overshoots, the bit will be subjected to unnecessary side forces, which can easily cause stalling.

Some snapshots from PID tuning of the toolface controller are shown in Figure 10.4, Figure 10.5 and Figure 10.6. Figure 10.4 shows a step response with a poorly tuned toolface PID controller. Oscillations occur when the toolface approaches the set point, indicating that the derivative effect should be increased. The proportional and integral gains could also be increased, to achieve a small overshoot, thereby making the controller more reactive. Figure 10.5 shows a step response with a well-tuned PID toolface controller when first entering the orienting state after running the script. The toolface starts in a random

orientation after exiting vertical drilling mode, and quickly orients itself to the set point. The controller overshoots by around $15\mathrm{deg}$ and then settles without much oscillation on the set point. This overshoot is too large for this system and the proportional and integral terms may be reduced. Figure 10.6 shows another PID toolface controller during a step response. This controller is tuned to be slow and therefore, takes a long time to reach the set point. This would be bad for a WOB controller in a faster system, such as the one used in 2018, which needed to react quickly to formation changes and drilled at a higher rate and WOB. It is however a good tuning for the slow system of this year's competition. The profile of this tuning is therefore similar to the one that will be used during the competition run.

10.2 Implementation in Control System

10.2.1 Implementation of Filtering in Control System

Downhole sensor data and measured WOB are the most important measurements for the control system. These are filtered in an unmodelled Kalman-filter. The measurement variance, R, was found for WOB and the sensor by measuring the variance of the data when the system was kept still. The system was assumed not to change between measurements, so A=C=1. No input was added to the system, so the coefficients of the inputs can be considered to be zero. Finally, the process noise matrix was tuned manually until the filter reacted appropriately to changes while drilling. Q can be any value from 0 to positive infinity. A low Q will lead to a slower system, while a higher Q will lead to a faster one. It was found that values between 0 and 1 tended to be the best. Both the drilling rate and the need for quick position corrections are expected to be low. It is, therefore, preferable to err on the side of slowness when tuning the filter, as this minimizes the effect of process noise on the filtered measurements and does not impact drilling performance to any noticeable degree. However, this means that safety-related WOB warnings should be detected based on unfiltered data, or that the safety factors between the physical limits and the control system limits are sufficient to terminate the script if the true WOB should be much larger than the filtered value.

10.2.2 Implementation of PID Controllers in the Control System

WOB PID Controller

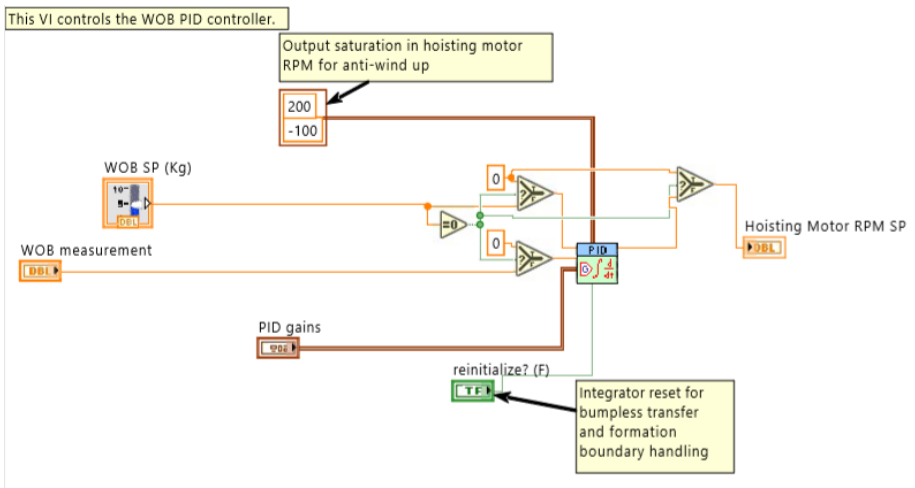

Figure 10.7: Figure showing the weight on bit PID controller in the control system

Figure 10.7 shows the WOB PID controller in the control system. Kalman-filtered WOB-data is input to NI LabVIEW's PID sub-Vi as the process variable. The control variable is the hoisting motor RPM SP, which is used by the internal PID of the hoisting motor. Each time the script changes drilling states, the integral reset is activated. This prevents integral wind-up after hoisting, orienting or entering the safety sequence. In the 2018 competition, the integral reset was also used to allow the PID controller to handle new rock formations without being influenced by the previous formation. If the setpoint is zero, the output RPM will automatically be set to zero, as that is easier for the system to achieve than to constantly perform small corrections to stay at zero.

The PID is only active when the control system is in one of the two drilling states. The program enters these states following tagging and a short hoist up sequence. The distance to the rock is therefore small and the integral effect does not build up too much. In addition to this, a maximum hoisting speed of 200 RPM, and a minimum of -100 RPM has been set in the PID.

Due to friction in the ball screw, the WOB offset between data taken when hoisting up and hoisting down can be as large as 15 kg. The WOB is tuned so that the actual WOB and the readings from the load cell are both zero after hoisting down. This means that if the PID attempts to hoist up in order to reduce the WOB, the WOB will appear to decrease drastically as soon as the hoisting begins, while the actual weight on the bit will be barely reduced. An overactive controller will, therefore, influence the measurements, which will further exacerbate the corrections.

Since the rock sample in this year's competition is uniform, the PID controller does not need to be as sensitive as it was in 2018. The priority has instead been to make a slow controller which does not overshoot too much, to avoid stalling the downhole motor. The controller has been tuned for the same sandstone that will be drilled in the competition.

10.2.3 Tool-face PID Controller

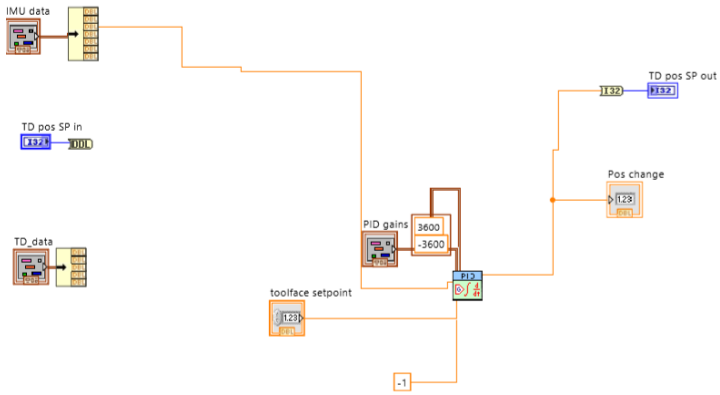

Figure 10.8: Figure showing the tool-face control PID controller in the control system

Figure 10.8 shows the PID toolface controller in the control system. The process variable in the toolface controller is the Kalman-filtered toolface and the control variable is the absolute top drive position. The TD position is limited to 360 degrees in either direction, with zero being the position at which the top drive switched from velocity control to toolface control and the position being the net distance in degrees that the motor has moved since then. Initially it was planned to set the limit to 180 degrees, to avoid complete rotation of the drill string. This did however mean that if the zero-position ended up being directly in the south direction, the controller would have no room to correct to one side after orienting itself correctly. As the motor should not need to rotate more than a full rotation, this was instead set at a limit. There is little reason to limit the output from the PID, because of the slowness of the system and the fact that magnetic north should not change drastically over the course of the competition. During the competition, the toolface set point will be zero. This means that the control system will always try to orient the sensor card towards the magnetic north, regardless of which direction it has previously gone.

10.2.4 Versions of the Competition Script

Because the competition script was not complete at the time of shipping the rig, two main versions exist. In order to keep working on the competition script after the rig was shipped, a simple simulation of the system was created. This script is fundamentally the same as the competition script, with the exception that all output from sensors and actuators that were shipped with the rig have been replaced with controls. It is, therefore, possible for the user to test how the logic in the script will react to different situations. Due to the time of the competition being a week after the delivery of this thesis, the program presented in this thesis will not be identical to the one used in the competition. Instead, a simulator script is shown in Appendix G to illustrate the simulated control system at the time of writing. Changes to the front panel and possible error states will most likely be made before the final competition. Details on how each sensor and actuator is implemented can be found in the instrumentation chapter 9.

10.2.5 Competition Script GUI

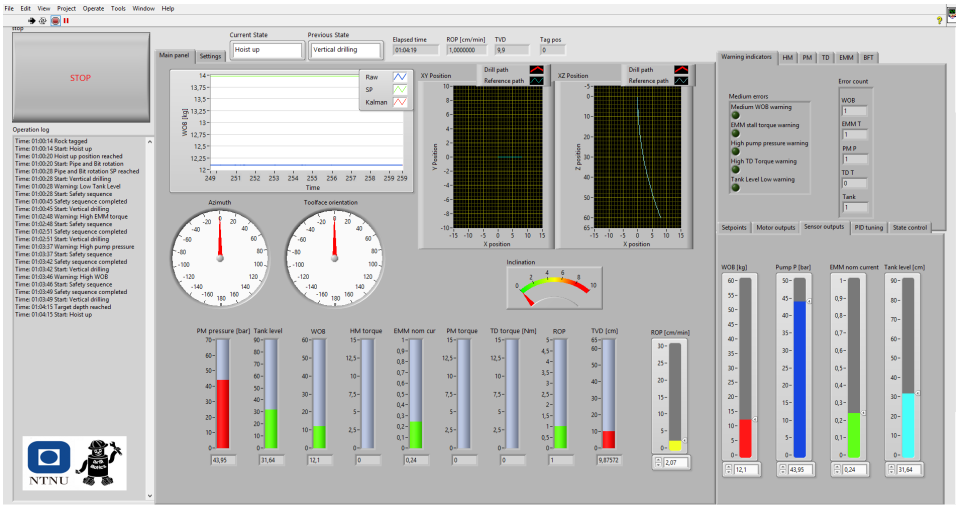

Figure 10.9: Figure showing the competition script simulator during a run

Figure 10.9 shows the front panel of the simulator version of the competition script during a run where several safety sequences have been triggered by the user. Important measurements such as pump pressure, WOB and EMM torque are displayed in colour coded bars in the middle frame of the panel. These bars change colour depending on whether the values are within the accepted range. Values within the normal and desired range of measurements show up as green, slightly abnormal values as orange, and measurements that are near a limit are displayed in red. This helps the operator pay attention to the most pressing issues at any time. The log to the left of the front panel can be closer observed

in Figure 10.10, and shows the history of states and warnings that the system has experienced. Additionally, a series of warning lights to the right of the panel informs the operator of which medium level errors are active, in case several errors should be active at the same time. If any errors develop past the safety limits, the program will automatically stop all motors and terminate the script. A large stop button is placed in the upper right corner, which will allow the user to stop the script in the same manner. The XY-plots show the planned path of the well, as calculated based on the input well path. When the well is drilled with a downhole sensor, the calculated trajectory is displayed in the same plot as the desired trajectory for comparison.

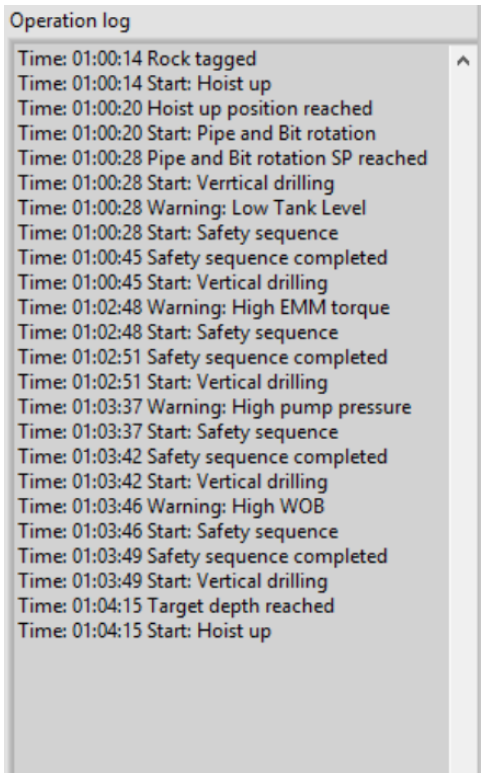

Figure 10.10: Figure showing the live log section of the front panel after a simulation run in which several warnings have been purposefully triggered to display the functions of the safety sequence

10.2.6 Structure of the Program

The main structure of the competition script consists of four sequential frames. The first frame initializes all relevant sensors, actuators and constants that are needed for the rest of the script to run. The second frame is the main section of the script, which runs while the rig drills. When the well is finished, or a serious error is detected, the script goes into the third frame, where communication with sensors and actuators is terminated. In the last frame, data from the drilling run is written to a text file. This structure is illustrated in Figure 10.11.

There are three while-loops in the second sequential frame. These loops all run in parallel and communicate using global variables. This is done to ensure that the top drive and sensor card have constant communication with the system. Delays in this communication leads to the top drive running jaggedly when its control is updated too infrequently and the sensor card readings suffering a time delay between the sensor is moved and the program can see the sensor response. The main while-loop collects all other sensor data, controls the other motors and actuators in the system and contains the state machine that controls the drilling process.

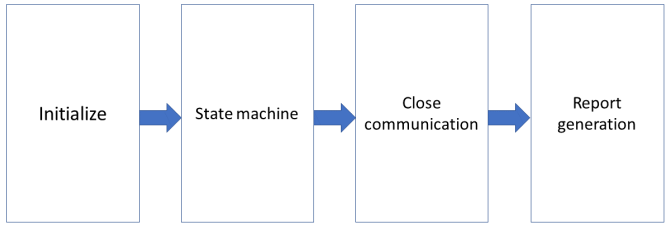

Figure 10.11: Figure showing the overall structure of the competition script

10.2.7 States of the State Machine

The state machine consists of the following states. These will be executed in the same order as they appear in the following list, with the exception of the safety sequence, which can be entered from the two drilling states:

- Tag
- Hoist up 1
- Start rotation
- Vertical drilling

- Hoist up 2
- Orient
- Directional drilling
- Trip out
- Safety sequence

Tag

In this state, the hoisting motor hoists down at 3 cm/min until the WOB exceeds the defined tagging WOB. Different tagging WOB have been tried and 8 kg has been found to be a good value. Once the rock is tagged, the hoisting speed is set to zero, a message is printed to the drilling log and the system enters the first hoist-up state.

Hoist up 1

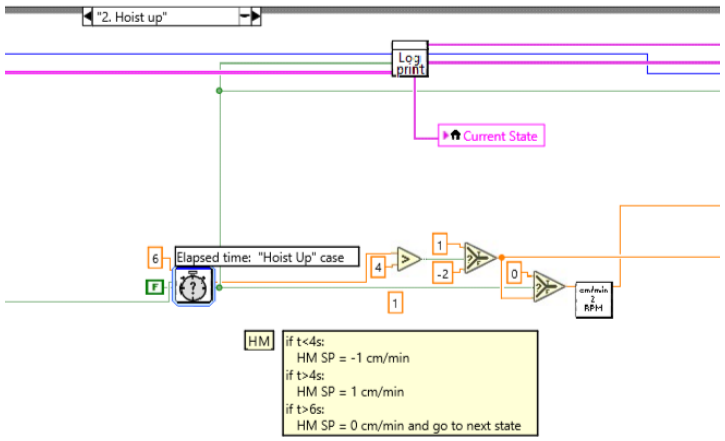

Figure 10.12: Figure showing the hoist up state.

Figure 10.12 shows the block diagram for the hoist-up state. The hoist up state hoists up for 4 seconds at -2 cm/min, before hoisting down for 2 seconds at 1 cm/min. This is done to get the bit free from the rock when rotation is started, while also ending with hoisting down, ensuring that the WOB measurements are as correct as possible when beginning the WOB PID controller in a later state. When hoisting is done, a message is printed to the log and the system will enter the next state.

Start Rotation

In start rotation state, top drive rotation, pumping and EMM rotation is started. If the EMM should prove unable to drill adequately in vertical mode, only the top drive and pump will be started in this mode. When measured rotation is similar to the set points, a log statement will be printed and the program will enter the vertical drilling state

Vertical Drilling

In this mode, the WOB PID controller controls the weight on bit, while motor rotation is maintained. The setpoint selector for vertical drilling is active and will reduce the WOB SP if the TD Torque or EMM torque surpasses an upper limit and the WOB SP will be reduced if the EMM torque goes below a predefined lower limit. The vertical drilling state will be exited if a medium level error is detected, or if the target depth for the vertical section has been reached.

Hoist up 2

This hoist up mode is the same as the first, but directs the program to orient mode instead of start rotation mode in preparation for drilling the vertical section. Hoisting up before orienting allows the top drive to turn the drill pipe more freely, as there is no WOB.

Orient

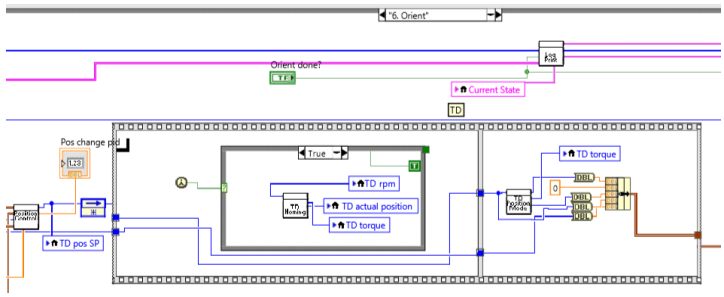

Figure 10.13: Figure showing the orient state block diagram

The top drive is set to tool-face control in this state, and a TD position is chosen. This position is given by the PID in the tool-face control sub-VI. In Figure 10.13, a front panel control must be manually toggled to exit orient mode. In the fully automatic version, this is replaced by a Boolean value that is true when the TD position is the same as the TD Position SP.

Directional Drilling

This mode combines the WOB PID control, the toolface PID control and the deviated version of the SP selector. The only difference between the version of the SP selector for deviated drilling and the one for vertical drilling is whether they take TD torque into account. As position adjustments should be small and the top drive can provide a lot more torque than the electrical motor, it is not expected that the top drive torque should be a limiting factor for the WOB SP.

One issue that may arise is that the EMM stalls during orienting, as digging action at both the sides and the front of the bit will increase the amount of rock that is attempted to be removed in each rotation and the EMM will likely already be using a large portion of the available torque. The torque required to drill with the sides of the bit is larger than the torque required to drill equal amounts of rock at the bottom of the bit, due to the distance from where the force is applied to the axis of the shaft. It has been observed during testing that the EMM stalls more easily when the sides of the bit are touching the rock.

No specific control action is made for this case, but the issue may be solved automatically by pre-existing features. If the change in torque happens gradually, the SP selector will decrease the WOB SP, stabilizing on a lower set point where the torque is within acceptable levels. If the change occurs too quickly for the SP selector to act, the medium level warning will activate and the safety sequence will be entered. When the safety sequence is exited again, the BHA will be hoisted down pointing in the correct direction. The bit should then be able to remove some of the rock from the side of the wellbore while hoisting down before it tags the rock and the torque is increased again.

Trip out

When the well has reached its planned depth, the script enters the trip out state. In this state, the hoisting motor hoists up at -50 cm/min until the starting position has been reached.

Safety Sequence

The safety sequence is activated when a medium level warning is detected. These warnings can be due to high WOB, high EMM torque, high pump pressure, high TD torque or low tank water level. Regardless of which error activated the safety sequence, the script will hoist up the same way as is done in the hoist up modes. If the problem is high WOB or high TD torque, this should remove the warning. If the error is due to high pump pressure, due to a clogged nozzle at the bit, hoisting up will remove the bit from the cuttings that are most likely clogging the nozzles. If the problem is a low tank level, the pump rate will be set to zero until the tank is partially refilled. The script will not leave the safety sequence until all warnings are resolved.

Critical Error

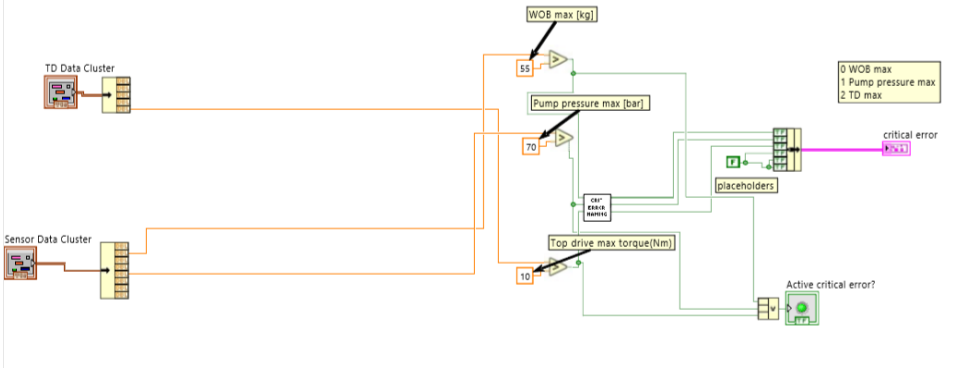

Figure 10.14: Figure showing the critical error detection block diagram

The block diagram in Figure 10.14 shows how the sub-VI detects critical errors. If WOB, pump pressure or TD torque reach a critical max and safety is at risk, the script will terminate. The critical error limits should be high enough that the only option when they are detected is to terminate the script, yet there should be some safety factor added to the theoretical limits of the system.

Medium Error

Medium errors occur if the system reaches the medium warning limits for high WOB, high EMM torque, high pump pressure, high top drive torque or low tank water level. It is important that the warning limits are well thought out and fit together with all other limits in the system. Medium warning limits should be lower than the critical error limit, by enough of a margin that the safety sequence is started before the script terminates due to a critical error. At the same time, using too conservative limits for the medium warning levels can lead to many unnecessary stops during drilling. If the pump pressure warning level is low enough that it will be reached under normal operation, the system may get stuck inside the safety sequence, since the pump pressure warning will not be resolved as long as the pump is on. This can be avoided by having a good understanding of the conditions the program will face under normal operation or by adjusting a relevant control parameter if the program encounters an error that does not resolve itself during the safety sequence. For example, the pump RPM can be decreased in the control system if the pump pressure is consistently too high to allow for drilling.

WOB SP Selectors

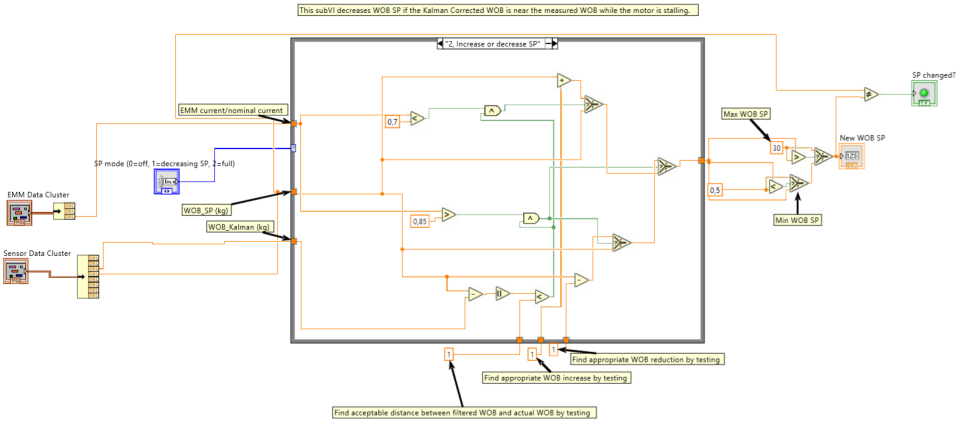

Figure 10.15: Figure showing the subVI for the WOB SP selector for directional drilling mode

Figure 10.15 shows the WOB SP selector for deviated drilling. If the EMM torque approaches either an upper or a lower limit and the filtered WOB data is near the WOB SP, the set point will be changed. This avoids changing the set point in response to a motor output that is not measured while drilling at set point. Several alternative options for the SP selectors have been made, depending on which section is being drilled, whether the vertical section should be drilled with an EMM or a PDM, as well as whether it is only desired that the WOB SP should be decreased automatically and not increased. The selectors also have a button for easy switching between drilling with and without SP selector while testing.

Log Print

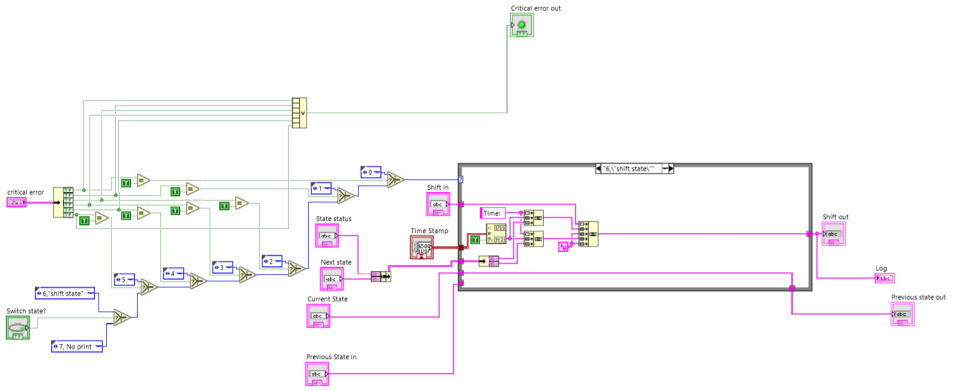

Figure 10.16: Figure showing the subVI block diagram for printing status to the live drilling log

Several subVI's work together to make the front panel log print. Each time a state is changed, the reason for the change and the next state will be printed. Inside each state there is a sub which determines what, if anything, should be printed in the current iteration of the while-loop. Outside of the while loop, these strings are input into the operation log subVI, which prints the strings to the log, along with a timestamp. Additionally, it is planned to implement the option of notifying the log whenever a WOB SP is changed automatically if it is decided to change the WOB SP rarely and in larger increments. If the SP is changed too often, the log will become cluttered by messages about changing the SP. The decision on how to tune the SP selector will be made after testing the set point selector in Germany. The new subVIs for logging this will require will be made ready before travelling to the competition, but the decision on whether to implement them in the final competition script will depend on how often the set point is changed. It is therefore currently unknown if this feature will be part of the final competition script.

Chapter 11

Tests, Results and Discussions

In this chapter, the performance of the PDM and electric motor is tested. Besides, the complete set of different drill bits is tested and compared later on. The results from these tests are also discussed in this chapter.

11.1 PDM Tests

After the last design iteration explained in Section 7.3.1, it was decided to test the performance of different lobe configurations. These tests include rpm, start-up flow rate and stalling WOB. Since proper tools were not available to perform a dynamometer test, simple procedures had to be implemented. Parameters like torque had to be theoretically calculated based on other parameters, to have an idea of the performance of the PDM.

11.1.1 Performance tests

Several theoretical methods exist that try to predict the performance of a PDM based on the internal geometry of the power section and other parameters such as friction losses and slippage across the motor. When creating a PDM from scratch, it is useful to have an idea beforehand of its performance and if such a performance will be enough to drill the rock sample in the competition. This is why three different methods have been implemented to have a rough estimate of the mud motor performance when tested on the miniature rig. It is important to mention that all of these methods are ideal, meaning no friction losses and flow slippage through the power section were considered in the calculations.

By using and comparing three different models, one can compare the accuracy of each with true measurements taken on the rig. This way the performance of future designs can be better estimated by selecting the most accurate model.

Model 1 by Kirk Townsend Lowe

The model developed by Kirk Lowe is based purely on the geometry of the power section and it is specifically derived for 1:2 lobe configurations only [33]. Since the equations that calculate the output Torque and RPM are not generalized for multi-lobe power sections, this model might introduce additional errors when trying to predict the performance of different lobe configurations.

Model 2 by T.C. Nguyen et. al.

The model developed by T.C. Nguyen et. al. is also based on the internal geometry of the power section, but with the difference that the performance equations are generalized for any type of rotor-stator configuration [36].

Model 3 by Robello et. al.

The model developed by Robello et. al. although older than the two previously mentioned, arrives to similar performance equations also based on the internal geometry of the power section. This model digs deeper into how to optimize this geometry when designing a PDM and analyzes the leakage and torque losses that occur in a real-case scenario [39].

Test Setup and Results

This test was performed with the old pump used in last year's competition rig. Due to increasing issues, this pump had to be replaced as it is mentioned in section 7.2. Besides, no wires were placed inside the drill pipe this time, meaning no downhole measurements were taken at this point.

A 4:5 lobe configuration was used to increase the torque and have moderate RPM with an interference fit of + .21 mm. To help overcome the initial friction inside the power section, an anti-washout grease was applied on the surface of the rotor. The operational flow rates used on this test were limited by the capacity of the pump.

The results are summarized below. RPM estimates are compared against measured RPM on a semi-logarithmic scale and torque estimates are also compared for the three different methods.

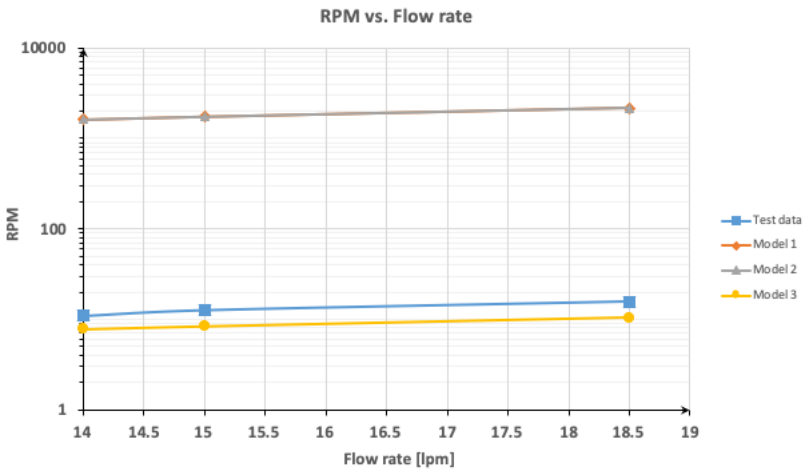

Figure 11.1: RPM vs. Flow rate

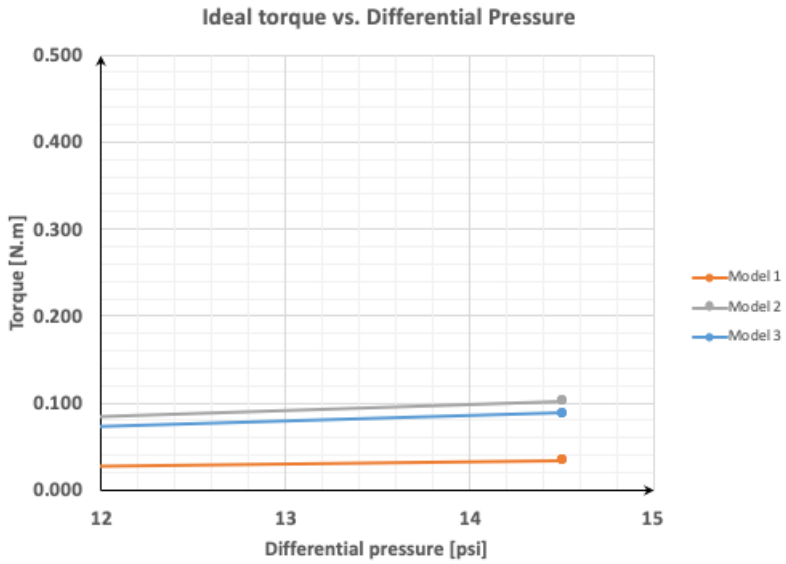

Figure 11.2: Torque vs Differential Pressure

When the measured RPMs are compared against the estimates, one can see that Model 1 and 2 almost overlap themselves but are well above the true RPM. On the other hand, Model 3 seemed the better estimate the real values got on the test.

As far as torque is concerned, the estimations provided by all three methods are relatively similar to each other.

Test Conclusions By comparing these three analytical methods, it was proved that the model suggested by Robello et. al. provides the best estimates when it comes to RPM. When getting torque estimates, all three methods seemed to provide somewhat similar results. Either way, according to the results one should not expect to have more than 0.1 Nm out of the current power section.

By increasing the fit of the power section, one could increase the pressure loss across the motor and therefore the output torque. These results considered a motor efficiency of 75% and ideal conditions as it was previously mentioned. Therefore, it is fair to expect that the true performance of the mud motor will be inferior to that predicted by the models.

11.1.2 Motor Start-up Tests

The interference fit inside a PDM's power section plays an essential role in its performance. This important parameter is illustrated in Figure 11.3 and can be defined as:

$$Fit = (Rotor\ major\ diameter - Lobe\ height) - Stator\ minor\ diameter \quad (11.1)$$

Having a rotor that is too small for the stator would create too much slippage (leakage between consecutive lobes) and the mud would simply flow through the power section without moving the rotor, this is sometimes also referred to as weak motor [41]. On the other hand, having a rotor that fits too tight inside the stator would create excessive friction and heat, eventually leading to elastomer chunking.

Downhole temperatures and the type of mud being used also influence this parameter. Sometimes it is common to decrease the fit of a power section where high downhole temperatures are expected. In this case, the additional rubber expansion due to temperature would create the correct fit for the motor. Some rubbers also react to the drilling mud by shrinking or swelling, so a proper fit would take the chemical compatibility between the rubber and the mud into account.

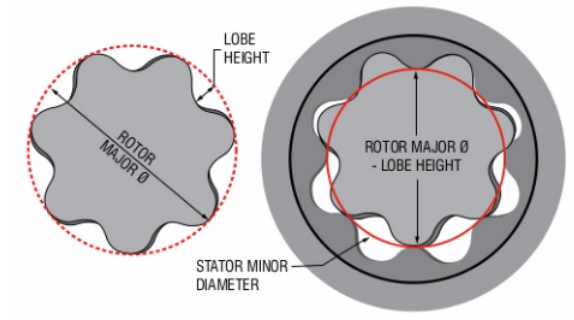

Figure 11.3: Interference fit definition [41]

The performance of a power section greatly depends on the materials used for the rotor and stator. To achieve the same results with a nitrile based rubber and a polyurethane material as a stator, for example, one would have to choose different interference fits, assuming the material of the rotor is the same and both surfaces have the same quality.

Several materials and fits have been tried throughout the project by combining different 3D-printed stators and rotors, as shown in Figure 11.4. Different lobe configurations were tested, but most of the tests were performed using a 4:5 lobe ratio between rotor and stator. Among all the materials that were tested, using PLA on the rotors and Ninjaflex on the stators proved to be the best working combination.

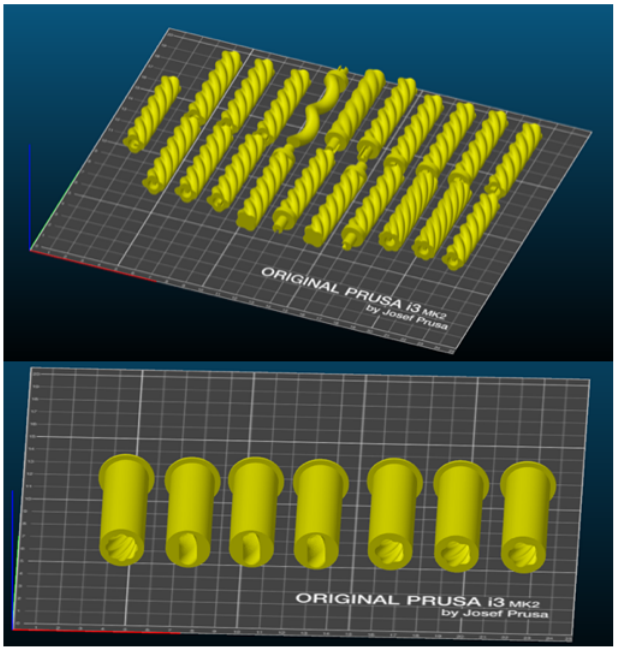

Figure 11.4: Different rotors and stators tested in the project.

Test Setup and Results

The main objective behind this test was to find the relation between the start-up flow rate of the motor and the fit and also to find the optimal operating point before reaching the pump pressure limit. For these tests, a 4:5 lobe configuration was used in the power section, by 3D-printing stators in Ninjaflex and rotors in PLA. The flow rate was recorded at the moment the drill bit started rotating and the internal friction inside the motor was calculated by recording the pump outlet pressure and subtracting the pressure losses before the power section, also as soon as the bit started turning. It is worth mentioning that this test assumes the internal friction inside the motor comes entirely from the power section, where in reality this is not true. The rest of the transmission adds more friction to the

system, especially in the bearing section and in the space between the bearing section and the bit sub.

After the optimal operating point is found for the current hydraulic system, one can expect that the performance of the power section is maximized as well. The results are shown in Figure 11.5.

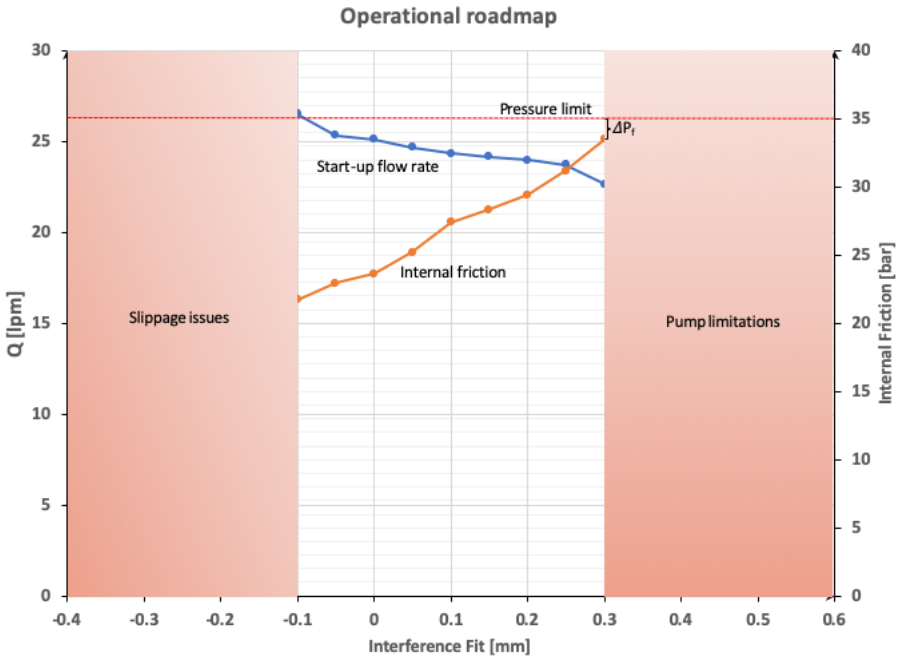

Figure 11.5: Operational roadmap for the PDM

Based on these results, one can see that the flow rate needed to start the PDM by itself decreases while increasing the interference fit in the power section. If the fit is too low, slippage issues appear and the motor might need help turning the bit from the outside to make it start. Sometimes the slippage in the power section is so high that even with outside help, the motor does not start. These issues appeared when fits of -0.1 mm were used, indicating that values lower than this would cause the same effect in the motor.

As the fits were increased, the internal friction showed an increase as well. When using a fit of + 0.3 mm, this friction reached about 33.6 bar. At this point, the pump reached its pressure limit and the motor never started. It is worth mentioning here that this result is directly influenced by the pressure loss above the power section. This test was performed with no sensor wires inside the drill pipe, which in turn influences the pressure made available for the PDM. In this case, this pressure loss (ΔP_f) is 1.4 bar but in the competition setup, wires and connectors will be placed inside the drill pipe and will, therefore, increase the pressure loss. This increase in pressure drop before the power section will cause the

upper operational limit (+ 0.3 mm) to decrease accordingly.

After analyzing the results of this test, one can say that the optimal operating point for this PDM could be achieved by choosing an interference fit between +0.2 mm and +0.3 mm. If one considers the competition setup, then a more conservative approach should be chosen and a fit of +0.2 mm would work best.

Working with Limitations

It has been shown that the torque provided by a PDM is directly proportional to the pressure drop across the power section. By increasing the interference fit, the pressure drop will increase accordingly and the PDM could generate enough torque to drill the rock sample.

As seen in the previous test, the upper operational limit of the PDM is controlled by the pump. By increasing the maximum pressure the pump can deliver, one could work with higher fits and have a functioning and better performing PDM. For this reason, it was decided to change the old pump for a new one that fits the requirements. The new pump can be seen in Figure 11.6 along with its specifications.

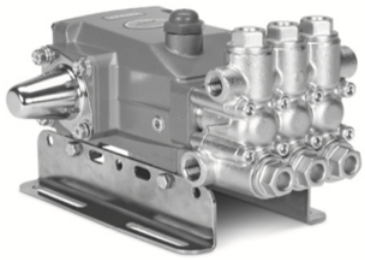

SPECIFICATIONS	U.S. Measure	Metric Measure
5CP6120		
Flow	6.0 gpm	23 lpm
Pressure Range	100 to 1600 psi	7 to 110 bar
RPM	1400 rpm	1400 rpm
Bore	0.787"	20 mm
Stroke	0.709"	18 mm
Weight	19.9 lbs.	9 kg

Figure 11.6: New pump and its specifications (*Courtesy of Cat Pumps*)

The new pump was changed and installed two days before the rig had to be shipped to the testing facility in Celle, Germany. Therefore, it was not possible to test it together with the PDM. Such a test will be performed before the competition day in Germany.

11.2 Electric BHA Tests

11.2.1 Initial ROP Test of Downhole EMM

Purpose of Test

Before reserve EMM were to be ordered, it was determined to perform drilling tests to verify whether it was feasible to use the motor for drilling during the competition. Testing from Phase I indicated that this would be the case [35], but there were several uncertainties. The torque output from the EMM was not much above the minimum found in Phase I and the friction in the BHA had not been tested. Thus, friction in the system could bring the effective torque at the bit below what was required to drill. Also, the previous tests had been run using the old BHA and the bit produced by Lyng Drilling for the 2018 competition. As torque varies between different bits, it was not certain that the same performance could be achieved with the new bits. There was also the issue of different hole sizes, with the 2018 bits being smaller than the 2019 bits. An attempt was made to correct for this by scaling up the torque requirements with the same factor as the area was increased with between the two bit sizes, but no testing could be done to verify the scaled results without a larger bit available. New tests were therefore carried out with the EMM in a sandstone once the 2019 BHA was ready.

Testing Procedure

When starting the hole, the BHA was supported by manually to prevent excessive bit walking. Water circulation during the test was provided by an external hose instead of being circulated through the drill pipe, BHA and bit, as the electric swivel shaft was in the workshop and there was, therefore, no barrier against water leaking out of the top of the hydraulic swivel. Once the hole was deep enough that the drill bit was prevented from bit walking by the hole walls, the housing was released and only the rig floor stabilizer worked to stabilize the drill string.

Error Sources

The tests were performed with the bent sub as part of the BHA, as no alternative without a bend was available. To avoid rotation of the drill pipe, counter torque was supplied by a wrench supported against the rig. The hole was drilled without a riser. These conditions contributed to the stability being poorer than could be expected if the BHA was supported by the riser.

The external water circulation likely affected the test by reducing hole cleaning and increasing friction between the different parts of the BHA, as cuttings entered the gaps between parts and the bit nozzles.

The hole cleaning was not optimal, particularly as the well grew deeper. Accumulation of cuttings around the bit cutters and at the bottom of the well were observed after pulling out of the hole. This is likely to have affected the drilling rate negatively and a higher ROP could be expected with better hole cleaning.

The ring sealer in the bearing assembly is designed to expand as pressure is increased within the bottom hole assembly. The bearing thus provides a seal against water flowing outside the U-joint. However, this also increases the friction between the rotating U-joint and the bearing. The magnitude of this friction force has not been measured but can be expected to cause lower effective torque at bit when drilling with internal water circulation.

Due to programming errors, the logged data from the test were incomplete. The hole depth therefore had to be measured by hand. Due to a lack of sandstone to drill, parts being in the workshop and time constraints, no repeat test was done.

Results

The hole was measured to be 8 cm, and the total drilling run time was 695 seconds. This corresponds to a ROP of nearly 0.7 cm/min. As the rock had to be tagged before drilling could start, some of this time was spent hoisting without touching the rock. This estimate for ROP is therefore conservative.

Discussion

If the same drilling rate could be achieved in the competition well as was achieved in these tests, the 60 cm well would be drilled in less than 87 minutes. However, several factors may cause the competition drilling rate to differ from the rate found in these tests. The lack of pressure in the BHA and the softness of the sandstone both contribute to the inaccuracies of this test. Even so, this test was considered sufficient proof that the EMM was a viable option for a down-hole motor. Spare miniature motors were ordered later that day.

11.2.2 Electric Motor Complete BHA Drilling Test

Purpose of Test

Once the swivels, BHA and programming for the EMM were ready, the first full scale tests were performed. The goal of these tests was to find any potential faults in the system, so that they could be corrected before the competition. Of particular interest was the build-up rate from in sliding mode with the bent sub, the robustness of the downhole electrical system, the ease of rig up and rig down and verifying which parts of the control system worked and which needed to be altered.

Procedure

The drilling tests were performed in a stone made of cement mix and sand. This mix was purposefully made slightly softer than the competition sandstone, to allow for faster testing. Drilling was done using the DSATS bit, with a depth of cut limitation of 2 mm. The top drive was still in the process of being set up, and therefore not included in the test. The sensor data did therefore not affect the decisions of the control system. The riser was also not used so that the drilling of the upper section of the hole could be more easily observed.

The first EMM had suffered some damage prior to the tests, presumably due to water or grease entering the motor through the shaft. This motor was therefore considered more expendable than the newer replacement motors. When this motor failed during testing, the procedure was to connect the wires from the EPOS4 drive directly to the motor wires to check if the motor still runs. If it did, the error had to be with the wires or connections further up, and testing could continue after fixing the faulty wire or connection. After this first motor was too damaged to run, the procedure became to immediately halt testing when the motor experienced a short circuit and check all wires and connections for visible faults. If nothing was visible, the motor was put in a heating cabinet for drying before being tested again. Even so, the first replacement motor failed on the first day it was tested.

Wire Management

Several runs were done, with and without the sensor card. Much work went into wire management. After connecting the sensor card and EMM wires, the card and the motor was run continuously while tightening connections in the swivel and BHA. It was thereby possible to detect when a connection was broken by the assembly process. It was found that assembly was easiest when the connecting point on the wires was several cm below the lower end of the swivel and all the wires exiting the swivel were wrapped in the shrinking tube from the top to connection point at the bottom. The stiffness of the shrinking tube then allowed the thinner, more fragile wires to be pushed down below the connection point of the drill pipe and removed the risk of damaging the wires when tightening the connection. It was discovered that it was important that the wires going through the drill pipe were thin enough to be easily pushed into the drill pipe.

Sensor Card Communication and Wire Connections

Many drilling runs ended a short time after the start of circulation due to communication with either the card or the motor failing. Two 5-pin quick connections were initially used to connect the two motor wires and four sensor wires going through the drill pipe. It did however prove too cumbersome to pull two connectors through the swivel. As the wires from the swivel are fragile and have needed fixing several times, ease of assembly and disassembly was a priority. There were also problems moving the wires away from the threaded parts when making up the drill string, which caused communication failure when

wires were squeezed while assembling the system. This was caused by the lack of space in the drill pipe and the necessity of having wires pass on the outside of the connector.

There were also issues with the 5-pin connections not being watertight, which led to unreliable connections when water flowed through the system. A plastic spray which had been by the previous year's team to isolate the sensor card was used on the connectors to reduce the chance of water shorting the wires. However, this did not solve the problem and the connection remained unreliable. It was, therefore, decided to try soldering the wires. The connection was then more stable but required the wires to be soldered on every time the rig was made ready for drilling.

Another challenge discovered during testing was that of avoiding damage to the electric downhole components. Plans were in place before testing for how to protect the sensor card and EMM from water damage, but testing was required to find out if these methods worked. The plastic spray from last year turned out to be too fragile to protect the sensor card, as it could be scraped off when inserting the card. Another option was shrinking glued heat shrinking tubes around the sensor card. This worked for a few minutes at a time before communication with the sensor was lost. When the card was later inspected, it was discovered that water had come in the seams of the shrinking tube. This could be partly due to a poorly glued tube and partly due to lack of space in the sensor housing. Using the shrinking tube as sealing added approximately 2mm of height to the card. This, coupled with the stiffness of the sensor wires at their connection to the sensor, hindered the card from being fully inserted into the sensor sub. When the drill pipe connection was torqued up, the edge of the sensor card shrinking tube was folded, which caused the glued seam to open. Several combinations of plastic spray, glues and shrinking tubes were used. The best solution turned out to be gluing the entire sensor card with 3M™ Scotch-Weld™ DP110 Gray glue, and using a thin, fast drying glue on the sensor wires as extra support. This protected the wire connections as well as keeping the card watertight, and communication was stable for most of the duration of the well. Communication with the sensor card was lost early, but the cause of this was identified to be bad connections in the drill pipe and swivels.

Water Sealing EMM

Sealing the EMM from water also proved challenging. The motor housing was designed with channels in the housing walls to minimize exposure to water, but the ends of the motor were potential leakage points. Particularly the wire holes, seams at the top of the motor body and between the motor and gear section and the bearing by the gear shaft at the bottom of the drive were considered high-risk areas. Attempts were made to seal these places with silicone, potting rubber and glue.

Before inserting the motor, the lower end of the housing was filled up with grease and all wire holes and seams along the housing were glued shut. After the motor had been inserted, the set screw was screwed in and a sealing substance was applied to the top of the motor and around the set screw hole. Two kinds of substances were tried: a removable potting rubber for electrical appliances and silicone. The rubber formed a plug around the top of

the motor, but did not stick well to the surface of either the motor or the housing walls. The silicone appeared more sealing, as it stuck to all surfaces, but was very time consuming to remove. The motor that was sealed with potting rubber ended up short-circuiting after 30 minutes of drilling with a low flow rate. This was considered to most likely be due to water damage. It was not possible to verify the source of the leak. However, previous drilling runs with the silicone sealing had lasted for longer than 30 minutes and the same procedure had been used to apply grease to the lower end of the motor in both cases. This indicated that the potting rubber was the issue. No further tests were done with the potting rubber, as it was considered too risky.

Water Sealing EMM-Grease

The EMM housing consists of two compartments near the bottom. The motor sits in the upper compartment, on top of a series of pins which enter the holes at the end of the gear body and restricts motor movement in the radial direction. A hole sits in the middle for the shaft to go through and in the compartment below, water exits the channels in the wall. Ideally, there should be no flow between these compartments. Grease should occupy all free space in the upper compartment, leaving no room for water to enter. High flow rates and pressures in the BHA may still displace the grease and over time allow water to seep into the gear, and from there into the motor. This is suspected to have happened during the first day of testing with a replacement motor.

A well was drilled in the soft mix of coarse sand and cement and the pump was run at between 800 and 1800 RPM. Several stops were made to test various aspects of the control system and the pump remained on for many of these stops in drilling. A total of 26 cm was drilled before the motor detected a short circuit. This was around 3 hours after the pump had initially been started, and after 51 minutes of the control system being active. This suggests that it may be possible to drill a competition well using grease as the only sealing method at the lower end, if the well can be drilled within one hour. This does however remain a risky option. It was therefore decided to attempt a tighter seal on the final electric motor that would be used in the competition. This was achieved by the use of a V-ring.

Another issue with using grease as the means of sealing the shaft was discovered when inspecting the faulty motors. Electric motors that experience water damage typically fail due to impurities in the water causing a short circuit. When the damaged motors where inspected with a multimeter, the resistance was 10^3 to 10^6 orders of magnitude larger in the damaged motors than in the undamaged motor. This result is consistent with what could be expected if grease had been forced into the motor by high water pressure, and created a non-conductive coating inside the motor. An alternative solution would be broken wires, but this was not observed in any of the motors. Work was started on cutting open one of the damaged motors to be able to observe the insides, but due to a lack of time, this work could not be finished. To be on the safe side, the last motor was sealed with a more viscous grease, which should be more difficult to displace into the motor.

Deviation

The drilled well appeared to have some slight deviation, but this could not be measured, due to time constraints and issues with the rig. The deviation appeared to be smaller than 1 cm, by very rough estimates. However, the well was drilled in a very soft sandstone without any measured WOB, due to the rock being so easily drilled. This is likely to have affected the deviation, as the contact points in the BHA were unlikely to have touched the wall at such low WOB. Too many uncertainties exist in this test to draw any conclusions on the deviation capacity of the system. In order to verify if the BHA builds the planned angle, a new test should be performed in a harder rock and the deviation should be measured by an accurate tool.

Results

At the longest, a 26 cm long well with a 36 mm diameter was drilled in sliding mode. The bit diameter was 31.75 mm, meaning that the well was over gauge. Sensor communication was established, but was not stable enough to gain downhole data while drilling. There appeared to be some small deviation, but no good measurements of this could be made without the sensor. A previously unused EMM failed, which indicated that the water sealing in the EMM housing was not sufficient.

Discussion

This test did not yield much in the way of theoretical results but clearly showed that several aspects of the system needed improvement. After the test, the process of designing a better water sealing solution for the EMM and identifying the weak points in the electric connections for the sensor was begun. It was concluded that gluing the sensor card was the best way to keep it safe from water damage and strengthen the connection between the wires and the card.

11.3 Rock Strength Test of Soft Sandstone

11.3.1 Purpose of Test

Initial drilling tests with the EMM were done in a soft sandstone of unknown origin. To be able to relate the results from these drilling tests to the expected drilling rate in the competition sandstone, a uniaxial compressive test was performed on the rock. The results from this test were the UCS, elastic modulus and Poisson's ratio from the sandstone.

11.3.2 Testing Procedure

Three core samples were extracted from the sandstone. One of these broke during preparation, so only two rock samples were tested. These were from opposite ends of the larger block. Preparation consisted of grinding the wet rock sample to achieve an even surface. It was observed during preparation of the cores that they appeared weaker when wet. The cores were therefore put in a heating cabinet overnight prior to testing.

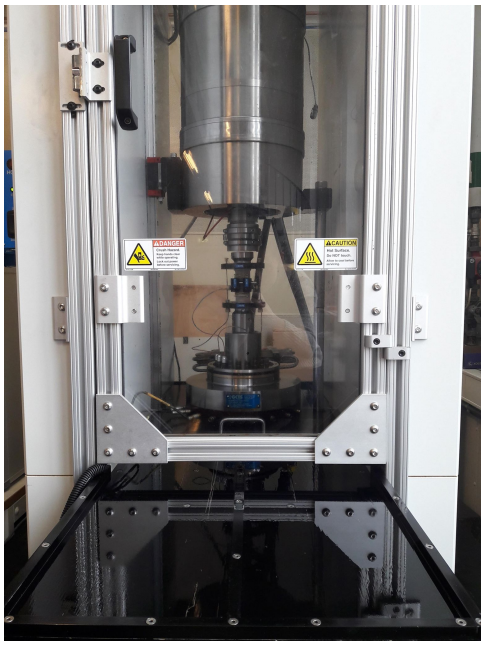

Figure 11.7: Picture showing a core sample being instrumented for a uniaxial unconfined test

A protective shrinking plastic was then wrapped around the core to keep rock fragments away from the testing apparatus. A hole was cut in the plastic to allow air to escape before applying heat to the shrinking plastic. A frame for the extensometer was then attached using set screws and a radial strain gauge was placed around the rock sample. The frame consisted of two circular parts, which were aligned using rods of equal length.

Two extensometers were placed between the two parts of the frame and adjusted to read 1.4 mm. The measurement was then put to zero before starting the test. The membrane and rock dimensions were then registered and the rock sample inserted into the GCTS RTR-4000 Rapid Triaxial Rock Testing System apparatus. The top of the press was lowered manually due to the low strength of the sandstone observed during preparation of the cores. This process can be seen in Figure 11.7 and Figure 11.8.

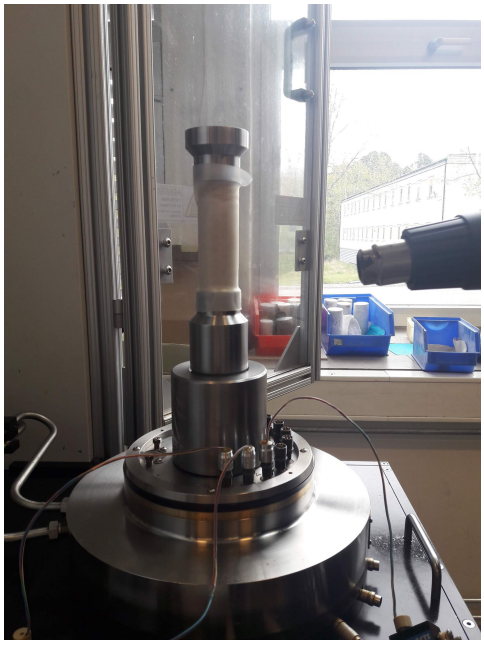

Figure 11.8: Picture showing a core sample in the rapid triaxial rock testing apparatus, going through a uniaxial unconfined test

The axial strain, radial strain and deviator stress were logged and the stress on the core sample was increased until failure.

11.3.3 Error Sources

An unevenness on one of the rock samples exceeded the ISRM's limit of 0.2mm [17] and meant that the sample did not stand firmly in the apparatus. Any air pockets in the shrinking wrap may have affected the measurements of radial strain.

Table 11.1: Results from the two cores tested for UCS

Core no.	D (mm)	L (mm)	Weight (g)	E-modulus (GPa)	UCS (MPa)	Poisson's ratio	Comment
1	34.29	93.2	177.97	10,12	35.5	0.58	
2	34.21	77.5	145.94	6,39	28	0.44	<1mm departure from end being perpendicular to axis

11.3.4 Results

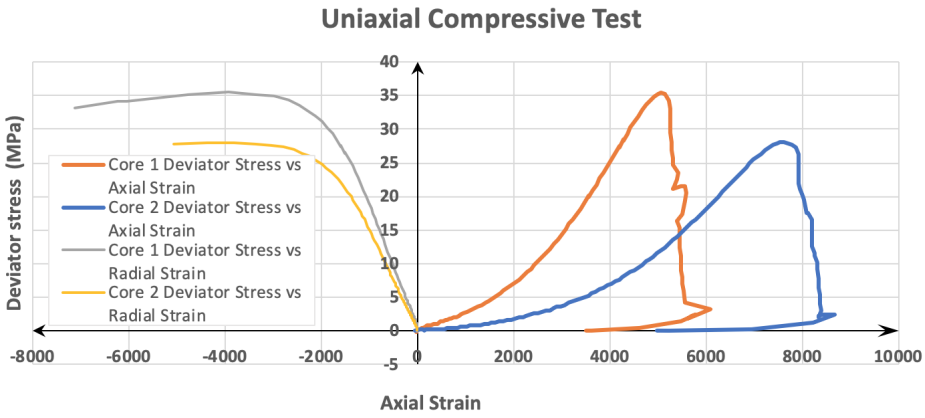

Figure 11.9: Uniaxial Compressive Strength test results

The dimensions, elastic moduli, uniaxial compressive strengths and Poisson's ratios of the two cores are presented in table Table 11.1.

11.3.5 Discussion

The sandstone that will be provided in the competition is expected to be between 31 MPa and 43 MPa [14]. The sandstone that was tested is therefore on average slightly weaker than the one that will be provided in the competition. The core that yielded the highest UCS was taken less than 5 cm from the test wells. The test wells have therefore most likely been drilled in a stone of similar strength to the competition sandstone. A slightly lower ROP can, therefore, be expected in the competition sandstone than in the stone that was used for initial testing of the EMM, when only considering the UCS. However, it was noted that the tested sandstone appeared weaker when wet, which may have caused a larger ROP during drilling than would be achieved in stone of similar strength and different composition.

11.4 Hoisting Position and Speed Accuracy Test

11.4.1 Purpose of Test

Position readings from the hoisting motor are crucial for the position control system. The readings are used to decide which drilling mode the system is in and to relate the heading from the sensors to the position of the BHA at any given time. It was therefore decided to test the accuracy of the position readings from the hoisting motor.

11.4.2 Testing Procedure

A laser measurer was attached next to the hydraulic swivel on the moving frame on the rig. The hoisting motor was run at different speeds in both directions and the position was measured both by the laser measurer and from the hoisting motor position when the hoisting system was still. Additionally, the RPM of the hoisting motor was integrated and this gave a third estimate of the position. These three position readings were logged and compared to each other.

11.4.3 Error Sources

The laser measurer was accurate to the closest millimeter, while the motor position was given to one-thousandth millimeter.

The hoisting motor position measurements come from an internal incremental encoder with 2048 pulses per revolution [31]. The sampling rate is 100 Hz. As the hoisting motor speed does not exceed 1000 RPM during normal drilling, the sampling rate and frequency of pulses from the incremental encoder are not expected to cause any major inaccuracies in the readings.

The laser measurer was attached to the moving frame by tape, which may have slipped and affected the measurements during testing. However, no evidence of this was observed.

11.4.4 Results

In the first round of the test, the hoisting motor started at a position where the laser measurer measured 891 mm down to the rig floor. The moving frame was hoisted down at -10 RPM for a few seconds before the next measurement was taken. Eleven measurements were taken this way. The hoisting motor measured RPM, position and the calculated ROP was logged in the software.

It was observed that the hoisting motor drive's measured HM velocity did not correspond with the set point for most of the run. This is illustrated in figure Figure 11.10 and lead to the ROP calculations based on hoisting motor speed being positive even when the set point

was zero. Furthermore, it was observed both visually and from the position measurements that the hoisting motor was still when the set point was zero, even though the measured velocity was nonzero. The cause of this inaccuracy was identified as an error in the conversion between double precision and integer numbers in the hoisting control sub-VI, which was fixed.

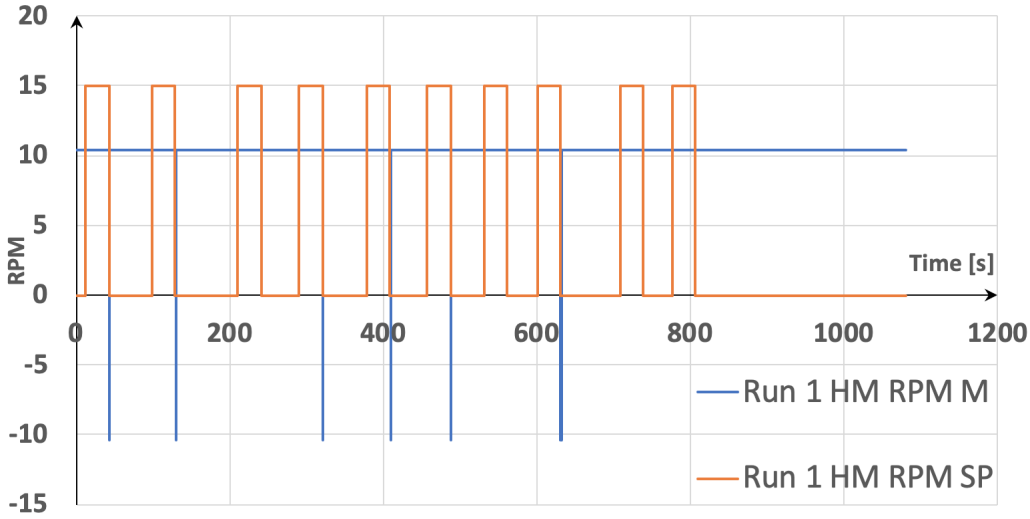

Figure 11.10: Hoisting motor measured velocity vs. set point

The position data from the drive corresponded well with the position measured with the laser sensor, with the difference between the measurements staying below 1mm. These results can be seen in table Table 11.2. For simplicity's sake, the HM Position refers to the distance from the initial position at the time of starting the script and the laser measurement at each point is converted to the position relative to this starting position. The position difference between the two measurements is defined as the laser position minus the HM position. The average position difference was 0.036mm.

Table 11.2: Table showing run 1 in the hoisting motor position accuracy test, with a low constant speed of hoisting down between measurements

Measurement no.	HM Pos. (mm)	Laser measurement (mm)	Laser pos. (mm)	Position difference
0	0	891	0	0
1	4.197	886	5	0.803
2	8.393	883	8	-0.393
3	12.590	878	13	0.41
4	16.843	875	16	-0.843
5	21.040	870	21	-0.04
6	25.236	866	25	-0.236
7	29.489	861	30	0.511
8	33.742	857	34	0.258
9	37.939	853	38	0.061
10	42.135	849	42	-0.135

Two more tests were performed, with varying hoisting times and speeds. The results from these are presented in table Table 11.3 and Table 11.4.

Table 11.3: Table showing run 2 in the hoisting motor position accuracy test, with varying hoisting speeds in both directions between measurements

Measurement no.	HM Pos. (mm)	Laser measurement (mm)	Laser pos. (mm)	Position difference
0	0	835	0	0
1	2.854	832	3	0.146
2	16.731	819	16	-0.731
3	20.928	814	21	0.072
4	33.462	802	33	-0.462

Table 11.4: Table showing run 3 in the hoisting motor position accuracy test, with varying hoisting speeds in both directions and using WOB PID controller to hoist between measurements

Measurement no.	HM Pos. (mm)	Laser measurement (mm)	Laser pos. (mm)	Position difference
0	0	752	0	0
1	156.119	596	5	-0.119
2	362.038	389	8	-0.962
3	151.138	602	150	-1.138
4	538.29	168	584	0.71
5	28.818	724	28	-0.818

The error fluctuates and does not appear to grow over time. The average error is slightly on the negative side, meaning that the hoisting position was slightly lower than the laser position. This could be due to the low number of samples taken. The magnitude of the error is mostly below 1mm and always below 1.5 mm.

11.4.5 Discussion

The test showed that the RPM readings from the hoisting motor were inaccurate and therefore not suitable in their current state for use in the control system. The position readings were much more accurate and mostly within a millimeter of the laser measurements. Since the laser only measured increments of one millimeter and a single millimeter difference in drilled length does not affect the performance of the rig very much, the hoisting motor's position readings are considered accurate enough to use in the control system. The drilling rate calculations will, therefore, be based on position and time instead of hoisting motor RPM.

11.5 Drill Bit Tests

The team had bits from three different sources to be tested. The sources were bits bought from Alibaba, the bits provided by DSATS and custom bits designed in cooperation between the team and Lyng Drilling as described in subsection 7.4.3. The Drillbotics competition allows the use of any kind of bit as long as it is designed by the team and within the required dimensions. All the bits were tested to see their performance with respect to ROP, WOB requirements and stability. The tests were performed with EMM to map the operational range of drilling parameters.

11.5.1 Drill Bit Tested with EMM

Before the hydraulic system was properly set up, the team decided to test the performance of the available bits with the EMM. The drilled cuttings were removed from the well by water from an external hose. Initially three bits with EMM were tested, as explained below. Ideally, many drilling runs should have been run per bit, but as sandstone was a limited resource, and the set up for these tests was very limited without internal water circulation, it was decided to save space in the sandstone so that more complete tests could be run later, and the Lyng bits could be included in these tests.

DSATS bit with inserts Firstly, one of the DSATS bits with a depth of cut limitation of 2mm was tested with a constant rpm of 87 while changing the WOB. The whole drill string experienced lot of vibrations right after touching the rock. This was due to the absence of the riser system and stabilizer. Due to the extensive bit walking the hole drilled was slightly overgauge. The picture of the drilled hole with this bit is shown in Figure 11.11.

Since, the circulation system was not active in the drilling test and cuttings were removed by external water supply, bit balling was observed. Also, in the picture below, it can be seen that the hole drilled not uniform which is due to the heterogeneous bit profile of DSATS bit. The Table 11.5 below shows the torque readings for the bit against the WOB. It is important to note that the torque mentioned in the table is the percentage of the nominal

torque provided by the motor against the WOB and the bit stalled at 17 kg. The nominal torque provided by EMM is 0.8 Nm.

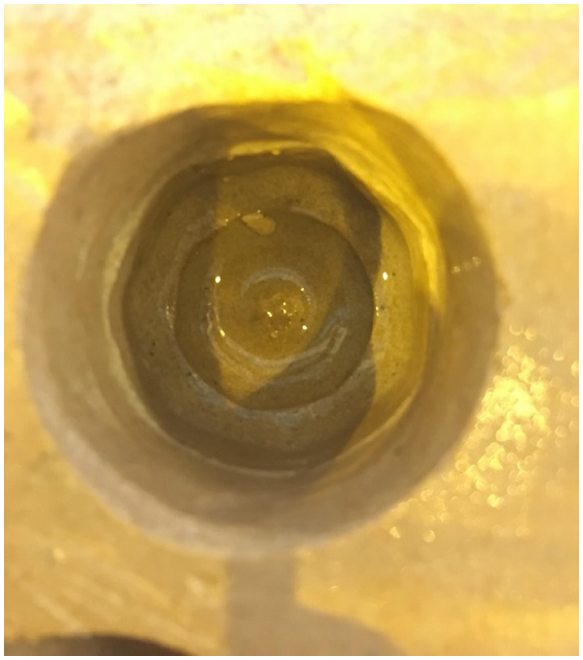

Figure 11.11: Hole drilled with DSATS bit

Table 11.5: DSATS bit torque against the applied WOB

WOB (kg)	% of Nominal Torque
6	45
9	61
12	86
14	95
15	98
16	99
17	100

DSATS bit without inserts In order to check the effect of the inserts, the team decided to test the bit provided by DSATS without putting inserts. The speed of the motor was held same the as for the previous test i.e. 87 rpm. As soon as the bit touched the rock surface, excessive bit walking was observed. This led to the whole drill string vibrating, which was stopped by manually stabilizing the bit. The hole drilled by this bit is shown in Figure 11.12.

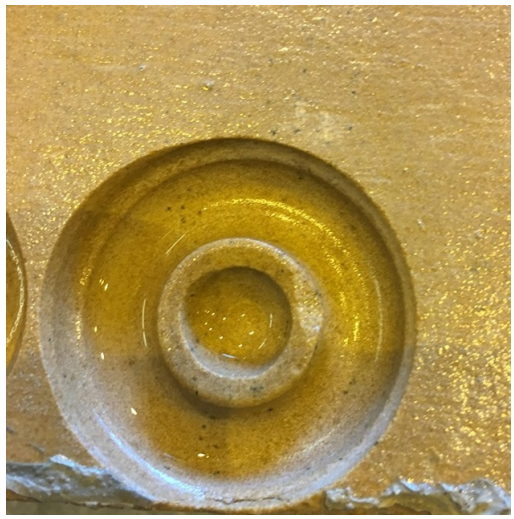

Figure 11.12: Hole drilled with DSATS bit (without inserts)

The hole drilled was over-gauge due to the bit walking and had a small undrilled section in the drilled hole as shown in Figure 11.12. The undrilled section was due to the absence of any cutters at the bit center and the bit moving in a circle withing the well, leading to the inner uncut circle. Eventually, the bit was unable to drill further and instead kept following the track it had made. It is clear that this bit will require better stabilization, preferably in the form of a pre-drilled pilot hole in order to be able to drill. The percentage of nominal torque against the applied WOB is shown in Table 11.6. Due to the undrilled ring in the center, the bit stop going down further and hence didn't experience more torque against the higher values of weight.

Table 11.6: DSATS bit (without inserts) torque against the applied WOB

WOB (kg)	% of Nominal Torque
3	17
5	18
8	24
12	32
14	52
16	57
19	75
22	85

Alibaba bit The Alibaba bit was also tested along with the DSATS and NTNU/Lyng Drilling bits. The drilling parameters remained the same as in the previous tests. The bit started walking as soon as it touched the rock surface but less than the DSATS bit without the inserts. The bit was kept static manually and after drilling the small hole, the Alibaba bit started drilling smoothly without any vibrations. The drilling speed was observed faster than the DSATS bit. The hole drilled by Alibaba bit is shown Figure 11.13.

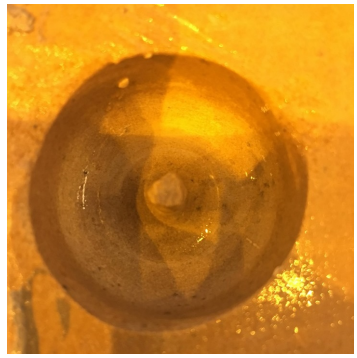

Figure 11.13: Hole drilled with Alibaba bit. The inner core visible in the middle of the well contributes to hole stability

The hole drilled was perfectly in gauge and smooth. However, a thin vertical undrilled section was observed after the drilling was stopped. This thin core was due to the absence of a cutter in the bit center. Due to that thin core, the bit gained support from the rock, causing stable drilling and a smoother and perfectly gauged hole. The percentage of nominal torque and the respective WOB for the Alibaba bit is shown Table 11.7. The nominal torque for the miniature EMM is 0.8 Nm.

Table 11.7: Alibaba torque against the applied WOB

WOB (kg)	% of Nominal Torque
3	36
6	48
8	66
10	67
12	90

The graph in Figure 11.14 shows the comparison of the initial drilling tests for three different bits and the Figure 11.16 shows the bits tested.

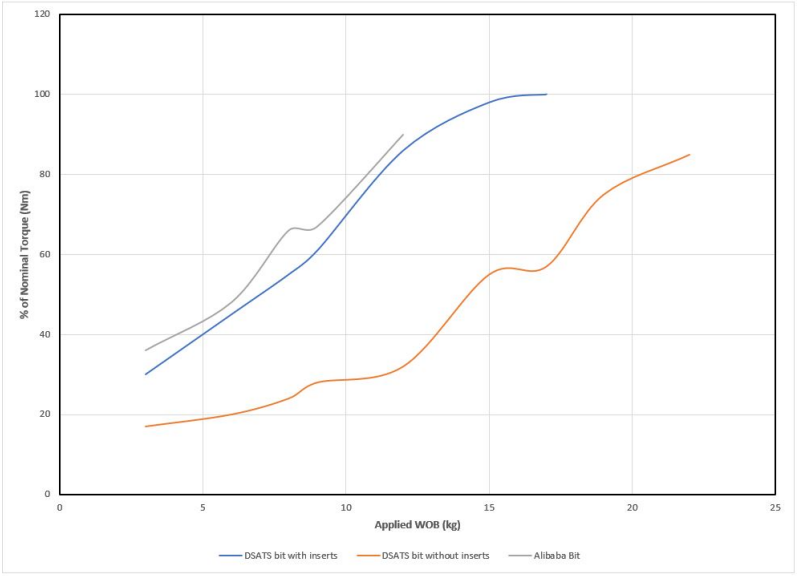

Figure 11.14: Comparison of Torques for three different bits

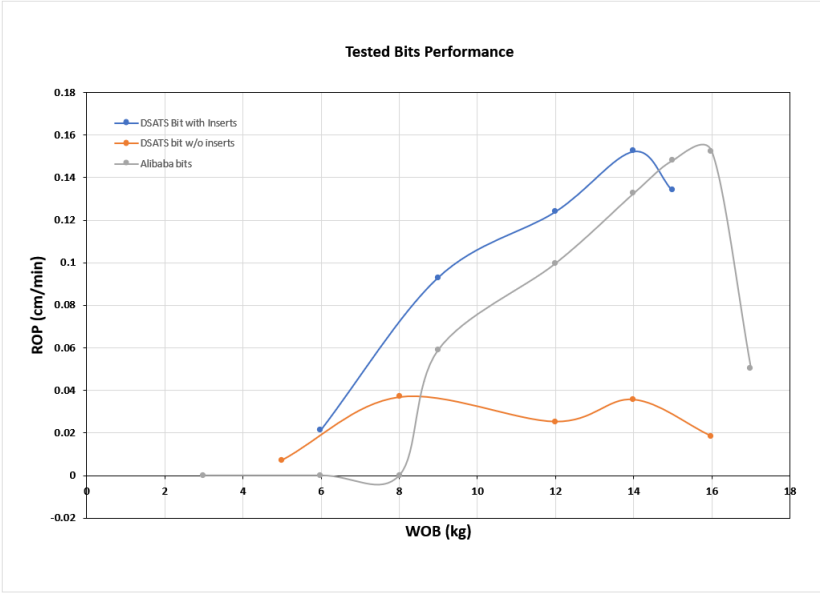

Figure 11.15: Comparison of ROPs for the tested bits

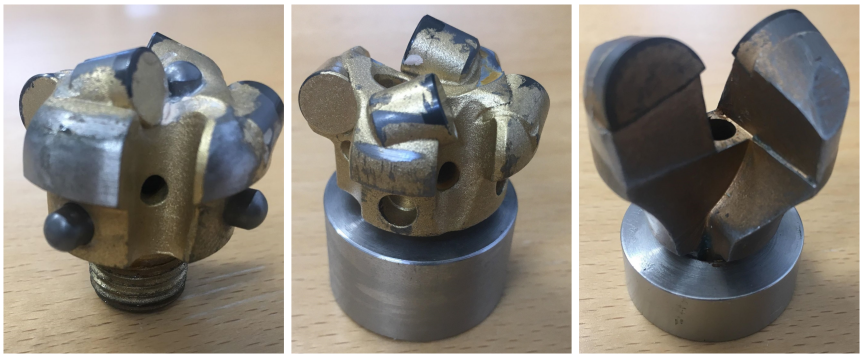

Figure 11.16: Tested bits (DSATS bit with inserts on right, without inserts in the center and Alibaba bit on the right)

Based on the comparison in Figure 11.14, the DSATS bit without inserts appears to be able to take a lot more WOB without stalling the motor. However, this is not due to efficient drilling, but rather due to the motor sliding around on a circular track of uncut rock without the cutters reaching the rock. This can be seen by Figure 11.15, where the ROP for this bit is much lower than for the other bits. As this would not have happened if proper stabilization was in place, it is not a good indicator of bit performance. It does however point towards the bit being a poor choice for drilling a pilot hole, as the rig floor stabilizer

was not enough to keep the bit stable. Ideally, further testing should be performed, but due to a lack of available sandstone, this test was not prioritized.

The DSATS bit with inserts limiting the depth of cut shows a smooth, slightly s-shaped curve as the relation between torque and WOB, stalling at around 16kg. The hole was slightly overgauge, which means some of the mechanical energy went towards drilling unnecessary rock. The bit profile has a shelf and bears evidence of the cutters not being evenly spaced. This bit is however probably the easiest to use when orienting during directional drilling, as it does not create the deep uncut sections of the Alibaba bit and unaltered DSATS bit. Therefore, less rock restricting is restricting side-wards force when the bit is at bottom and attempting to turn. It also has a higher ROP than the Alibaba bit for most WOB, but the effect tapers off more quickly. The maximum ROP is the same for the two different bits. This is likely due to hole cleaning issues, as sand accumulation was observed around the cutters towards the end of the run, where the ROP was higher. A high ROP means that more cuttings were generated. At the same time, the well got progressively deeper with each increase in SP, which made the hole more difficult to clean with the external hose.

The Alibaba bit had the highest torque at any given WOB and the best stability. The central cylinder of undrilled rock at the center of the bit ensured stability and a smooth borehole, but would probably have caused major issues when orienting in deviated mode, as the extra torque the EMM would have to provide in order to break this cylinder would limit the available torque for cutting at the sides of the wellbore, which could cause already slow drilling to nearly come to a halt.

The plan was to test the custom design bits with the same drilling parameters as for the other bits. But due to the delay in the arrival of the custom bits, top drive failure and swivel connection issues, these bits could not be tested for performance. However, a top drive performance test with the custom bit proved that the custom NTNU/Lyng Drilling bits can have good performance while drilling vertically. As the bits have been carefully designed for the requirements of the team, it is planned to use a custom bit in the competition, despite the team not having had the chance to compare drilling performance between these bits.

Chapter 12

Challenges

In any technical project involving designing and manufacturing, different unpredicted events, experiences and challenges can happen. These experiences can affect the overall performance of the project. During the Drillbotics competition, the team experienced a lot of mechanical and logistical challenges, some of the challenges were overcome permanently while some got temporary solution. This chapter explains all the challenges throughout the Drillbotics project.

12.1 Project Management

The Drillbotics team is a multidisciplinary team with students from petroleum and cybernetics backgrounds. The team members from petroleum background had a steep learning curve when working with setting up communication with new sensors and learning the basics of the theory related to the downhole measurements. The team member with a cybernetics background helped the team greatly in understanding the lower level of the control system, as well as the basics of downhole measurements.

Different components for the rig were ordered from around the world. For each part ordered, a contact person within the team was assigned to follow-up the orders to avoid any unnecessary delays. The machining of small components in the university workshop was also followed up, as the support crew always has multiple projects at the same time. During the last week before the rig shipping, a lot of testing was expected to be done. Different communication and hardware problem appeared during the last week and the team dedicated long days to solve the problems that arose.

12.2 Down-sizing of BHA

The original main plan was to use a PDM in a BHA with a bent housing to deviate the hole at specific angle. In the industry, PDMs are used frequently for directional drilling. The size of the PDM in a drilling operation in the petroleum industry varies from 4 m to 12 m, depending upon the vendors and design [12]. The down-sizing of the BHA from several meters to a few centimeters was a big challenge. The team first spent time on understanding the working principle of the PDMs before applying the theoretical concept into the CAD design. With different iterations, especially in the power section of the PDM, the team managed to down-size the whole BHA to 16.4 cm, which fit within the space constraints of the minature rig. The secondary solution of using a downhole EMM as a power section also faced some challenges related to the size of the BHA. Finding a sufficiently strong motor within the size limitations proved challenging and finding a way of water sealing such a miniscule motor was a task that was worked on until the very end of the project. The whole BHA and its designed is explained in section 7.3.1.

12.3 Manufacturing of BHA Parts

The designing of the PDM was done on the basis of available papers and in-house knowledge . When the designing challenge was over, the challenge of machining the whole BHA came in. The team contacted different vendors for machining the PDM power section and EMM housing, but the parts were too small and complex. Particularly challenging were the parts with internal features, such as the inner surface of the stator and the water channels in the EMM housing walls. Manufacturing these features would require the parts to be made in several pieces and then later put together. Instead, team decided to go for metallic 3D printing of the PDM power section and EMM housing, due to this manufacturing method's capabilities of making complex designs relatively quickly based on CAD files. The designs were sent to multiple vendors for the best possible proposal and team ended up using the services of a company in Sweden. The rest of the BHA, such as bent housing, stabilizers, bit sub, and sensor subs were machined in the university workshop by the support crew and off-the-shelf parts such as u-joints and bearings were ordered separately.

12.4 Elastomer Coating of Stator/Rotor

When drilling with a PDM, keeping the leakage between the rotor and stator to a minimum is extremely important for the performance of the motor. In the industry, the stator is commonly coated by an elastomer layer, which creates a positive fit between the rotor and stator. This prevents water leaking between the sealing lines in the configuration, and ensures that the majority of the flow rate goes towards driving the motor. The team initially planned to use a similar solution. Covering the internal surface of the stator was considered

impractical, due to the size and tolerances of the part, in case the coating would have to be applied by hand. It was therefore desired to apply an elastomer coating to the rotor instead. This would also reduce the metal to metal contact, which was expected to cause wear over time. Several avenues were tried and the team found a supplier willing to provide an elastomer coating for free. However, this would require a custom metal mould to be created. This would be complicated for all the same reasons that made manufacturing the rotor and stator to be complicated. 3D printing a mould would be expensive. It would also be an inflexible solution, as one rotor/stator fit would have to be decided on for each mould. As the team considered it likely that different rotor/stator fits would have to be tested in order to make the PDM solution work, this option was discarded, and the modular design in 3D printed plastic was instead designed. The detail of different designs is explained in section 7.3.1.

12.5 Pump Pressure

The PDM works with the hydraulic energy provided by the pump. There should be enough pressure and the flow for the PDM to work properly. During the testing phase, the pump started struggling with providing the enough pressure to overcome the resistance in the power section. The expectations from the pump were to provide around 80 bar of pressure so that the PDM could rotate, but the pump gave up at maximum 36 bars pressure. Towards the end of the project, the pump had become a major limitation for PDM testing. Finally, two days before the rig shipment, the worn out pump was replaced with a relatively newer pump available in the workshop.

12.6 EMM Water Sealing

The EMM with the bent housing is used as one of the options for the directional hole. To remove the cuttings from the drilled hole, a continuous flow of water through the drill string is necessary. The EMM is placed inside the EMM housing,which has channels inside its walls for water flow. It is necessary to have a near perfect motor seal to avoid short circuiting the motor. The team spent much time in sealing the area above the motor and shaft area with different option as explained in section 11.2.2. Due to the importance of conserving one EMM for the competition, the final water sealing solution has not been tested.

12.7 Electrical Swivel Wiring Problem

The electrical swivel provides the connection point between the downhole wiring and the topside wiring. During the testing phase, the team experienced problems related to the wiring in the electrical swivel, due to weak copper wires going from the hydraulic swivel to the electric swivel. Finally a decision was made to create all new connections with less fragile wires connecting the wires between the two swivels. As with the EMM water sealing, this solution is expected to work better than the old one, but has not been tested due to time limitations before the rig being shipped.

12.8 Wiring Inside the Drill Pipe

All the wires from the sensor card and EMM have to pass through 7 mm ID drill pipe. The two relatively thick power wires from EMM and 4 wires from the sensor card pass from the BHA through the drill pipe. These wires then have to connect with the wires coming from the electrical swivel at the drill pipe hook up point. Different options for connection was tested, but none of them showed satisfactory results for the whole run. The soldered option appeared to have good robustness, but making the connections was time consuming and the connection while drilling could not be tested for a full well length, due to the unstable connection through the swivel. Finally, 11-pin nano-connectors were ordered and the plan is to use these and to apply glued shrinking tubes before drilling to avoid water seeping into the connections.

12.9 Magnetic Distortions to Sensor Card

The sensor card is surrounded with the steel all around that caused magnetic distortion and poor downhole measurements. Different precautionary measurements, such as using a stainless steel riser and riser guide system, were taken to minimize the distortion. Furthermore, the decision was made to use an electromagnet outside the rock to provide an active magnetic ranging to the magnetometer inside the sensor card for correct downhole measurements.

12.10 Sensor Card Water Tightening

Similar to EMM, the sensor card is also sensitive to water. Initially the sensor card was properly sealed with the glued shrinking tube. This worked for some time, but later during the test the sensor card stopped responding. Water damage was observed. An epoxy layer was then applied on the sensor card surface to protect it from water, and tested by putting in water glass for 2 of hours. This solution of sensor card sealing worked and thus will be used in the competition. The two tested options for sensor sealing are shown in Figure 12.1.

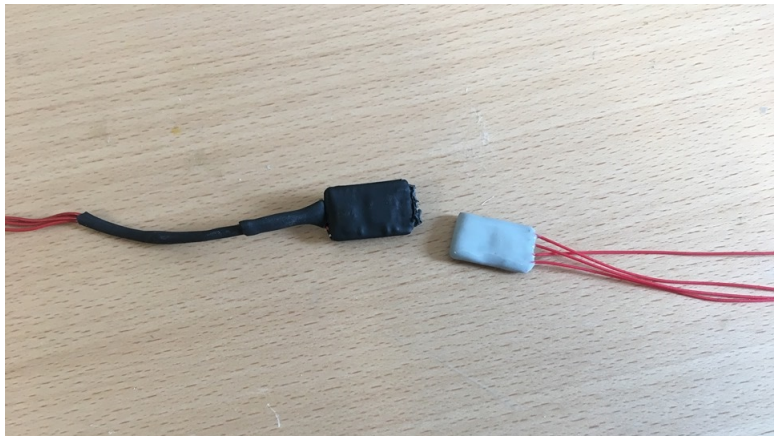

Figure 12.1: Sensor cards sealing, shrinking tube seal on left and epoxy seal on right

12.11 Top Drive Servo Communication

The servo drive communication was a real challenge and it caused a lot of delays in testing. One of the support crew had been working to set up the communication but due to communication protocol issues and delays in the missing parts, it was not possible to set it up early. Much communication with the vendor was required before a solution was found. After continuous effort and dedication by the senior engineer, the communication of servo motor with its drive was set up a few days before shipment. The team received the final instruction in the control of the top drive the evening before shipping.

12.12 Delays

In the planning phase of the project, team has added the possible delays from ordered parts in the time planner. However, some of the delays of were also experienced from the missing parts and the ordered parts which do not work as first assumed. Most of the delays didn't effect the overall time line of the project but the sum of deliveries combined with hardware and software issues have caused intensive down time which prevented the team from proceedings as planned. Due to these combined delays, the team could not manage to test the complete set up properly before the competition.

12.13 Budget Limitation

As explained in section 6.3, the budget of the project is limited to USD 10,000 only. To remain within the budget was a great challenge itself. Different ideas, such as testing of different PDM designs with steel printing and elastomer inside and more EMMs for testing its exact operational range were discarded due to budget limitations.

Chapter 13

Conclusions

The current thesis has shown the work done by NTNU for the Drillbotics competition. With a special focus on implementing a steerable BHA while using downhole measurements as feedback control.

The team worked on two solutions throughout the semester to try to limit the risks involved with each of them. Several changes had to be made to the rig to be able to steer inside the rock sample, as the Drillbotics guidelines require. Among the most important changes are the top drive and a more powerful pump.

This year HSE was improved by the control system instead of mechanically changing the rig. The competition script included a series of safety sequences that allow the driller to reduce NPT by not stopping the rig completely in case of a drilling dysfunction. Besides, the GUI was improved by adding a live log panel that displays all important events from the drilling operation, as well as colour coding important data in the front panel for easier reading.

As repeatedly mentioned throughout this report, the challenges with the BHA were numerous. Even though there was not enough time to properly tune and improve the PDM's performance, the learning curve behind the whole manufacturing process was steep. The team is certain this solution can still be improved and the operational state would have been reached with more time.

Working with downhole measurements proved to be a challenge as well. The proximity of the magnetometer with many static and moving steel parts, called for an additional method to properly track the azimuth of the well. By implementing an active magnetic ranging method, it was possible to keep track of the magnetic North and partially solve this issue.

By including two alternatives to deviate the well, the risks were minimized to a certain degree. Towards the end of the project, the downhole communication with the sensor card

proved to be an additional bottle neck. Since many wires had to be fed inside the drill pipe, the weak connections between wires kept going on and off, hindering complete setup tests before the competition.

In order to keep minimizing these risks while the rig was being shipped to Germany, the NTNU team kept the parts that needed to be fixed and tuned before the competition. With the majority of the challenges solved, the NTNU rig will compete against five other universities on June 13th in Celle, Germany.

Chapter 14

Future work

The focus of this project has been on making the rig ready for the competition. Working on two separate solution for a down-hole power section was a choice made to limit the risk of spending all resources on a solution that had a very real risk of being impossible to implement within the limitations of the competition. The trade-off for this was that the two solutions were in competition for resources. Time spent by the workshop staff manufacturing parts, monetary budget, rig time and work hours from the team members all had to be split between the solutions. The delays caused by this competition between the solutions, combined with long lasting problems with the top drive, a failing pump and the broad scope of the competition means that there are many avenues of work for future teams.

14.1 PDM Development

Further development of the PDM design could be done to increase the RPM and torque output of the solution. A dedicated workbench for PDM testing could improve the design process by giving more accurate measurements of the performance of the PDM, as well as limiting the amount of time lost due to waiting on rig. Such a workbench would need a tachometer for measuring the RPM, a device to measure the torque and pressure sensors to measure the pressure loss over the PDM. A strong pump would be required, as a lack of available pressure proved to be a limitation to testing many of the designs that seemed promising in theory. When the performance of the PDM is proven, drilling tests can begin. If a design is considered promising enough, the rotor could be 3D printed in metal to reduce friction.

A good investigation of the performance of the PDM would also ease the inclusion of the PDM in the control system, by finding how to more accurately detect stalling from readings of pressure change, vibrations from the downhole sensor or changing ROP.

Using a modular design and 3D printing parts for the PDM turned out to be an efficient method of testing different fits and configurations of the PDM. However, the accuracy of the printer could influence both leak rates and wear in the system, as uneven sides on the rotor or the stator could create paths for leakage, or cause wear due to the lack of a smooth finish. It could therefore be worth looking into acquiring a more accurate 3D printer, or simply using a smaller nozzle diameter. Variables such as infill density and pattern can affect the compressibility of the stator and the effect of changing these parameters should be looked into if work on the 3D-printed modular design is continued.

Efforts could also be made to reduce the length of the other components of the BHA, leaving more for the power section. A longer power section would mean a higher torque output. The long double U-joints are currently taking up much of the length in the BHA and replacing these with a shorter alternative could free several centimeters for a longer power section.

14.2 Testing System Limitations

Several aspects of the current rig could be investigated to get a better understanding of the current design. A complete well has never been drilled in the sliding mode in a real sandstone and the calculated deviation has therefore not been compared to the actual deviation that will be achieved. As the manufacturing process and measuring of this bend angle carry some uncertainties, it would give a better understanding of the deviation capabilities of this system to perform more deviated drilling tests with a down-hole sensor to measure the deviation.

Theoretical buckling limits depending on drilled depth can be adapted for deviated wells by testing the buckling limit of the lower section of the pipe at different well deviations and depths. The results of this can be implemented in the control system, to change the maximum allowed weight on bit depending on drilled depth. This was not necessary this year due to the weak downhole motor being considered a larger limiting factor than the buckling limit but could increase the drilling performance of the system if the down-hole motor is improved to such a degree that the drill pipe risks buckling before the motor stalls.

14.3 Improve Weak Parts of the Design

Some parts of the design needed a lot of work to function during everyday testing, and improving these would improve quality of life. A better method of sealing the EMM would lead to a lower risk of motor failure and less time and money spent replacing damaged motors. A wireless solution for down-hole communication would decrease the system's dependency on unstable connections in the drill pipe and electric swivel. Motor power could still go through this system, as the thicker wires have proven less likely to fail.

Efforts could be made to reduce the magnetic disturbances for the sensor card. Remaking the BHA in a non-magnetic material, such as aluminium, would reduce the requirements

for sensor calibration, and most likely lead to more accurate sensor readings. The power section should then also be made as non-magnetic as possible, which could be achieved by using a non-magnetic material in the PDM.

14.4 Improvements to Control System

The goal of the Drillbotics competition is to create a fully autonomous drilling rig. Improving the autonomous control system would, therefore, be a natural way forward for the project. To achieve this, the amount of input from the user should be reduced, the drilling performance should be optimized and the rig should be able to handle a wider scope of drilling issues.

Currently, the starting set point for weight on bit is set by the user and the computer changes it only if it detects that EMM torque values go outside a predefined range. The output from the motor could be more optimally used if the WOB was continuously changed to maximize the performance of the EMM, based on EMM torque. This could be done using a PID controller for the hoisting motor with EMM torque as input.

A similar system to the one used in 2018 could be an option, where the control system switches between torque control and WOB control for the hoisting motor, depending on which is the limiting factor. Accurate measurements of the down-hole motor torque would then be needed, to avoid limiting the drilling performance further. Any safety factors included to make up for inaccuracies in the torque measurements would restrict the operating range of the down-hole motor, which in the case of the EMM could lead to drastic decreases in drilling rate.

The top drive RPM during vertical drilling is currently completely manually decided. Allowing the control system to increase or decrease the RPM as needed, based on drilling performance, downhole motor performance, limits for internal electric wires and drill string limits would allow for more efficient drilling performance.

Pump RPM is also set to a constant in the control system. For the PDM, this is not an issue, as it is generally wanted to keep the flow rate and available pressure as high as possible. However, when drilling with an EMM that is sensitive to water, it could be an advantage to adjust the pump output as the well is drilled, to always keep the pressure at a minimum. This could perhaps be done by finding the relation between flow rate, pressure and pump RPM and combining it with hole cleaning calculations to determine how much water is needed to be pumped through.

On the position control side, steering could be improved by aiming towards a predefined path or target coordinates instead of constantly steering towards the local magnetic north. This would allow the control system to get back on track if an offset was detected, instead of drilling parallel to the planned path.

Bibliography

[1] Area moment of inertia. https://www.engineeringtoolbox.com/area-moment-inertia-d_1328.html/. [Online; accessed 21-May-2019].

[2] Determining yaw, pitch, and roll from a rotation matrix. http://planning.cs.uiuc.edu/node103.html. [Online; accessed 5-June-2019].

[3] EHS Today. https://www.ehstoday.com/safety/safety-practices-oil-and-gas-industry-infographic/. [Online; accessed 14-May-2019].

[4] Functions of drilling fluids. https://petrowiki.org/Functions_of_drilling_fluid. [Online; accessed 17-April-2019].

[5] HIWIN Corporation. HIWIN Ballscrew. http://wpstatic.idium.no/aratron.no/2014/12/Hiwin-Ballscrews.pdf. [Online; accessed 21-May-2019].

[6] HIWIN Linear guideway. https://www.hiwin.com/pdf/linear_guideways.pdf. [Online;accessed 19-April-2019].

[7] Kelly vs. Top Drive Rigs. https://www.petroprophet.com/kelly-vs-top-drive-rigs/. [Online; accessed 18-April-2019].

[8] MechanicalCalc. https://mechanicalc.com/reference/column-buckling. [Online; accessed 21-May-2019].

[9] National Instruments. http://www.ni.com/en-no/support/model.usb-6212.html/. [Online; accessed 21-May-2019].

[10] PDC bit design. https://petrowiki.org/PDC_bit_design. [Online; accessed 5-April-2019].

[11] PDC bit profile. https://petrowiki.org/PDC_bit_profile. [Online; accessed 8-April-2019].

[12] ”Positive Displacement Mud motor, Micon Downhole Tools”. https://micon-drilling.de/Download/Catalog_PDM_EN.pdf. [Online; accessed 06-June-2019].

[13] Principles of PID Control and Tuning. https://www.eurotherm.com/temperature-control-us/principles-of-pid-control-and-tuning/. [Online; accessed 05-May-2019].

[14] Rock strength. https://drillbotics.com/rock-strength/. [Online; accessed 15-May-2019].

[15] Steerable PDC bits require balanced design. https://www.ogj.com/articles/print/volume-97/issue-21/in-this-issue/drilling/steerable-pdc-bits-require-balanced-design.html. [Online; accessed 18-April-2019].

[16] Strength of materials. https://pressbooks.bccampus.ca/powr4406/chapter/bending-moment-stress/. [Online; accessed 28-May-2019].

[17] Suggested methods for determining the Uniaxial Compressive Strength and Deformability of rock materials. https://www.isrm.net/fotos/gca/1129631264isrm_sm_uniaxial_compressive_strength_and_deformability-_1979.pdf. [Online; accessed 5-May-2019].

[18] ”TDK Invensense, World’s Lowest Power 9-Axis MEMS MotionTracking Device”. https://www.invensense.com/products/motion-tracking/9-axis/icm-20948/. [Online; accessed 21-May-2019].

[19] M. L. Arnø. The design and implementation of a control system for an autonomous miniature drilling rig. Master’s thesis, NTNU, 2018.

[20] N. J. Bahr. *System safety engineering and risk assessment: a practical approach*. CRC press, 2018.

[21] A. T. Bourgoyne, K. K. Millheim, M. E. Chenevert, and F. S. Young. Applied drilling engineering. 1986.

[22] B. A. Brechan, A. N. Corina, T. B. Gjersvik, S. Sangesland, and P. Skalle. *Drilling, Completion, Intervention and P&A –design and operations*. NTNU - Department of Petroleum Engineering and Applied Geophysics, 2016.

[23] G. Bruton, R. Crockett, M. Taylor, D. DenBoer, J. Lund, C. Fleming, R. Ford, G. Garcia, and A. White. Pdc bit technology for the 21st century. *Oilfield Review Summer*, 2014.

[24] R. Clayton and B. Ivie. Development of whirl resistant pdc bits. *LACPEC*, 1994.

[25] M. J. Economides, L. T. Watters, S. Dunn-Norman, et al. *Petroleum well construction*. John Wiley & Sons West Sussex, England, 1998.

[26] S. Health and Executive. Safety topics in engineering industry, May 2019.

[27] T. Inglis. *Directional drilling*. Graham - Trotman, 1987.

[28] F. Irgens. *Fasthetslære*. Fagbokforlaget, 7. utgave edition, 2014.

[29] S. Knoop. Design and optimization of a miniature autonomous drilling rig-contribution to the drillbotics competition 2018. Master's thesis, NTNU, 2018.

[30] B. Larsen. *Måle- og reguleringsteknikk*. Instrutek A/S, 1994.

[31] Lenze. *Automation systems Drive solutions*. Lenze, 1 edition, 2013.

[32] A. Lescoeur, M. A. Olsen, M. Vasantharajan, and R. L. Egeland. Design and construction of an autonomous, miniature drilling rig-contribution to the drillboticstm competition 2017. Master's thesis, NTNU, 2017.

[33] K. T. Lowe. Selection and integration of positive displacement motors into directional drilling systems. *University of Tennessee Honors Thesis Projects*, 2004.

[34] S. Menand, H. Sellami, C. Simon, A. Besson, and N. D. Silva. How bit profile and gauges affect well trajectory. *SPE Drilling and Completion*, 2003.

[35] J. M. Montoza, M. U. Azam, M. Naamdal, and H. E. Helle. Design report ntnu - drillbotics 2018 phase 1. 2018.

[36] T. Nguyen, E. Al-Safran, and V. Nguyen. Theoretical modeling of positive displacement motors performance. *Journal of Petroleum Science and Engineering*, 2018.

[37] M. B. Nåmdal. Design and implementation of instrumentation and control system for an autonomous miniature drilling rig. Master's thesis, NTNU, 2019.

[38] C. S., R. Arfele, S. Anderle, and J. Romero. A new theory on cutter layout for improving pdc-bit performance in hard-and transit-formation drilling. In *SPE Intelligent Energy International Conference and Exhibition*, Utrecht, The Netherlands, 2014.

[39] G. R. Samuel and S. Miska. Analytical study of the performance of positive displacement motor (pdm): Modeling for incompressible fluid. *Society of Petroleum Engineers*, 1997.

[40] L. Sinor, J. Brett, T. Warren, and S. Behr. Field testing of low-friction-gauge pdc bits. *SPE Drilling and Completion*, 1993.

[41] N. O. Varco. *Motor Handbook*. National Oilwell Varco, 7 edition, 2011.

[42] U. Zalluhoglu, H. Gharib, J. Marck, N. Demirer, and R. Darbe. Steering advisory system for mud motors. *SPE/IADC International Drilling Conference and Exhibition*, March 2019.

[43] T. Åström, Karl J.; Hägglund. *PID Controllers- Theory, Design and Tuning*. ISA, 1995.

Appendix A

Drillbotics Guidelines 2019

Society of Petroleum Engineers
Drilling Systems Automation
Technical Section (DSATS)
International University Competition
2018 – 2019

Drillbotics™ Guidelines

Revised 26 November 2018

1. Introduction

This year marks the fifth competition for the title of Drillbotics champion and a chance for students to learn about the drilling process from industry experts and for winning team(s) to travel and present a paper at the next SPE/IADC Drilling Conference and at an event organized by DSATS. The past years involved undergraduates, masters and doctoral students from a variety of disciplines who built innovative drilling machines and downhole tools while developing a deeper understanding of automating the drilling process. The university teams freely share lessons learned, which more rapidly advances the science of drilling automation. Everyone involved claims to have had a lot of fun while learning things that are not in the textbooks or published papers. Students also participated in related events at conferences, workshop meetings and networking with industry leaders in drilling automation. This year's contest promises to be just as challenging and hopefully as much fun.

How did the competition first come about? The origins began in 2008 when a number of SPE members established the Drilling Systems Automation Technical Section (DSATS) to help accelerate the uptake of automation in the drilling industry. DSATS' goal was to link the surface machines with downhole machines, tools and measurements in drilling systems automation (DSA), thereby improving drilling safety and efficiency. Later, at an SPE Forum in Paris, the idea of a student competition began to take shape. A DSATS sub-committee was formed to further develop the competition format and guidelines. Several universities were polled to find out the ability of academic institutions to create and manage multi-disciplinary teams. The Drillbotics committee began small in 2014-2015 to see if the format could succeed. With fine tuning, we continue along those lines as we start the 2019 process.

Version	Date	Section	Description
2019.01	10 Sept 2018	All	New Challenge, updated drillbit and formation, mandatory sensor requirements
2019.02	19 Nov 2018	3.1, 3.2, 3.4, 3.5, 3.7, 3.15, 8.2, Appendix A"	Modification to directional drilling target/objective/scoring, add details to bit specifications
2019.3	26 Nov 2018	3.2 3.5 and 3.6 3.7 7.0	Consolidated section Renumber/re-arrange section, allow for pilot hole and revise shipping info Bit diameter Timeline to reflect co-located tests

The 2019 competition has a few changes worth highlighting here:

- During previous competitions, the main focus was autonomously dealing with drillstring mechanics. Of course, this remains a concern, but the new test will focus on autonomous directional drilling.
- The 2019 rock sample shall be a homogeneous sandstone of known strength. Strength valuation will be provided well in advance of the competition date by the Drillbotics committee.
- Closed loop control of the rig based on downhole data is mandatory in this year's competition, not integrating this data set into the control algorithm is considered a "F - Failing grade" in this year's competition.
- Teams will kick off from vertical and are required to exit the rock sample within a defined target area, obtaining as much displacement as possible from well center along the north axis of the rock sample.
- The drill bit will be increased in diameter from last year's competitions by 1/8". Details will be provided via a post to the Drillbotics blog once the design is complete.
- Teams can choose to compete in a Group B Competition, which would use the prior year's rules/guidelines.
- The competition is to take place at a single industry facility in the USA and another facility in Europe. All teams are permitted to attend the presentations and Q&A of the other teams. All competitors at each location will start drilling at the same time.
- To attain a higher rating by the judges, the Phase I report should include a summary paragraph or table in the design report containing details of the control algorithm proposed. See section 3.4. This should be updated for the Phase II presentation to judges at the on-site test.
- The 2019 design should allow for third-party plug and play interface. See section 3.15.5. This is optional for 2019, but it will likely be mandatory in 2020.

The DSATS technical section believes that this challenge benefits students in several ways. Petroleum, mechanical, electrical and control engineers gain hands-on experience in each person's area of expertise that forms a solid foundation for post-graduate careers. They also develop experience working in multi-disciplinary teams, which is so important in today's technology driven industries. Winning teams must possess a variety of skills. The mechanical and electrical engineers need to build a stable, reliable and functional drilling rig. Control engineers need to architect a system for real-time control, including selection of sensors, data handling and fast-acting control algorithms. The petroleum engineers need an understanding of drilling dysfunctions and mitigation techniques. Everyone must work collectively to establish system functional requirements understood by each team member, properly model the drilling issues, and then to create a complete package working seamlessly together.

The oil and gas industry today seeks lower costs through efficiency and innovation. Many of the student competitors may discover innovative tools and control processes that will assist drillers to speed the time to drill and complete a well. This includes more than faster ROP, such as problem avoidance for dysfunctions like excessive vibrations, stuck pipe, and wellbore stability issues. Student teams built new downhole tools using 3D printing techniques of designs that would be difficult, if not impossible to machine. They used creative hoisting and lowering systems. Teams modeled drilling performance in particular formations and adjusted the drilling parameters accordingly for changing downhole conditions. While they have a lot to learn yet about our business, we have a lot to learn about their fresh approach to today's problems. Good Luck!

the DSATS Drillbotics Committee

Shashi Talya	(chair)	Pat Derkacz	Joachim Oppelt
Aaron Logan	(co-chair)	Frode Efteland	Neil Panchal
Fred Florence	(co-chair)	James Franks	Luis Pereira
Trey Adams		Jana Hochard	Marco Perez
Víctor Hugo Soriano Arámbulo		Mark Hutchinson	Bhavesh Ranka
Mike Attrell		Jayesh Jain	Geir Skaugen
Vimlesh Bavadiya		John Macpherson	Sami Sultan
Sylvian Chambon		George Michalopulos	Majid Tariq
John Clegg		Alex Ngan	Suresh Venugopal
Dmitriy Dashevskiy		Nii Nunoo	Kurt West

Contents

Objectives for the 2019 Competition

1.1. During the school year beginning in the fall of 2018, a team of students will organize themselves to solve a drilling related problem outlined in item 3 below. The team should preferably be a multi-disciplinary team that will bring unique skills to the group to allow them to design and construct hardware and software to demonstrate that they understand the underlying physics, the drilling issues and the usual means to mitigate the issues. We cannot stress enough the need to involve students with different technical training and backgrounds. They will need to develop skills to understand drilling dysfunctions and mitigation strategies, but they must also have the mechanical engineering capabilities to design the rig/drilling package. In past years, some entrants have not adequately considered the control network and algorithms needed for autonomous drilling. They have often misunderstood the need for calibrated sensors and fast, accurate data handling. All of this and more is needed to build and operate a complete automated drilling system.

1.2. The students could produce novel ideas leading to new drilling models, improved drilling machines and sensors, and the ability to integrate the data, models and machines that will hopefully create new, more efficient ways to drill wells in the future. Any such innovation will belong to the students and their university in accordance with the university's written policies. DSATS and SPE waive any claims to students' intellectual property.

1.3. The students, working as a multi-disciplinary team, will gain hands-on experience that will be directly applicable to a career in the upstream drilling industry.

2. Background

2.1. What is DSATS?

2.1.1. DSATS is a technical section of the Society of Petroleum Engineers (SPE) organized to promote the adoption of automation techniques using surface and downhole machines and instrumentation to improve the safety and efficiency of the drilling process. More information is available about DSATS at the DSATS homepage (http://connect.spe.org/DSATS/Home/).

2.1.2. The Drillbotics website at www.Drillbotics.com includes official updates to the competition guidelines and schedule, as well as FAQs, photos, and previous entrants' submittals and reports. Any updates to the guidelines posted on the Drillbotics website via blog entries from the

Committee is considered to be an official revision to these Guidelines. Questions and suggestions can be posted there, or teams can email the sub-committee at 2019@Drillbotics.com.

2.2. Why an international competition?

2.2.1. DSATS, as part of the SPE, is a group of volunteers from many nations, connected by their belief that drilling automation will have a long-term, positive influence on the drilling industry. This diversity helped to shape the direction of the organization. The group feels that the industry needs to attract young professionals from all cultures and disciplines to advance drilling practices in all areas of the world. The winners of the Group A competition will receive a grant for economy class transportation and accommodations to attend the next SPE Drilling Conference and will present an SPE paper that will be added to the SPE archives of One Petro[1]. Winners of Group B will publicly receive recognition of their achievement, and have the opportunity to publish an SPE paper that will be added to the SPE archives of One Petro. DSATS believes recognition at one of the industry's leading technical conferences will help encourage student participation. Also, the practical experience with drilling automation systems increases the students' visibility to the companies that are leading automation activities.

3. Competition Guidelines

3.1. Problem statement for the 2018-2019 competition:

Design a rig and related equipment to autonomously drill a well, using downhole sensors, that obtains as much horizontal displacement from surface as possible along the rock's "north" direction, as quickly as possible while maintaining borehole quality and integrity of the drilling rig and drillstring.

3.2. 2018-2019 High Level Challenge and Judging Changes

3.2.1. The competition will take place on the same day for all teams in North America, and the same day (likely different from the North American date) for all teams in Europe. (see 3.1.6, 3.5 and 7.0)

3.2.2. Inclination and Azimuth directionality is part of the competition for 2019. (see 3.5) The wellbore must be started vertically and then kicked off below a specified depth to build as much angle as

[1] Publication is subject to the SPE program committee's acceptance of the abstract/paper. If the abstract is not accepted, DSATS will solicit other SPE events try to get the paper into OnePetro.

possible along a specific well path. Teams score more points if the displacement is in the north direction along the centerline of the rock (see Appendix "A" for scoring details)

3.2.3. Downhole sensors are mandatory, and it is also mandatory to implement their data into the control algorithm of the rig. A severe penalty will be applied to teams who do not use downhole sensors. Closed loop control of the rig based on downhole data is mandatory in this year's competition, not integrating this data set into the control algorithm is considered a "F- Failing grade" in this year's competition.

3.2.4. A homogeneous sandstone Rock Sample will be provided by Drillbotics at the test sites. (see 3.6)

3.2.5. DSATS to provide a new bit with 1/8" larger diameter (1.25" new diameter) and 2" length. Students are permitted to use their own drillbit for the 2019 competition. (see 3.7)

3.2.6. Groups A&B

3.2.6.1. All returning teams must enter Group A, and are judged according to these guidelines. First time entrants may join Group A or Group B. Group B competitors will be judged by the previous year's guidelines (2017-2018).

3.2.6.2. New teams may choose in which Group they will compete with six (6) weeks' notice before the earliest drilling competition date. This notice is required for the committee to build and ship the custom rock sample.

3.2.6.3. Prizes are described in sections 9 and 10 below.

3.2.6.3.1. The "big prize" will be awarded to the winner of challenge Group A: an SPE Whitepaper published in OnePetro, economy class transportation and accommodations to attend and present at the next SPE Drilling Conference, with their rig presented at the drilling conference, subject to conference guidelines.

3.2.6.3.2. The winning Group B team will have an opportunity to present and publish a SPE Whitepaper, subject to the conference guidelines, and they will also receive recognition of the accomplishment at the conference

3.2.7. Additional information regarding the judging of the competition is detailed in section 3.16.

3.3. Two Project Phases

Fall Semester 2018

The first phase of the project is to organize a team to design an automatic drilling machine to solve the project problem. It is not necessary to build any equipment in this phase, but it is okay to do so. Design considerations should include current industry practices and the team should evaluate the advantages and shortcomings of today's devices. The design effort may be assisted by university faculty, but the students are encouraged to introduce novel designs for consideration. The level of student, faculty and technical staff involvement shall be reported when submitting the design. For returning teams, the Phase I Design should include an analysis of data and learnings from previous ("offset") wells drilled.

Spring Semester 2019

During the second phase, the finalist teams selected by DSATS proceed to the construction and drilling operation will use the previous semester's design to build an automated drilling machine. As per industry practices, it is common during construction and initial operations to run into problems that require a re-design. The team may change the design as needed in order to solve the problem subject to section 4.3.4. Teams may use all or part of a previous year's rig.

See section 7 for detailed timeline information.

3.4. Phase I – Design Competition

Design an automated drilling machine in accordance with the rules below.

3.4.1. DSATS envisions a small (perhaps 2 meters high) drilling machine that can physically imitate the functionality of full-scale rig machinery. (Since the winning machines will be presented at the SPE conference, there may be height restrictions imposed by the conference facility, so machines that are too tall may not be allowed on the exhibit floor.) The machine will be the property of the university and can be used in future research and competitions. New and novel approaches that improve on existing industry designs are preferred. While innovative designs are welcome, they should have a practical application to drilling for oil and gas.

3.4.2. The drilling machine will use electrical power from the local grid not to exceed 25 horsepower. Lower power consumption resulting from energy efficient designs will receive additional consideration.

3.4.3. The design must provide an accurate and continuous measurement of Weight-On-Bit (WOB), inclination, azimuth, and depth; as well as other drilling parameters, that should be presented as a digital record across the period of the test. All depth related measurements shall use the rig floor as the datum, not the top of the rock. Appropriate statistical measurements should be made at frequencies and with an accuracy and appropriate frequency content for the dynamics of the drilling system both at surface and downhole. Discussion of such choices should be included in the design report.

3.4.4. The proposed design must be offered in Phase I of the project, but changes are allowed in Phase II, as long as they are reported to the Committee via students' monthly reports. A summary of all significant changes, including the reason modifications were necessary, must be included in the students' final report.

3.4.5. Design submittal by the students shall include:

3.4.5.1. Engineering drawings of the rig concept, mechanical and electrical and auxiliary systems, if any

3.4.5.2. Design notes and calculations

3.4.5.2.1. All engineering calculations shall be included in the Phase I report, even if the rig is built using previous years' designs. This ensures that the 2019 team reviewed and understood the previous design assumptions and calculations.

Calculations should include each formula considered in the design, a reference that shows the origins of the formula, why is was chosen, what engineering assumptions were made, a definition of all variables and the values used in the calculation.

Example

Buckling limit	Euler's Equation	(1) cite a reference here or in the reference section of your design report

The critical buckling load, bcr, is calculated:

$Pbcr = \pi 2 * E * I /(K * L)^2$

$Pbcr$: Critical buckling load

E: Modulus elasticity of the aluminum drill pipe

I: Area moment of inertia

L: Length of the column

K: Column effective length factor (explain how you chose the appropriate k or n factor)

3.4.5.2.2. The report should include a table that summarizes ALL calculations.

Example

Calculations	***Formula***	***Reference***	***Results***
Moment of Inertia	$I = \pi / 64\ (dp\ 4 - idp\ 4)$	*Thin wall approx. or ID/OD calc separately or other? List your reference*	$0.000546\ in4$
Buckling Limit	$Pbcr = \pi 2 * E * I /(K * L)^2$	*Euler's Eq*	$18.9\ kg$

3.4.5.3. Control system architecture. (The response time of measurements, data aggregation and control algorithms should be estimated.)

3.4.5.4. Key features for any models and control software.

3.4.5.5. Proposed data handling and display.

3.4.5.6. Specification for sensors, signal processing and instrumentation, (verifying their accuracy, precision, frequency response and environmental stability), including the methods planned for calibration before and after the Phase II testing.

3.4.5.7. Plan for instrumentation of sensors in the BHA, as well as a method to synchronize all measurements and utilize both the surface and downhole sensors for real-time control of the drilling process.

3.4.5.8. An explanation of the implementation of the output of the BHA sensors to improve the trajectory of the wellbore, drilling efficiency and other drilling concerns.

3.4.5.9. An explanation of the algorithm used to autonomously control the drilling rig based on the output of the BHA sensors

3.4.5.10. An explanation of the principles being applied to directionally steer the wellbore into the defined target area (see Appendix "A") with the intent to score the maximum amount of points

3.4.5.11. Cost estimate and funding plan

3.4.5.12. A design summary video used to outline the design submittal not to exceed five (5) minutes in length. Videos shall be the property of the university, but DSATS shall have the rights to use the videos on its websites and in its meetings or events.

3.4.5.13. All design, construction and operation of the project are subject to the terms and conditions of section 11.

3.4.5.14. A safety case shall be part of the Phase I design. Include a review of potential hazards during the planned construction and operation of the rig, and for the unloading and handling of any rock samples or other heavy items. An example of a safety case will be posted on the Drillbotics.com website.

3.4.6. A committee of DSATS members (the Committee) will review the Phase I designs and select the top five (5) teams[2] who will progress to Phase II of the competition.

3.4.7. DSATS shall also award a certificate of recognition and publication on its website for the most innovative design. The design video will also be shown at the DSATS automation symposium at SPE conferences.

3.4.8. DSATS will not fund any equipment, tools, software or other material, including labor, for the construction of the rig. Student teams are encouraged to find external funding from industry participants and suppliers.

[2] The number of finalists could be increased or decreased by the DSATS Board of Directors subject to available funding.

3.5. Phase II – Drilling Competition

3.5.1. In the spring term of 2019, qualifying teams will build the rig and use it to drill rock samples provided by DSATS. Drilling a well, deviated toward the defined target area (see Appendix "A"), efficiently though the sample while controlling drilling dysfunctions is the primary technical objective of the competition. The exit point of the drillbit will be judged based on how much displacement from well center is obtained, with weighting applied according to the direction of the displacement. The use of both surface and downhole measurements to control the drilling process in real-time is mandatory, failure to do so will result in a failing grade. To avoid disqualification due to a downhole sensor failure, redundant or immediately replaceable items should be part of the design and implementation. Time to replace a sensor will be added to the drilling time for calculation of ROP.

3.5.2. The teams are to use manual control to pre-drill a vertical pilot hole not more than 1" deep measured from the rock's top face. This hole is to be drilled using the competition drilling rig. Location of this pilot hole will be marked on each sample by the committee at the intersection of two lines drawn from opposite corners of the rock sample.

3.5.3. Teams may use glue or use a mechanical fastener to attach a bell nipple or diverter housing to the top of the rock to allow connection of a flowline for return mud flow. The maximum allowable length of the bell nipple is 8 inches. If you use a fastener, be careful not to break the rock.

3.5.4. When the competition drilling begins, Teams competing in Group A will be required to continue to drill the pilot hole vertically to the kick off point. The kick off point may be at any depth greater than 4" below the surface of the rock.

3.5.5. Navigation shall be done autonomously, without any manual intervention.

3.5.6. No lateral forces are allowed to be applied above the rocks top face

3.5.7. No forces are allowed to be applied external to the rock that will force the drillbit in a particular direction

3.5.8. External magnetic field effects from the drilling rigs will be present on the directional sensors used to drill the wellbore. The industry has accepted practice of magnetic ranging, and this may be a technique worth investigating to improve the signal to noise of magnetic measurements

3.5.9. Once drilling commences, the test will continue until the drillbit exits the rock sample, or three (3) hours, whichever comes first.

3.5.10. Drilling performance will be observed and measured by Drillbotics judges invited to attend and witness the test.

3.5.11. DSATS will judge the competitors primarily on their ability to obtain as much displacement from well center as possible along the north axis of the rock sample; closer proximity to this axis and larger amounts of displacement point receives higher marks in this category (see Appendix "A" for details)

3.5.12. DSATS will run a flexible "casing" into the wellbore, and use this to gauge the borehole quality

3.5.12.1. Casing will be nearly equal in diameter to the 1.25" drillbit

3.5.12.2. An over gauge, and under gauge Casing will also be used as a no-go measurement

3.5.13. The final test will be scheduled late in the school year or soon after graduation. The test will occur at two locations, so teams must allow time to ship their rig from their university in accordance with the timeline per section 7 below.

3.6. Rock Samples

3.6.1. DSATS will prepare a set of nearly identical homogeneous sandstone samples appx. 12"W x 24"L x 24"H (30 x 60 x 60 cm) that will be shipped to each test site. It will not be sent to the schools. A smaller sample could be provided (no smaller than 12"W x 12"L x 24"H), which will be announced not later than March 1st.

3.6.2. The rock sample will be homogeneous sandstone, and rock compressive strength values will be provided for the sandstone samples furnished by DSATS. The Drillbotics committee will mark the surface of rock to indicate the well center where drilling will start. It will be located at the intersection of two lines drawn from opposite corners of the rock sample.

3.6.3. The university and/or students may acquire or produce rock samples as needed to verify the design and allow students to practice using their machine prior to the test. Drilling of the samples provided by DSATS prior to Phase II testing is not allowed and could lead to disqualification, except for the pilot hole.

3.6.4. The sandstone sample will be oriented during drilling so that it rests on a 12”x24” face so that the drilled depth will be 24”.

3.7. Bits

3.7.1. Upon request, DSATS will send a drillstring and bit to the finalist teams for use in Phase II. It is expected that the BHA and pipe will cause some difficulty, both for causing drilling dysfunction and for sensor integration and data telemetry. The judges will look for creative concepts supported by sound reasoning showing an understanding of how the BHA, bit and drillstring function together, and how the downhole system measures, samples and transmits the drilling data.

3.7.2. Upon request, the bit shall be returned to the Committee following Phase II testing for reconditioning for use in future competitions.

3.7.3. One (1) PDC bit will be provided by DSATS to be used during the Phase II tests. For 2018-2019 the bit will be:

3.7.3.1. A micro-bit 1.25" in (31.75 mm) diameter and 2.0” in total length.

3.7.3.2. Low axial aggressiveness and high side aggressiveness (i.e. high bit anisotropy).

3.7.3.3. An error when posting information about the bit diameter may have led to confusion and could affect teams who designed equipment based on the erroneous diameter. Therefore, teams may substitute a bit of their own design or a purchased bit not to exceed 1.5 inches in diameter and not more than 2 inches long. While this may allow some additional space for building the downhole equipment, it could also affect the build rate of the directional wellbore. It may also induce additional torque that could affect drillstring forces. Teams must evaluate the benefits and drawbacks of each and are encouraged to provide this analysis in their Phase I design report that describes what different forces are expected and their impact on drilling operations.

3.7.4. Students are encouraged to consider bit wear prior to the final test and its impact on drilling performance during the onsite testing. Based on prior competitions, bit wear should be minimal but some cutter damage is always possible.

3.7.5. Student teams may build or buy similar drill bits to test their design with the rock samples they sourced.

3.7.6. For the final competition, the students may use the directional drill bit provided by DSATS, or use their own bit design. However, the dimensions of their bits must not exceed 1.5 inches in diameter and 2 inches long. This provision is made to enable students to fully optimize the bit design for their specific directional system.

3.8. Drillpipe

3.8.1. The drill string provided by DSATS, if requested by the student teams, will be chosen to ensure drilling dysfunctions will be encountered. How these dysfunctions are mitigated is a key objective of the competition. Final details of the construction of this drill string will be furnished in late fall of 2018 to all entrants upon request. Preliminary specifications are listed below to assist with the mechanical and electrical design of the rig.

3.8.2. The drill pipe specifications for the 2018-2019 competition are subject to change, but should be:

3.8.3. Round Aluminum Tube 3/8 inch diameter x 36 inches long; 0.049 inch wall or equivalent

3.8.4. The material from KS Precision Metals is a typical low alloy material: "Our Aluminum tubing with wall thickness of .035 or .049 is 6061 T6"

3.8.5. DSATS will provide, upon request, the finalists four (4) joints of pipe. Any additional pipe needed can be purchased by the student teams or university if needed.

3.8.6. The use of a metric equivalent of the tubing is permitted.

3.8.7. Tubing is usually available from various hobby shops such as K-S Hobby and Craft Metal Tubing and via Amazon and other suppliers.

http://www.hobbylinc.com/htm/k+s/k+s9409.htm

ROUND ALUMINUM TUBING

OUTSIDE DIAMETER INCHES	WALL THICKNESS	ID
3/64 (.047)	.014	.019
1/16 (.0625)	.014	.035
5/64 (.078)	.014	.050
3/32 (.094)	.014	.066
	.016	.062
7/64 (.109)	.014	.081
1/8 (.125)	.014	.097
9/64 (.141)	.014	.113
5/32 (.156)	.014	.128
11/64 (.172)	.014	.144
3/16 (.187)	.014	.159
	.022	.143
	.035	.117
	.049	.089
13/64 (.203)	.014	.175
7/32 (.219)	.014	.191
	.022	.175
	.035	.149
15/64 (.235)	.014	.207
1/4 (.250)	.014	.222
	.016	.218
	.022	.206
	.035	.180
	.049	.152
9/32 (.281)	.014	.253
	.016	.249
5/16 (.312)	.014	.284
	.016	.280
	.035	.242
	.049	.214
11/32 (.344)	.016	.312
3/8 (.375)	.016	.343
	.035	.305
	.049	.277
13/32 (.406)	.016	.374
7/16 (.437)	.016	.405
	.035	.367
15/32 (.468)	.016	.436
1/2 (.500)	.016	.468
	.035	.430
17/32 (.531)	.016	.499
9/16 (.562)	.016	.530
5/8 (.625)	.016	.593

3.9. Tool joints

3.9.1. Students may design their own tooljoints as long as the design concept is included in the Phase I proposal.

3.9.2. Alternately, students may use commercially available connectors/fittings attached to the drillpipe using threads, epoxy cement or other material, and/or may use retaining screws if desired, as long as the design concept is included in the Phase I proposal.

3.9.2.1. A fitting used somewhat successfully in 2017 is available from Swagelock. In 2018, the winning team used a fitting from Vertex.

3.9.2.2. A fitting used successfully in 2016, but which did not work well in 2017, is available from Lenz (http://lenzinc.com/products/o-ring-seal-hydraulic-tube-fitting/hydraulic-straight-connectors) that uses a split-ring to allow a torque transfer across the fitting.

3.9.3. Students must state WHY they choose a tooljoint design in the Phase I proposal.

3.10. Bit sub/drill collar/stabilizers

3.10.1. It is expected that each team will design and build their own bit sub, instrumentation of the bit sub is ideal for directional sensors

3.10.2. Additional weight may be added to the bit sub, or surface weight/force (above the rock sample) may be applied to provide weight on bit and drillpipe tension

3.10.3. Stabilizers are permitted but will be limited in length. Advise the committee of your choice and why and include this in the Phase I design for committee consideration.

3.10.4. Students must add sensors to the drillstring, but are not permitted to instrument the rock samples. They must have a smaller diameter than the stabilizers and bit by at least 10%. Please include design concepts in the Phase I design.

3.10.5. The addition of along-string sensors to measure vibrations, verticality and/or tortuosity or other parameters will receive extra consideration. They must have a smaller diameter than the stabilizers and bit by at least 10%.

3.11. Automated Drilling

3.11.1. Drilling automation should be considered a combination of data, control AND dynamic modeling so that the control algorithm can determine how to respond to differences between the expected and actual performance. Process state detection can often enhance automation performance. Refer to documents posted on the DSATS website for more information.

3.11.2. Once drilling of the sample commences, the machine should operate autonomously. Remote operation and/or intervention is not allowed.

3.11.3. All directional steering should be autonomously controlled by the drilling rig

3.12. Sensors

3.12.1. The team may elect to use existing oilfield sensors or may look to other industries for alternate sensors.

3.12.2. The team may develop its own sensors if so desired.

3.12.3. Sensor quality differs from data quality. Both are important considerations in this competition.

3.12.4. The final report shall address which sensors were selected and why. The sensor calibration process shall also be explained.

3.13. Data collection and handling

3.13.1. The team may elect to use standard data collection and recording techniques or may develop their own. Data handling techniques and why they were chosen should be described in the Phase I submittal.

3.13.2. The final report shall address which data systems were selected and why.

3.13.3. The observed response time of measurements, data aggregation and control algorithms should be compared to the Phase I estimates.

3.14. Data visualization

3.14.1. Novel ways of presenting the data and progress of drilling in real time while drilling will receive particular attention from the judges.

3.14.2. Visualization of the processes (automation, optimization, drilling state, etc.) should be intuitive and easily understood by the judges, who will view this from the perspective of the driller operating a rig equipped with automated controls.

3.14.3. Data must be presented in a format that allows the judges to easily determine bit depth, elapsed drilling time, ROP, MSE, verticality/inclination, vibration, and any other calculated or measured variable used to outline the drilling rigs performance to the judges. Lack of an appealing and usable Graphic User Interface (GUI) will be noted to the detriment of the team.

3.14.4. All depths shall use the industry-standard datum of rotary/kelly bushing interface (RKB), which should be the top of the rig's "drill floor."

3.15. Measure and analyze the performance

3.15.1. The drilling machine should react to changing "downhole" conditions to select the optimal drilling parameters for improved performance, as measured by the rate of penetration (ROP), mechanical specific energy (MSE), verticality, cost per foot or meter, and other standard drilling measures or key performance indicators. Adding parameters such as MSE, or similar features, to the control algorithms will receive special attention from the judges.

3.15.2. Design limits of the drilling machine shall be determined and shall be incorporated in the programming of the controls during the construction phase.

3.15.3. Downhole measurements from directional sensors are to be used for adjusting drilling parameters and control of drilling machines used to aid in directional drilling

3.15.4. The final report (see Clause 3.19) shall outline drilling performance and efficiency criteria and measured results.

3.15.5. One of DSATS' goals is to promote plug and play capability to accelerate the implementation of drilling automation. A DSATS committee is preparing definitions and examples of proposed data communication protocols and interfaces. Once this is available, the Drillbotics competition will require the use of these standard protocols. This will not be a requirement for 2019 but it will be included in future competitions. Links to these standards will be added to the Drillbotics.com website when they are published.

3.16. The test well:

3.16.1. The competition will take place on the same day for all teams in North America, and the same day (likely different from the North American date) for all teams in Europe. The competition will take place at a facility capable of hosting all drilling rigs at the same time, and capable of having all drilling rigs start drilling at the same time (Group A and B). Location of drilling to be conducted indoors, in a location that does not have an unusually distorted magnetic field.

3.16.2. Prior to the commencement of the test, teams will attach a bell nipple per 3.5.3. They will then manually drill the pilot hole not to exceed 1" deep.

3.16.3. When the test begins, the teams will start drilling autonomously by continuing to drill the pilot hole, keeping the wellbore as vertical as possible until reaching the kick-off point. All rigs start the drilling competition at the same time (Group A and Group B)

3.16.4. The teams will kick off from vertical at any depth below the 4" vertical surface hole

3.16.5. The teams will target an exit of the directional wellbore within the defined target area. The target of exit is a primary judging metric, landing within the defined target area scoring points as described in Appendix "A"

3.16.6. No lateral forces may be applied above the rock.

3.16.7. Drilling will stop at 3 hours or when the last team exits the rock sample.

3.16.8. Should be drilled with a maximum allowable Weight-On-Bit dependent on the rig and dynamic drillstring integrity.

3.16.9. Will not require a closed-loop fluid circulation system, but could be of advantage for directional drilling, the bit and machinery should be cooled with air or fluid/water if needed. The design of the fluid system, if any, should be included in the Phase I design.

3.16.10. The rock sample will be homogeneous and will be capable of aiding in closed-loop fluid circulation. Note that the rock samples will leak once the drillbit punctures a rock face, so a rig design that includes a containment system is required.

3.16.11. Will require casing to fit in the directional wellbore. The ability to "run casing" is the secondary judging metric. Judges will run a "flexible" casing used as a gauge of borehole quality

3.16.12. Will not require a rig move, walking or skidding, but the mobility of the rig will be considered in the design phase.

3.17. Not included in the 2018-2019 competition

3.17.1. The drilling will not include automating the making or breaking of connections. If connections are necessary due to the rig and drillstring design, connections should be made manually, and the time involved with the connections will be included with respect to its effect on drilling performance (rate of penetration reduction).

3.18. Presentation to judges at Phase II Testing

3.18.1. The judges will arrive at the centralized test site facility to meet with the student teams and advisors immediately prior to the Phase II testing. DSATS will provide a suitable meeting room for discussion lasting about two hours.

3.18.2. The students will present a BRIEF summary of their final design, highlighting changes from their Phase I design, if any. Include an explanation of why any changes were necessary, as this indicates to the judges how much students learned during the design and construction process. Explain what measurement and control features have been deployed. Describe novel developments or just something learned that was worthwhile. Also include how actual expenses compared with the initial estimate. (Previous teams used a short PowerPoint presentation of about ten slides or so. Use any format you like.) Be sure to include all your team members as presenters, not just one spokesperson. At some time during your talk, let us know who the team members are and what background they have that pertains to the project.

3.18.3. Judges will ask questions to ascertain additional details about the design and construction process and to see if all team members have a reasonable understanding how all the various disciplines used for the rig design and construction fit together.

3.18.4. All teams may sit in for the presentations and Q&A of the other teams. The order of presentation will be determined by drawing lots.

3.19. Project report

3.19.1. The student team shall submit to DSATS a short monthly project report that is no more than one page in length (additional pages will be ignored) due on or before the last day of each month that will include:

3.19.2. Phase I

- Key project activities over the past month.
- Rig design criteria, constraints, tradeoffs, and how critical decisions were determined
- Cost updates
- Significant new learning, if any

3.19.3. Phase II

- Construction issues and resolution
- Summary of recorded data and key events
- Drilling parameters [such as WOB] and how they impact the test
- Other items of interest

3.19.4. Report content

3.19.4.1. To teach students that their work involves economic trade-offs, the monthly report should include at a minimum a summary estimate of team member labor hours for each step in the project: design, construction, testing, reporting, and a cost summary for hardware and software related expenditures. Also include labor for non-students that affect the cost of the project. Labor rates are not considered, as to eliminate international currency effects. Labor is not considered in the cost limits of item 6.1, but should be discussed in the report and paper.

3.19.5. File naming convention

3.19.5.1. To avoid extra work by the committee to rename all files, please use this convention for:

3.19.5.1.1. Monthly reports

Year-Month# University Name (abbreviated)

(note this is the competition year (spring term))

Example 2019-09 UDC

3.19.5.1.2. Design reports

Year University Name (abbreviated)

(note this is the competition year (spring term))

Example 2019 University of Drillbotics Competition

3.20. Final report and paper

3.20.1. The finalists shall prepare a project report that addresses the items below. We suggest you use the format of most SPE papers. For reference, please see http://spe.org/authors/resources/

3.20.2. The winning team of Group A and Group B shall update the report as needed to comply with SPE paper submittal guidelines to write a technical paper for publication by the SPE at its Annual Drilling Conference. SPE typically requires that the manuscript is due in the fall following the Phase II test. While the Drillbotics committee will make every effort to have the paper presented during the Drilling Conference, the SPE Program Committee has authority over which papers will be accepted by the conference. If the paper is not accepted by the conference, the Drillbotics committee will endeavor to have it presented at the DSATS Symposium and will use its contacts to have the paper published via other related SPE conferences.

3.20.3. The report, paper and all communications with DSATS shall be in the English language. The presentation will be made by at least one member of the student team.

3.20.4. The timing for submittal of the abstract and paper will be the published deadlines per the call for papers and conference guidelines as posted on the SPE's website (www.spe.org).

3.20.5. The abstract must generate sufficient interest with the SPE review committees to warrant publication, although DSATS will help promote acceptance where possible

3.20.6. The paper should address at a minimum

3.20.6.1. The technical and economic considerations for the rig design, including why certain features were chosen and why others were rejected.

3.20.6.2. The setup of the experimental test, the results and shortcomings.

3.20.6.3. Recommendations for improvements to the design and testing procedures.

3.20.6.4. Recommendations for improvements by DSATS of the competition guidelines, scheduling and provided material.

3.20.6.5. Areas of learning gained through the competition not covered in the university course material.

3.20.6.6. A brief bio or CV of the team members and their sponsoring faculty.

4. Team Members

4.1. DSATS envisions that the students would be at least senior undergraduate or Masters level, well versed in the disciplines needed for such a project. The maximum number of students per team is five (5) and the minimum shall be three (3). Any team that loses team members during the project can recruit a replacement.

4.2. At least one member of the team must be a Petroleum Engineering candidate with sufficient coursework completed to understand the physics relating to the drilling problems and the normal industry practices used to mitigate the problem.

4.3. Students with a background in mining, applied mathematics, mechanical and electrical engineering, as well as controls, mechatronics and automation or software development, are the most likely candidates, but students with any applicable background is encouraged.

4.4. A multi-disciplinary team simulates the working environment in the drilling industry today, as most products and services are produced with the cooperation of technical personnel from differing backgrounds and cultures.

4.5. A university may sponsor more than one team but must submit only one team/design for Phase II evaluation.

4.6. Students shall register their team not later than 30 November using the registration form on the Drillbotics website. Any changes to the team members or university supervisor over the course of the competition should be reported in the monthly reports.

5. Expenditures

5.1. Teams selected to advance to the second phase must limit the cost of the rig and materials to US$ 10,000 or its equivalent in other currencies. The students shall find a source of funding and report the source in the Phase I proposal. All funding and procurement should comply with university policy.

These funds are intended to cover the majority of expenses for hardware, software and labor to construct and operate the team's equipment. DSATS shall not be liable for any expenditure other than DSATS provided material and specified travel expenses.

5.2. DSATS will assist when possible to obtain free PLCs or similar control devices from suppliers affiliated with the DSATS organization. Such "in-kind" donations shall not be included in the team's project costs.

5.3. Students and universities may use other "in-kind" contributions which will not be included in the team's project costs. Such contributions may include modeling software, laboratory equipment and supplies, and similar paraphernalia usually associated with university laboratory projects.

5.4. Any team spending more than US$ 10,000, or its equivalent in other currencies, may be penalized for running over budget.

5.5. DSATS reserves the right to audit the team's and university's expenditures on this project.

5.6. Any devices built for the project will become the property of the university and can be used in future research and competitions. Any maintenance or operating costs incurred after the competition will not be paid by DSATS.

6. *Other Considerations*

6.1. The design concepts shall be developed by the student team under the supervision of the faculty. Faculty and lab assistants should review the designs to ensure student safety.

6.2. Construction of the equipment shall be supervised by the student team, but may use skilled labor such as welders and lab technicians. The use of outside assistance shall be discussed in the reports and the final paper. DSATS encourages the students to gain hands-on experience with the construction of the rig since this experience will be helpful to the career of individuals in the drilling industry.

6.3. University coursework and credit: Each university will decide whether or not this project qualifies as a credit(s) towards any degree program.

7. *Project Timeline*

Phase I - Design:	Fall 2018
Submit monthly reports	On or before the final day of each month
Submit final design to DSATS	31 Dec 2018, midnight UTC
Submit an abstract to DSATS*	31 Dec 2018, midnight UTC

*DSATS will submit an abstract to the SPE that will include excerpts from the student abstracts by the conference paper-submittal deadline, typically in mid-summer, for consideration of a paper by the conference program committee.

Phase II – Construction and Testing	Spring 2019
DSATS to announce finalists	On or about 15 Jan 2019
Construction	Spring 2019
Monthly reports	On or before the final day of each month
Drilling Test	Specific on-site test locations and dates for the North American and European locations will be arranged not later than 31 March 2019. The testing will typically occur in late May and/or early June.
The timeline for the Phase II tests:	Day 0 Students arrive Day 1 Students rig up; judges arrive Day 2 Students present to judges Day 3 Performance tests Day 4 Students rig down and depart
Shipping of rig to test site	The rig should be shipped to arrive no earlier than 10 days before the test date. Each team will coordinate with the committee and provide any documentation necessary.
Prepare and submit paper	Per SPE deadline*
Prepare and submit presentation	Per SPE deadline
Present paper at the Drilling Conf	Per SPE and DSATS schedule

8. *Evaluation Committee*

8.1. DSATS will select an evaluation committee from its membership

8.2. Criteria/Weighting (see chart):

Criteria	Parameter	Weighting
Phase I:		
a. Safety	Safety: construction and operation	10
b.Mobility of rig	Rig up, move, rig down	5
c.Design considerations and lessons learned		10
d.Mechanical design and functionality, versatility		25
e.Simulation/Model/Algorithm		25
f.Control scheme	Data, controls, response times	25
	Total	100%
Phase II:		
a.Creative Ability	Analysis, concepts, development	10
b.Engineering Skills	Problem/Goal, design criteria, feasibility	10
c.Construction Quality		10
d.Cost Control		10
e.Performance		30
Various parameters such as:	ROP, MSE, Landing Bit, Inclination, and other	
Are these used within the control algorithms		
Exit of drillbit within defined target area (see Appendix "A" for details)	Optimal landing of bit	
f.Quality of wellbore	Tested using the Go-No-Go flexible 'Casing'	10
	Verticality, tortuosity, caliper, other	
g. Data	Data handling, data visualization, data comparison to judges' wellbore logs, and other	20
h. Downhole Sensor Data Used in Control Algorithm	**Pass/Fail**	**Pass/Fail**
	Total	100%
Intangibles	Additional score may be added or subtracted by the judges at their discretion	

9. Group A Prizes

9.1. The winning team of Group A will be sponsored by DSATS to attend the next SPE/IADC Drilling Conference to present a paper that explains their project in detail.

9.1.1. The program committee of the Drilling Conference awarded the Drillbotics subcommittee a permanent slot in one of the drilling sessions at the conference. As per SPE's customary procedures, the paper will be archived in OnePetro. In addition, SPE has agreed to furnish a booth in the exhibition area during the conference where the team can erect their rig and describe its operation to the conference attendees. This is an excellent opportunity for students to network with the industry.

9.2. Upon submittal to DSATS of a valid expense statement (typically a spreadsheet supported by written receipts) of covered expenses will be reimbursed by the treasurer of DSATS for the following:

9.2.1. Reasonable shipping costs of the Drillbotics rig to and from the conference as long as charges are pre-approved by the chair or co-chair of the Drillbotics subcommittee.

9.2.2. Round trip economy airfare for the team and one university sponsor/supervisor to the gateway city of the next SPE/IADC Drilling Conference. Entrants should use the SPE approved carrier where possible to minimize cost. Airfares that exceed the SPE rate must be pre-approved by the committee or the reimbursement will be limited to the SPE rate. Information of reduced fare flights is available on the conference website. Please note that reservations must be made before the SPE published deadline. The departure point will be a city near the university, the student's home, or current place of work, subject to review by the Committee. Alternately, a mileage reimbursement will be made in lieu of airfare should the entrants decide to drive rather than fly to the conference. The reimbursement is based on current allowable mileage rates authorized by the US Internal Revenue Service.

9.2.3. One rental car/van at the gateway city for those teams that fly to the conference.

9.2.4. Lodging related to one hotel room per team member will be reimbursed at a rate not to exceed the SPE rate. Note that the room reservations are limited, so entrants must book their rooms early. Room and taxes for the night before the DSATS symposium, the night of the symposium and for the nights of the conference are covered. Charges for the room on the last day of the

conference need to be pre-approved by the Committee as most conference attendees depart on the last day of the conference unless there are unusual circumstances.

9.2.5. A per diem will be pre-approved by the Committee each year, which will vary with the cost of living in the gateway city. The per diem is intended to cover average meals (breakfast, lunch and dinner) and incidentals.

9.2.6. ATCE registration will be reimbursed. Students should register for the conference at the student rate. Early registration is appreciated.

9.3. Individual award certificates will be presented to all participants upon request, with special certificates given to all finalists.

9.4. DSATS may provide additional awards, at its sole discretion.

9.5. The evaluation and all decisions on any matter in the competition by the DSATS judges and DSATS board are final.

10. Group B Prizes

10.1. The winning team of Group B will submit a SPE Whitepaper that explains their project in detail. If the quality of the abstract is approved by the SPE Conference Program Committee, as per SPE's customary procedures, the paper will be archived in OnePetro

10.2. Individual award certificates will be presented to all participants upon request, with special certificates given to all finalists.

10.3. DSATS may provide additional awards, at its sole discretion.

10.4. The evaluation and all decisions on any matter in the competition by the DSATS judges and DSATS board are final.

11. Terms and conditions

11.1. In no event will SPE, including its directors, officers, employees and agents, as well as DSATS members and officers, and sponsors of the competition, be liable for any damages whatsoever, including without limitation, direct, indirect, special, incidental, consequential, lost profits, or punitive, whether based on contract, tort or any other legal theory, even if SPE or DSATS has been advised of the possibility of such damages.

11.2. Participants and Universities agree to indemnify and hold harmless SPE, its directors, officers, employees and agents, as well as DSATS members and officers, and sponsors of the competition, from all liability, injuries, loss damages, costs or expenses (including attorneys' fees) which are sustained, incurred or required arising out of participation by any parties involved in the competition.

11.3. Participants and Universities agree and acknowledge that participation in the competition is an agreement to all of the rules, regulations, terms and conditions in this document, including revisions and FAQs posted to the DSATS and Drillbotics websites (see section 2.1).

11.4. Winning teams and finalists must agree to the publication of their names, photographs and final paper on the DSATS web site.

11.5. All entries will be distributed to the Drillbotics Committee for the purpose of judging the competition. Design features will not be published until after all teams have been judged and a winner is announced. Previous years' submittals, reports, photos and similar documentation will be publicly available to foster an open exchange of information that will hopefully lead to faster learning for all participants, both new and experienced.

11.6. DSATS and the SPE cannot provide funding to sanctioned individuals and organization per current US law.

11.7. Participants must comply with all local laws applicable to this contest.

12. Marketing

12.1. Upon request, DSATS will provide a link on its website to all participating universities.

12.2. If university policy allows, various industry journals may send a reporter to witness the tests and interview students to publicize the project.

- End -

Appendix

A. Directional Objective Scoring

The following attached pages describe the directional target area, as well as the scoring for the directional competition objective. The maximum score is obtained by drilling at least 2 3/8” from well center along the north axis of the rock sample (see page A-A1 for details). Deviation from the north axis results in a reduced score for the same amount of displacement (see page A-A2 for a scoring example).

Directional Control Scoring Target

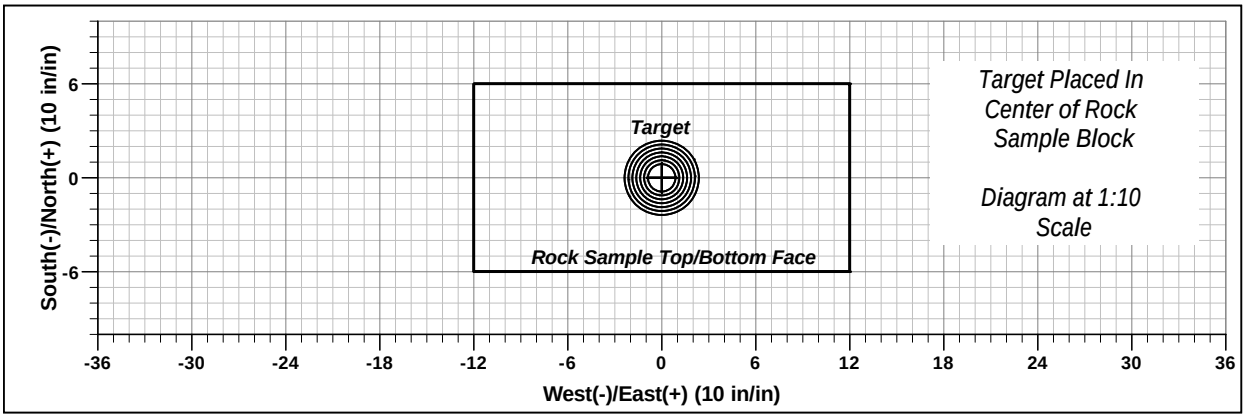

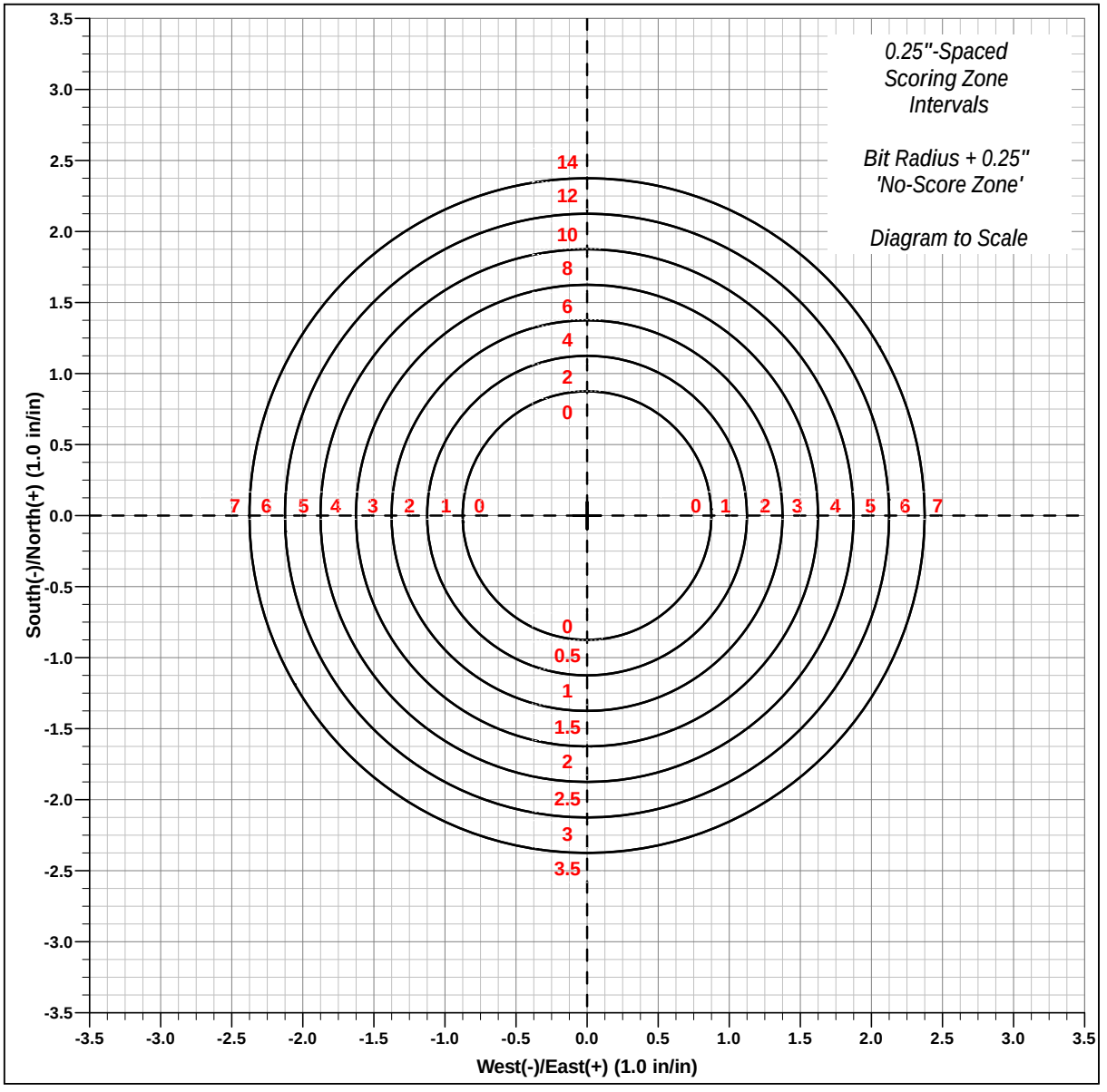

Directional Control Scoring Target Example

$$Total\ Score = [Min\ Score] + ([Max\ Score] - [Min\ Score]) * \frac{90° - [Deviation\ from\ Max\ Score]}{90°}$$

Max Score = 10 (North axis score)

Min Score = 5 (East axis score)

Deviation from Max Score = x = 35°

$$Total\ Score = [5] + ([10] - [5]) * \frac{90° - 35°}{90°}$$

$$Total\ Score = 5 + 5 * \frac{55°}{90°}$$

$$Total\ Score = 5 + 5 * \frac{55°}{90°}$$

$$\boldsymbol{Total\ Score = 8.06}$$

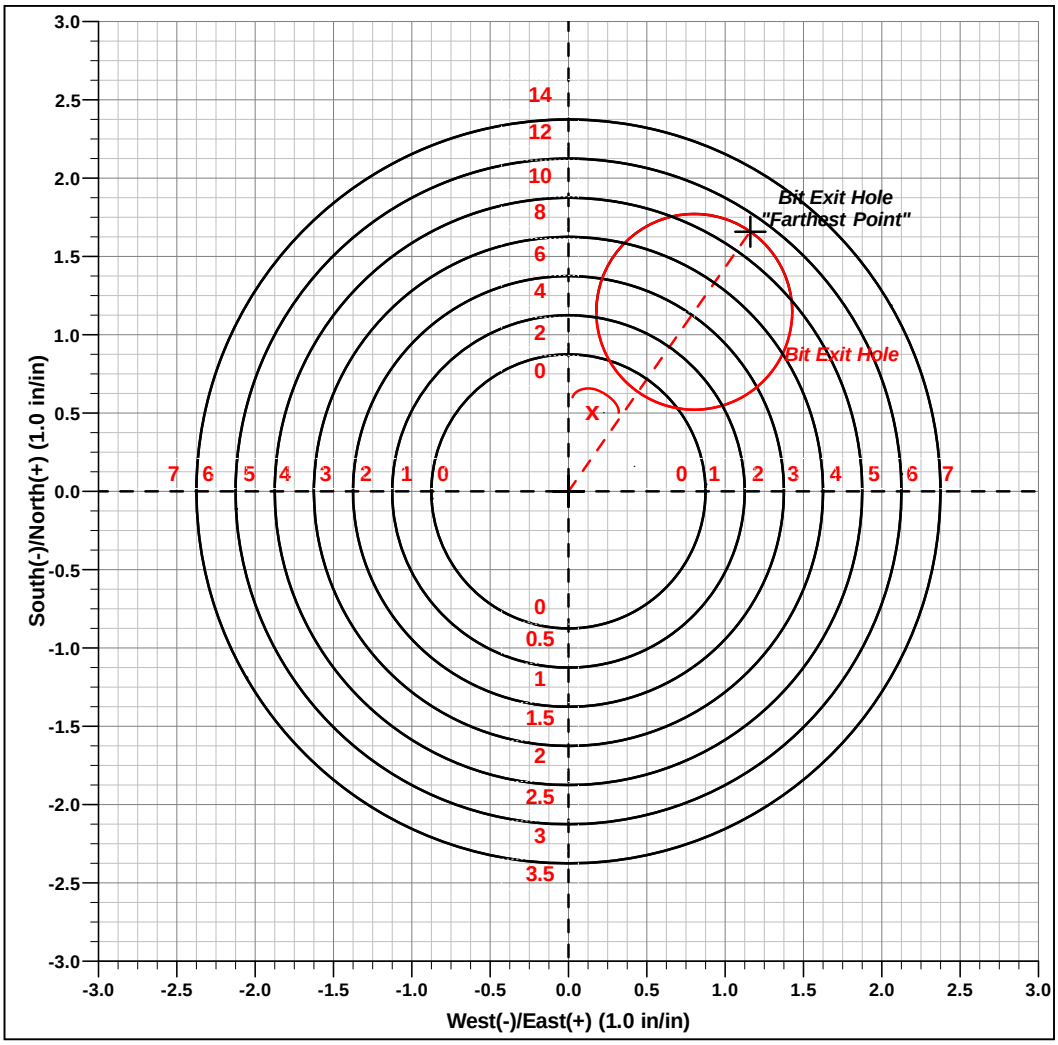

A.1 DSATS Drill bit

BAKER HUGHES a GE company

PDC Micro-Bit for 2019 SPE Drillbotics Competition

For the 2019 Drillbotics directional drilling challenge, a generic directional PDC micro-bit has been designed. Several changes have been implemented to aid directional drilling. The length has been significantly reduced and the bit anisotropy increased. Additionally, provisions are made to let participants adjust the axial and side aggressiveness of the bit before a run by changing the exposure of the blunt tungsten carbide elements on the gage pads and on the bit face.

PDC Micro-Bit

Micro-Bit face view

Specifications:

Overview	Steel body bit with 4 PDC cutters
Bit Diameter	1.25"
Bit Length	1.25"
Cutter Diameter	0.323"
Chamfer	0.010" x 45^0 (No ground flats)
Back Rake Angle	Cone Cutters (1-2): 25^0 Shoulder Cutters (3-4): 20^0
Clearance at Gage Pads	Configurable* 0"- 0.150"
Depth-of-cut Control	Configurable** (No bit body rubbing)
Hydraulics	Two ports (Not shown in the image)
Connection	1/4" NPT Threads (Not to be modified)

*Four tungsten carbide ovoid elements will be provided to adjust the gage configuration. The elements can be installed at a designed exposure using brazing or a special adhesive to adjust the clearance at the gage between 0" and 0.150"
**A tungsten carbide ovoid element will be provided to adjust the depth-of-cut control configuration. The element can be installed on the bit face at a designed exposure using brazing or a special adhesive.

Figure A.1: DSATS drill bit

Appendix B

Risk Assessment

	Situation	Estimated likelihood	Consequence	Possible risk mitigating actions
Electric downhole motor	Too many wires in drill pipe. Wires touch wall and get disconnected	Somewhat likely	Lost drilling time. While reconnecting wires.	Only using crucial wires from motor. Train team members in efficient reconnection of wires. Ensure wires are appropriate length.
	Not enough usable wire slots in electric swivel.	Likely	Need to buy new swivel. Extra cost. Long delivery time of swivel could lead to delays in testing.	Investigate whether a new swivel is needed. If there is any doubt as to whether a new one is needed, buy a new one to avoid unnecessary delays.
	Permanent installation of wires to el. motor interfering with sensor wires when drilling with PDM	Somewhat likely	Loss of downhole sensor communication, necessitating reconnection before drilling deviated section. Lost time.	Allow for disconnection of el. motor wires at top if possible. Train team members in efficient reconnection of sensor wires.
	Electric motor not providing enough torque	Likely	Slow drilling, not finishing competition within time limits.	Minimize friction in BHA. Do not use a too aggressive drill bit.
	Water damage to electric motor	Likely	Motor needs to be replaced. Extra cost and wait time	Buy motors to keep in reserve at once if motor proves to be strong enough.

Downhole PDM	Elastomer coating unavailable	Likely	Excessive negative interference between rotor and stator leading to poor PDM performance, and slow drilling.	Use simple alternatives, like grease and epoxy, to increase interference.
	Low flow rates at competition location	Likely	Low RPM, frequent drilling breaks. Slow drilling.	Use pre-filled water tanks to mitigate this effect. Pause drilling to fill up tanks, so drilling will be efficient.
	Not enough room for U-joint to rotate within housing	Somewhat likely	No rotation of drill bit, requiring re-design of BHA.	3D print plastic version to check fit before ordering expensive metal parts.
General BHA	Slow manufacturing of parts due to small size and complicated design	Very likely	Delayed testing	3D print most complicated BHA parts, plan for other tasks to work on while waiting for parts
	Thin internal BHA parts breaking.	Somewhat unlikely	Potential limitation to output of PDM, and therefore drilling speed. Can cause delays in testing if changing shafts is too time consuming.	Calculate theoretical mechanical limits of vulnerable parts. Always keep spare parts, limit torque by controlling WOB. All team members should learn to assemble BHA quickly.
	Sand particles interfering with function of thrust bearing	Very likely	Excessive friction while drilling, causing wear to bearing and slow drilling.	Keep spare bearings. Consider using grease to limit inflow of sand.
	Design or manufacturing errors on 3D printed parts	Somewhat likely	Risk of going over budget due to high price of 3D printed metal parts.	Print plastic versions of parts and check all relevant fits and functions of parts before ordering them in metal.

General project risk	High workload on team members due to tight deadlines and large project	Extremely likely	Long working days near competition date. Final set up not being properly tested.	Evaluate new tasks before putting a lot of work into them. Prioritize critical tasks and be ready to discard whichever BHA solution works least well.
	Team members being absent due to illness, traveling etc.	Certain	May lead to delays in execution of critical tasks if not planned for.	Ensure sharing of important file and knowledge between team members, so others can pick up the slack if necessary. Team members planning to be absent should finish important tasks before leaving.

Table B.1: Table showing different risks in the project

Appendix C

Bit design

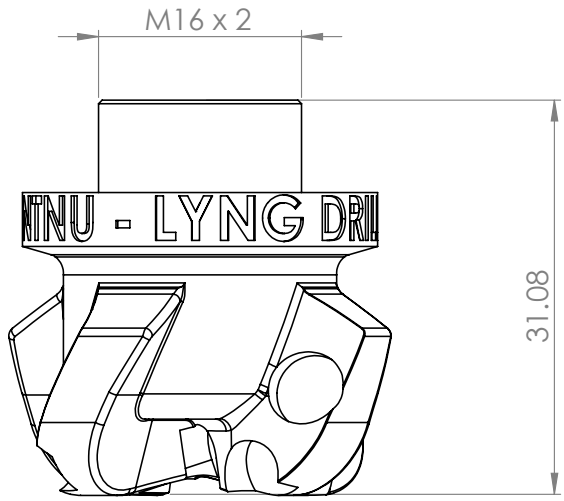

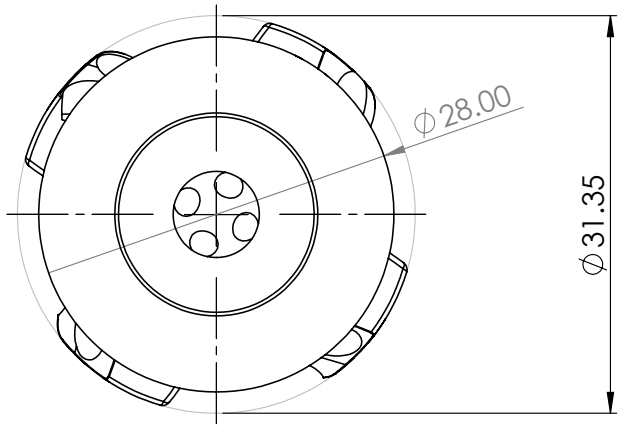

UNLESS OTHERWISE SPECIFIED: DIMENSIONS ARE IN MILLIMETERS SURFACE FINISH: TOLERANCES: LINEAR: ANGULAR:		FINISH:		DEBURR AND BREAK SHARP EDGES		DO NOT SCALE DRAWING	REVISION
	NAME	SIGNATURE	DATE			TITLE:	
DRAWN							
CHK'D							
APPV'D							
MFG							
Q.A				MATERIAL:		DWG NO. Design1a	A4
				WEIGHT:		SCALE:1:1	SHEET 1 OF 1

SOLIDWORKS Educational Product. For Instructional Use Only.

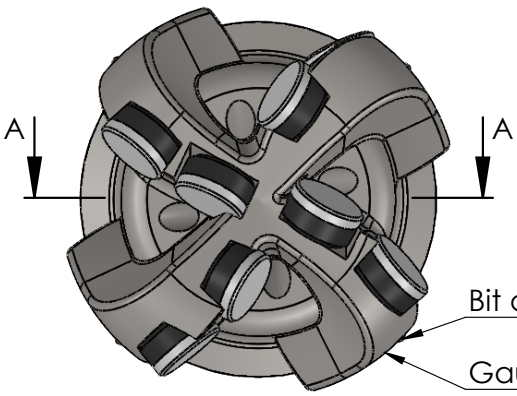

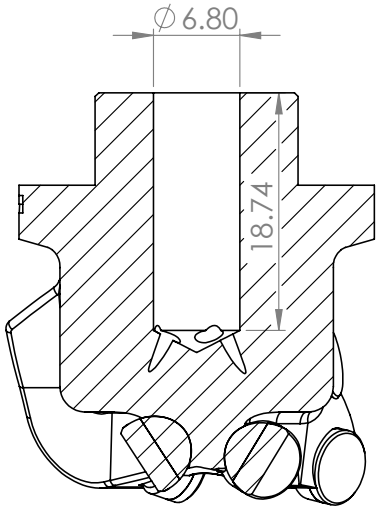

Section A-A

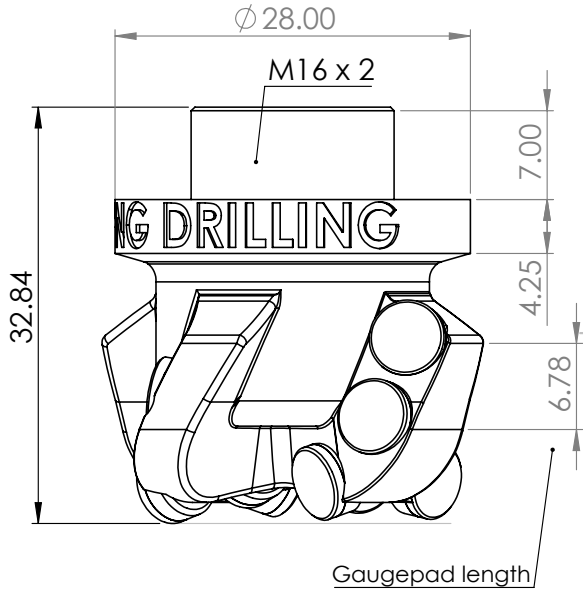

UNLESS OTHERWISE SPECIFIED: DIMENSIONS ARE IN MILLIMETERS SURFACE FINISH: TOLERANCES: LINEAR: ANGULAR:		FINISH:			DEBURR AND BREAK SHARP EDGES		DO NOT SCALE DRAWING	REVISION
	NAME	SIGNATURE	DATE				TITLE:	
DRAWN								
CHK'D								
APPV'D								
MFG								
Q.A				MATERIAL:			DWG NO. Design1b	A4
				WEIGHT:			SCALE:1:1	SHEET 1 OF 1

SOLIDWORKS Educational Product. For Instructional Use Only.

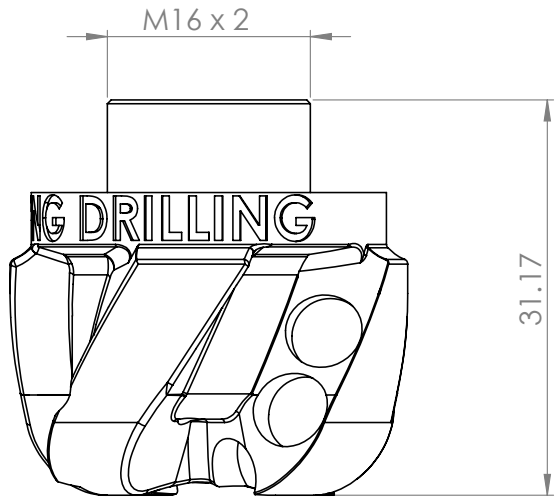

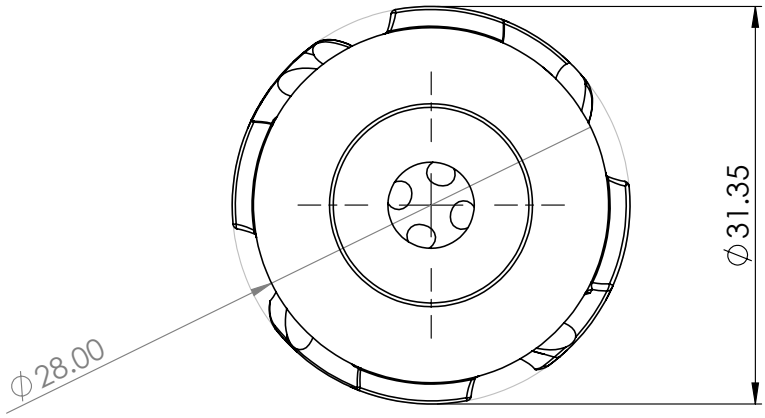

UNLESS OTHERWISE SPECIFIED: DIMENSIONS ARE IN MILLIMETERS SURFACE FINISH: TOLERANCES: LINEAR: ANGULAR:	FINISH:	DEBURR AND BREAK SHARP EDGES	DO NOT SCALE DRAWING / REVISION

	NAME	SIGNATURE	DATE
DRAWN			
CHK'D			
APPV'D			
MFG			
Q.A			

TITLE:

MATERIAL:

DWG NO. Design2a

A4

WEIGHT:

SCALE:1:1

SHEET 1 OF 1

SOLIDWORKS Educational Product. For Instructional Use Only.

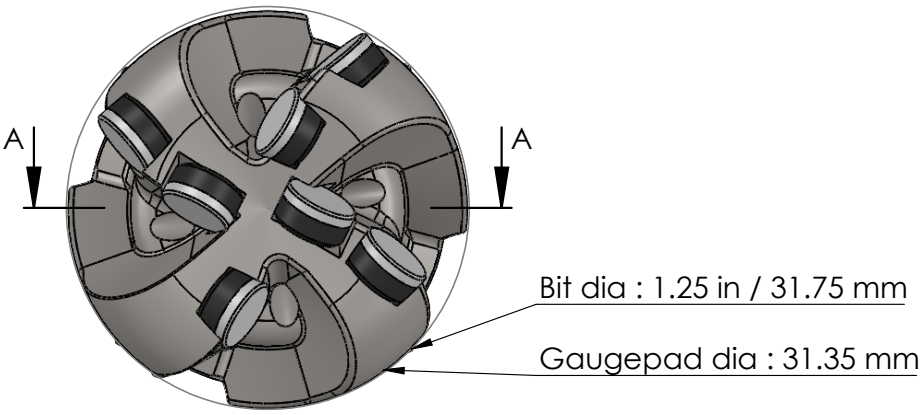

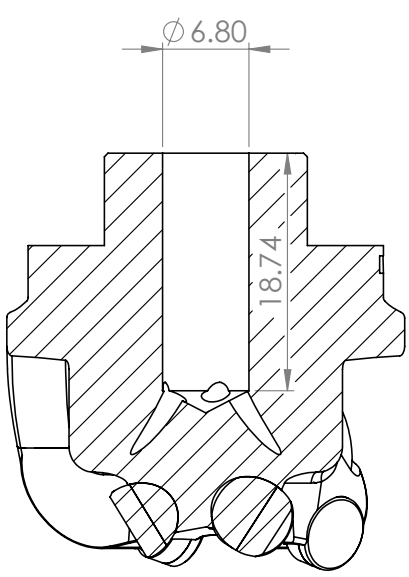

SECTION A-A

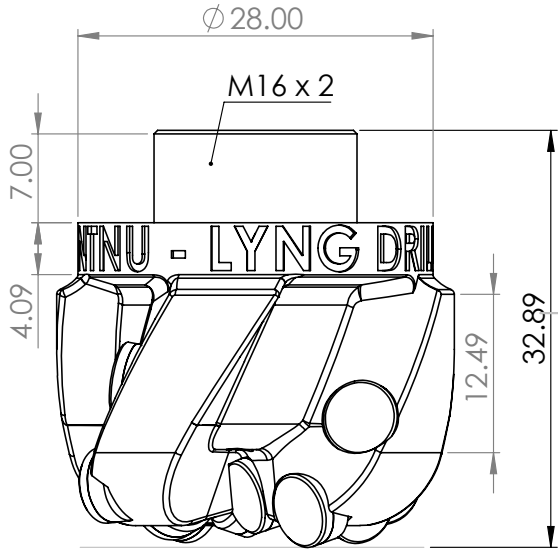

UNLESS OTHERWISE SPECIFIED: DIMENSIONS ARE IN MILLIMETERS SURFACE FINISH: TOLERANCES: LINEAR: ANGULAR:	FINISH:		DEBURR AND BREAK SHARP EDGES		DO NOT SCALE DRAWING	REVISION	
	NAME	SIGNATURE	DATE			TITLE:	
DRAWN							
CHK'D							
APPV'D							
MFG							
Q.A				MATERIAL:		DWG NO. Design2b	A4
				WEIGHT:		SCALE:1:1	SHEET 1 OF 1

SOLIDWORKS Educational Product. For Instructional Use Only.

Appendix D

Downhole EMM Technical Specifications

maxon motor
driven by precision

Configured drive

Motor - DCX19S GB KL 48V
Planetary gearhead - GPX19HP 138:1
Sensor - ENX 10 EASY XT 1024IMP

Part number: B7A0C6FBA57E Revision number 2

Orders are processed and shipped from Switzerland within 11 working days.
General Terms and Conditions: https://www.maxonmotor.ch/maxon/view/content/terms_and_conditions_page

To open the integrated CAD file, please save this document and open it in Acrobat Reader. The STEP file is available after a double-click on the pin icon.

B7A0C6FBA57E.stp (STP AP 214)

Open configuration: ?ConfigID=B7A0C6FBA57E

Motor - DCX19S GB KL 48V
Planetary gearhead - GPX19HP 138:1
Sensor - ENX 10 EASY XT 1024IMP

ISO 5456-1

Axial play gerahead: 0...0.1mm

maxon motor
driven by precision

Drawing not to scale!

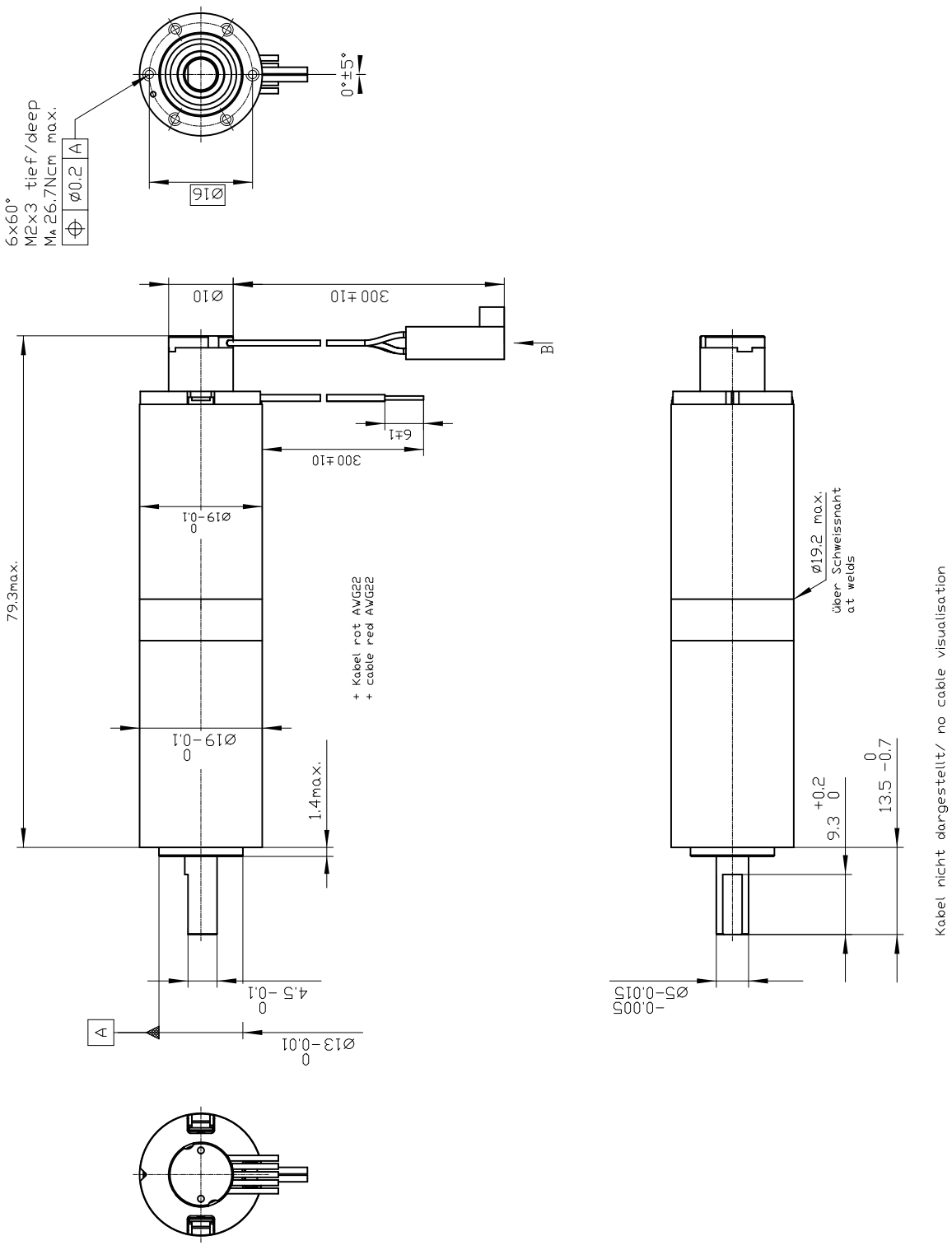

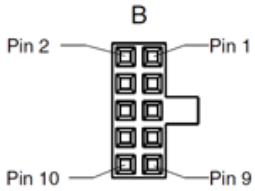

Connector type, encoder	
Molex 22-55-2102	
Pin 1	NC
Pin 2	VCC
Pin 3	GND
Pin 4	NC
Pin 5	NC
Pin 6	Channel A
Pin 7	NC
Pin 8	Channel B
Pin 9	NC
Pin 10	Channel I

Summary of your selected configuration

Total weight of the drive: 116 g

	DCX19S GB KL 48V	
Product detail		
	Commutation	Graphite brushes
	Nominal voltage	48 V
	Motor bearings	Preloaded ball bearing
Electrical connection, motor		
	Electrical connection, motor	Cable
	Cable length	300 mm

	GPX19HP 138:1	
Product detail		
	Gearhead type	High Power
	Reduction	138
	Number of stages	3

	ENX 10 EASY XT 1024IMP	
Product detail		
	Counts per turn	1024

Legend for part designation

EB	Precious metal brushes	GB	Graphite brushes	CLL	Spark suppression	BL	Brushless
A	Hall sensors	B	Sensorless	KL	Ball bearings	SL	Sintered bearings
GPX	Planetary gearhead	ENX	Encoder	ENC	Encoder	IMP	Pulses
ST	Number of stages	HP	High Power	S/M/L	Short/medium/long	HS	High Speed
STE	Sterilizable	INT	Integrated	STD	Standard	SP	Speed
ABS	Absolute	LN	Reduced noise level	A	Standard	LZ	Reduced backlash
C	Ceramic bearing			STEC	Sterilizable, Ceramic bearing		

Selected operating point

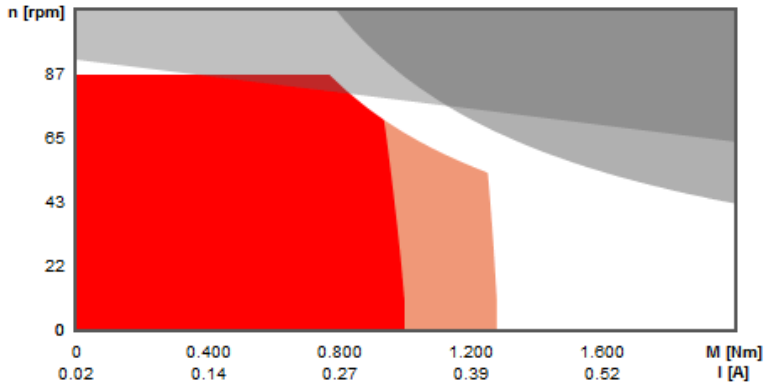

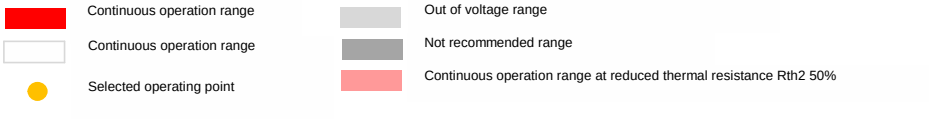

DCX19S GB KL 48V

Product specification	
Values at nominal voltage	
Nominal voltage	48 V
No load speed	12700 min^{-1}
No load current	18.7mA
Nominal speed	10800 min^{-1}
Nominal torque (max. continuous torque)	11.4 mNm
Nominal current (max. continuous current)	0.338 A
Stall torque	74.5 mNm
Stall current	2.09 A
Max. efficiency	82.3 %
Characteristics	
Max. output power continuous	16.1 W
Terminal resistance	23 Ω
Terminal inductance	1.32 mH
Torque constant	35.6 mNm A^{-1}
Speed constant	268 min^{-1} V^{-1}
Speed/torque gradient	173 min^{-1} mNm^{-1}
Mechanical time constant	4.92ms
Rotor inertia	2.72 gcm^2
Thermal data	
Thermal resistance housing-ambient	17.6 KW^{-1}
Thermal resistance winding-housing	6.5 KW^{-1}
Thermal time constant of the winding	11.5 s
Thermal time constant of the motor	312 s
Ambient temperature	-40…100 °C
Max. winding temperature	125 °C
Mechanical data	
Max. permissible speed	16000 min^{-1}
Axial play	0…0.1 mm
Preload	2.5 N
Radial backlash	0.02 mm
Max. axial load (dynamic)	2.5 N
Max. force for press fits (static)	30 N

	Static, supported shaft	440 N
	Max. radial load 5 mm from flange	16 N
	Measurement from the flange	5 mm

Further specifications		
	Number of pole pairs	1
	Number of commutator segments	9
	Motor weight	51.3 g
	Motor length	33.75 mm
	Typical noise level	40 dBA (6000 min^{-1})

Information about motor data: http://www.maxonmotor.com/medias/CMS_Downloads/DIVERSES/12_049_EN.pdf

GPX19HP 138:1

	Product specification	
Gearhead data		
	Reduction	138:1
	Absolute reduction	341550/2470
	Number of stages	3
	Max. continuous torque	1.6 Nm
	Max. intermittent torque	2 Nm
	Direction of rotation, drive to output	=
	Max. efficiency	65 %
	Average backlash no-load	1.3 °
	Mass inertia	0.528 gmc^2
	Max. transmittable power (continuous)	7 W
	Max. short-time transferable output	9 W
Technical data		
	Output shaft bearing	Wälzlager
	Max. radial play, 5 mm from flange	max. 0.1 mm
	Axial play	0…0.1 mm
	Max. permissible radial load, 5 mm from flange	120 N
	Max. permissible axial load	40N
	Max. permissible force for press fits	100 N
	Max. continuous input speed	12000 min^{-1}
	Max. intermittent input speed	15000 min^{-1}
	Recommended temperature range	-40..100 °C

Information about gearhead data: http://www.maxonmotor.com/medias/CMS_Downloads/DIVERSES/12_203_EN.pdf

ENX 10 EASY XT 1024IMP

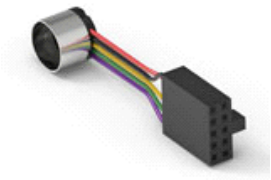

	Product specification	
Sensor data		
	Counts per turn	1024
	Number of channels	3
	Line Driver	No
	Max. electrical speed	90000 min^{-1}
	Max. mechanical speed	30000 min^{-1}
Technical data		
	Supply voltage Vcc	5 V ±10 %
	Output signal	INC
	Output signal driver	Single Ended / EIA RS 422
	Output current per channel	-20...20 mA
	State length	20…160 °el
	Signal rise time/Signal fall time	20/20 ns
	Min. state duration	125 ns
	Direction of rotation	A before B CW
	Index position	A low & B low
	Index synchronously to AB	Yes
	Index pulse width	90 °el
	Typical current draw at standstill	23 mA
	Max. moment of inertia of code wheel	0.09 gcm^2
	Operating temperature range	-55…125 C°
	Number of autoclave cycles	0

Datasheet: http://www.maxonmotor.com/medias/CMS_Downloads/DIVERSES/ENXEASY_EN.pdf

	Product specification	
Motor		
	DC motors up to	250 W
	EC motors up to	250 W
Sensor		
	Without sensor (DC motors)	Yes
	Sensorless (EC motors)	
	Digital incremental encoder (2-channel, single-ended)	Yes
	Digital incremental encoder (2-channel, differential)	Yes
	Digital incremental encoder (3-channel, differential)	Yes
	Digital Hall sensors (EC motors)	Yes
	SSI absolute encoder	Yes
	Analog incremental encoder (2-channel, differential)	Yes
Operating modes		
	Current controller	Yes (Torque)
	Speed controller (open loop)	
	Speed controller (closed loop)	Yes
	Positioning controller	Yes
Electrical data		
	Operating voltage VCC	10..50 VDC
	Logic supply voltage VC optional	10.. 50 VDC
	Max. output voltage (factor * VCC)	0.9 *
	Max. output current Imax	15 A
	Max. duration of peak output current Imax	15 s
	Continuous output current Icont	5 A
	Switching frequency of the power stage	50 kHz
	Sampling rate, PI current controller	25 kHz
	Sampling rate, PI speed controller (closed loop)	2.5 kHz
	Sampling rate, PID positioning controller	2.5 kHz
	Max. efficiency	98 %
	Max. speed (DC motors)	100000 min-1
	Max. speed (1 pole pair), block commutation	100000 min-1
	Max. speed (1 pole pair), sinusoidal commutation	50000 min-1
	Built-in motor choke per phase	15 uH
Inputs		
	Hall sensor signals	H1, H2, H3
	Encoder signals	A, A\, B, B\, I, I\

	Max. encoder input frequency	6.2 MHz
	Digitale Eingänge	8
	Functionality of digital inputs	limit switch, reference switch, general purpose
	Analog inputs	2
	Resolution, range, circuit	12-bit, -10…+10V, differential
	Functionality of inputs	general purpose
	Potentiometers	
	Functionality of the potentiometers	
	DIP switch	
	Functionality of the DIP switch	CAN Node-ID, Autobitrate, CAN-Bus Termination, I/O-level (TTL, PLC)

Outputs		
	Digital outputs	3
	Functionality of digital outputs	holding brake, general purpose
	Analog outputs	2
	Resolution, range	12-bit, -4…+4V
	Functionality of analog outputs	coming soon

Voltage outputs		
	Hall sensor supply voltage	see "Sensor supply voltage"
	Encoder supply voltage	see "Sensor supply voltage"
	Auxiliary output voltage	+5 VDC, max. 150 mA
	Output voltage (reference)	

Ambient conditions		
	Temperature – operation	-30.. 50 °C
	Temperature – storage	-40 .. 85 °C
	Temperature – extended range	+50…+80 °C, Derating: -0.167 A/°C
	Humidity (non-condensing)	5 .. %

Mechanical data		
	Weight	206 g
	Dimensions (L x W x H)	105 x 83 x 38.7 mm
	Mounting	Flange for M4 screws

Appendix E

Downhole EMM Drive Technical Specifications

RECOMMENDED

EPOS4 Module 50/5, digital positioning controller, 5 A, 10 - 50 VDC

Part number 534130

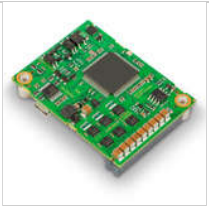

Enlarge image

Compare product
Add to wish list
Make a request
Send to a colleague

Price scales		
Price per unit	1-4	**€276.09**
	5-19	**€243.18**
	20-49	**€209.00**
	from 50	**On request**

Prices excluding VAT and shipping costs

Start combination

Order quantity 1 Add to cart

Print specifications

Description

The **EPOS4 Module 50/5** is a dynamic OEM positioning controller module for integration into customer systems. Designed for use with brushed DC motors with encoders and brushless EC motors (BLDC) with Hall sensors and encoders up to 250 W / 750 W.

Specifications

Product		
	Weight	17 g
Motor		
	DC motors up to	250 W
	EC motors up to	250 W
Sensor		
	Without sensor (DC motors)	Yes
	Digital incremental encoder (2-channel, single-ended)	Yes
	Digital incremental encoder (2-channel, differential)	Yes
	Digital incremental encoder (3-channel, differential)	Yes
	Digital Hall sensors (EC Motors)	Yes

	Absolute encoder (SSI)	Yes
	Analog incremental encoder (2-channel, differential)	Yes
Operating modes		
	Current controller	Yes (Torque)
	Speed controller (closed loop)	Yes
	Position controller	Yes
Electrical data		
	Operating voltage V_{CC} (min.)	10 V
	Operating voltage V_{CC} (max.)	50 V
	Logic supply voltage V_C (min.) optional	10 V
	Logic supply voltage V_C (max.) optional	50 V
	Max. output voltage (factor * V_{CC})	0.9
	Max. output current I_{max}	15 A
	Max. time of peak output current I_{max}	3 s
	Continuous output current I_{cont}	5 A
	PWM clock frequency of power stage	50 kHz
	Sampling rate PI current controller	25 kHz
	Sampling rate PI speed controller	2.5 kHz
	Sampling rate PID positioning controller	2.5 kHz
	Max. efficiency	97 %
	Max. speed (DC)	100000 rpm
	Max. speed (EC; 1 pole pair) block commutation	100000 rpm
	Max. speed (EC; 1 pole pair) sinusoidal commutation	50000 rpm
Inputs		
	Hall sensor signals	H1, H2, H3
	Encoder signals	A, A\, B, B\, I, I\
	Max. encoder input frequency	6.2 MHz
	Sensor signals	A, A\, B, B\, I, I\, Clock, Clock\, Data, Data\
	Digital inputs	8
	Functionality of digital inputs	limit switch, reference switch, general purpose
	Analog inputs	2
	Resolution, range, circuit	12-bit, -10…+10V, differential
	Functionality of analog inputs	general purpose
Outputs		
	Digital outputs	3
	Functionality of digital outputs	holding brake, general purpose
	Analog outputs	2
	Resolution, range	12-bit, -4…+4V
	Functionality of analog outputs	General Purpose

Voltage outputs		
	Hall sensor supply voltage	see "Sensor supply voltage"
	Encoder supply voltage	see "Sensor supply voltage"
	Sensor supply voltage	+5 VDC, max. 100 mA
	Auxiliary output voltage	+5 VDC, max. 150 mA
Interface		
	RS232	Yes
	USB 2.0 (full speed)	Yes
	CAN	Yes
	CANopen	Slave
	CANopen application layer	CiA 301
	CANopen frameworks	CiA 305
	CANopen profiles motion control	CiA 402
	Gateway function RS232-to-CAN	Yes
	Gateway function USB-to-CAN	Yes
	EtherCAT	IEC 61158 Type 12 Slave (optional)
	CoE (CAN application layer over EtherCAT)	CiA 402
	FoE (File transfer over EtherCAT)	Yes
	Distributed Clocks Support	Yes
	Variable PDO mapping	Yes
Display		
	Status indicator "Ready"	green LED
	Status indicator "Error"	red LED
Protective functions		
	Protective functions	current limit, overcurrent, excess temperature, undervoltage, overvoltage, voltage transients, short-circuits in the motor cable, loss of feedback signal
Ambient conditions		
	Temperature – Operation (min.)	-30 °C
	Temperature – Operation (max.)	45 °C
	Temperature – Extended Range	+45…+75 °C, Derating: -0.167 A/°C
	Temperature – Storage (min.)	-40 °C
	Temperature – Storage (max.)	85 °C
	Humidity (non-condensing) (min.)	5 %
	Humidity (non-condensing) (max.)	90 %
Mechanical data		
	Weight	17 g
	Dimension (length)	53.8 mm
	Dimension (width)	38.8 mm
	Dimension (height)	11.1 mm
	Mounting	mountable on socket terminal strips pitch 1.27 mm, mounting holes for M2.5 screws

Software	
Installation program	EPOS Setup
Graphical User Interface	EPOS Studio
Operating system	Windows 10, 8, 7
Windows DLL for PC	32-/64-bit
PC master	IXXAT, Vector, National Instruments, Kvaser
Programming examples	MS Visual C#, MS Visual C++, MS Visual Basic, MS Visual Basic.NET, Borland C++, Borland Delphi, NI LabView, NI LabWindows/CVI
Linux Shared Object Library	X86 32-/64-bit, ARMv6/v7/v8 32-bit, ARMv8 64-bit
CAN Interfaces	IXXAT, Kvaser
Programming example	C++

Functions	
CANopen Profile Position Mode	Yes
CANopen Profile Velocity Mode	Yes
CANopen Homing Mode	Yes
CANopen Cyclic Synchronuous Position	Yes
CANopen Cyclic Synchronuous Velocity	Yes
CANopen Cyclic Synchronuous Torque	Yes
Position Control Feed Forward	Yes
Velocity Control (Feed Forward)	Yes
Dual loop position and velocity control	Yes
Quickstop	Yes
Enable	Yes
Control of holding brakes	Yes
STO (Safe Torque Off)	based on IEC61800-5-2
Advanced automatic control settings	Yes

Downloads

Catalog page

Katalogseiten (deutsch, PDF 433 KB)	Version 2018
Catalog page (english, PDF 418 KB)	Version 2018
カタログページ (日本語, PDF 337 KB)	Version 2017

Software/firmware

English

Setup EPOS2, EPOS2 P, EPOS3, EPOS4 and MCD's - Studio 3.5 (english, ZIP 1 GB)	Version 32
EPOS Setup Release Notes (english, PDF 172 KB)	Version November 2018
EPOS Command Library Documentation (english, PDF 9 MB)	Version November 2018
EPOS Windows 32-Bit and 64-Bit DLL (english, ZIP 96 MB)	Version 6.5.1.0
EPOS .Net Library (english, ZIP 32 MB)	Version 6.5.1.0
EPOS LabVIEW VI's (english, ZIP 18 MB)	Version 6.5.1.0

Appendix F

Phase I control system theory

This section is taken directly from the Phase I project report handed in from the NTNU team to DSATS in December 2018.

4.3 Control Theory

4.3.1 PID Controller

A PID controller, or a proportional-integral-derivative controller, is a highly used closed loop feedback controller within process/performance control in many industries. The team will use this controller to control the rig response during the drilling operation. Figure 15 shows an overview of the PID control scheme.

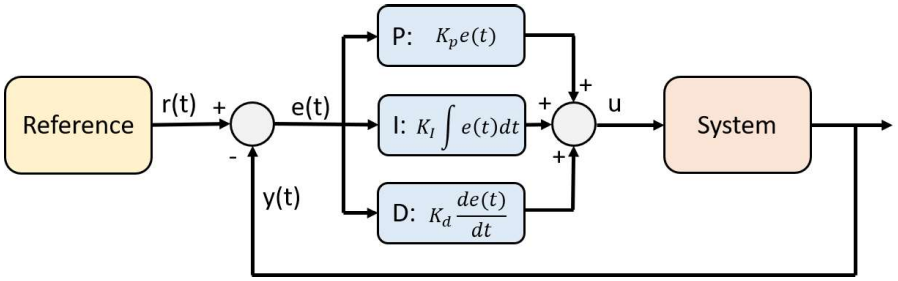

Figure 15: Overview of PID control scheme

The working principle of the PID controller starts with measuring the control state $y(t)$. This is further used in feedback to the controller where an state error $e(t)$ is calculated compared to a chosen set point. The error is then fed into the controller where proportional, integral and derivative effect is applied to calculate the new input to the system. The main goal by using a PID controller is to minimize the state error and to achieve a steady state response. A mathematical expression of the controlled input u can for a PID controller be defined as

$$u(t) = [K_p e + K_I \int e(t)dt + K_d \frac{de(t)}{dt}] \tag{19a}$$

where the equation in the frequency domain becomes

$$u(s) = e(s)[K_p + \frac{K_I}{s} + sK_d] \tag{19b}$$

To better explain how the PID controller effects the system response, a graphical illustration is presented in Figure 16. Along with the figure, the effects can be explained accordingly:

- **P:** The proportional effect determines how fast the output response is going to the reference. That is, a large proportional gain K_p results in a small rise time. The rise time is the time it takes for the system to reach a set percentage of the reference value after an impulse response. The rise time is shown in the figure.
- **I:** The integral effect eliminates the error between the set point and the measurement, often referred to as the steady state error. That is, large integral gain K_I results in a response eliminating the steady state error, moving the response up to the desired reference. The steady state error is shown in the figure.
- **D:** The derivative effect, also known as the dampening effect, dampens out oscillations on the response. By adjusting the derivative gain K_d, the controller can determine how fast oscillations should be dampened out. That is, the derivative gain determines the settling time which is the time it takes for the system to find a steady state after a impulse response.

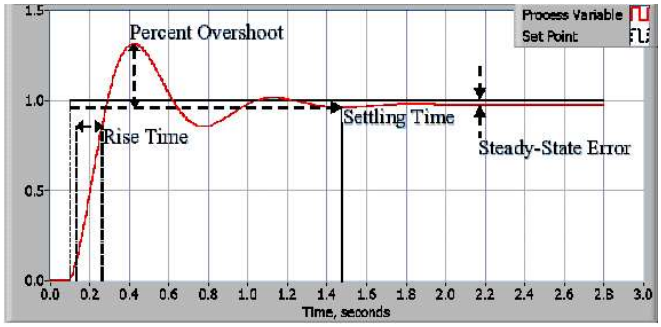

Figure 16: Overview of PID control response [24]

The autonomous control system will during the drilling operation perform impulse responses when switching between different set points for the control states. Hence, a proper tuning of these effects will be important to achieve an appropriate response. All theory used for this short description of the working principles of a PID controller is based on literature written by Jens G. Balchen et al.[29].

4.3.2 Kalman Filter

A Kalman filter is an optimal estimation algorithm that predicts a parameter of interests, such as location, speed and direction in the presence of noise in the measurement. It is often used to predict variables of interest that can only be measured indirectly. In this project the problem case is to measure and control the position of the drill bit in a directional drilled well. Hence, the position cannot be measured directly, so it needs to be estimated by using the measured ROP, the measured arc length of drill pipe and by measuring the orientation of the bit using down hole sensors. With the expectations of high-frequent noise on the down hole measurements, a Kalman filter is highly suited. To explain how a Kalman filter works, it's useful to start by explaining how a state observer works.

State Observer
A state observer is primarily a mathematical model that estimates the measured output and compares it with the real measurement. A state observer is shown in Figure 17. The model takes in the system input u and calculates an estimated output $\hat{y}$. The estimated output $\hat{y}$ is then compared with the measured y and an error e_y is calculated. The loop is closed by feeding the error e_y multiplied with the observer gain L back into the system. The overall goal is to eliminate the estimator error by finding to best value for the observer gain L. This is where a Kalman filter comes in.

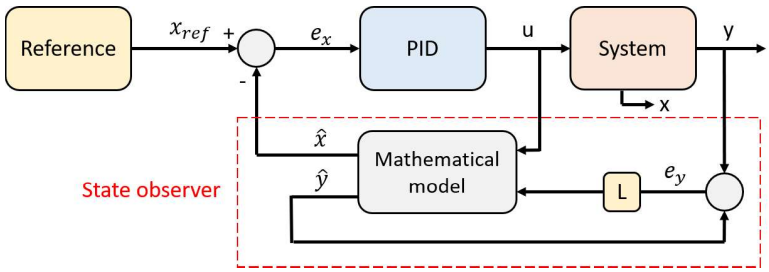

Figure 17: Overview of state estimator scheme

Measurement Noise Co-variance
When taking a measurement, as the angle between the orientation of our drill bit and the magnetic north, it can be expected that the measurement value will vary around the true measurement. If the variance is small and the power spectral density is constant, this noise can be defined as white noise. In Figure 18 the covariance of a signal is shown, where μ is the zero mean, σ is the variance and σ^2 is the covariance.

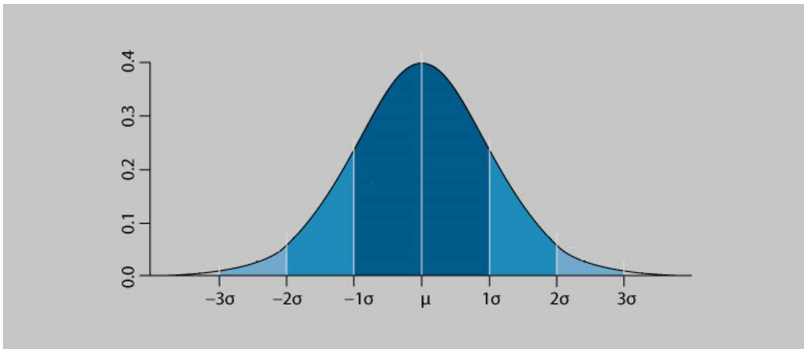

Figure 18: Graphical illustration of the covariance σ^2, showing the variance σ relative to the mean value μ

The working principle of a Kalman filter
Using the above and simple probability, it can be defined that our estimated state $\hat{x}$ is most likely the mean of the covariance of the measurement (state). In Figure 19, an illustration of the working principle of the Kalman filter is presented as a probability density function. First, an initial estimated state $\hat{x}_{k-1}$ is made. Comparing this to the state $\hat{x}_k$ in the next time step, it can be seen that the variance increases and the probability for estimating the correct state value decreases. This is the point where our true measurements come in. By multiplying the covariance of $\hat{x}_k$ and y_k, the optimal estimate can be found by taking the mean of the newly combined covariance. The Kalman filter finds these optimal estimates by iterating through an algorithm using the principles explained above.

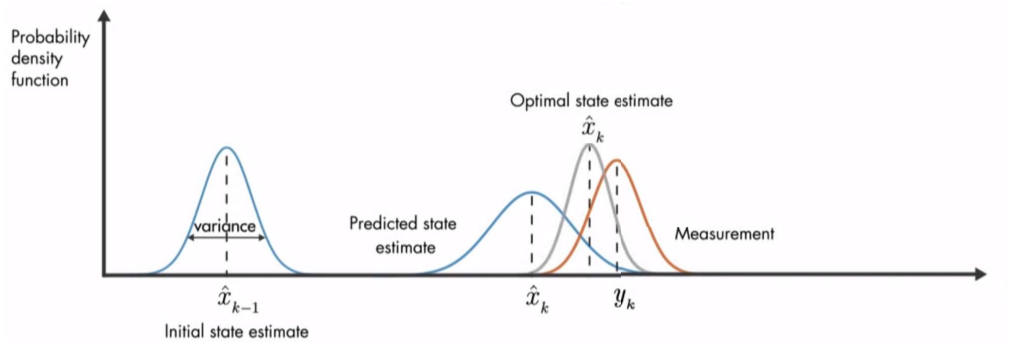

Figure 19: Illustration on how a Kalman filter finds the optimal state estimation [51].

Algorithm
The discrete time Kalman filter algorithm iterates through 4 steps. For a general process model we have:

$$x[k+1] = A_d x[k] + B_d u[k] + w[k],\ y[k] = Cx[k] + v[k] \tag{20}$$

By assuming the noise and disturbance are unbiased and white, we have:

$$E[v[k]] = 0,\ E[w[k]] = 0,\ E[v[k]v[l]^T] = \delta[k,l]R_d,\ E[w[k]w[l]^T] = \delta[k,l]Q_d \tag{21}$$

The algorithm initializes at

$$\hat{x}^-[0] = E[x(0)],\ and\ P^-[0] = E[(x[0] - \hat{x}^-[0])(x[0] - \hat{x}^-[0])^T] \tag{22}$$

and iterates through the following steps:

$$1.\ L[k] = P^-[k]C^T(CP^-[k]C^T + R_d)^{-1} \tag{23a}$$
$$2.\ \hat{x}[k] = \hat{x}^-[k] + L[k](y[k] - C\hat{x}^-[k]) \tag{23b}$$
$$3.\ P[k] = (I - L[k]C)P^-[k](I - L[k]C)^T + L[k]R_dL[k]^T \tag{23c}$$
$$4.\ \hat{x}^-[k+1] = A_d\hat{x}[k] + B_du[k],\ P^-[k+1] = A_dP[k]A_d^T + Q_d \tag{23d}$$

At each iteration, the Kalman algorithm uses the prior estimated state $\hat{x}^-[k]$ and the prior error covariance $P^-[k]$, to calculates a new Kalman gain L[k]. The Kalman gain is used to calculate the new estimated state $\hat{x}[k]$ and the new error covariance $P[k]$. Finally, the algorithm calculates next iteration's prior estimated state $\hat{x}^-[k+1]$ and prior error covariance $P^-[k+1]$ that is used to initialize the next iteration. The algorithm returns to start and continues the same way.

4.3.3 Cohen-Coon tuning method

The Cohen-Coon tuning method is a well used PID tuning method that has proven to work well on most self-stabilization processes, such as a drilling operation. The method is based on open loop testing, where the goal is to find a transfer function for the system which can be used to identify the appropriate PID gains for an ideal system response. The method was successfully used to tune the WOB- and torque controllers in Drillbotics 2018 [9]. Hence, the team will use this as inspiration for tuning the new controllers in 2019. A commonly used transfer function is the first-order plus dead time (FOPDT), and can be defined in the frequency domain as follows [15]:

$$H(s) = \frac{Kw^{-t_ds}}{\tau s + 1} \tag{24}$$

where t_d is the dead time, τ is the time constant and K is the process gain defined by

$$K = \frac{\Delta PV\%}{\Delta CO\%} \tag{25}$$

where PV is the process variable input and CO is the controller output.

The Cohen-Coon tuning method can be described through several steps where we will perform a step response to go from one steady state to another. The steps can be described as follows including a graphical illustration in Figure 20 [46]:

1. Choose a constant CO value and wait for the systems PV to settle at a steady state.
2. Perform a step response by changing OV a few percents and want for the system to settle at a new steady state.
3. Calculate K by using Equation 25

4. Find the maximum slope on the PV curve (inflection point) and draw a tangential line that intersects with the original level of PV. This is shown in Figure 20.
5. Calculate t_d which is the time between the beginning of the step response and the tangential intersection with original PV.
6. Calculate τ which is the time between after the dead time t_d to the time where PV has reached 63% of its total change.
7. Redo step 1-6 until you can produce similar values with small variance on the calculated constants, and use the average values in the next steps.
8. Use Cohen-Coon tuning rules in Table 3 to calculate the new controller settings. Note that these rules uses quarter-amplitude damping response, which is a rather fast response that quickly eliminates steady state error but slightly overshoots and oscillates a few times around the set point before it settles at a steady state.

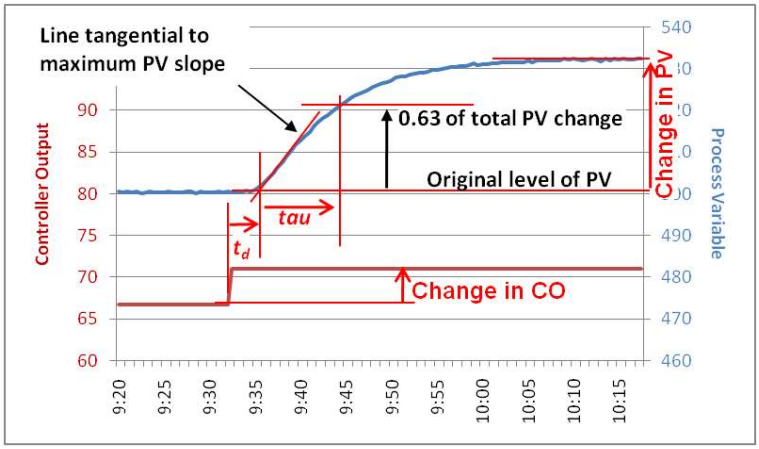

Figure 20: Cohen-Coon tuning with step response [46]

Table 3: Cohen-Coon tuning rules

	Controller Gain	**Integral Time**	**Derivative Time**
P	$K_c = \frac{1.03}{K}(\frac{\tau}{t_d} + 0.34)$		
PI	$K_c = \frac{0.9}{K}(\frac{\tau}{t_d} + 0.092)$	$T_I = 3.33t_d\frac{\tau + 0.092t_d}{\tau + 2.22t_d}$	
PD	$K_c = \frac{1.24}{K}(\frac{\tau}{t_d} + 0.129)$		$T_D = 0.27t_d\frac{\tau + 0.324t_d}{\tau + 0.129t_d}$
PID	$K_c = \frac{1.35}{K}(\frac{\tau}{t_d} + 0.185)$	$T_I = 2.5t_d\frac{\tau + 0.185t_d}{\tau + 0.611t_d}$	$T_I = 0.37t_d\frac{\tau}{\tau + 0.185t_d}$

The team will use this method as a starting point for tuning the WOB and torque controllers, but further fine tuning will most likely be performed. Since a drilling operation can be described as a "slow" process, a quick controller that overshoots will not be necessary. The tuning process using the Cohen-Coon tuning method will be further described with the implementation in phase 2.

4.3.4 First order Explicit Runge-Kutta

The first order explicit Runge-Kutta method (ERK1), also known as the Euler's method, is a simple but important integration scheme. The method uses last known function value and calculates a new value based on the function derivative multiplied by a step length. This derivation is based on literature written by Olav Egeland and Tommy Gravdahl [13]. A numerical expression of the solution can be computed using:

$$y_{n+1} = y_n + hf(y_n, t_n) \tag{26}$$

where h is the step length and $f(y_n, t_n)$ is the time-derivative of the function $y(t)$. The method is step-wise linear and highly suitable for calculating the discrete time position of a first order differential equation, or for a system with relatively slow dynamics like a directional drilling operation. The stability function for the method can be defined as

$$R(h\lambda) = 1 + h\lambda \tag{27a}$$

where stability is ensured whenever

$$|R(h\lambda)| \leq 1 \tag{27b}$$

That is, the method has a stability region inside a unity circle around $Re = -1$. This is shown in Figure 21. For real eigenvalues λ, stability is ensured whenever

$$h \leq -\frac{2}{\lambda} \tag{27c}$$

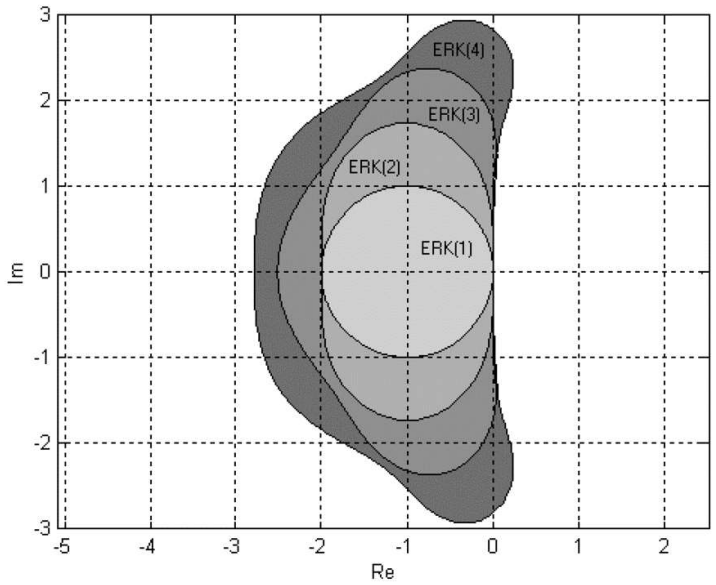

Figure 21: Explicit Runge-Kutta stability regions [13]

The Euler's method will be used to calculate the position of the drill bit in reference to a world frame located on top of the rock sample. This will be further described in subsection 9.3.

Appendix G

LabVIEW Control System

This section shows a selection of the most important, interesting and relevant VI's and sub-VI's in the control system. The main file of these is the competition script, from which all other VI's are called. This competition script shows the simulated version of the system, in which all motor and sensor outputs except those belonging to the top drive are user given inputs. In the version that will be used on the competition day, these are replaced by the real motor and sensor outputs. Some changes will also be made to the front panel, and possibly the safety logic.

Competition_Script_simualtion_v2.vi
C:\Users\Drillbotics\Desktop\Drillbotics backup\Drillbotics 2019\Autonomous Control\Competition Script\Competition_Script_simualtion_v2.vi
Last modified on 08.06.2019 at 23:04
Printed on 09.06.2019 at 02:12

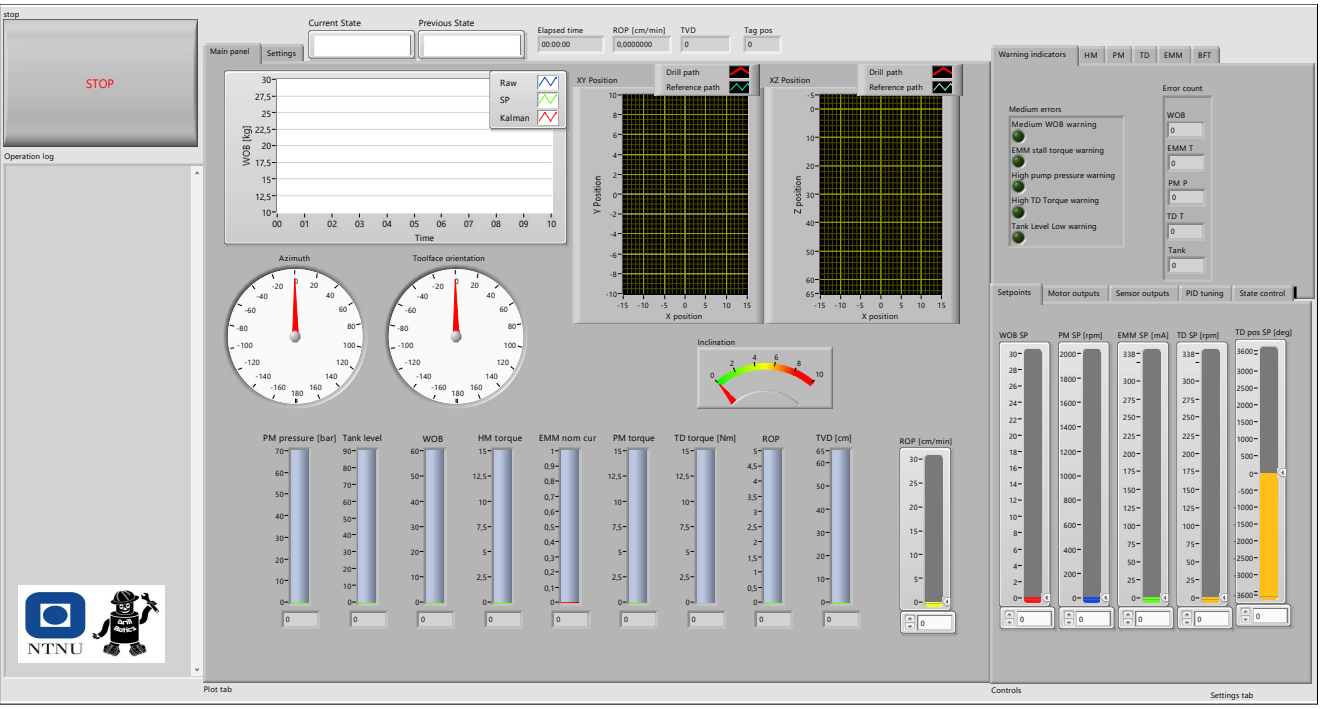

Competition_Script_simualtion_v2.vi
C:\Users\Drillbotics\Desktop\Drillbotics backup\Drillbotics 2019\Autonomous Control\Competition Script\Competition_Script_simualtion_v2.vi
Last modified on 08.06.2019 at 23:04
Printed on 09.06.2019 at 02:12

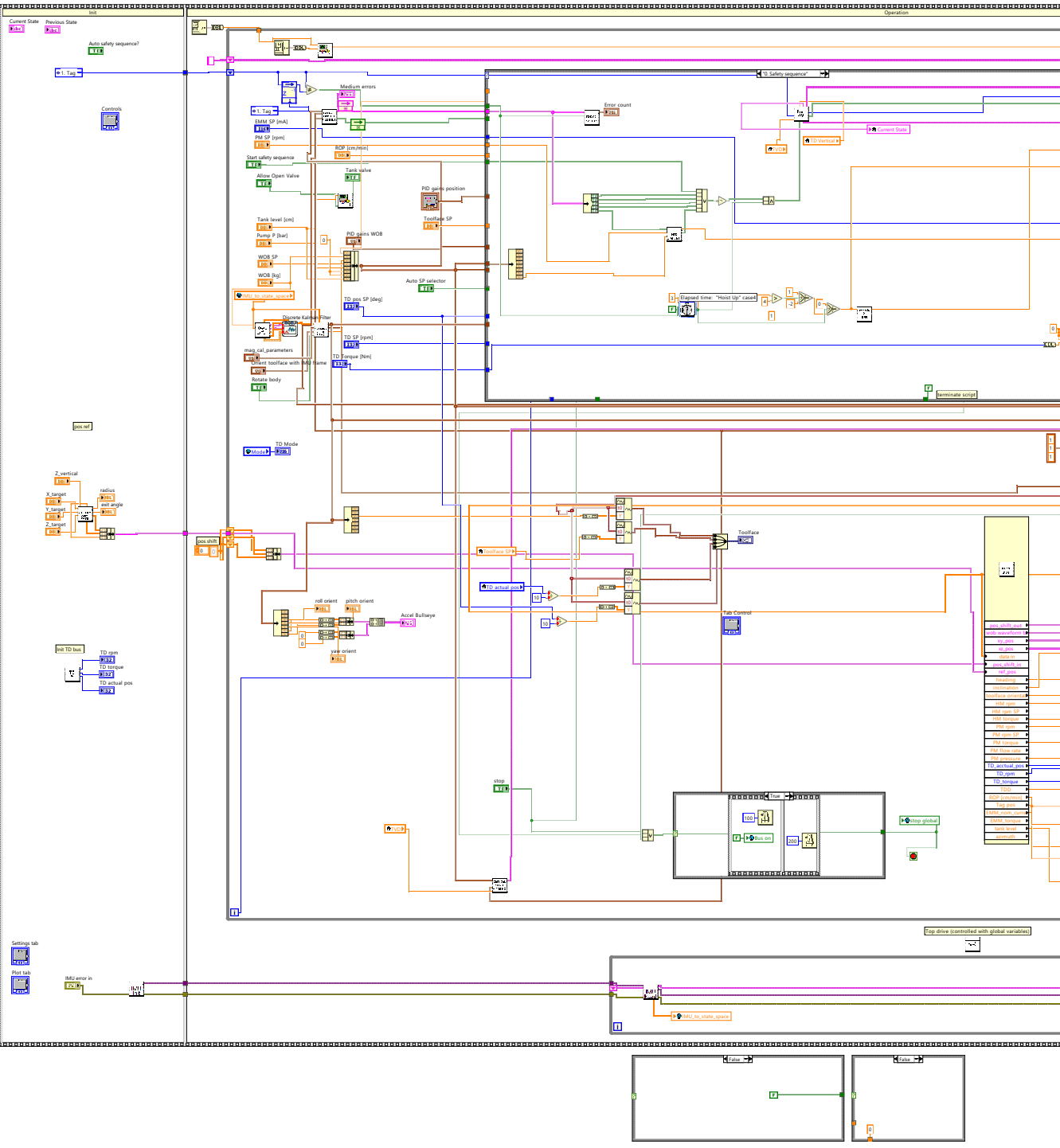

Competition_Script_simualtion_v2.vi
C:\Users\Drillbotics\Desktop\Drillbotics backup\Drillbotics 2019\Autonomous Control\Competition Script\Competition_Script_simualtion_v2.vi
Last modified on 08.06.2019 at 23:04
Printed on 09.06.2019 at 02:12

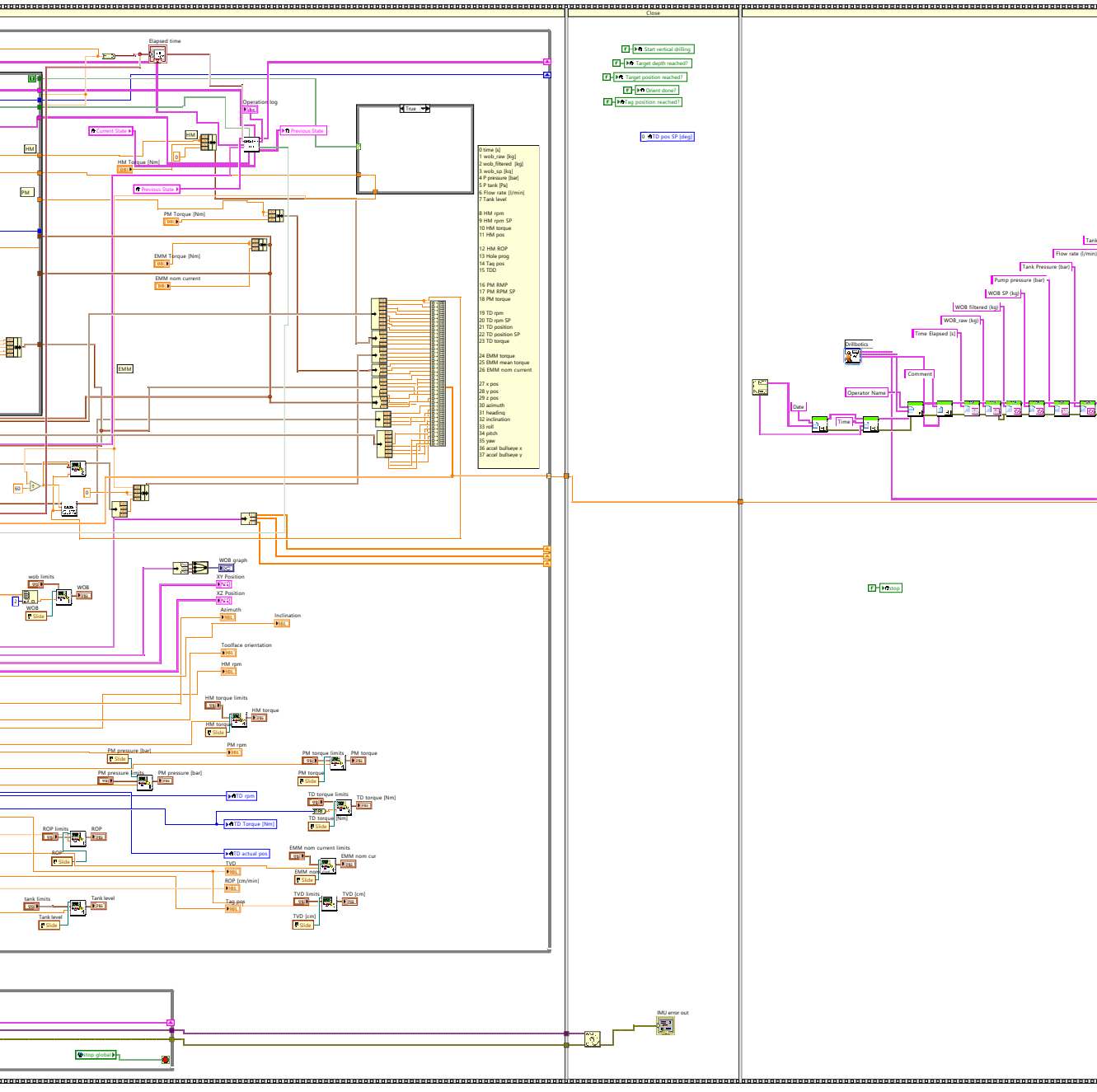

Competition_Script_simualtion_v2.vi
C:\Users\Drillbotics\Desktop\Drillbotics backup\Drillbotics 2019\Autonomous Control\Competition Script\Competition_Script_simualtion_v2.vi
Last modified on 08.06.2019 at 23:04
Printed on 09.06.2019 at 02:13

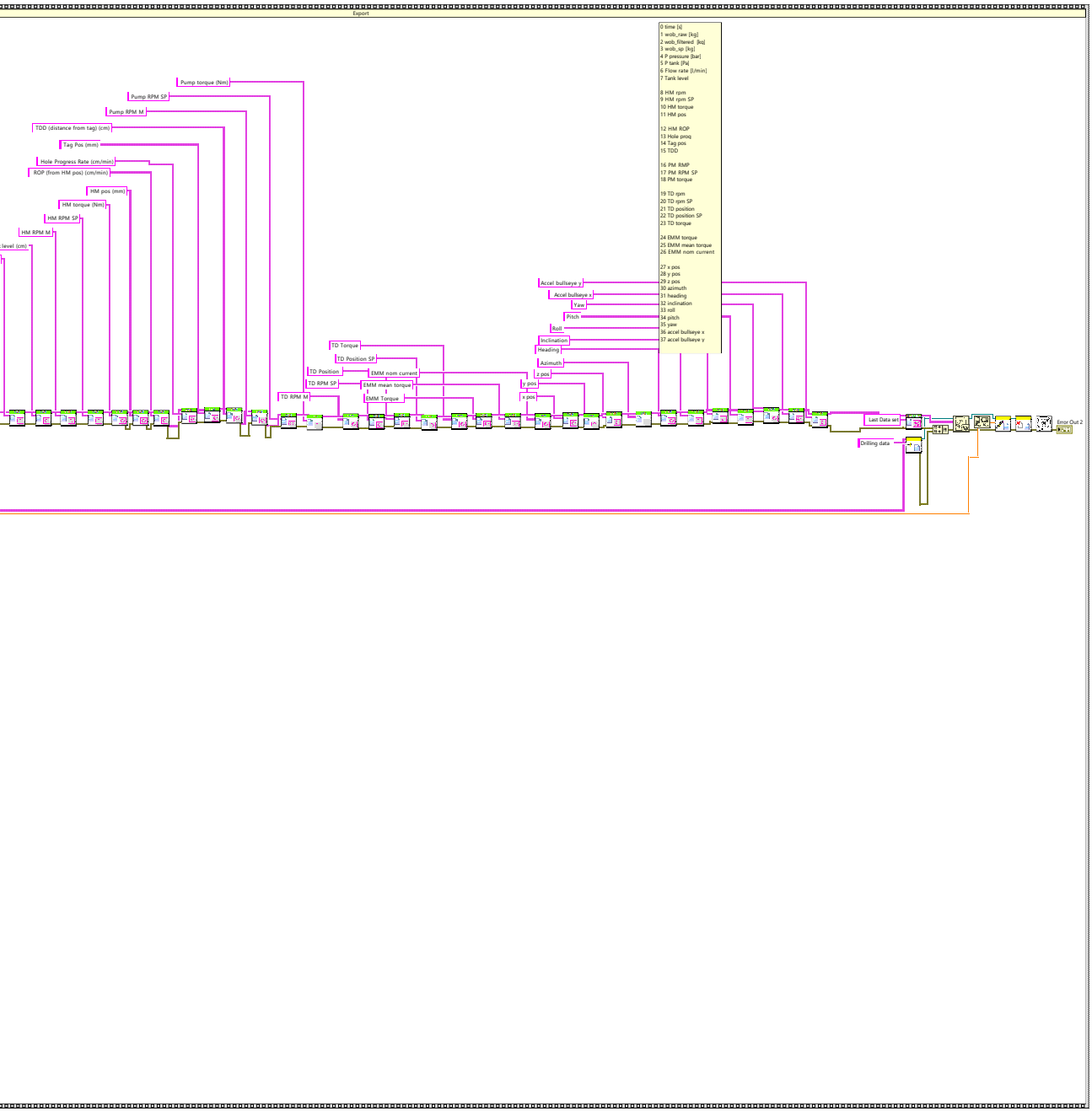

Competition_Script_simualtion_v2.vi
C:\Users\Drillbotics\Desktop\Drillbotics backup\Drillbotics 2019\Autonomous Control\Competition Script\Competition_Script_simualtion_v2.vi
Last modified on 08.06.2019 at 23:04
Printed on 09.06.2019 at 02:13

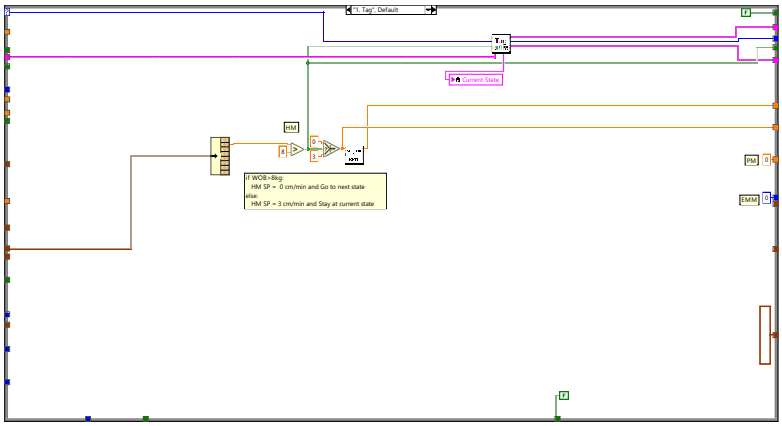

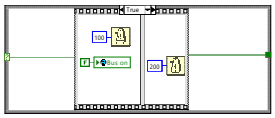

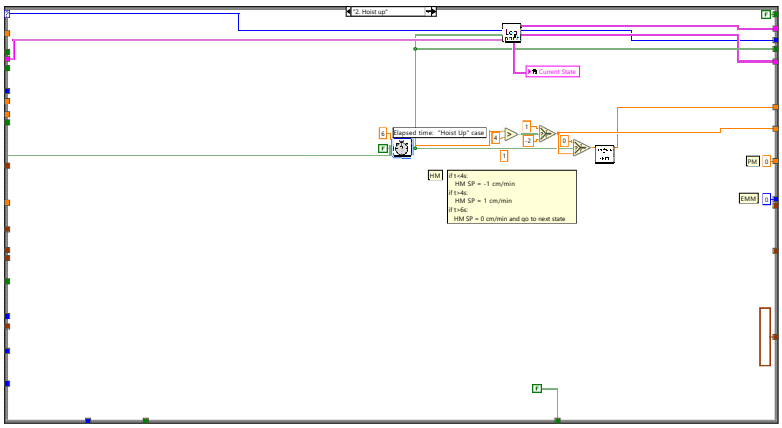

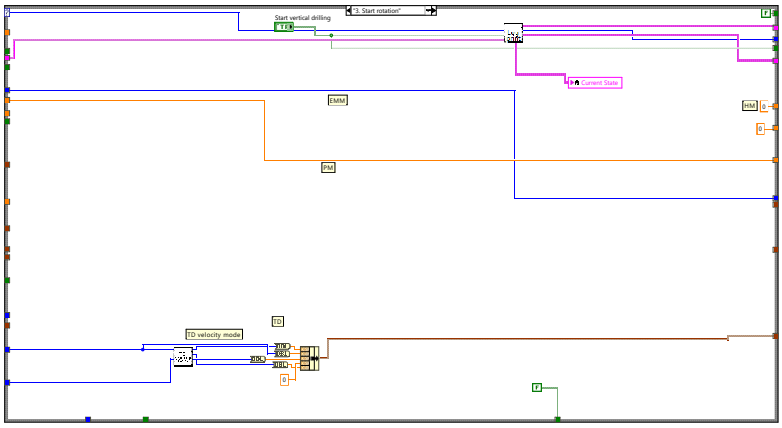

Competition_Script_simualtion_v2.vi
C:\Users\Drillbotics\Desktop\Drillbotics backup\Drillbotics 2019\Autonomous Control\Competition Script\Competition_Script_simualtion_v2.vi
Last modified on 08.06.2019 at 23:04
Printed on 09.06.2019 at 02:13

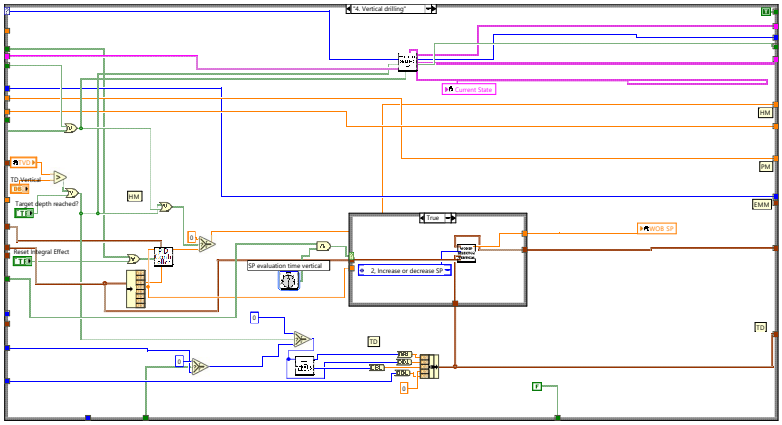

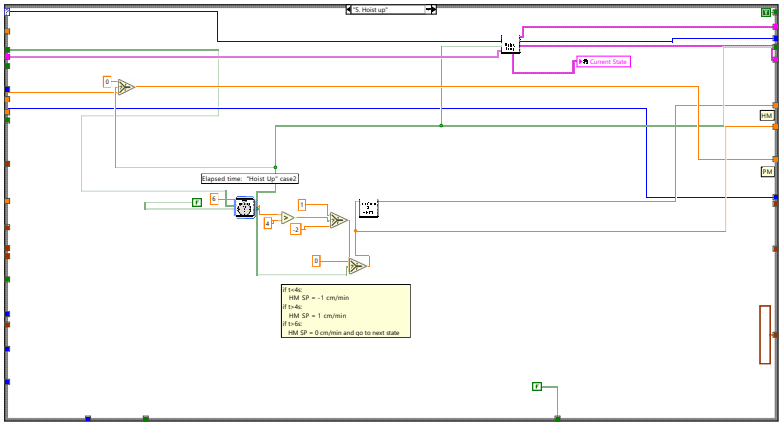

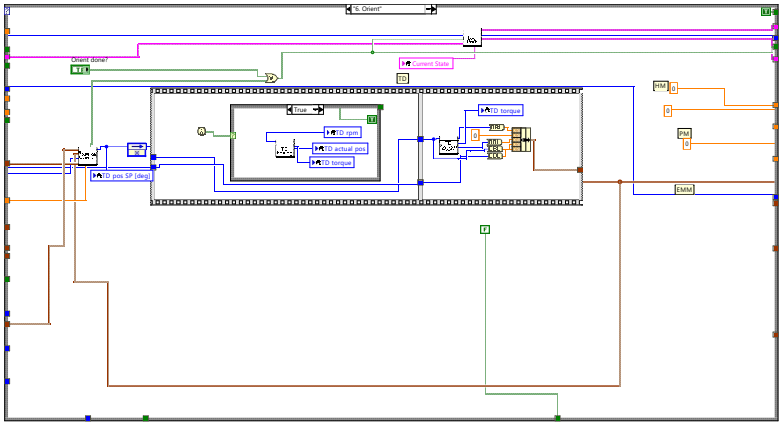

Competition_Script_simualtion_v2.vi
C:\Users\Drillbotics\Desktop\Drillbotics backup\Drillbotics 2019\Autonomous Control\Competition Script\Competition_Script_simualtion_v2.vi
Last modified on 08.06.2019 at 23:04
Printed on 09.06.2019 at 02:13

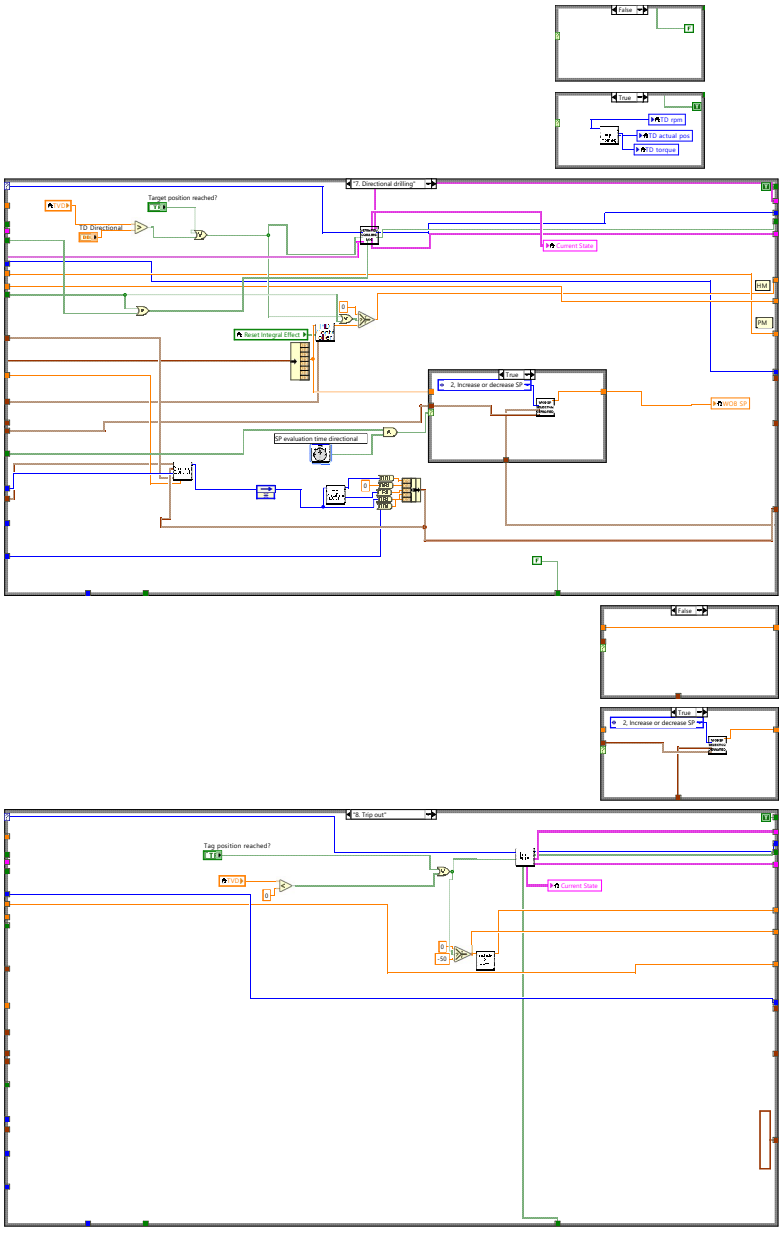

Competition_Script_simualtion_v2.vi
C:\Users\Drillbotics\Desktop\Drillbotics backup\Drillbotics 2019\Autonomous Control\Competition Script\Competition_Script_simualtion_v2.vi
Last modified on 08.06.2019 at 23:04
Printed on 09.06.2019 at 02:13

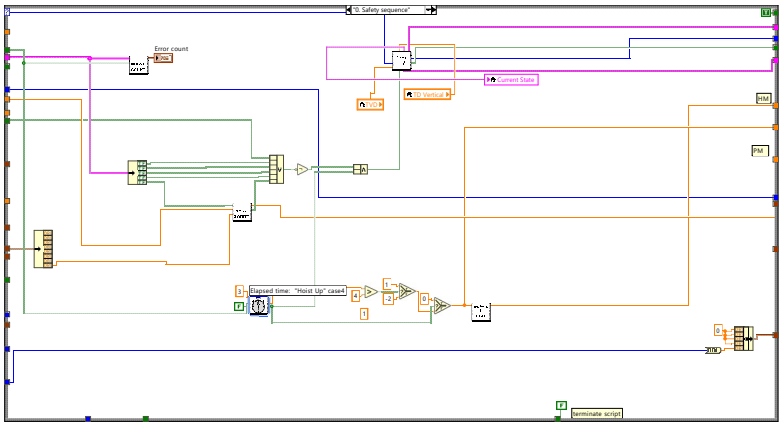

Critical_error_sub_Hilde.vi
C:\Users\Bruker\Desktop\Drillbotics backup 05062019\Drillbotics 2019\Autonomous Control\Sub-VIs\Hilde subVI 29mai\Critical_error_sub_Hilde.vi
Last modified on 04.06.2019 at 08.25
Printed on 05.06.2019 at 20.43

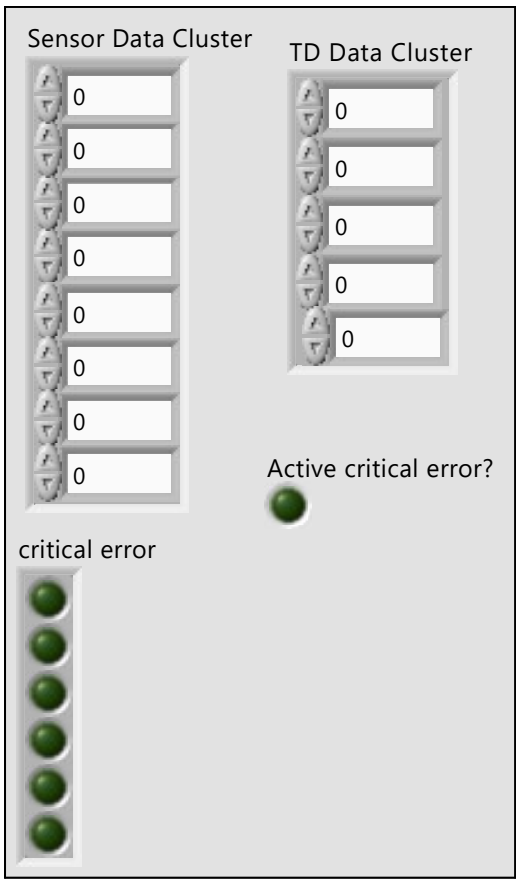

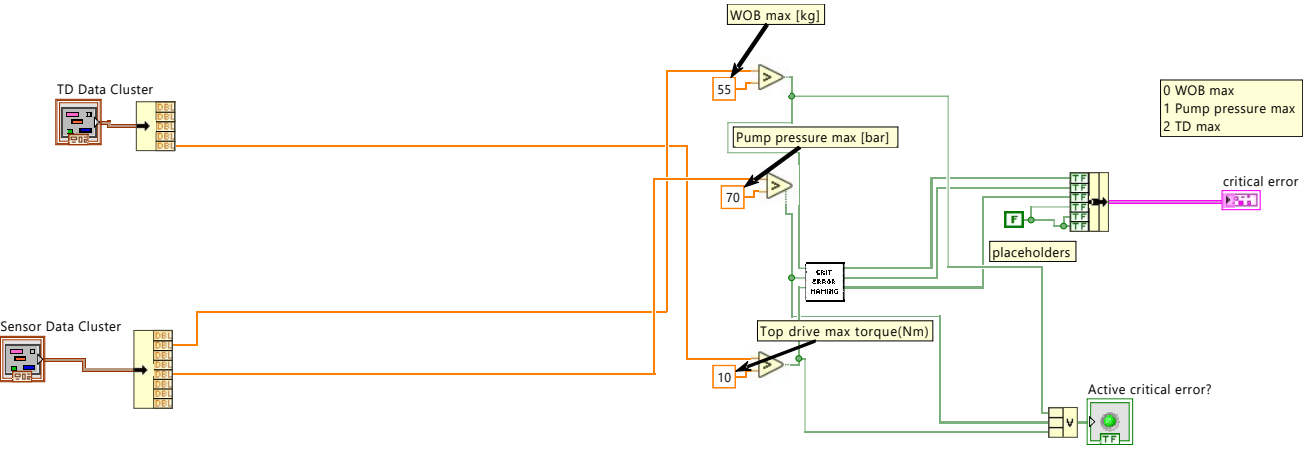

detect_medium_warning.vi
C:\Users\Bruker\Desktop\Drillbotics backup 05062019\Drillbotics 2019\Autonomous Control\Sub-VIs\Hilde subVI 29mai\detect_medium_warning.vi
Last modified on 03.06.2019 at 20.24
Printed on 05.06.2019 at 20.42

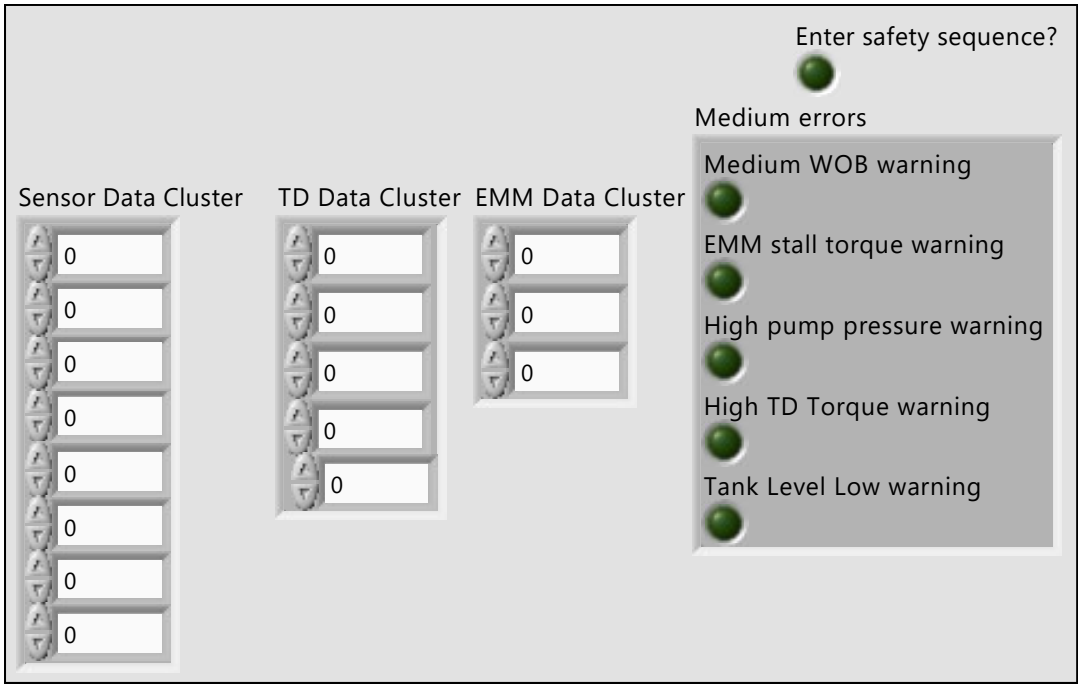

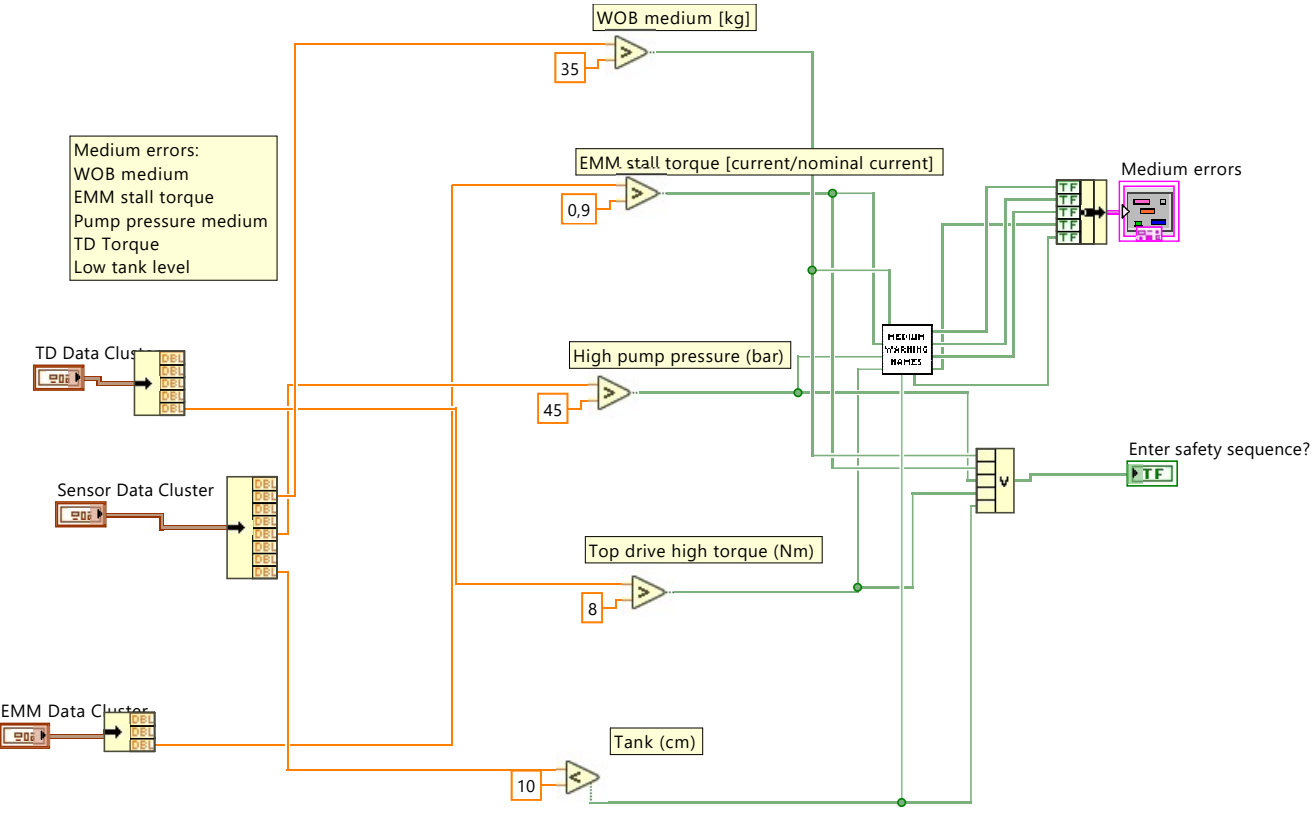

deviated_drilling_log_sub_Hilde.vi
C:\Users\Bruker\Desktop\Drillbotics backup 05062019\Drillbotics 2019\Autonomous Control\Sub-VIs\Hilde subVI 29mai\deviated_drilling_log_sub_Hilde.vi
Last modified on 04.06.2019 at 14.23
Printed on 05.06.2019 at 20.41

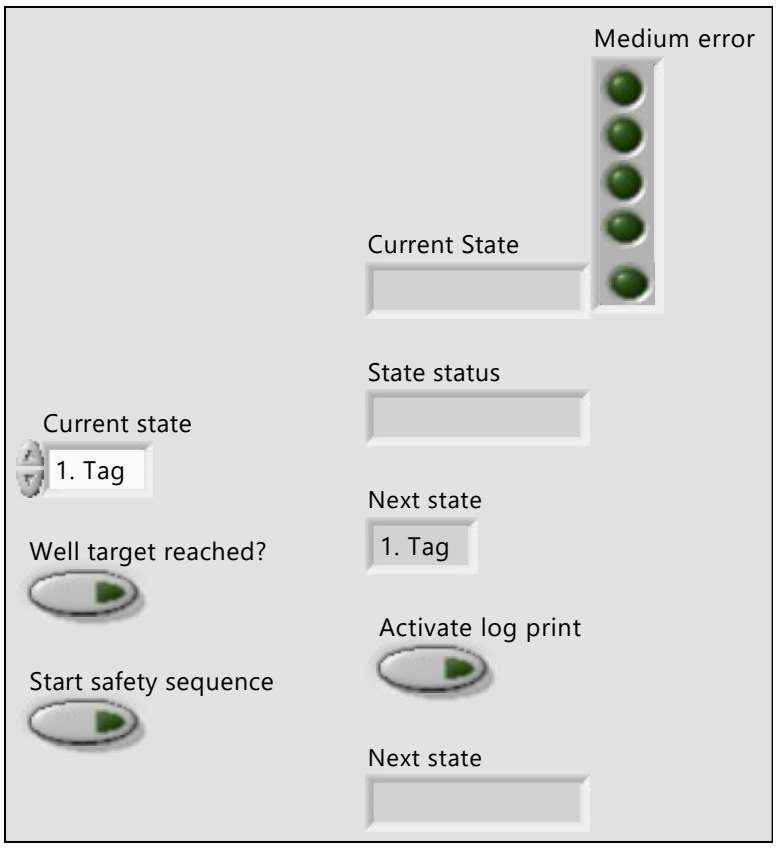

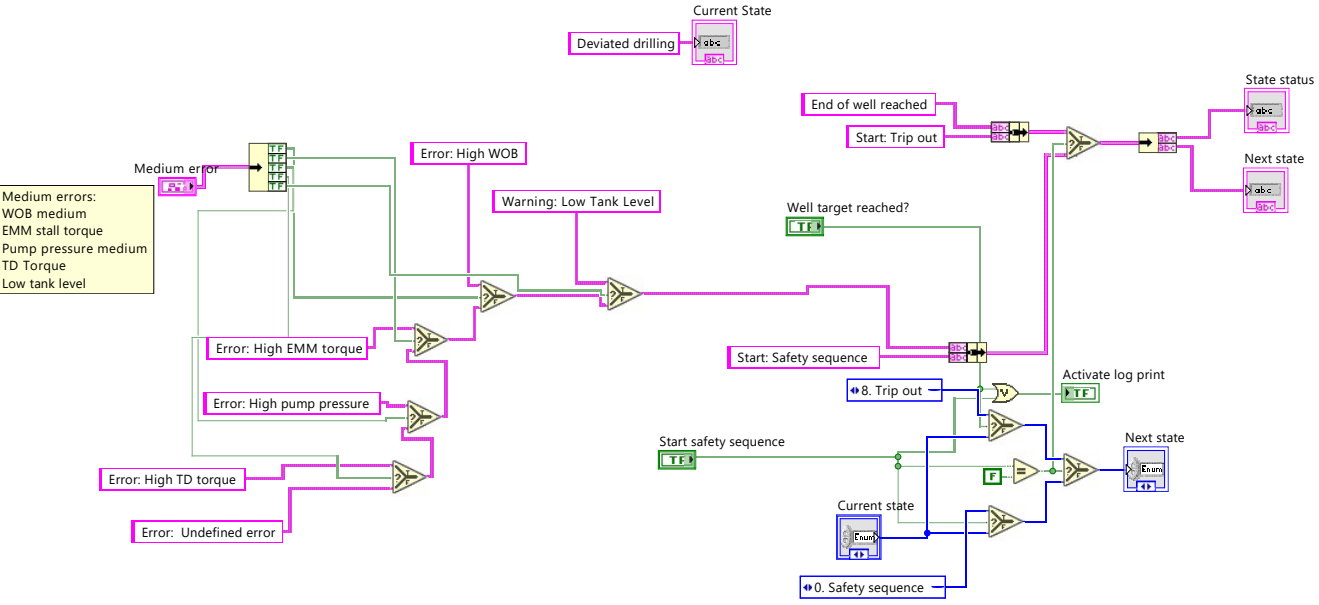

WOB_SP_selector__deviated_Hilde.vi
C:\Users\Bruker\Desktop\Drillbotics backup 05062019\Drillbotics 2019\Autonomous Control\Sub-VIs\Hilde subVI 29mai\WOB_SP_selector__deviated_Hilde.vi
Last modified on 31.05.2019 at 04.42
Printed on 05.06.2019 at 20.38

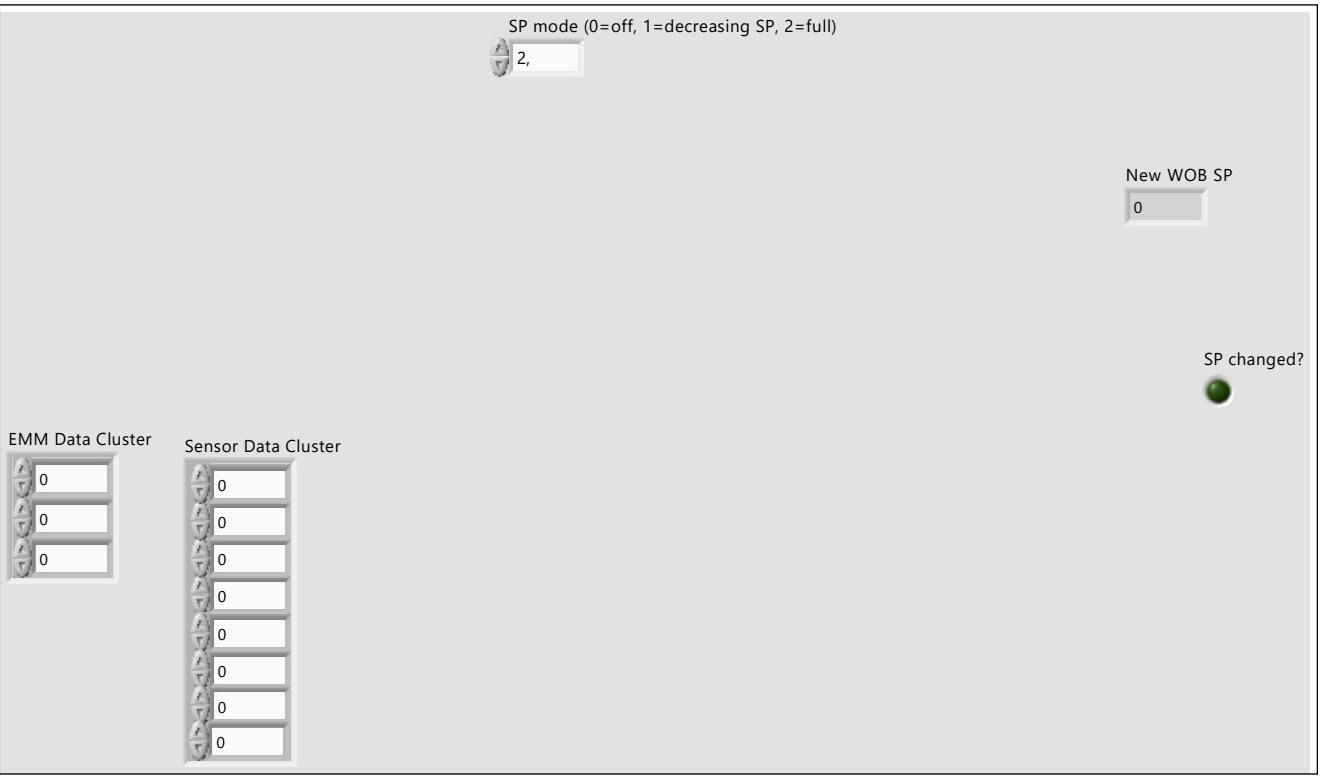

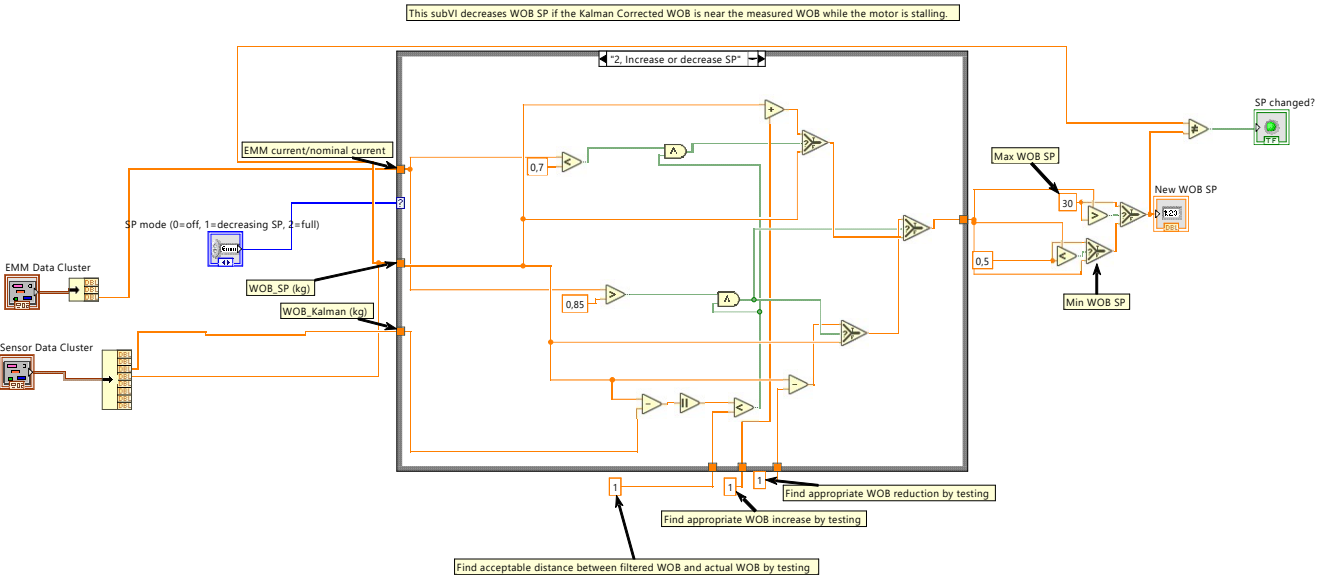

WOB_SP_selector__deviated_Hilde.vi
C:\Users\Bruker\Desktop\Drillbotics backup 05062019\Drillbotics 2019\Autonomous Control\Sub-VIs\Hilde subVI 29mai\WOB_SP_selector__deviated_Hilde.vi
Last modified on 31.05.2019 at 04.42
Printed on 05.06.2019 at 20.38

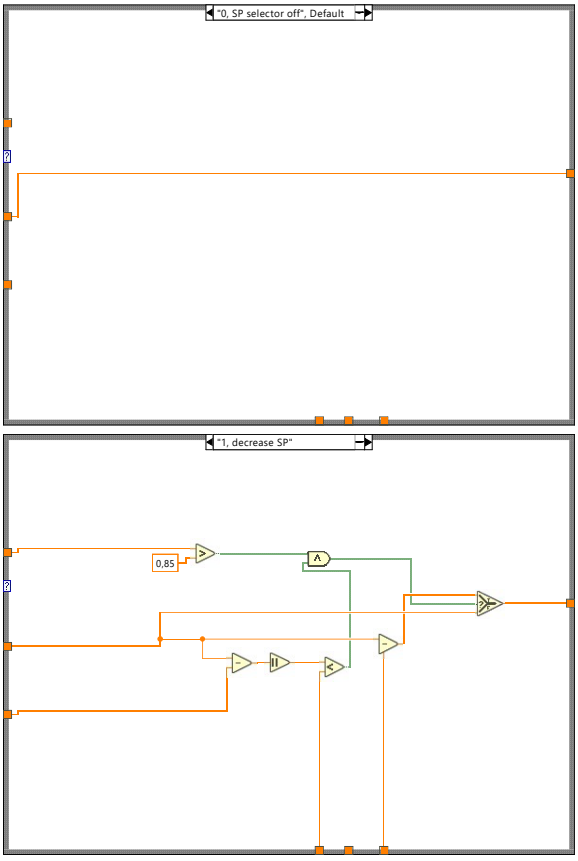

Operation_log_sub_Hilde.vi
C:\Users\Bruker\Desktop\Drillbotics backup 05062019\Drillbotics 2019\Autonomous Control\Sub-VIs\Hilde subVI 29mai\Operation_log_sub_Hilde.vi
Last modified on 04.06.2019 at 15.58
Printed on 05.06.2019 at 20.40

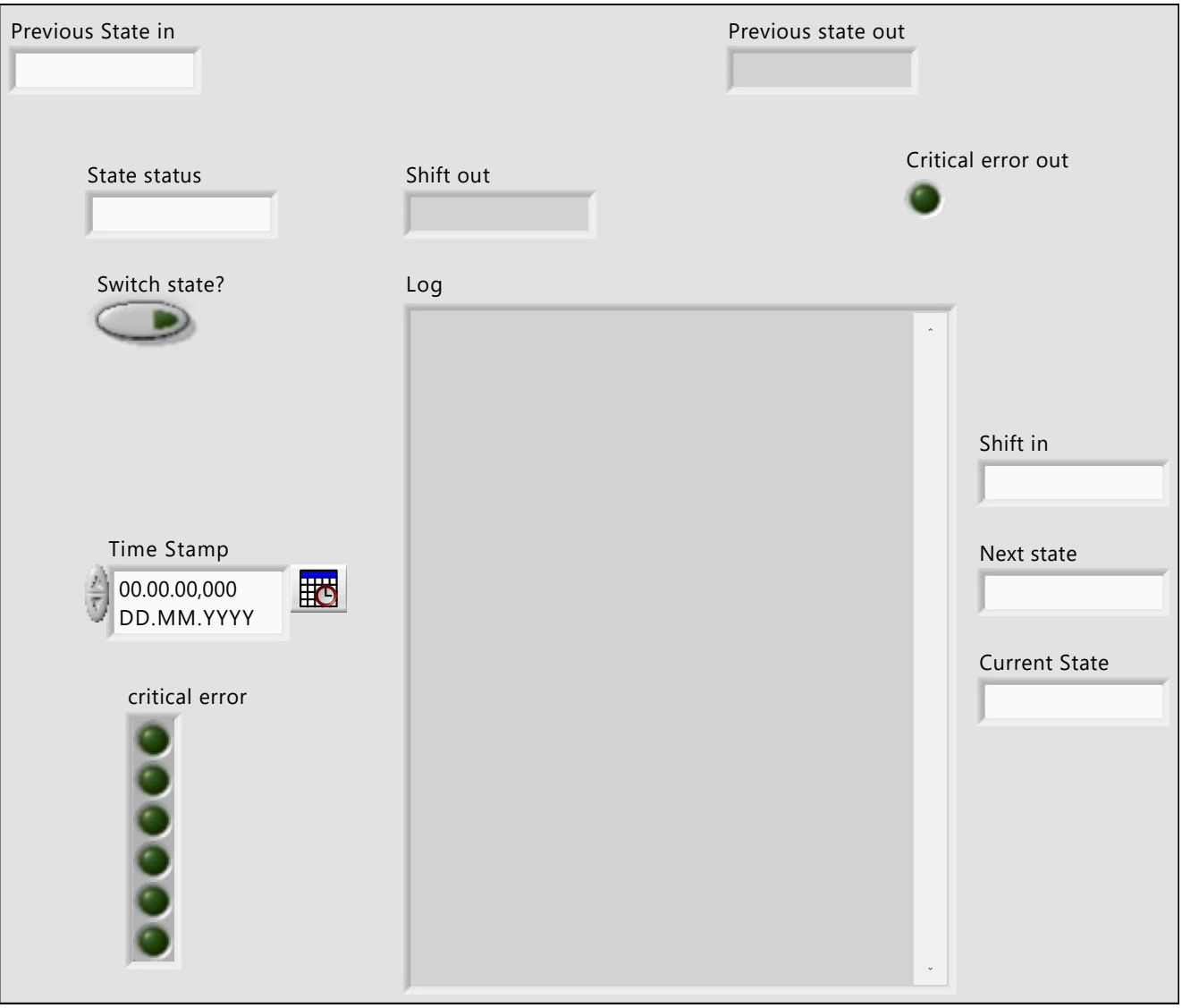

Operation_log_sub_Hilde.vi
C:\Users\Bruker\Desktop\Drillbotics backup 05062019\Drillbotics 2019\Autonomous Control\Sub-VIs\Hilde subVI 29mai\Operation_log_sub_Hilde.vi
Last modified on 04.06.2019 at 15.58
Printed on 05.06.2019 at 20.41

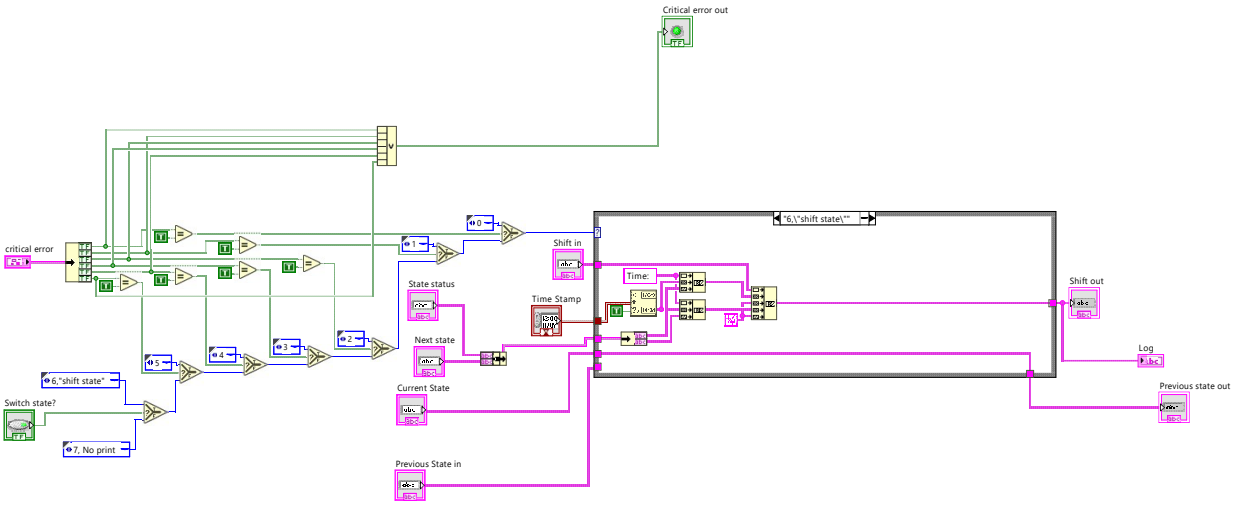

Critical errors:
0 WOB max
1 Pump pressure max
2 TD max torque
3, 4, 5 Placeholder
6 Shift state

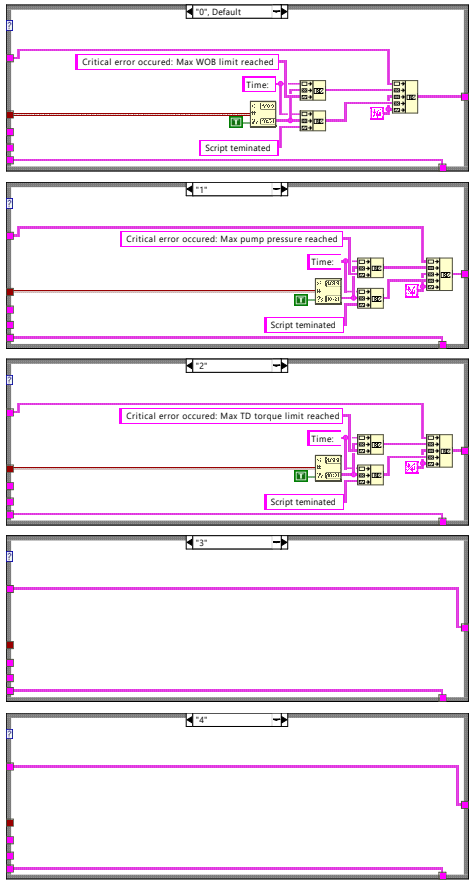

Operation_log_sub_Hilde.vi
C:\Users\Bruker\Desktop\Drillbotics backup 05062019\Drillbotics 2019\Autonomous Control\Sub-VIs\Hilde subVI 29mai\Operation_log_sub_Hilde.vi
Last modified on 04.06.2019 at 15.58
Printed on 05.06.2019 at 20.41

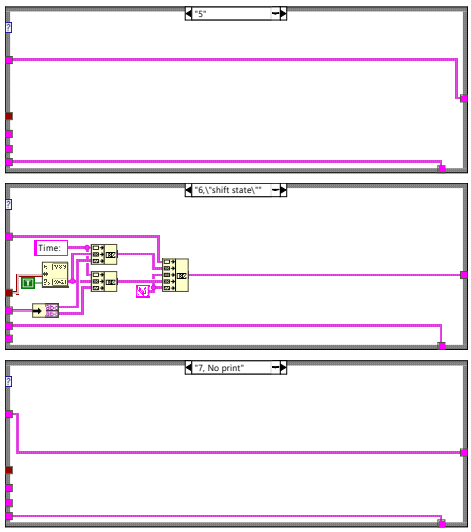

PID_WOB (SubVI).vi
C:\Users\Bruker\Desktop\Drillbotics backup 05062019\Drillbotics 2019\Autonomous Control\Sub-VIs\PID_WOB (SubVI).vi
Last modified on 04.06.2019 at 21.10
Printed on 05.06.2019 at 20.45

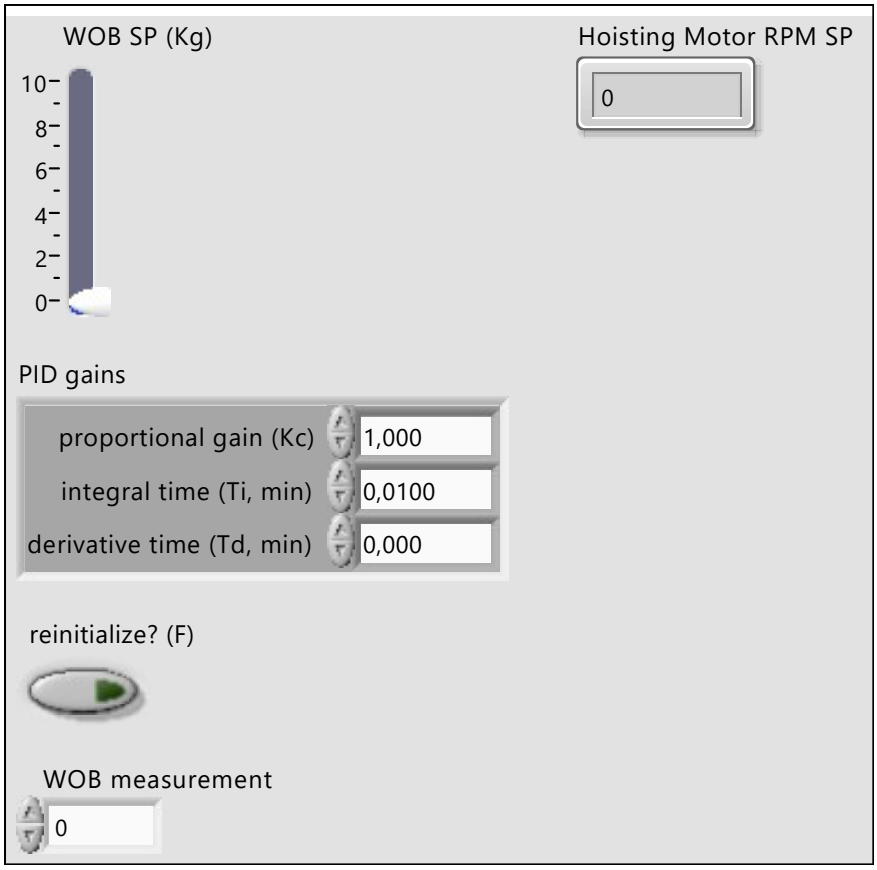

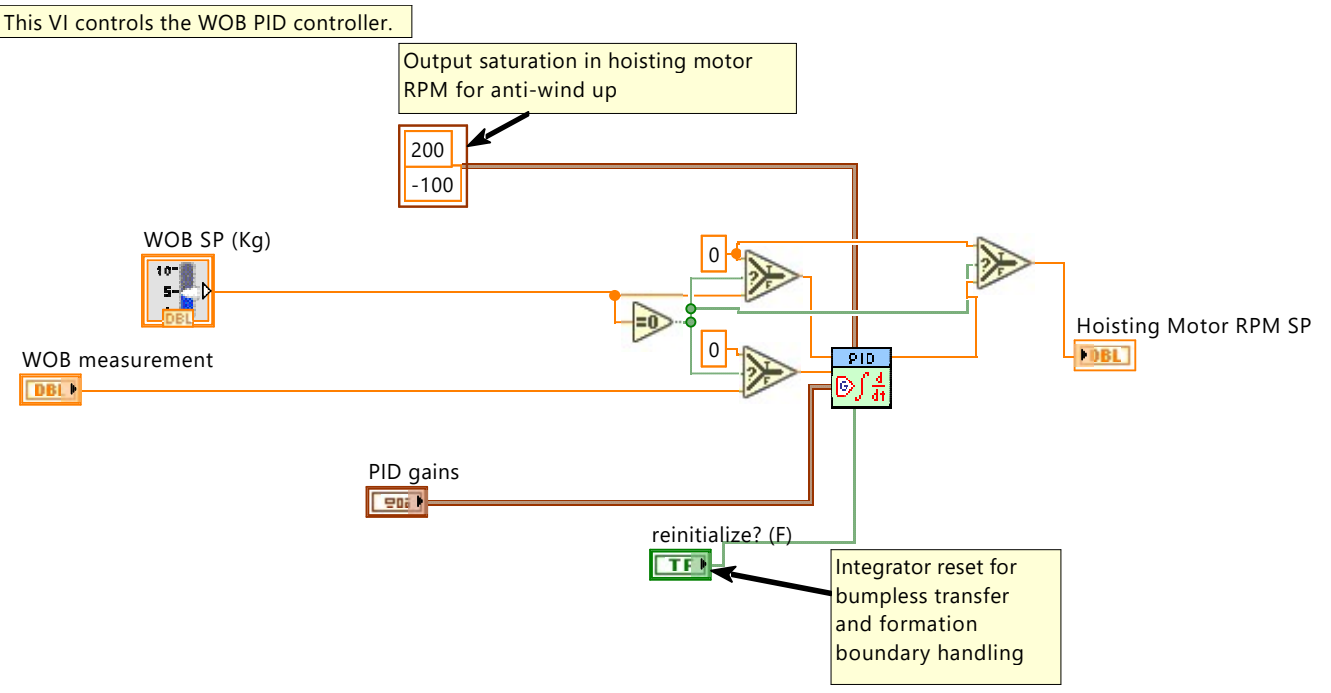

position_control_sub.vi
C:\Users\Bruker\Desktop\Drillbotics backup 05062019\Drillbotics 2019\Autonomous Control\Sub-VIs\position_control_sub.vi
Last modified on 05.06.2019 at 11.11
Printed on 05.06.2019 at 20.46

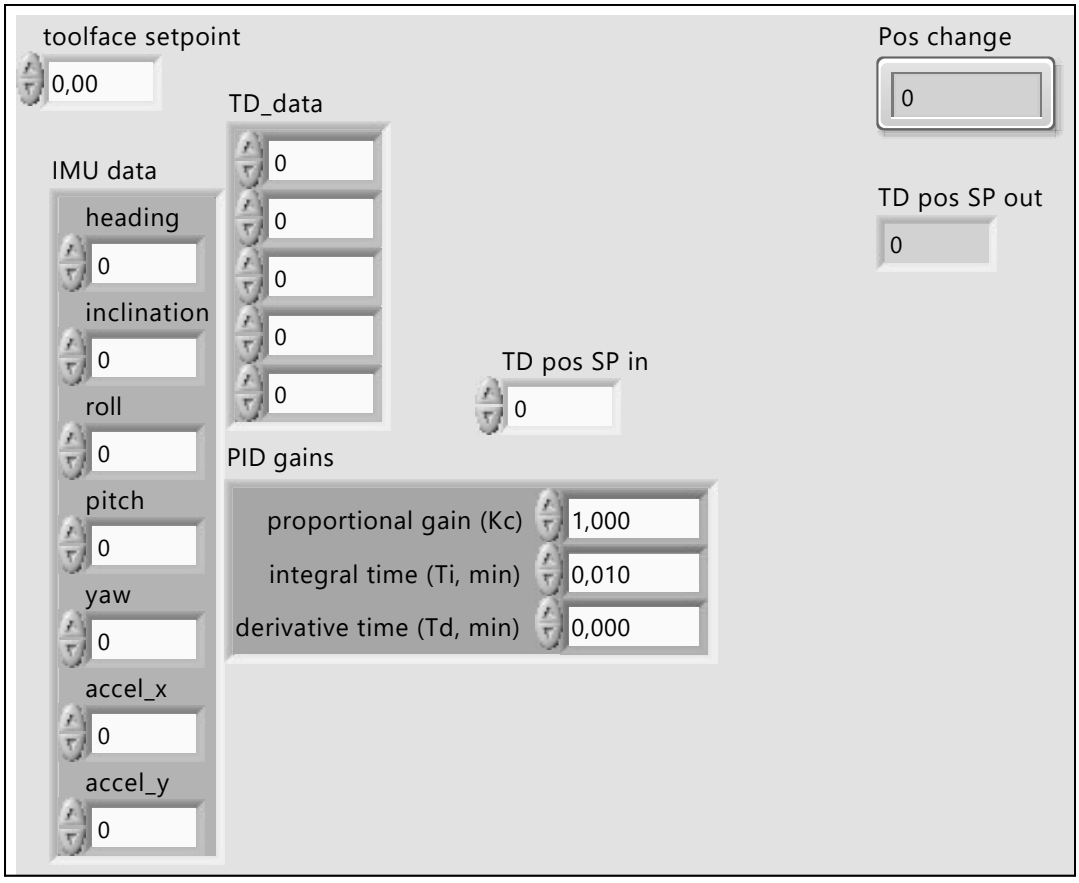

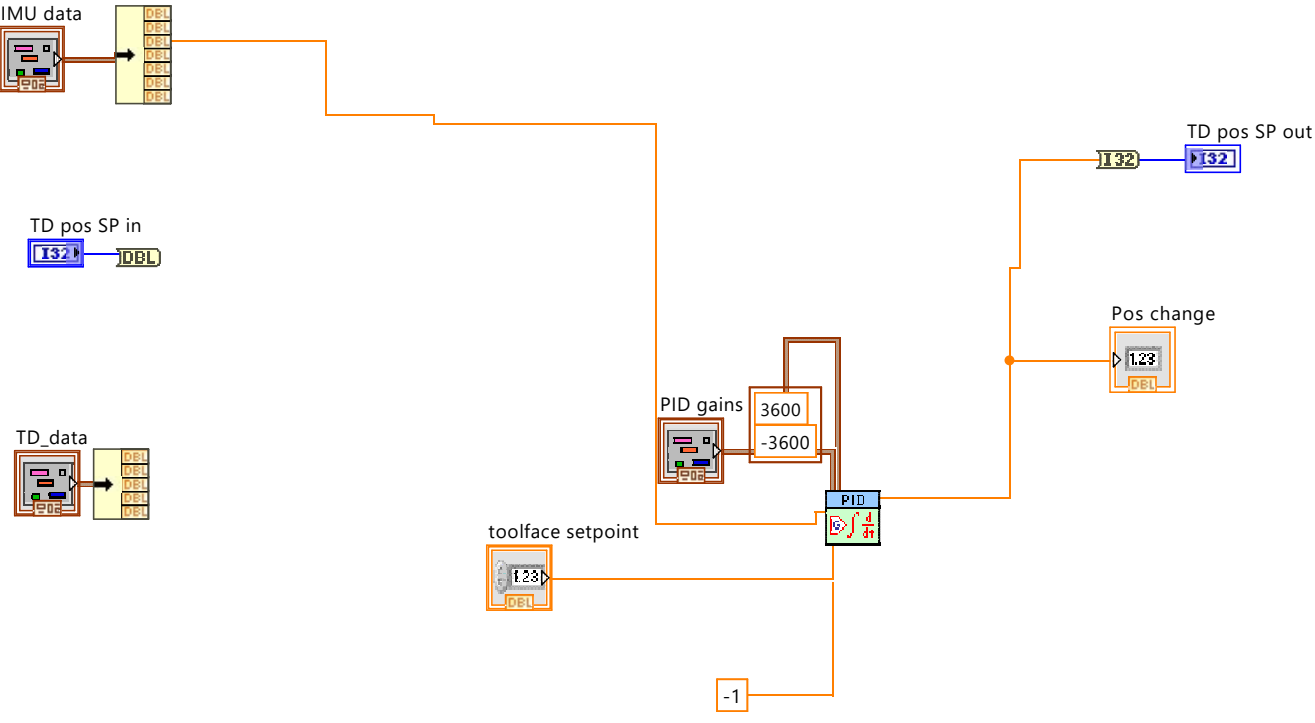

state_space_model_kalman_sub.vi
C:\Users\Bruker\Desktop\Drillbotics backup 05062019\Drillbotics 2019\Autonomous Control\Sub-VIs\state_space_model_kalman_sub.vi
Last modified on 05.06.2019 at 18.33
Printed on 05.06.2019 at 20.47

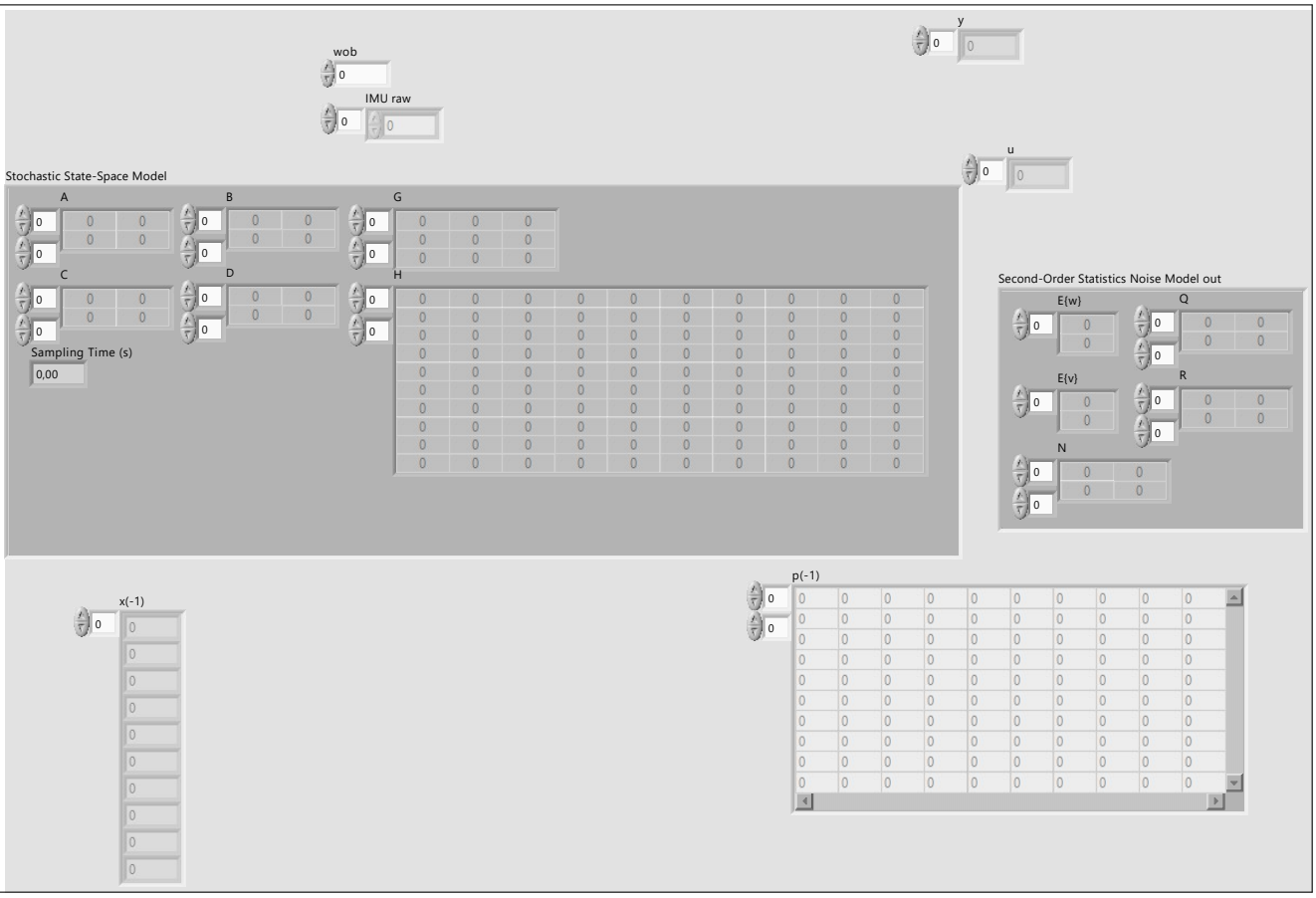

state_space_model_kalman_sub.vi
C:\Users\Bruker\Desktop\Drillbotics backup 05062019\Drillbotics 2019\Autonomous Control\Sub-VIs\state_space_model_kalman_sub.vi
Last modified on 05.06.2019 at 18.33
Printed on 05.06.2019 at 20.47

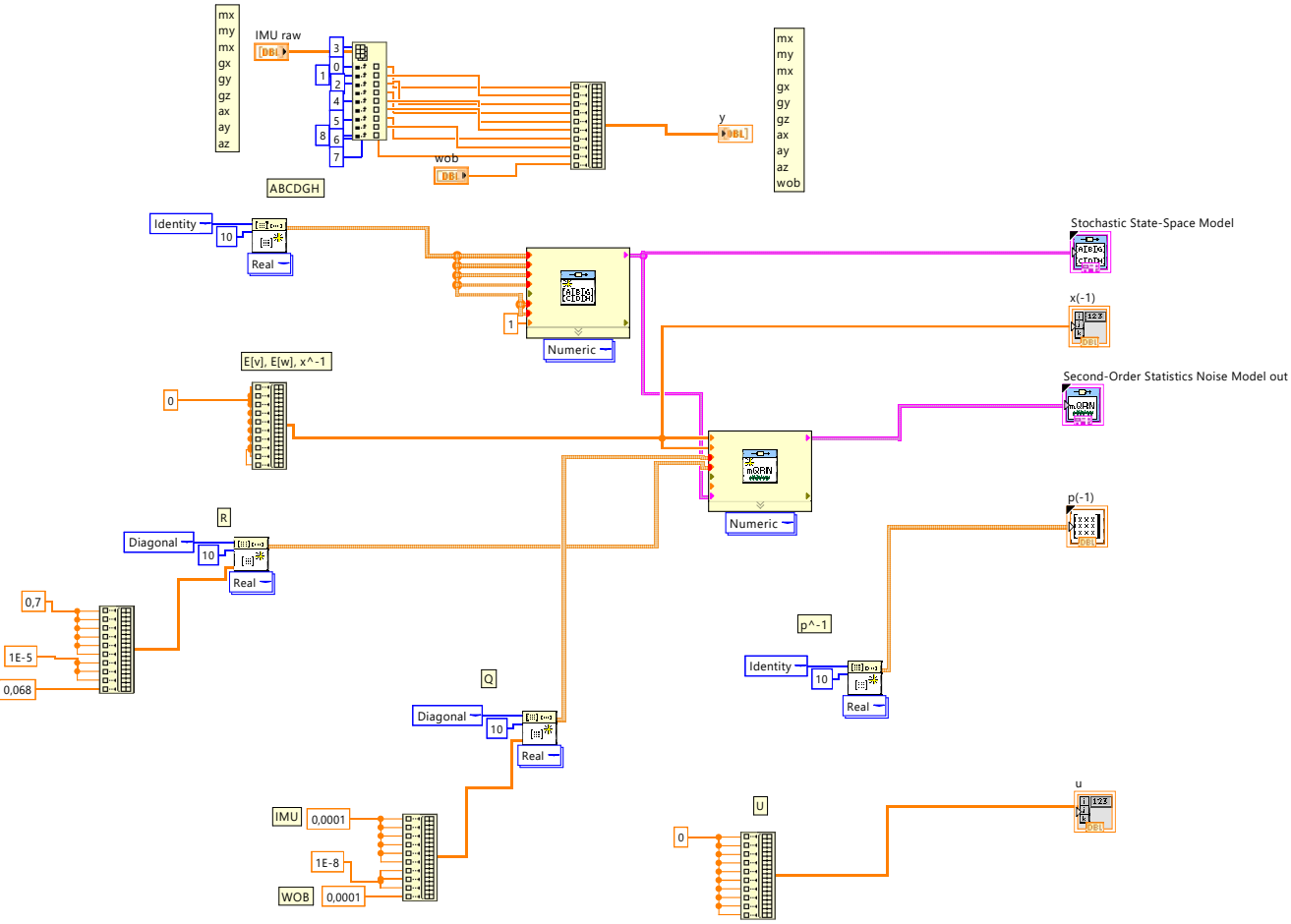

vertical_drilling_log_sub_Hilde.vi
C:\Users\Bruker\Desktop\Drillbotics backup 05062019\Drillbotics 2019\Autonomous Control\Sub-VIs\Hilde subVI 29mai\vertical_drilling_log_sub_Hilde.vi
Last modified on 04.06.2019 at 14.29
Printed on 05.06.2019 at 20.40

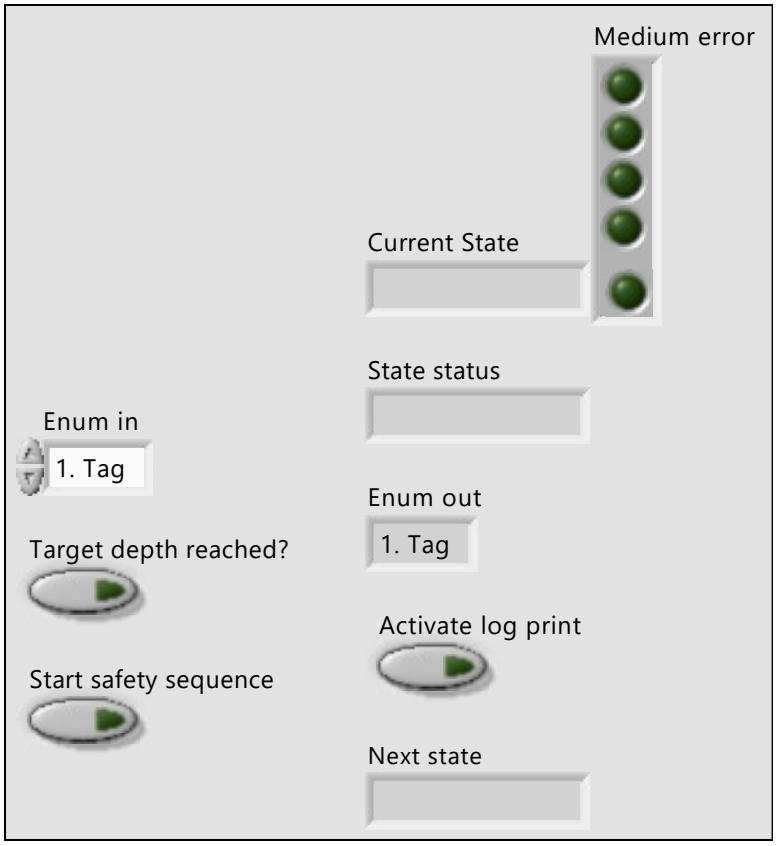

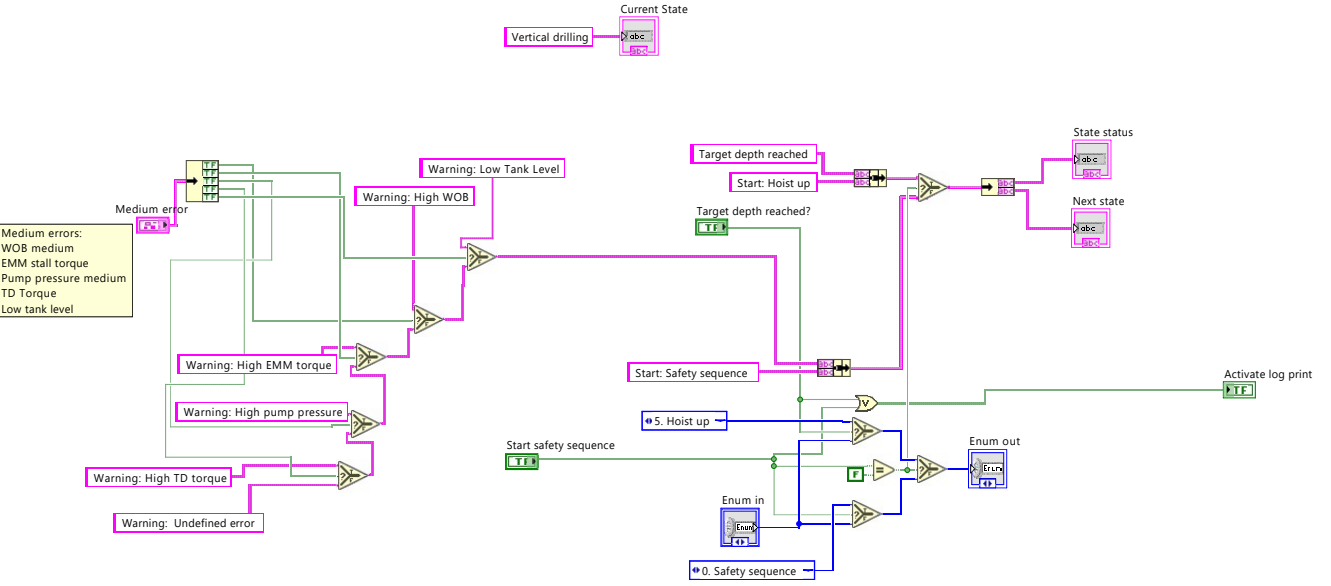

vertical_drilling_log_sub_Hilde.vi
C:\Users\Bruker\Desktop\Drillbotics backup 05062019\Drillbotics 2019\Autonomous Control\Sub-VIs\Hilde subVI 29mai\vertical_drilling_log_sub_Hilde.vi
Last modified on 04.06.2019 at 14.29
Printed on 05.06.2019 at 20.40

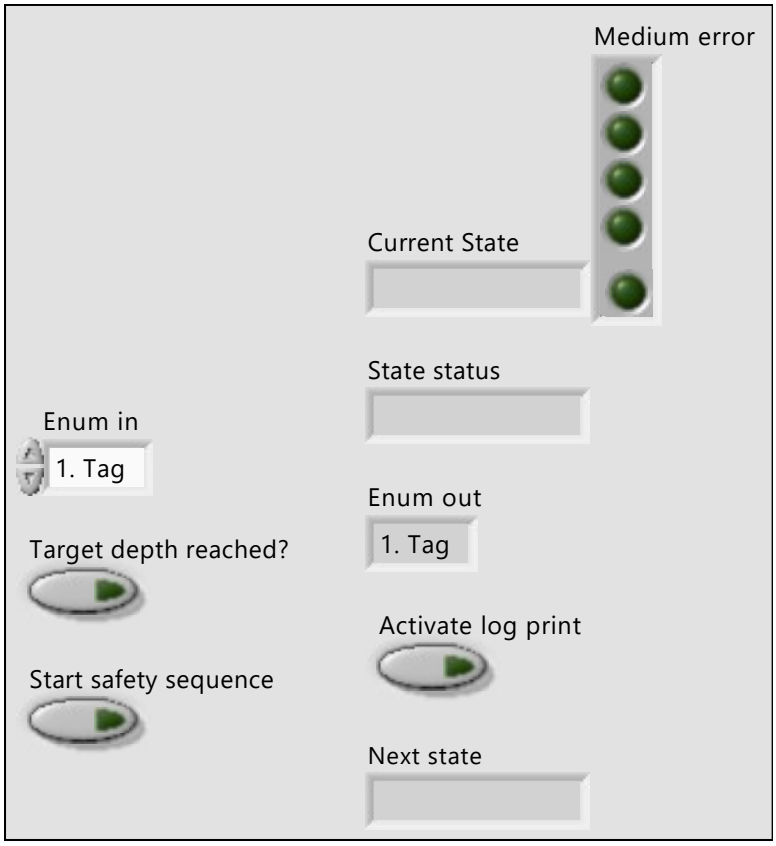

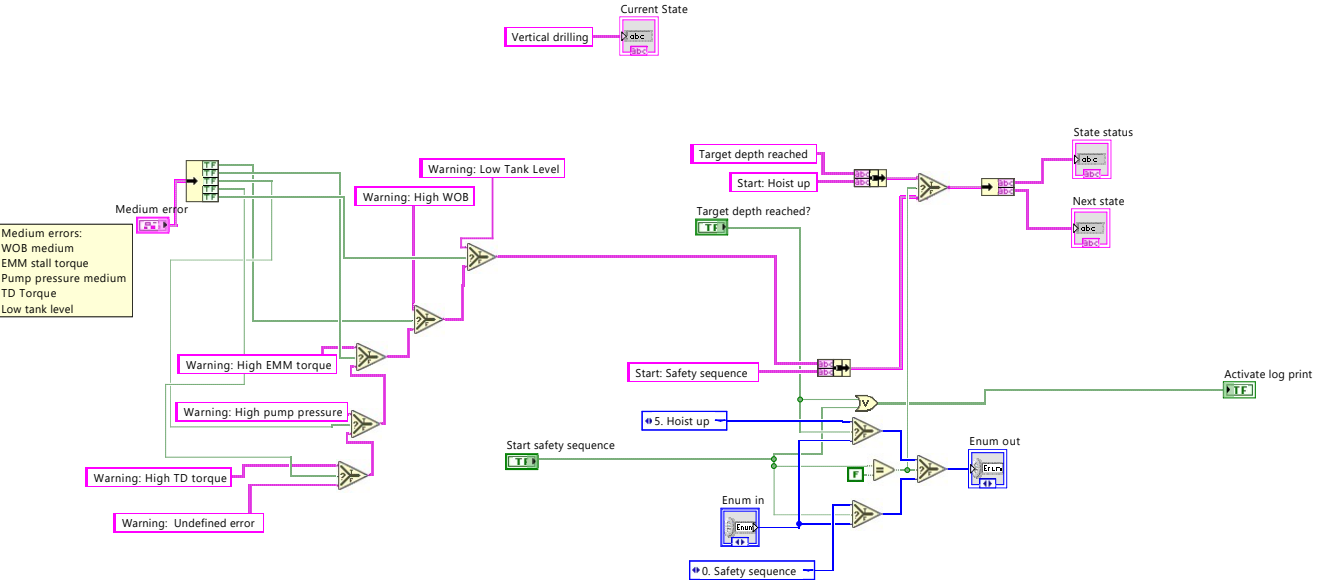

WOB_SP_selector__vertical_Hilde.vi
C:\Users\Bruker\Desktop\Drillbotics backup 05062019\Drillbotics 2019\Autonomous Control\Sub-VIs\Hilde subVI 29mai\WOB_SP_selector__vertical_Hilde.vi
Last modified on 04.06.2019 at 16.37
Printed on 05.06.2019 at 20.38

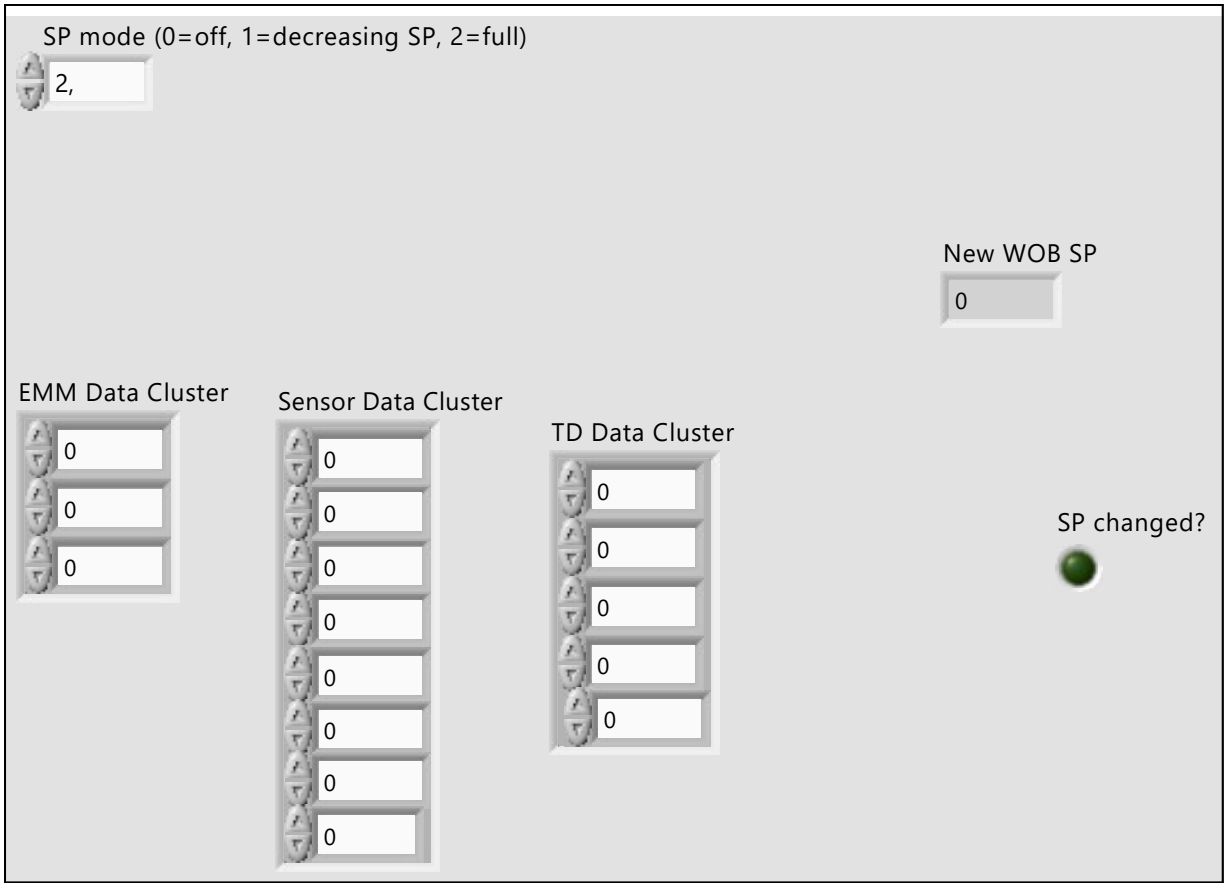

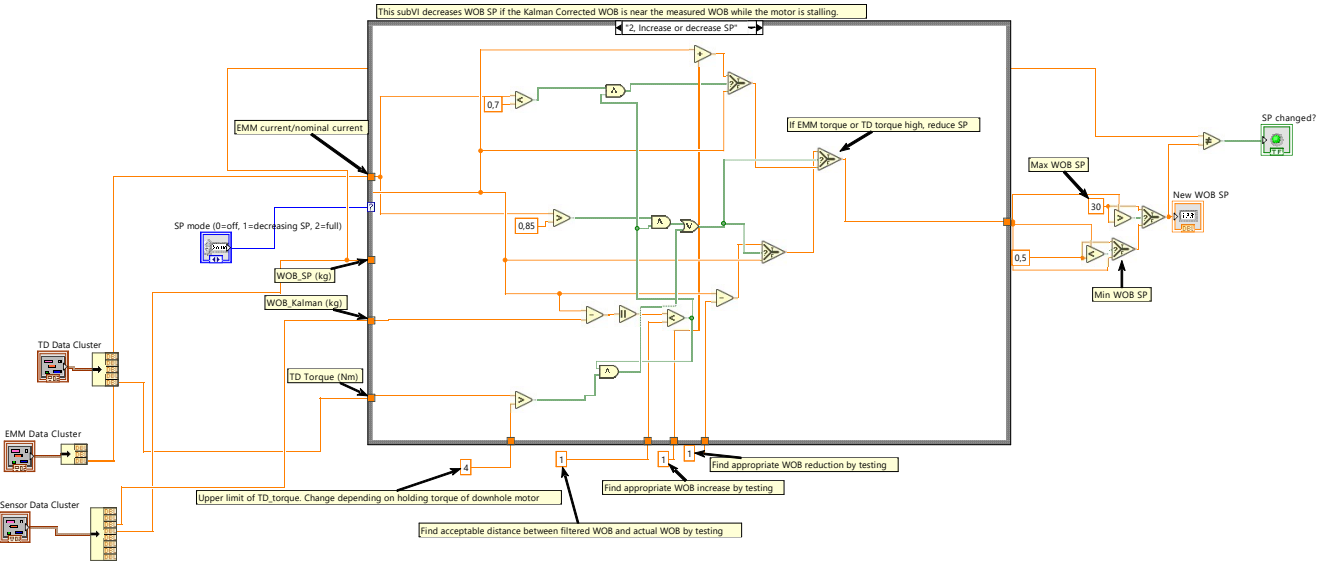

WOB_SP_selector__vertical_Hilde.vi
C:\Users\Bruker\Desktop\Drillbotics backup 05062019\Drillbotics 2019\Autonomous Control\Sub-VIs\Hilde subVI 29mai\WOB_SP_selector__vertical_Hilde.vi
Last modified on 04.06.2019 at 16.37
Printed on 05.06.2019 at 20.38

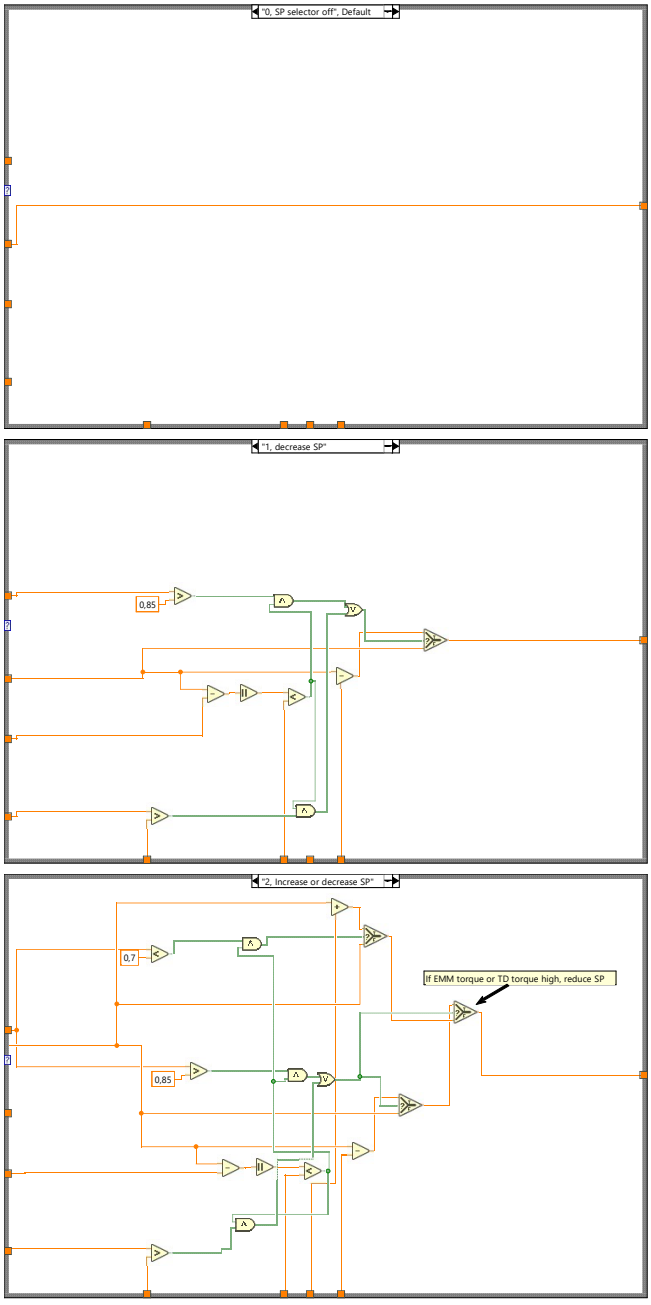

Appendix H

New Riser Design and Calculations

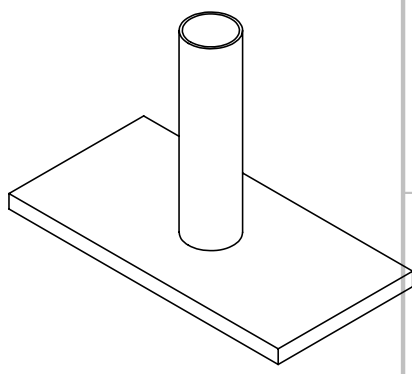

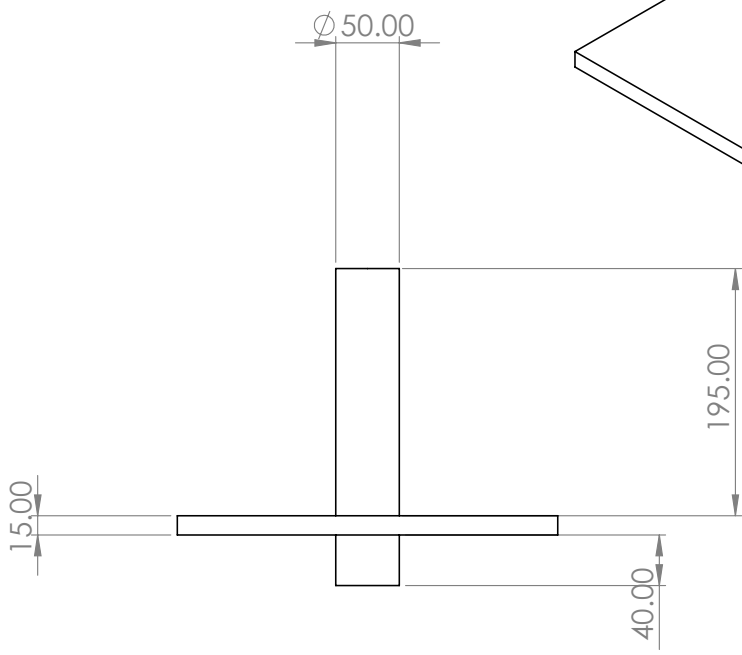

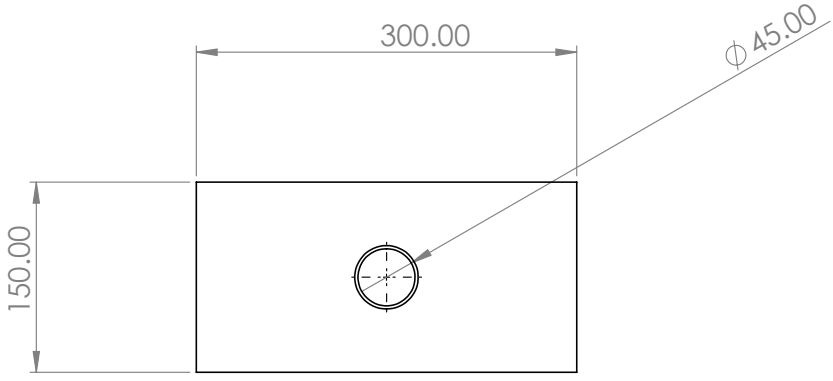

UNLESS OTHERWISE SPECIFIED: DIMENSIONS ARE IN MILLIMETERS SURFACE FINISH: TOLERANCES: LINEAR: ANGULAR:		FINISH:		DEBURR AND BREAK SHARP EDGES		DO NOT SCALE DRAWING	REVISION
	NAME	SIGNATURE	DATE			TITLE:	
DRAWN							
CHK'D							
APPV'D							
MFG							
Q.A				MATERIAL:		DWG NO. Riser_final_8.05	A4
				WEIGHT:		SCALE:1:5	SHEET 1 OF 1

SOLIDWORKS Educational Product. For Instructional Use Only.

Riser Size Calculations

Angle of bend (deg)	3
Length of bent sub below bend (mm)	10
Bit sub length (mm)	15
Bit length (mm)	45
Total length after angle	70
Bit diameter (mm)	36
Horizontal distance from BHA center before bend to bit center (mm)	3.66351694
Horizontal distance from center of end bit to bit edge (mm)	17.9753316
Max radius of BHA with bit	21.6388486
Minimum required riser diameter (mm)	43.2776971

Maximum height of riser should allow for some room between top of riser and rig floor, both because this section is very stable against buckling and because misalignment between the stabilizers/ball bearings may lead to fatigue if the distance is too short		
Provided Rock height	0.61	m
Height of lumber under rock	0.0445	m
Height of platform under rock	0	m
Height at top of rock	0.6545	m
Riser height	0.25	m
Rig floor height	0.95	m
Drill pipe length	0.9144	m
V. sect. Length	0.1016	m
Curve hor. Displ	0.060325	m
Curve ver. Displ	0.508	m
RC	2.16910987	m
angle	0.23639298	rad
Curve length	0.51276234	m
Total well length	0.61436234	m
Distance top riser/rig floor	0.0455	m
Well length+riser height+distance riser/rig floor	0.90986234	m

Figure H.1: Riser calculations

NTNU
Norwegian University of
Science and Technology